MECHANISMS OF BIOMATERIAL MEDIATED FIBROTIC RESPONSES AND STRATEGIES TO IMPROVE TISSUE REACTIONS TO BIOMATERIAL IMPLANTS

by

PAUL TODD THEVENOT

Presented to the Faculty of the Graduate School of

The University of Texas at Arlington in Partial Fulfillment

of the Requirements

for the Degree of

DOCTOR OF PHILOSOPHY

THE UNIVERSITY OF TEXAS AT ARLINGTON

May 2010

ACKNOWLEDGEMENTS

A number of individuals have contributed to my development as a researcher here at the University of Texas at Arlington and have therefore been instrumental in the development of this dissertation. I would like to take this opportunity to express my gratitude to them for their contributions.

I would first like to thank my dissertation committee, Dr. Robert Eberhart, Dr. Malgosia Wilk-Blaszczak, Dr. Jian Yang, Dr. Chi Zhang, and Dr. Liping Tang, for their guidance and suggestions during development of this dissertation. Specifically, I would like to acknowledge my advisor, Dr. Liping Tang, for the opportunity to pursue my research interest and wisdom in developing and focusing the outline of this dissertation.

In addition, I would like to thank members of my lab group for their assistance as part of this dissertation and prior work. I would like to acknowledge Dr. Jinhui Shen, Dr. Hong Weng, and Dr. Wu for assistance with animal studies. In addition I would like to thank David Baker, Richard Tran, and Ashwin Nair for their patience in assisting me with working out mechanisms and interactions as well as audience reviews of presentations in preparation for this dissertation. Finally from our laboratory I would like to acknowledge Cheng-Yu Ko and Yi-Ting Tsai for technical assistance.

Finally, I would ultimately like to thank my family and friends for their support which has made this entire venture possible. To my wife, Ashley Thevenot, I would like to express my sincerest appreciation for patience during long nights of study and time away from home. Without her companionship and the hope that this in some way could contribute to a better life for her and my son, this work would not have been possible. I would also like to thank my mother and father, Terry Thevenot and Robert Thevenot, for believing in me and supporting throughout the academic career. Thanks to Phillip, Veronique, and Oliver Zayas for allowing me

to invade their home during the final preparation for my defense. My family would also like to express their sincerest appreciation and apologies for inheriting a less than desirable roommate. I would also like to remember and dedicate this work to my close friend Adam Puckett, who established a legacy of success and model lifestyle which will serve as a lasting template for which I will continually strive.

March 15, 2010

ABSTRACT

MECHANISMS OF BIOMATERIAL MEDIATED FIBROTIC RESPONSES AND STRATEGIES TO IMPROVE REACTIONS TO BIOMATERIAL IMPLANTS

Paul Todd Thevenot, PhD

The University of Texas at Arlington, 2010

Supervising Professor: Liping Tang

Despite considerable advancements in biomaterial synthesis and modification techniques, most tissue engineering scaffolds elicit fibrotic reactions resulting in implant encapsulation, secluding cells and/or therapeutic agents within a thick collagenous matrix. Therefore, strategies to minimize these responses while improving the functionality of recruited/transplanted cells are required. This work set out to improve the host response to biomaterials and identify what cellular responses were attributed to biomaterial-mediated fibrosis. Two strategies were investigated involving two different targets. In the first approach, PLGA scaffolds were RFGD modified to bear -NH_2 (amine), -COOH (carboxyl), and -OH (hydroxyl) groups altering surface wettability and charge properties. Surface modified scaffolds altered fibrinogen adsorption and RAW 264.7 (macrophage) cytokine secretion *in vitro*, subsequently effecting macrophage chemotaxis to preconditioned media from different modified scaffolds. *In vivo* scaffolds were able to slightly alter inflammatory cell influx while increasing cell infiltration density and matrix production. However surface modification exerted only minor influence over the thickness of the fibrotic capsule.

In the second approach, SDF-1α was incorporated with scaffolds to increase recruitment of host-derived stem cells while reducing fibrotic responses. Increased stem cell recruitment was able to significantly alter interface collagen deposition, in addition to increasing angiogenic progenitor recruitment thus improving angiogenesis and altering the local cytokine environment. By varying cytokine delivery onset and duration, the effects of SDF-1α were linked with a stabilized mast cell response upstream. This led us to consider whether the mast cell responses were primarily regulating the biomaterial-mediated fibrotic response, and specifically what cells where responsible for collagen production at the biomaterial interface.

Fibrocytes and fibrocyte-derived myofibroblasts were identified as primary contributors to collagen deposition. Fibrocytes recovered from the biomaterial implantation site predominantly migrated in response to SDF-1α. Targeting this link with the anti-inflammatory drug dexamethasone did not alter fibrocyte responses; however SDF-1α neutralization significantly reduced the influx of fibrocytes and generation of fibrocyte-derived myofibroblasts. This led to significant reduction in fibrotic responses. Since mast cells influence the acute inflammatory response to biomaterial implants, we hypothesized that creating different degrees of mast cell responses would result in differential stimulation of SDF-1α producing cells while reducing inflammatory stimuli. Stabilizing mast cells with Cromolyn was able to significantly reduce macrophage influx along with fibrocyte and fibrocyte-derived myofibroblast influx. This led to significant reduction in fibrotic encapsulation and collagen I structure at the biomaterial interface, implicating mast cells as the initiator of the biomaterial-mediated fibrotic response. Based on these results, we propose a hypothetical sequence of events leading to the formation of fibrotic tissue around biomaterial implants, which depends upon the degree of mast cell activation and subsequent fibrocyte responses. Therefore, this study has identified the critical involvement of the mast cell response in biomaterial-mediated fibrosis, as well as identifies a strategy to reduce mast cell activation while improving host-derived stem cell responses to improve the response to biomaterial scaffolds in the subcutaneous space.

TABLE OF CONTENTS

ACKNOWLEDGEMENTS iii

ABSTRACT v

LIST OF ILLUSTRATIONS xii

LIST OF TABLES xv

Chapter Page

1. INTRODUCTION 1

1.1 Tissue Engineering Background 1

1.2 Current Clinical Progress and Barriers Limiting Translation of Tissue Engineering 3

1.3 The Host Response to Biomaterial Implants 4

1.3.1 Protein Interactions 4

1.3.2 The Mast Cell Response 5

1.3.3 The Acute Inflammatory Response 5

1.3.4 Granulation Tissue and Fibrotic Encapsulation 6

1.4 Strategies to Improve the Host Response 6

1.4.1 Anti-Inflammatory Drugs 6

1.4.2 Surface Modification 7

1.4.3 Control of Cytokine/Chemokine Systems 8

1.4.4 Growth Factors to Improve Tissue Integration 9

1.5 Aims of This Dissertation to Improve These Strategies 10

1.5.1 Surface Modified Scaffolds to Improve In Vivo Host Responses 11

1.5.2 Incorporation of Stem Cell Chemokines to Improve In Vivo Host Responses 11

1.5.3 Evaluation of Mast Cell Responses in Facilitating Biomaterial Mediated Fibrosis 11

2. THE INFLUENCE OF SURFACE FUNCTIONALITY ON SCAFFOLD INFLAMMATORY AND FIBROTIC RESPONSES 13

2.1 Introduction 13

2.2 Fabrication and Characterization of Surface Modified Scaffolds 13

2.2.1 Purpose 13

2.2.2 Materials and Methods 13

2.2.3 Results 16

2.3 In Vitro Quantification of Protein and Inflammatory Cell Interactions with Surface Modified Scaffolds 20

2.3.1 Purpose 20

2.3.2 Materials and Methods 21

2.3.3 Results 24

2.3.4 Discussion 30

2.4 Interface Interactions with Surface Modified Scaffolds at 2 Weeks Implantation 35

2.4.1 Purpose 35

2.4.2 Materials and Methods 35

2.4.3 Results 36

2.4.4 Discussion 38

2.5 Host Response to Scaffold Implants at 6 Weeks 40

2.5.1 Purpose 40

2.5.2 Materials and Methods 41

2.5.3 Results 42

2.5.4 Discussion 46

2.6 Conclusions 49

3. THE INFLUENCE OF SDF-1α RELEASE ON INFLAMAMTORY AND FIBROTIC RESPONSES TO PLGA SCAFFOLDS 50

3.1 Introduction 50

3.2 Methodology 52

3.3 SDF-1α Background 53

3.3.1 Structure, Properties, and Physiological Function during Homeostasis 53

3.3.2 Influence on Stem Cell Mobilization 53

3.3.3 Influence on Inflammatory and Fibrotic Responses 54

3.3.4 Hypothesized Interactions in the Context of Biomaterial Mediated Responses 54

3.4 In Vitro Evaluation of SDF-1α Releasing PLGA Scaffold System to Induce MS Chemotaxis and Engraftment 56

3.4.1 Purpose 56

3.4.2 Materials and Methods 56

3.4.3 Results 57

3.4.4 Discussion 60

3.5 Influence of Short Tern Scaffold Treatment with SDF-1α on MSC Responses In Vivo 60

3.5.1 Purpose 60

3.5.2 Materials and Methods 61

3.5.3 Results 63

3.5.4 Discussion 70

3.6 The Effects of Improved MSC Responses on the Inflammatory Response to PLGA Scaffolds 71

3.6.1 Purpose 71

3.6.2 Materials and Methods 72

3.6.3 Results 72

3.6.4 Discussion 90

3.7 Influence of SDF-1α Dosing Time and Duration on Biomaterial Medaited Tissue Responses 94

3.7.1 Purpose 94

3.7.2 Materials and Methods 95

3.7.3 Results 96

3.7.4 Discussion 112

4. THE INFLUENCE OF MAST CELL RESPONSES ON THE RECRUITMENT OF FIBROCYTES AND FACTORS DICTATING THEIR SUBSEQUENT PARTICIPATION IN BIOMATERIAL-MEDIATED FOREIGN RESPONSES 115

4.1 Introduction 115

4.2 Characterization of the Cell Populations which Constitute the Granulation and Fibrotic Tissue in Biomaterial Implants 119

4.2.1 Introduction 119

4.2.2 Materials and Methods 119

4.2.3 Results 121

4.2.4 Discussion 123

4.3 Influence of Inflammatory Cytokines on Fibrocyte Recruitment In Vitro and In Vivo 126

4.3.1 Introduction 126

4.3.2 Materials and Methods 127

4.3.3 Results 128

4.3.4 Discussion 130

4.4 Effects of Dexamethasone Treatment on Fibrocyte Responses 130

4.4.1 Introduction 130

4.4.2 Materials and Methods 131

4.4.3 Results 132

4.4.4 Discussion 135

4.5 Effects of SDF-1α Neutralization on Fibrocyte Recruitment and Collagen Deposition 136

4.5.1 Introduction 136

4.5.2 Materials and Methods 137

4.5.3 Results 138

4.5.4 Discussion 141

4.6 Influence of Different States of Mast Cell Activation on Fibrocyte Responses and Collagen Deposition 144

4.6.1 Purpose 144

4.6.2 Materials and Methods 145

4.6.3 Results 146

4.6.4 Discussion 153

5. SUMMARY AND CONCLUSION 156

5.1 Summary 156

5.2 Conclusion 158

5.3 Future Perspectives 159

REFERENCES 161

BIOGRAPHICAL INFORMATION 176

LIST OF ILLUSTRATIONS

Figure Page

1.1 The Tissue Engineering Design Strategy 2

1.2 Factors Limiting the Clinical Translation of Tissue Engineering 4

2.1 Characterization of Functionalized Scaffolds. 18

2.2 Characterization of Surface Pore Structure of Unmodified and Plasma Modified PLGA Scaffolds by SEM 20

2.3 Scaffold Absorption of a Hydrophilic Dye 24

2.4 Fibrinogen Adsorption on RFGD Modified PLGA scaffolds 25

2.5 Effects of Serum Protein Adsorption on Macrophage Chemotaxis. 26

2.6 Macrophage Migration to Macrophage Preconditioned Media from each Scaffold Modification Group 28

2.7 Macrophage Migration to Inflammatory Cell Preconditioned Media from each Scaffold Modification Group 30

2.8 H&E Staining of the Skin Side Interface Tissue between the Scaffold Implant and the Native Healthy Tissue 36

2.9 CD11b Inflammatory Cell Responses in the Interface Tissue Between the Scaffold Implants and the Native Healthy Tissue. 38

2.10 Collagen Deposition at the Interface of Surface Modified Scaffolds after 2 Weeks 43

2.11 Collagen Deposition 6 Weeks after Implantation 44

2.12 Collagen Deposition inside the Scaffold 46

3.1 Hypothesized Interactions of SDF-1α in Biomaterial-Mediated Foreign Body Responses. 55

3.2 In Vitro Model of Bone Marrow-Derived MSC Chemotaxis and Engraftment. 58

3.3 MSC Homing and Engraftment to SDF-1α and SDF-1α Modified Scaffolds In Vitro 59

3.4 Pluripotency of Implant Recruited MSC Following Biomaterial Implantation 64

3.5 Preferential Migration of Bone Marrow Derived MSC to SDF-1α Treated Scaffolds 65

3.6 SDF-1α (CXCL12) Distribution in the Matrix Surrounding Scaffold Implants..... 66

3.7 Visualization of MSC Recruited to the Interface of SDF-1α Treated and Untreated Scaffolds. (A) SSEA-4^{+} CD45^{-} MSC phenotype with nuclear DAPI, (B) control MSC, (C) SDF-1α MSC 67

3.8 Density and Kinetics of MSC Recruited to the Scaffold Implantation Site. (A) Kinetics of MSC recruitment, (B) Intra-scaffold MSC density 68

3.9 HSC Recruitment to the Biomaterial Interface in SDF-1α Treated Scaffolds. (A) c-kit control density, (B) c-kit SDF-1α treated scaffolds..... 69

3.10 Recruitment Density of HSC at the Scaffold Interface..... 69

3.11 Mast Cell Behavior in the Inflammatory Response to SDF-1α Treated Scaffolds 74

3.12 SDF-1α Alters Downstream Mast Cell Responses..... 75

3.13 Neutrophil and Macrophage Infiltration 3 Days after Implantation..... 77

3.14 Neutrophil and Macrophage Infiltration 7 Days after Implantation..... 78

3.15 Buildup of Inflammatory Cells at the Scaffold Interfaces 79

3.16 Histological Characterization of Scaffold Interface and Cross-Section after 3 Days 80

3.17 Characterization of Granulation Tissue at the Interface of SDF-1α Treated Scaffolds 82

3.18 Comparison of 1 Week Cell Infiltration among Scaffold Treatment Groups 83

3.19 Cell Behavior at the Interface and Within the Scaffold Cross-Section 2 Weeks after Implantation..... 85

3.20 Inflammatory Cell Stabilization in Week 2 Scaffold Interfaces..... 86

3.21 SDF-1α Treated Scaffolds have Reduced Fibrotic Responses at 5 Weeks after Implantation..... 88

3.22 Mosaic Image of H&E Stains in a Column through the Center of the Scaffold 89

3.23 Delayed SDF-1α Delivery Results in Intermittent MSC and Inflammatory Cell Responses 97

3.24 Stem Cell Expression at the Interface of SDF-1α Pump Scaffolds..... 99

3.25 Quantified Stem Cell Responses in SDF-1α Pump Scaffolds 100

3.26 Effects of Controlled SDF-1α Release on Inflammatory Cell Responses 102

3.27 Controlled SDF-1α Delivery Reduces Interface Density and Increases Interface Vessel Formation 103

3.28 Histology of 2 Week SDF-1α Pump Implants 104

3.29 Analysis of Macrophage and Macrophage Phenotypes at the Tissue Interface 106

3.30 Endothelial Progenitor Cell Participation in Interface Vessel Formation Due to SDF-1α Delivery 107

3.31 Blood Vessel Formations at SDF-1α Scaffold Interfaces and Intra-Scaffold 109

3.32 Collagen Deposition at the Interface of Treated and Untreated Scaffolds 110

3.33 Inflammatory Cytokine Expression in the Scaffold and Adjacent Tissue 112

4.1 Biomaterial-Mediated Fibrotic Responses 116

4.2 Characterization of Cells in the Fibrotic Tissue Surrounding Biomaterial Implants 122

4.3 Characterization of Stem Cell and Myofibroblast CD90 Expression at the Biomaterial Interface 123

4.4 Fibrocyte Expression and Chemotaxis 129

4.5 Characterization of Inflammatory and Fibrotic Cells in Response to Dex 133

4.6 Effects of Dex on Interface Cell MSC Marker Expression 134

4.7 Characterization of the Fibrotic Response to Chalcone-4 Loaded PLGA Films 139

4.8 Compositional Changes in Fibrocyte Density at the Interface of Chalcone-4 Implants 140

4.9 Effects of Fibrocyte Intervention on Differentiation of Fibrocytes to Myofibroblasts 141

4.10 Interfacial Responses and Collagen Deposition in the Context of Variable Mast Cell Responses 148

4.11 Fibrocyte, Macrophage, CD90, and Stem Cell Responses Due to Variable Mast Cell Responses 151

4.12 Effect of Mast Cell Response on Cell Populations at the Biomaterial Interface 152

LIST OF TABLES

Table Page

2.1 Plasma Deposition Conditions and Surface Wettability
of the Polymer Films Generated to Coat the PLGA Scaffolds 19

CHAPTER 1

INTRODUCTION

1.1 Tissue Engineering Background

TE is a discipline of regenerative medicine for which the basic goal is to provide a temporary matrix to replace damaged extracellular matrix upon which cells can be seeded and synthesize new ECM as the temporary matrix degrades [1]. A common TE design diagram is summarized in Figure 1.1. The standard approach employs either physiological decellarized ECM or synthetic polymer cast into a porous matrix in which the gross structure resembles the physiological ECM, either of which represents the biomaterial component of the design. The second portion consists of cells which ideally would be, fully differentiated cells, though in most instances these are difficult acquire and expand cells in vitro [2]. To address this problem, stem cells have become a popular cell of choice in TE. Due to their unique pluripotency and regeneration properties, stem cells have been intensively studied as powerful therapeutic tools for a variety of diseases and conditions, including articular cartilage regeneration [3], multiple sclerosis [4], spinal cord repair [5], and cardiac muscle recovery after heart attack [6]. Based on these findings, stem cells have been extensively employed in TE research and product development, including designs for regenerating the retina [7], myocardial tissue [8, 9], bladder [10], and skeletal tissue [11, 12]. Unless limited by properties or leachables from the scaffolds, it is often straightforward to facilitate cell adherence and proliferation on protein adsorbed porous scaffolds [13], especially with FDA approved polymers such as PLGA and PLLA. However, the foreign biomaterial component of the TE design presents significant problems when translating designs to the in vivo system [14]. The host response to biomaterials significantly hampers the intended functionality of many designs [14]. These limitations are mostly due to the destructive properties of the inflammatory response and the encapsulating

processes of the fibrotic response [15]. These processes ultimately function to segregate the scaffold from the native healthy tissue, thereby limiting the therapeutic potential intended for the design [16]. As a result, the clinical impact of TE has been limited due to tissue responses (inflammatory and fibrotic reactions) to both the biomaterial and cell components of the designs [17].

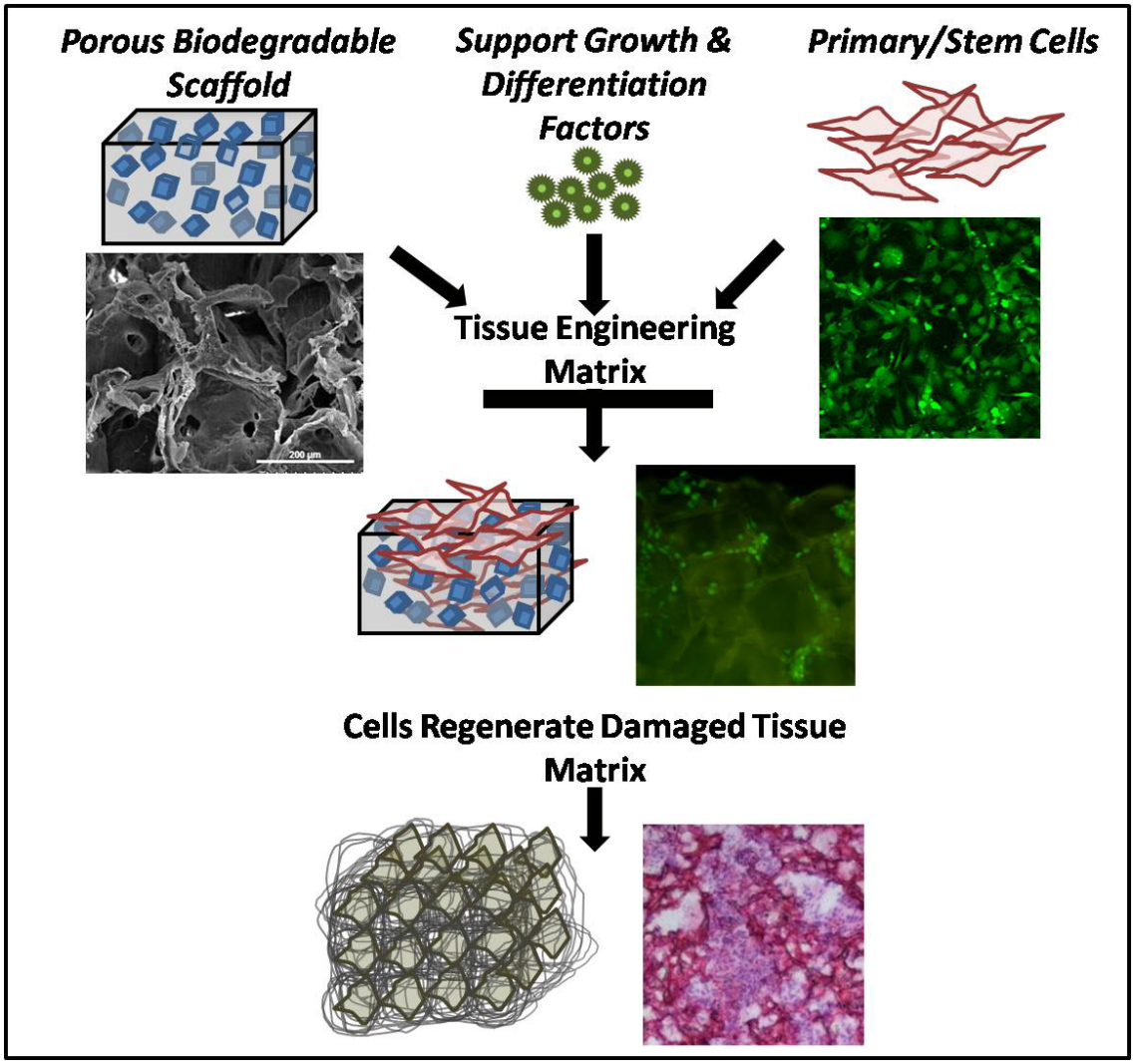

Figure 1.1 The tissue engineering design strategy. A combination consisting of a porous matrix, differentiation/growth factors, and progenitor or terminally differented cells is cultured to produce a confluence, 3D block of tissue matrix. This matrix can then be implanted into a defect to induce regeneration of the damaged tissue.

1.2 Current Clinical Progress and Barriers Limiting Translation of Tissue Engineering

Despite considerable academic effort, there are very few clinical applications [18], with current products limited to only a few tissue types [19, 20]. Many have suggested that clinical translation of TE has been limited due to our inability to control/circumvent the inflammatory and fibrotic responses while quickly and adequately vascularizing scaffold implants [20-23]. The inflammation and fibrotic reactions as well as wound healing and angiogenesis are critical to the survival and behavior of seeded cells in the short term and dictate long term functionality and integration [24]. Therefore, the ability to control, or at least minimize, the inflammatory response has emerged as a critical design parameter which may ultimately dictate the success of TE designs in vivo [24-26].

The inflammatory and fibrotic response to biomaterial implants will be covered in the subsequent section. Though, within the context of the inflammatory response to TE implants, many limitations exist concerning angiogenesis. In order for cells to survive in vivo, it has been shown that the cell must be within 200μm of a capillary bed [22, 27]. Therefore, in most full thickness designs, seeded constructs will not be adequately vascularized after implantation resulting in a necrotic or bare core as shown in many recent publications [1, 28-30]. In fact, many studies have shown that cells seeded below the scaffold exterior surface do not survive and require some degree of prevascularization in vitro to survive in vivo [21, 23]. In fact, even in vitro, cells tend to prefer the exterior of the scaffold (Figure 1.2) despite ample pore space for invasion [31]. In a recent investigation, MSC seeded by various methods onto scaffolds implanted subcutaneous showed the majority of cells die within 2 weeks [21]. In conjunction with this, many scaffold implants induced very little short term cell infiltration, resulting in cell buildup at the tissue:material interface, inducing a significant fibrotic response effectively walling off the biomaterial implant (Figure 1.2). To overcome the need for near immediate angiogenesis with pre-seeded constructs many have suggested seeding scaffolds with endothelial or endothelial progenitor cells prior to implantation [32, 33]. However, pre-seeding

with endothelial cells in vitro does not necessary guarantee that these cells will make functional connection with existing vasculature in vivo [22]. Failure to address these design strategies in small animal models will only become more complex with scaled up structures for clinical application [34].

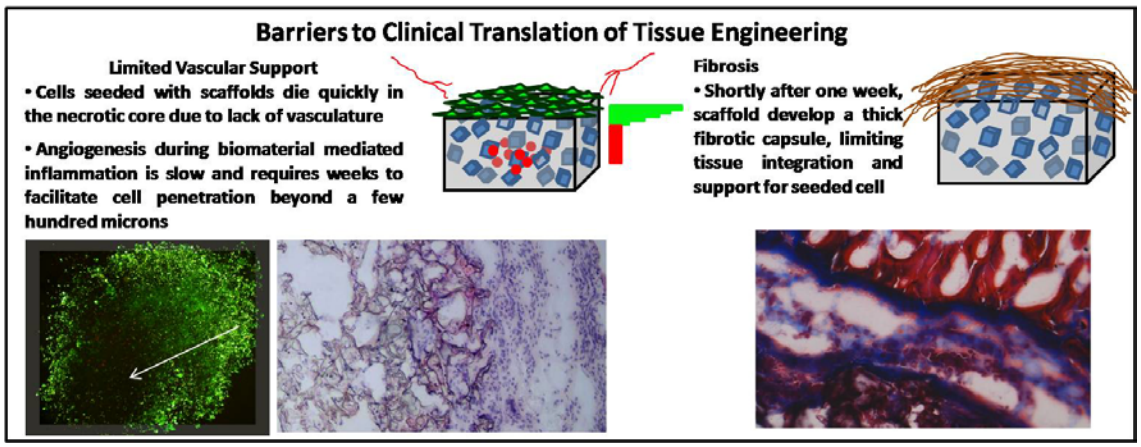

Figure 1.2 Factors limiting clinical translation of tissue engineering. Both in vitro and in vivo, cells have a limited capacity to survive inside the scaffold without adequate nutrient support. In vivo, this process if limited due to poor scaffold integration and the fibrotic response which encapsulates the implant with collagen, limiting vessel infiltration and nutrient exchange.

In addition most TE designs incorporate differentiated stem cells which may not have the interaction potential of pluripotent stem cells and cannot adapt to local stimuli as those stem cells recruited through the injury mechanism [17]. This idea ties in with the overall problem of clinical translation, owing to the fact that our understanding of the influences of site specific foreign body reactions, undesired cell infiltration, and cytokines is underdeveloped [20].

1.3 The Host Response to Biomaterial Implants

1.3.1 Protein Interaction

The first step which initiates the host response to biomaterials is the nonspecific interaction of serum proteins with the biomaterial [14, 16]. Serum protein components, such as fibrinogen, adsorb to the biomaterial and denature. The adsorption of protein and denatured protein conformations appear to be linked to the chemical properties of the biomaterial surface [14, 35, 36]. Based on the denatured protein conformations, certain epitopes of the protein

become exposed which serve as recognition sites for inflammatory cell adherence to the biomaterial [14, 37-39]. In addition to creating sites for inflammatory cell interactions, binding of complement components results in the release C3a and C5a which serve as locally stimulate the inflammatory response by recruiting cells to the implantation site [15].

1.3.2 The Mast Cell Response

Mast cells have been linked to the infiltration of inflammatory cells following biomaterial implantation [40]. It is generally believed that the products of protein interactions (C3a and C5a) initiate mast cell activation [15, 41]. These protein interactions serve to activate mast cells causing degranulation and release of cytokines and chemokines (such as TNF-α and IL-1β) which propagate the inflammatory response [15, 41]. These factors include histamine, tryptase, and other factors which dilate local vessels and activate the endothelium to facilitate neutrophil infiltration and monocyte diapedesis to the implantation site [16, 42]. Additionally, recent work has shown that mast cells can interact with fibrinogen adsorbed to tissue culture substrates, which can also subsequently influence their behavior [43]. However, our recent studies have shown that mast cells are predominantly present in the developing reaction tissue surrounding the implants, not in direct contact with the biomaterial during these acute responses [44].

1.3.3 The Acute Inflammatory Response

Though the specifics of neutrophil influence in the biomaterial-mediated foreign body response are not well established, histamine antagonists have been shown to reduce neutrophil infiltration [39]. Therefore, after mast cell degranulation, neutrophils influx the implantation site with the likely role of facilitating the removal of pathogens and debris from the implantation site and contribute to development of a local environment in which the foreign body response can begin to develop. This is supported by the fact that the neutrophil response is transient, with resolution resulting in macrophage infiltration mediated through neutrophil release of monocyte chemoattractants [45]. In contrast, macrophage involvement at this stage of the biomaterial mediated response has been well classified [16, 46]. Macrophages which have reached the

implantation site through chemotactic signals, take up residence at the implant interface in the developing matrix of infiltrated cells which is beginning to form around the implant [16]. At this site, macrophages assume an activated phenotype and transcription regime, secreting cytokines and chemokines which serve to activate fibroblasts and facilitate the early stages proliferation which will form the basis of the fibrotic capsule [16].

1.3.4 Granulation Tissue and Fibrotic Encapsulation

At this point, roughly 1-2 weeks post-implantation, the interface of cells surrounding the implant consist mainly of macrophages, fibroblasts, and neovascularization in the implant vicinity [16]. This granulation tissue forms the precursor to what will become the fibrotic capsule [16]. Macrophage activation in the granulation tissue causes cytokine and chemokine profile excretions which influence fibroblast precursors and terminal fibroblasts as well as influence the recruitment of additional macrophages [15, 16]. Factors such as TGF-β1 and PDGF released from macrophages influences the transition of fibroblast precursors to contractile myofibroblast capable of producing collagen and their proliferative capabilities, respectively [15].

The proliferation and differentiation of these cells, in the presence of elevated levels of TGF-β1 [15], marks the beginning of fibrotic capsule formation. Elevation of this cytokine leads to production of collagen I and collagen III by myofibroblasts, resulting in a disorganized matrix forming a thick scar layer around the implant [15]. The contractile myofibroblasts then facilitate capsule shrinkage around the biomaterial. The fibrotic capsule presents a permanent barrier to both scaffold intergration with host tissue and a nutrient diffusion barrier limiting the likelihood of any functional component placed within the scaffold from performing its designed duty [14].

1.4 Strategies to Improve the Host Response

1.4.1 Anti-Inflammatory Drugs

The first logical approach to minimizing the foreign body response to biomaterials would be to administer or incorporate anti-inflammatory drugs to minimize the cellular response. Drugs such as glucocorticoids act by reducing cytokine transcription as well as receptor

transcription, thereby reducing actuator elements of the inflammatory response [47]. Additionally, coatings such as heparin can reduce leukocyte diapesis decreasing inflammatory cell infiltration [48]. This results in a dampening of the inflammatory response. However, many of these down-regulated cytokines and chemokines are multi-functional (pleiotropic) and required for many aspects of the healing and regenerative responses [47, 49]. It is now understood that in addition to their role in the inflammatory response, these inflammatory cells, especially macrophages, play critical roles in modulating tissue remodeling and angiogenesis [50-52]. These processes are critical to wound healing and the regeneration of functional tissue following injury. Thus a blanket approach to reducing inflammatory cell activation has many consequences related to the ability of the host to regenerate the damaged tissue. In fact, glucocorticoids have been shown to reduce VEGF production and inhibit wound healing responses [53]. Therefore, our focus has shifted from this approach to strategies which can alter the activation of inflammatory cells without losing their regenerative potential.

1.4.2 Surface Modification

Several approaches to surface modification of biomaterials to improve biocompatibility have been investigated and are well reviewed in literature [47, 54, 55]. Most of these approaches aim to prevent, reduce, or alter the deposition and adsorption of proteins and cells to the biomaterial in an effort to control opsonization, leading to the activation of inflammatory responses [47, 54]. While anti-biofouling approaches are relevant for certain biomaterial applications, in TE some degree of host interaction is desired [56], and may likely be required to initiate host integration and productive regeneration.

Common methods include modifying surface chemistry, introducing functional groups with charge or wettability properties, alteration of surface roughness, and immobilization of cell attachment sequences [54, 57]. The limitations of these approaches can be summarized by three main drawbacks. The first two limitations are interrelated. Studies of surface roughness and immobilization of cell attachment sequences, show many potential benefits in vitro [54].

Even a well seeded scaffold must survive through inflammatory responses and integrate into the host tissue. Therefore, while these strategies may be successful at facilitating cell attachment in vitro [55], there functionality in improving TE translation by modulating foreign body responses is still unclear, with few studies examining influence on inflammatory and foreign body responses [57].

In situations where modifications are designed to improve in vivo responses in the absence of cells, the influence of surface modification may only be related to the cells which interact first with the adsorbed protein layer [54]. The link between the behavior of first responders and downstream events necessitates detailed monitoring which has not been adequately characterized in the in vivo system [58]. Though in vitro studies have shown cell responses, especially inflammatory cells, can be modulated through surface modification [16, 24, 46], the effects of surface functionality as investigated with thin films of implanted biomaterials appears to be minimal downstream, though some differences in early histology and cellular responses have been noted [14, 59, 60]. The final limitation is that most hypotheses underlying surface functionality investigations assume a direct relationship between the inflammatory response (assessed by monitoring the macrophage) and the fibrotic response [24]. However, several lines of evidence suggest this relationship may not be so direct and likely involves the participation of other potent effecter cells [24, 61]. As such, the next evolution of biocompatibility strategies involves modulation of the signaling and activation systems to achieve a more measurable and magnified response on both short term and long term responses.

1.4.3 Control of Cytokine/Chemokine Systems

The previously mentioned approaches can be arbitrarily broken down into two systems, the cytokine/chemokine system (discussed in this section) and the growth factor system (discussed in the subsequent section). It is well established that most inflammatory cells reach the damaged tissue by following chemokine gradients to the local circulation and subsequently

crossing the activated endothelium into the damaged tissue [24, 40, 62, 63]. In addition to chemokines role in increasing the sensitivity of chemokine receptors, thus facilitating migration, chemokines and additionally cytokines serve a critical role in the activation of cells [46]. Following activation, the cells can assume a particular phenotype and secrete additional cytokines and facilitate certain cellular interactions [46]. Recently, more focus has been placed on characterizing the effects of this system in biomaterial-mediated foreign body responses. A product of these investigations is new evidence that shows that based on the initial response to the biomaterial, macrophages of different phenotypes may be recruited to the implantation site, with function dependent upon phenotype at the injury site [52, 64]. However, as mentioned in the anti-inflammatory strategies section, a purely anti-inflammation approach may not yield desirable TE results given the necessity for host integration and functional regeneration. For instance, while studies which neutralizing/antagonizing inflammatory cytokines (such as TNF-α and IL-1) and interfering with inflammatory cell chemotaxis (MCP-1 and MIP-1) and diapedesis mechanisms have been successful at limiting inflammatory responses [40, 47, 65], their side effects on stalling wound healing responses has not been quantified from a biomaterial and TE perspective. Additionally, several groups have begun to link the effects of topography and surface functionality on altered cytokine release from inflammatory cells [57, 66]. These approaches will likely provide better translatable alternative in comparison to neutralization approaches, though in vivo characterization of these responses as well as overall effectiveness are still limited [57].

1.4.4 Growth Factors to Improve Tissue Integration

Due to the design strategy of TE and the primary use of stem cells, several growth factors have been employed in TE in the in vivo system [67, 68]. Factors such as VEGF, FGF, and PDGF has been incorporated to influence and accelerate implant vascularization [34]. Several bone tissue engineering approaches incorporate BMPs and TGF-β to influence mineralization and differentiation [69]. However, most of these investigations were not primarily

focused on their short term effects on biomaterial:tissue interactions in the context of the inflammatory and fibrotic responses, but rather long term regeneration of damaged tissue. As a result, many of these studies overlook potential influences on inflammatory and immune cell interactions and thus are difficult to translate to different biomaterials and tissue compartments, since of these factors regulate fibrotic tissue development [70-72]. One such study showed that local delivery of VEGF was able to increase neoangiogenesis, though dexamethasone (Dex) was required to suppress inflammation and fibrosis [73]. This highlights the shortcomings of pharmaceutical management strategies in biomaterial mediated responses, requiring many growth factor combinations, leading potentially to many unintended interactions and general translation complications due to design complexity [74].

In general, the short growth factor half lives and pleiotropic actions along with biomaterial dependent responses requiring variable dosing regimes, contribute to difficulty assessing these responses in vivo [67]. Despite these limitations, if simple, short term growth factor interactions can be used to alter an upstream response to initiate a modified cascade of response, the effectiveness of these strategies may become substantially more attractive in clinical TE applications [74].

1.5 Aims of this Dissertation to Improve These Strategies

The aim of this dissertation is to examine the in vivo outcomes of two different strategies to improve the host response biomaterials. In the context of examining these outcomes, we are specifically interested in monitoring cellular responses at the interface at different time points with particular focus on the kinetics of different cell responses and their translation to tissue histology, specifically related to fibrosis and fibrotic outcomes downstream. The ultimate goal is not only to identify strategies which improve the host response, but ideally to implicate cell or cell cascade interactions which can be directly linked to fibrotic outcomes. The summary of these aims breaks down as follows.

1.5.1 Surface Modified Scaffolds to Improve In Vivo Host Responses

As previously mentioned, many several groups have reviewed the topic of improving biocompatibility through surface modification [54, 55, 58, 75]. However, the in vitro systems employed in these studies are in most cases highly oversimplified and facilitate cell:material interactions in a manner not representative of the physiological response [58]. Thus to critically analyze the utility of this approach, the in vivo system is required. Several studies in our laboratory and others have looked at the short term influence of surface functionality using biomaterial films and microparticulate systems. Though these studies provide a framework of the short term response, the geometry of the material is not readily translatable to TE designs [59, 60]. Therefore, this study is set up to examine the effects of surface functionality downstream during the inflammatory response at 2 weeks and downstream into the fibrotic response at 6 weeks. The specific focus of this test is to analyze how surface functionality alters the inflammatory cell responses at the interface, and the relationship to fibrotic encapsulation at 6 weeks.

1.5.2 Incorporation of Stem Cell Chemokines to Improve In Vivo Host Responses

The second aim is consists of an approach for which very little literature has been reported in the context of biomaterial mediated responses. Therefore, evaluation of chemokine incorporated scaffolds will cover a broader range of time points, specifically with more coverage of the acute response. Focus in this aim is to examine whether release of the chemokine can indeed improve MSC responses locally. However, the primary focus is to quantify what effects the chemokine and recruited MSC exert on the host response. Specifically we are interested in observing whether MSC interactions can improve host response to the scaffold, increasing cellular integration and decreasing fibrotic outcomes.

1.5.3 Evaluation of Mast Cell Responses in Facilitating Biomaterial Mediated Fibrosis

After analyzing the responses of the two strategies, our findings potentially implicated the mast cell as a critical first determinant of downstream responses, in contrast to macrophage.

In this final aim, we set out to examine mast cell responses in a series of experiments designed to quantify mast cell influence over cell recruitment to the biomaterial interface and fibrotic reactions. Holding biomaterial properties constant, we created non-porous biomaterials with different tendencies to activate mast cells, and used this variable response system to characterize in vivo responses downstream. Finally, the link between the mast cell and fibrocyte was analyzed for its primary role in correlating to the fibrotic potential of a biomaterial implant.

CHAPTER 2

THE INFLUENCE OF SURFACE FUNCTIONALITY ON SCAFFOLD INFLAMMATORY AND FIBROTIC RESPONSES

2.1 Introduction

This study begins with implementation of a strategy to improve the tissue response and fibrotic outcomes to TE scaffolds by modifying the surface functionality of the scaffold. The justification for this approach lies in previous findings which show that material properties alter interactions with serum proteins and thus influence inflammatory cell interactions in the context of the foreign body response. Using PLGA salt leached scaffolds RFGD modified with different functional group containing monomers, we investigated the 2 week and 6 week response to these scaffolds in a subcutaneous implant model. Evaluation of the implants focused on inflammatory cell interactions at the implant interface and fibrotic outcomes at both time points.

2.2 Fabrication and Characterization of Surface Functionalized Scaffolds

2.2.1 Purpose

Though the influence of surface functionality on tissue responses has been investigated, the in vitro models and biomaterials used in these investigations provide little information on this influence from a TE perspective. Therefore we set out to create porous TE scaffolds fabricated from PLGA (75:25) using sieved NaCl as a leachable porogen, which could then be RFGD modified using schemes detailed in previous publications. We were primarily interested in ascertaining whether the scaffolds maintained accessible surface porosity post-modification and characterizing the application of each functionality to the scaffold.

2.2.2 Materials and Methods

2.2.2.1 Scaffold fabrication

All chemicals were purchased from Sigma-Aldrich (St.Louis, MO) unless otherwise specified. Scaffolds will be fabricated as outline in our previous publications. Briefly, PLGA salt-

leached scaffolds were fabricated following established procedure[31]. Briefly, PLGA (75:25, 113kDa, Medisorb Inc., Birmingham,AL) was dissolved in chloroform at 10% (w/v). The PLGA polymer solution was then added evenly over a Petri dish. Sodium chloride (porogen weight fraction of 90%, sieved at (150–250 mm) was then spread evenly on PLGA solution with continuous stirring in a fume hood until the solvent–polymer solution became pasty. After 72 h, the scaffold was placed under vacuum to complete solvent evaporation overnight. For the salt-leaching process, all scaffolds were submersed in distilled water and placed on an orbital shaker at 100 rpm. The water was changed every 30 min at room temperature until chlorides could not be detected by addition of 0.1M silver nitrate.

2.2.2.2 RFGD surface modification and film characterization

The EO2V, AA, and VAA monomers were purchased from Aldrich (Milwaukee, Wisconsin) and were of the highest purity available. They were outgassed repeatedly before use but were not subjected to any additional purification steps. Radiofrequency gas discharge plasma polymerization was used to coat the scaffolds. In an effort to achieve efficient coating, a 360-degree rotatable plasma reactor was used. The scaffolds were loaded inside the borosilicate glass reactor and the reactor was evacuated to 5 mTorr background pressure. After this background pressure was achieved, an oxygen-plasma pretreatment was conducted at 100 W average power to remove any carbonaceous contaminants. Subsequently, the plasma enhanced chemical vapor desposition (PECVD) process was initiated using one of the three monomers. In each case the polymerization was carried out using a monomer pressure between 50 and 100 mTorr. The film thicknesses deposited were limited to approximately 5 to 10 nm. The film deposition rates, and thus thickness, were determined in separate experiments using polished silicon substrates and an Alpha-Step profilometer (Tencor, San Jose, California).

The structures of the plasma-deposited polymer films produced from each of the three monomers used were characterized using Fourier transform–infrared (FT-IR) spectroscopy. A Bio-Rad, Model FTS-40 (Richmond, California), operated at 8 cm–1 resolution and transmission

mode, was used for the FT-IR characterizations. Additional characterization of these films included measurement of surface wettability using a Rame-Hart sessile drop goniometer, as described elsewhere [76]. For this purpose, as well as for the FT-IR measurements, these film characterization measurements were made on flat substrates coated in the plasma reactor under identical conditions to those used to coat the scaffolds. Polished silicon substrates were used for the water contact angle measurements and KBr discs for the FT-IR determinations. We have already shown that the film compositions are independent of substrate composition after deposition of the first few monolayers of polymer [77]. The surfaces of the PLGA scaffolds were modified using pulsed plasmas to control the chemical composition of the plasma-generated thin polymeric films. Under the pulsed condition the extent of retention of the functional group in a given monomer increases as the duty cycle used during the plasma polymerization is decreased [78]. The average power input is defined as: average power (W) = (duty cycle) × peak power (W), where the duty cycle represents the ratio of the plasma on time divided by the plasma (on + off) time. In the present study the plasma duty cycle used for each monomer was adjusted to generate films that maximized the surface functionalities of the desired chemical group, to achieve sufficient adhesion of the polymer to the biomaterial to resist dissolution of the films when immersed in aqueous solution based on our preivous studies [59]. As the average power input increases the extent of polymer cross-linking increases, while the retention of monomer functional groups decreases. After modification, scaffolds are sterilized by submersion in 70% ethanol in a sterile cell culture hood for 30min. Finally scaffolds are exposed to UV for 30min on both sides before pre-wetting through an ethanol:PBS series to 100% PBS.

2.2.2.3 Scaffold characterization

The porosity of the scaffolds was estimated using the ethanol displacement methods as previously described [79]. SEM was performed on each scaffold surface and cross-section to ensure integrity of the surface and cross-sectional porous structure as previously reported in our

studies using similar fabrication protocols [31]. To examine the cross-section of the scaffold, specimens were freeze fractured after submersion in liquid nitrogen for 30 seconds. Specimens were sputter-coated with silver before observation using a Hitachi S3000N scanning electron microscope (Hitachi High Tech Inc., Tokyo, Japan). Pore sizes of each treatment group were verified using Image J. FTIR was used to confirm the presence of the desired functional groups on the surface of the scaffold. Scaffolds were stored under vacuum to prevent damage to the generated surface chemistries until implantation or in vitro experimentation.

2.2.3 Results

2.2.3.1 Scaffold Fabrication and Characterization

The porosity of PLGA salt leached scaffolds fabricated using this technique have previously been published by our group and are similar to those reported in literature using similar techniques. The porosity of the salt leached scaffolds was estimated using ethanol displacement and approached the anticipated porosity based on polymer to salt ratio of ~95% [31, 80]. In addition, analysis of surface and cross-section SEM of the PLGA revealed uniform porosity and pore sizes consistent with the range of sieved NaCl used as the porogen, ranging from 150 – 250 μm, with a mean pore size of 212.87 ± 35.9 μm [31].

2.2.3.2 Verification of Scaffold Surface Modification

FT-IR identified the structural features of the coatings and confirmed the presence of each chemical functional group introduced onto the surface of the PLGA scaffolds. The spectra are arranged in the order poly(allyamine), poly(vinyl acetic acid), and poly(diethyleneglycol vinyl ether) reading top to bottom (Figure 2.1). The plasma parameters used during the synthesis of the coatings are detailed in Table 2.1. The allyamine group (AA) spectrum confirms the presence amine functional groups via the broad absorption band located near 3400 cm^{-1}. The vinyl acetic acid spectrum has a broad absorption band extending beyond 3500 cm^{-1} to below 3000 cm^{-1} which is characteristic of the presence of carboxyl groups. The absorption band

present at 1700 cm^{-1} is also characteristic of a carbonyl stretch which is associated with the carboxyl group. The diethyleneglycol vinyl ether spectrum displays an absorption band at 3400 cm^{-1} characteristic of the hydroxyl stretch as well as a C-O stretch. All three coatings imparted hydrophilic behavior as expected. The sessile drop static water contact angles ranged from 40 to 48 degrees (Table 2.1). Our previous studies have shown that this technique provides coatings with identical properties and morphology on substrates of different composition and geometries [77].

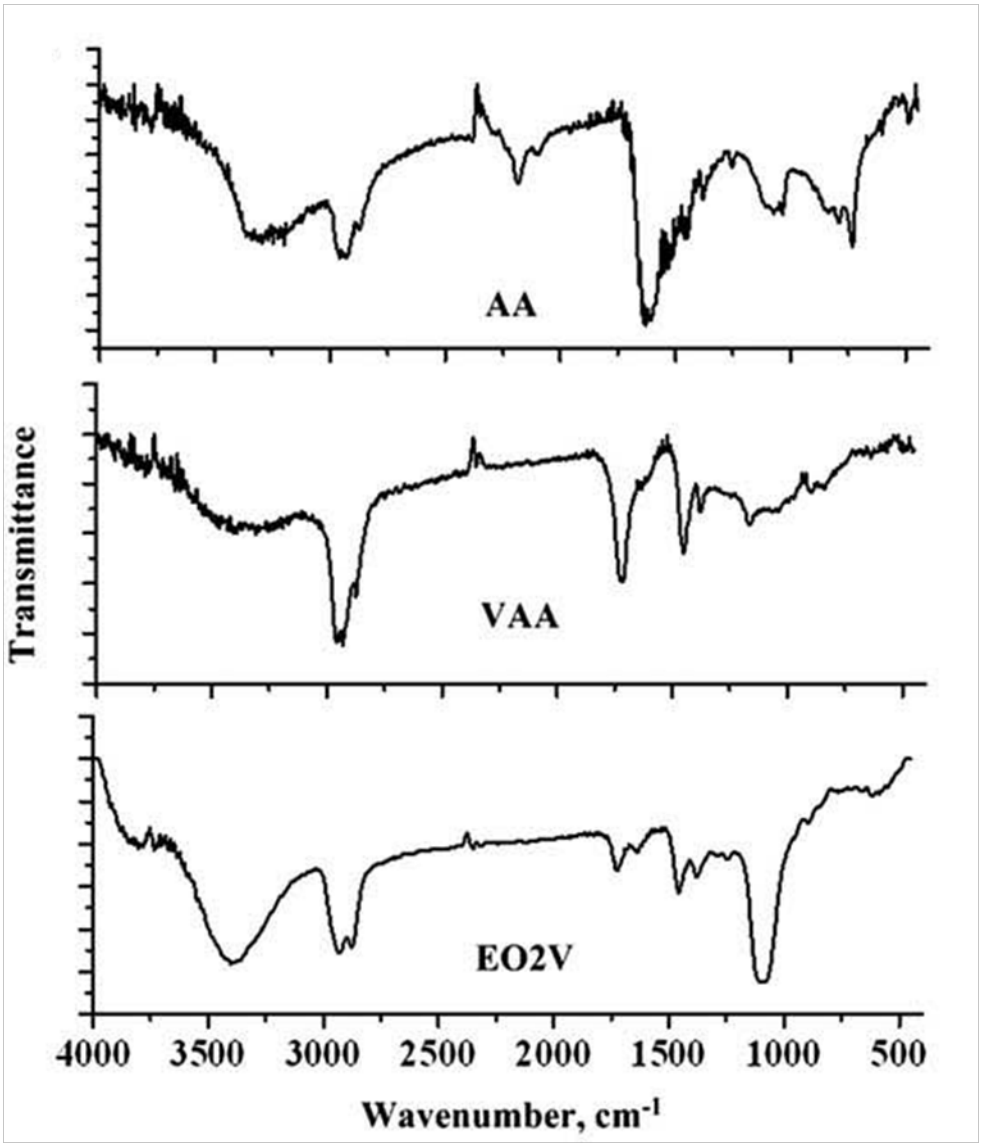

Figure 2.1 Characterization of functionalized surfaces. FT-IR transmission spectra of polymer films used to coat PLGA scaffolds. Spectra are arranged in the following order from top to bottom, allylamine (AA), vinyl acetic acid (VAA), and diethyleneglycol vinyl ether (EO2V) [published in Thevenot et al. Nanomedicine 4(3):226-236].

Table 2.1 Plasma deposition conditions and surface wettability of the polymer films generated to coat the PLGA scaffolds [published in Thevenot et al. Nanomedicine 4(3):226-236].

Monomer	RF peak power input (W)	Ratio of plasma on/off times (msec)	Monomer pressure (mTorr)	Water contact angle
Allyamine	300	10/200	240	40
Vinyl acetic acid	150	0.7/20	284	48
Diethyleneglycol vinyl ether	200	10/160	56	45

2.2.3.3 Scaffold Surface Morphology Post Modification

SEMs of unmodified and surface functionalized were obtained and compared to ensure preservation of the surface porosity of the scaffolds following plasma modification. As shown in our previous reports, the salt leached PLGA scaffolds displayed uniform porosity with pore sizes distributed over the range of sieved NaCl sizes used during fabrication (Figure 2.2). SEM of each modification group revealed no drastic alteration in surface porosity with numerous surface pores evident and measuring in the premodification porosity range. There is no apparent occlusion of the pore space by the deposited polymer films.

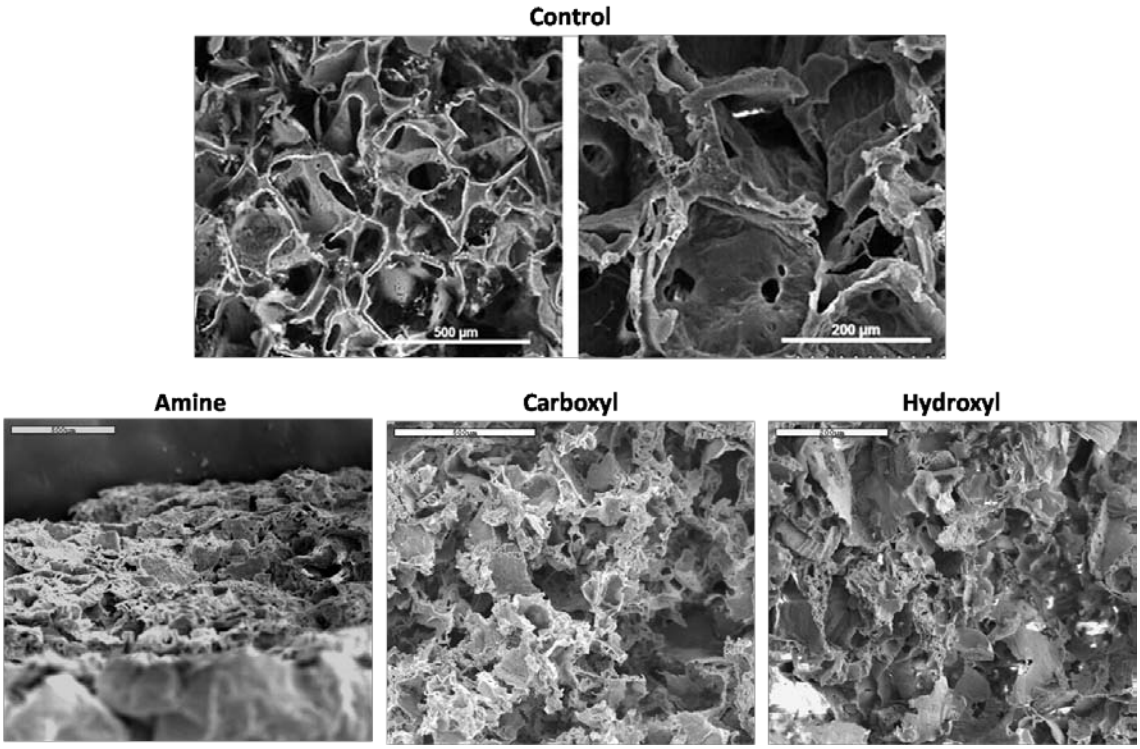

Figure 2.2 Characterization of surface pore structure of unmodified and plasma modified PLGA scaffolds by SEM. Scale bars for amine and carboxyl modified scaffolds are 500µm in length, while the hydroxyl scale bar is 200µm in length.

2.3 In Vitro Quantification of Protein and Inflammatory Cell Interactions with Surface Modified Scaffolds

2.3.1 Purpose

Previous studies have shown that macrophage behavior can be influenced by the functionality of the biomaterial surface, altering cell interactions with the material including activation and cellular secretions [57, 81-83]. The purpose of this study is to monitor the effects of a surface functionalized scaffold on serum protein interactions, mast cell interactions, and macrophage interactions prior to surface adherence. The reasoning behind this approach is to more closely approximate the in vivo influence of the scaffold in terms of linking protein interactions to subsequent cellular responses while avoiding forced interactions between the cells and scaffold in an manner which does not closely approximate those processes observed in vivo. In this study, we will examine the influence of scaffold modification on the adsorption of

protein from the cell culture media by analyzing protein depletion from the media. Then, using these conditioned media, we will analyze the influence of biomaterial:protein interactions on inflammatory cell chemoattraction using mast cells and macrophages.

2.3.2 Materials and Methods

2.3.2.1 Scaffold Adsorption of Aqueous Dye

In order to estimate the depth of the hydrophilic coating, scaffold samples were dried under vacuum for 24 hours, cut into thin cross-sections using a razor blade, and then placed into the hydrophilic dye Alcian Blue for 30min under vacuum. After soaking, scaffolds were rinsed in DI and imaged to visualize the dye stain and compared with scaffolds prior to dye treatment.

2.3.2.2 Fibrinogen Adsorption Study

The interaction of a model protein with the scaffolds was monitored using an established protocol. Briefly, fibrinogen (Sigma Aldrich, St. Louis, MO) was dissolved at 1mg/mL in phosphate buffer 100mM. Scaffolds of each functionality were placed in 4 well plates (n=3) and submersed in 1ml of fibrinogen and allowed to incubate for 3 hrs. Control scaffolds and blank TCPS well surfaces were also submersed in 1ml of fibrinogen solution. After 3 hrs, the fibrinogen solution was removed and scaffolds washed 3X with PBS. Scaffolds were then submersed in 2% SDS solution for 18hrs to remove fibrinogen adsorbed to the scaffolds and well plates. The amount of adsorbed fibrinogen was then calculated using BCA assay (Thermo Scientific Pierce, Rockford, IL) and quantified using albumin standards provided with the assay kit.

2.3.2.3 Scaffold Preparation for Cell Culture

Scaffolds were sterilized by submersion in 70% ethanol for 30 min. Ethanol was then exchanged with increasing concentrations of PBS in the following sequence PBS:ethanol (25:75. 50:50, 75:25. 100:0) with submersion for 10 min on an orbital shaker set to 100 RPM. Prewet scaffolds were then removed from PBS and used in the subsequent experiments.

2.3.2.4 Serum Preconditioning of Surface Modified Scaffolds

Scaffolds were preconditioned with serum proteins by incubation in cell culture media consisting of DMEM with 10% FBS for 3 hrs. Following incubation, scaffolds were removed from the media and the media analyzed using BCA assay to insure protein depletion from the media. Serum absorbed scaffolds were then placed into corresponding transwell migration chambers for subsequent studies.

2.3.2.5 Cell Sources and Culture

Primary bone marrow derived mast cells were differentiated and culture as previously described [84, 85]. Briefly, bone marrow cells were flushed from the cavity of femurs obtained from Balb/c mice after CO_2 asphyxiation. Cells were then cultured in RPMI1640 media supplemented with 20ng/ml SCF, 20ng/ml IL-3, and ultra-low IgE 10% FBS. Cells were subcultured every 4 days to remove adherent cells. After 4 weeks, cells were analyzed for c-kit expression and stained using Toluidine Blue to ensure >95% mast cell population. RAW 264.7 macrophages were obtained from ATCC. Cells were cultured in low bicarbonate DMEM with 10% FBS.

2.3.2.6 Transwell Inflammatory Cell Migration Studies

The chemotactic activity of serum adsorbed surface functionalized scaffolds was assessed using transwell migration assays as previously described [86, 87]. Briefly, prior to assay, RAW 264.7 were starved in serum free media overnight while transwells were prewet with DMEM. Cells were seeded 3hrs prior to media addition to the lower chamber to allow cell attachment to the membrane inserts. To quantify the effects of serum protein adsorption, media was placed in the lower chamber along with a serum preabsorbed scaffold. Macrophages were seeded in the upper chamber at 1×10^5 cells/well and allowed to incubate for 4 hrs. After 4 hrs, inserts were removed, fixed in 100% cold methanol, and swabbed on the upper surface to remove cells that did not migrate through to the lower surface. Membranes were then stained using H&E and the quantified.

2.3.2.7 Effects of Macrophage Conditioning on Subsequent Macrophage Chemotaxis

We next examined the effects of macrophage responses on subsequent macrophage chemotaxis were examined. To generate macrophage conditioned media, scaffold groups were seeded with 5 x 10^5 RAW 264.7 for 3 days to generate surface functionality specific conditioned media. After 3 days, scaffolds were removed and the preconditioned media centrifuged to remove cell and scaffold contaminants. Prior to assay, some samples from each scaffold preconditioning groups were treated with neutralizing antibodies for MCP-1 and MIP-1 (R&D Systems). The amount of neutralization antibody required was estimated from previous published RAW 264.7 seeded biomaterial cytokine quantification studies and estimated at ranges between 15-30ng/mL based on total cell values [57]. MCP-1 (30µg/ml) and MIP-1 (2µg/ml) were added to preconditioned media samples 30min prior to assay and incubated at 37°C. The preconditioned media was placed in the lower chamber with RAW 264.7 seeded in the upper chamber consistent with previous experiments. After 4 hrs, the migration of cells was quantified on the lower surface of the membrane as per previous experiments.

2.3.2.8 Effects of Mast and Macrophage Conditioning on Macrophage Chemotaxis

Finally, the effects of mast cell and macrophage exposure on macrophage chemotaxis were observed. To generate mast cell and macrophage preconditioned media, scaffolds were seeded with 5 x 10^5 RAW 264.7 with cells allowed to attach for 3hrs. After attachment, 5 x 10^5 primary murine mast cells, verified as >95% by Toluidine Blue staining, were added to the wells and the combined culture allowed to progress for 3 days. Preconditioned media from each test group was then collected and centrifuged to remove cells and placed in the lower with chamber with RAW 264.7 placed in the upper chamber as described in previous studies. Some samples were neutralized from MCP-1 and MIP-1 as described in the previous study. Quantification of chemotaxis was assessed as described in previous studies after 4hrs incubation.

2.3.3 Results

2.3.3.1 Hydrophilic Dye Adsorption

The depth of the hydrophilic coating was estimated by soaking scaffolds in the dye Alcian Blue (Figure 2.3). After washing of excess dye in DI water, it was observed that scaffolds differentially stained with the dye to differing depths within the scaffold. Control unmodified scaffolds (top-left) absorbed very little dye, with most of the surface dye washing away in DI water. The -COOH modified scaffolds (top-right) stained with a thin layer from around the exterior edges of the scaffold with very little infiltration. In contrast, $-NH_2$ modified scaffolds (bottom left) stained prominently on both the surface and cross section of the scaffold. Finally, -OH modified scaffold (bottom-right) absorbed dye well along the exterior borders with some penetration, leaving a blank central spaced where dye was unable to bind.

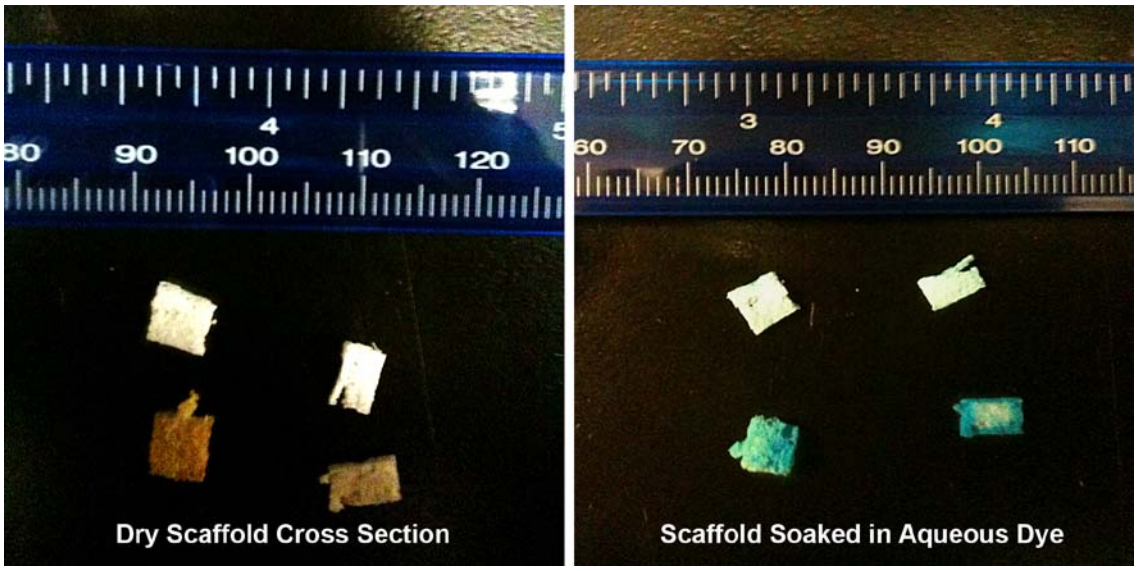

Figure 2.3 Scaffold absorption of a hydrophilic dye. Dry scaffolds soaked in Alcian Blue for 30min under vacuum differentially stain through the cross-section. Control (top-left), -COOH (top-right), $-NH_2$ (bottom-left), -OH (bottom-right).

2.3.3.2 Fibrinogen Adsorption

It is well established that biomaterials adsorb serum proteins after implantation, and these proteins, including fibrinogen, mediate the attachment of inflammatory cells to the

biomaterial. Here we investigated whether surface modification would alter fibrinogen adsorption, as reported studies using biomaterial films (Figure 2.4). The adsorption of fibrinogen to TCPS was quantified to account for fibrinogen adsorption to the well plate. Interestingly, control scaffolds adsorb only a slight amount of fibrinogen. COOH and OH functionalized scaffolds adsorbed slightly (5%) more fibrinogen than control scaffolds. As expected from previous literature, -NH_2 scaffolds adsorbed significantly more fibrinogen (> 20%) than other test groups.

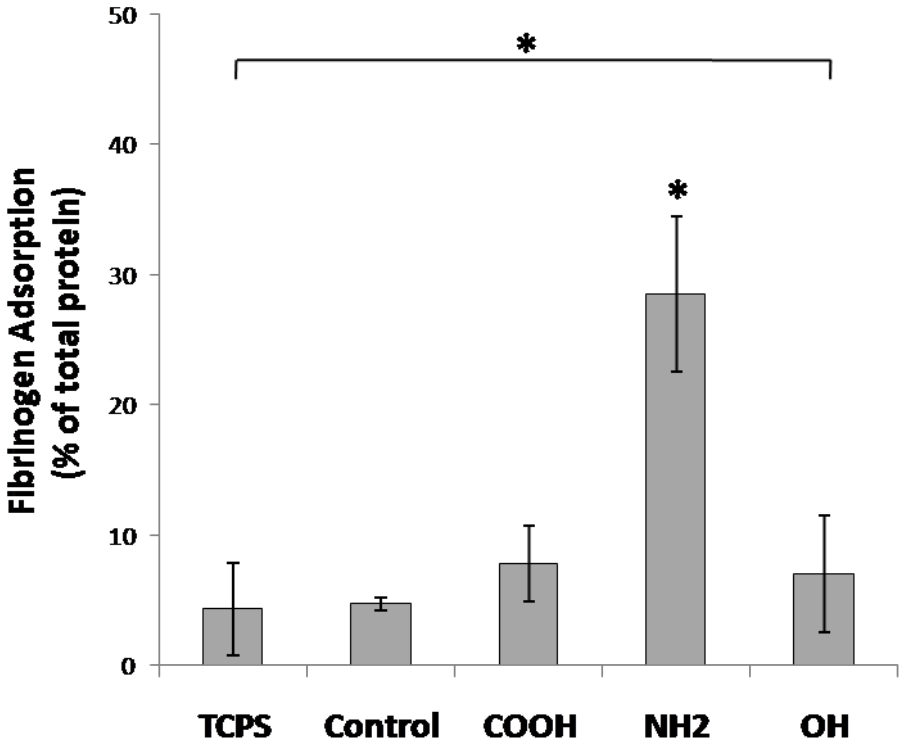

Figure 2.4 Fibrinogen adsorption on RFGD modified PLGA scaffolds. Values are plotted as the percentage of total fibrinogen to which scaffolds were exposed with protein concentration determine by BCA assay. -NH_2 modified scaffolds adsorbed substantially more fibrinogen in comparison to other scaffold modification groups and TCPS. Bracket and * represent significant ANOVA test at $P<0.05$. The * above groups represents significant Dunnett test verses control $P<0.05$

2.3.3.3 Effects of Scaffold : Protein Interactions on Macrophage Chemotaxis

We next examined the effects of protein interactions on macrophage responses. Scaffolds modified with $–NH_2$ were able to attract approximately 3X more macrophages than both control and other scaffold treatment conditions (Figure 2.5). Surprisingly, control, -OH, and –COOH modifications elicited approximately equivalent tendency to attract macrophages from protein adsorbed scaffolds. ANOVA testing revealed significant differences among the means ($P < 0.05$) and Dunnett intergroup comparison revealed $-NH_2$ modification and subsequent protein adsorption led to a significant increase in macrophage chemotaxis.

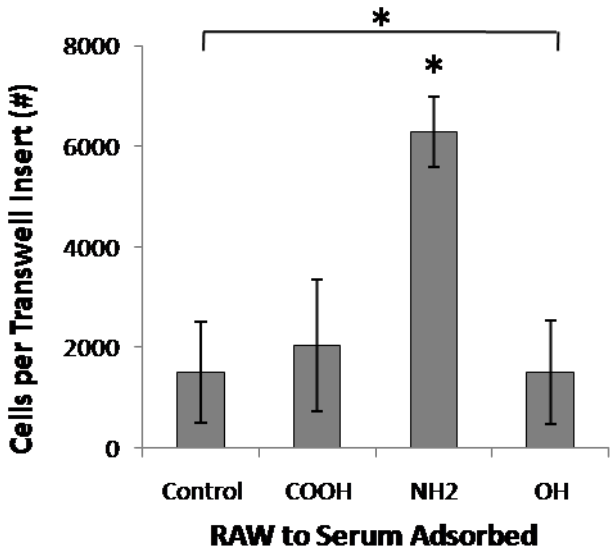

Figure 2.5 Effects of serum protein adsorption on macrophage chemotaxis. Transwell migration assay was used to quantify the migration of RAW 264.7 macrophages to each scaffolds treatment condition. Bracket and * represent significant ANOVA test at $P<0.05$. The * above groups represents significant Dunnett test verses control $P<0.05$

2.3.3.4 Effects of Macrophage Preconditioning on Macrophage Chemotaxis

The effects of surface functionality on mediating differential macrophage responses with regard to cytokine secretions has been investigated, with data supporting surface functionality does alter cytokine release profiles. However, here we are interested in determining whether that can modeled to an in vivo phenomenon, wherein aggravated initial macrophage response,

leads to an increase in inflammatory chemokines and thus an increase in inflammatory cell infiltration. This was examined through seeding macrophages onto surface modified scaffolds and using the preconditioned media to assess macrophage chemotaxis (Figure 2.6). As expected, macrophage interactions with surface modified scaffolds appear to lead to differential release of macrophage chemokines. The -COOH and -OH modified scaffolds migrated significantly fewer (3X – 4X) macrophages across the transwell membranes compared to control and -NH_2 modification. We next compared the effects of MCP-1 and TNF-α neutralization to survey potential chemokines regulating this process and whether neutralization decreased macrophage migration compared to untreated preconditioned media. Interestingly, neutralization of either MCP-1 or TNF-α was effective at limiting macrophage migration for control and surface modified scaffolds with exception to -COOH modified scaffolds. However, there were also differences between the effective neutralization antibodies. Both MCP-1 and TNF-1α were able to substantially reduce macrophage migration in control preconditioned group. Neutralizing antibodies were ineffective in the -COOH group, where macrophage migration was already relatively low. Regarding -NH_2 modified scaffolds, only TNF-α was able to significantly reduce migration ($P<0.05$). In the -OH macrophage preconditioned scaffolds, significance was found between chemokines, but neither were significantly lower than control -OH values.

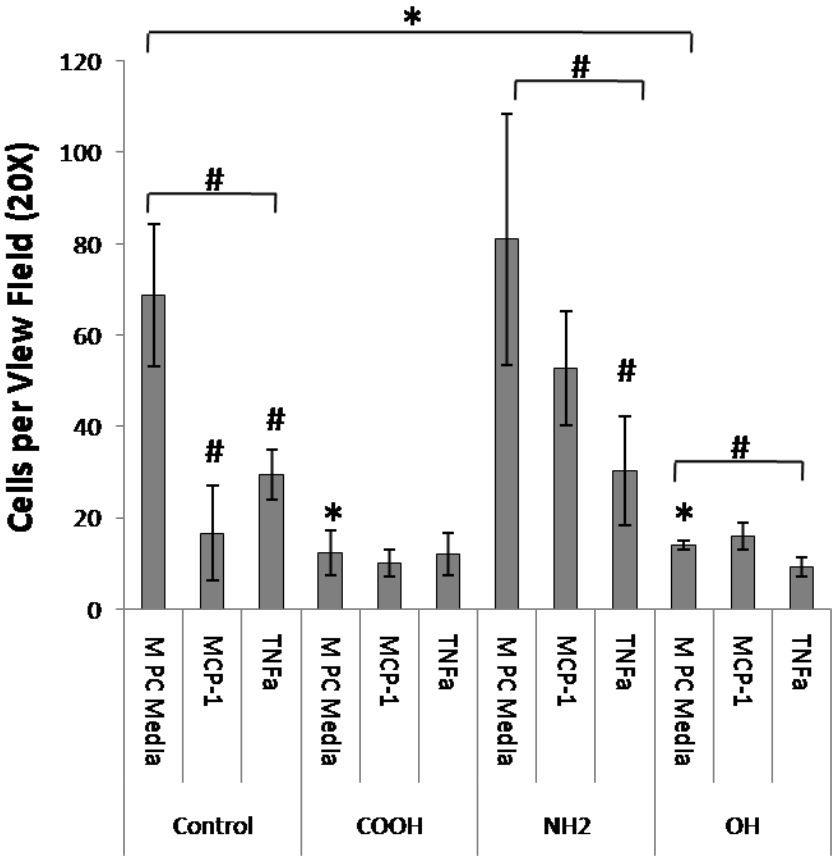

Figure 2.6 Macrophage migration to macrophage preconditioned media from each scaffold modification group. Migration of RAW 264.7 was assessed using transwell assays and determine by total cells per high powered view field (n=3). MCP-1 and TNF-α were neutralized for preconditioned media from each treatment group (n=3) and quantified in a similar manner. Bracket and * represent significant ANOVA test at $P<0.05$ for macrophage preconditioned media groups. The * above M PC media groups represents significant Dunnett test verses control $P<0.05$. Bracket and # represent significant ANOVA test between M PC media and neutralized media $P<0.05$, while # above groups indicates significance from control by Dunnett test $P<0.05$)

2.3.3.5 Effects of Macrophage and Mast Cell : Macrophage Interactions on Macrophage Chemotaxis

Despite the prevalence of in vitro investigation of cell verses biomaterial, very few of these investigations model the in vivo system. As a result, many significant alterations to biomaterials systems observed in vitro, do not result in substantial responses in vivo. In an attempt to generate a closer estimate of the in vivo environment, we attempted a co-culture

study consisting of mast cells exposed to serum preadsorbed scaffolds, followed by macrophage seeding onto the same scaffolds. To more closely approximate the in vivo environment, where macrophages are not always in direct contact with biomaterials, macrophages which became dislodged or overflowed from the scaffolds after seeding where left as adherent to well plates to generate 3 day preconditioned media. Preconditioned media was then analyzed for chemotactic activity using transwell chambers. Interestingly, using this system, we find less significant divergence of chemotaxis between treatment groups. Scaffold surface modification only resulted in a significant decrease in macrophage migration in the -COOH modified scaffolds. Even more surprising, chemokine neutralization resulted in less drastic alterations between treatment groups, with only MCP-1 neutralization in the control group significantly decreasing macrophage migration.

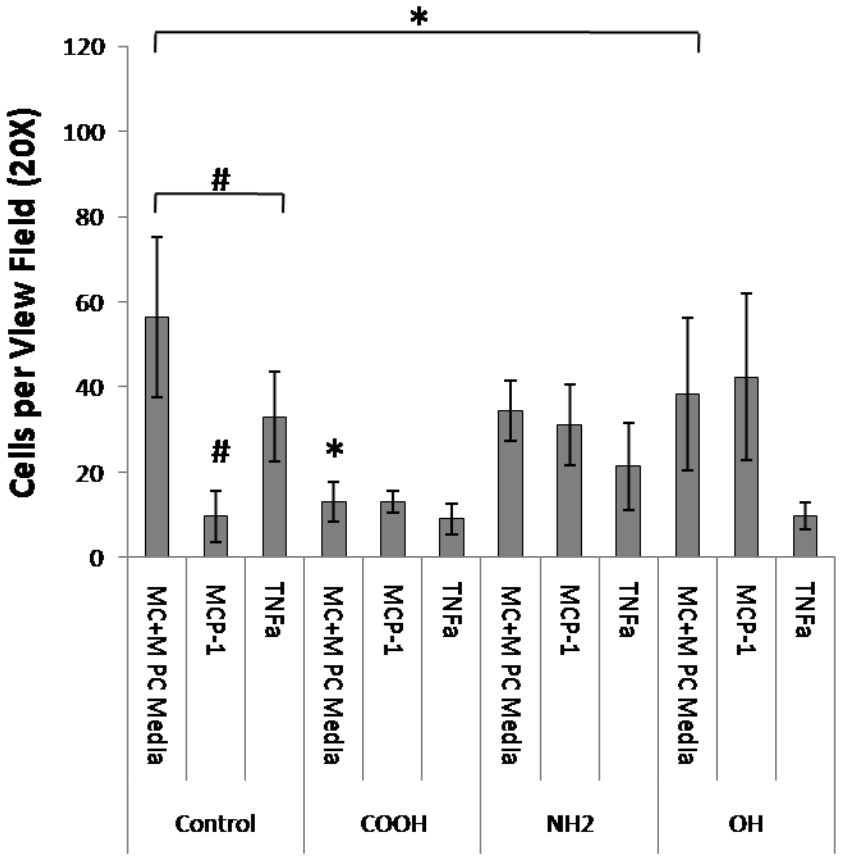

Figure 2.7 Macrophage migration to inflammatory cell preconditioned media from each scaffold modification group. Migration of RAW 264.7 was assessed using transwell assays and determine by total cells per high powered view field (n=3). MCP-1 and TNF-α were neutralized for preconditioned media from each treatment group (n=3) and quantified in a similar manner. Bracket and * represent significant ANOVA test at $P<0.05$ for macrophage preconditioned media groups. The * above M PC media groups represents significant Dunnett test verses control $P<0.05$. Bracket and # represent significant ANOVA test between M PC media and neutralized media $P<0.05$, while # above groups indicates significance from control by Dunnett test $P<0.05$)

2.3.4 Discussion

The purpose of this study was to analyze the in vitro effects of scaffold surface modification. Though biomaterial:macrophage interactions have been previously investigated [57, 62, 81, 82], these investigations have lacked a translatability to either tissue engineering or the in vivo system. In addition, many of these studies were not performed on 3D porous structures [81-83]. Though inherently, material interactions with cells could presumable occur regardless of the orientation of the material, in vivo studies have shown that porous structures generally develop less inflammatory cell interface density and fibrotic encapsulation compared

to solid film structures [88]. Therefore we set out to both characterize the in vitro scaffold inflammatory response, and additionally to increase the complexity of the model of exposure to more closely approximate the in vivo system.

Several different strategies exist for introducing functional groups onto biomaterial surfaces [14, 75]. The plasma modification technique employed in these studies was chosen due to its quality and reliability as established in our previous investigations using microparticulate systems [14, 59, 60, 77]. However, we have yet to test this technique on 3D porous polymer constructs. Others have shown that plasma source and operation parameters can dictate the depth of scaffold functionality modification [75, 89]. Therefore we investigated the penetration depth of scaffolds surface modification using a hydrophilic dye similar to approaches used in previous studies [89]. As expected, the operational parameters appeared to influence the depth of functionality potentially creating different penetration depths. Polyamine monomer was able to more deeply penetrate scaffolds compared EO2V which generated a slightly penetrated halo, and vinyl acetic acid which generated only a scaffold surface modification based on Alcian Blue dye staining. Although SEMs were taken of the scaffold surface to qualitatively assess the influence of film deposition, more detailed assessments of surface:volume ratio after modification may provide additional information regarding the effects of monomer deposition on scaffold surface properties.

Several previous groups have reported on fibrinogen adsorption to different biomaterials and different functional group modified biomaterials [90], showing a general trend of decreasing fibrinogen adsorption as hydrophilicity increases. Fibrinogen characterization provides insight into the possibilities of inflammatory potential [90], however our group and others have previously established that the conformation state of adsorbed fibrinogen is more predictive of inflammatory potential than the amount [14, 39, 63, 91]. Amine functionality has previously been linked with potent fibrinogen adsorption due to hydrogen bonding [14], and thus due to exposure of immune system recognition site, inflammatory cell adherence and activation.

In agreement with these simulations [92], we find the -NH_2 modified scaffolds lead to potent fibrinogen adsorption compared to other treatment groups. In these same simulations, -COOH and -OH functionalities had less prominent chemical interactions with surface, possibly indicating a more reversible interaction with the protein [92]. Though fibrinogen adsorption may allude to a high inflammatory potential [39, 63], subsequent studies were required to determine whether this potential led to quantitative differential outcomes. This response was further investigated by investigating serum protein adsorption using FBS. FBS is standardized in cell culture practice, as well as in vitro biomaterial:cell interaction studies. Interestingly, we find that adsorption of serum proteins does not significant vary among treatment groups for this diverse protein mixture. Some serum proteins such as fibronectin have been investigated for their functionality dependent adsorption patterns as well as downstream studies which shown effects on cell attachment, proliferation, and differentiation [93]. Several links have been drawn between surface properties such as charge and wettability with cell functionality such as adherence, growth, and mineralization [14]. More important to biomaterials and tissue engineering are the links between biomaterial properties, protein interactions, and subsequent inflammatory cell responses.

For the past few decades, a few research groups have focused on defining these mechanisms through progressively more complex evaluations, particularly of macrophage behavior on biomaterial surfaces [57, 66, 81-83]. These findings show that surface properties affect inflammatory cell adhesion, morphology, expression, cytokine secretion, and fusion to form foreign body giant cells. Additionally, protein interactions with surfaces are likely the primary initiator of the inflammatory response [41, 62, 94, 95], with soluble protein products release after adsorption physically mediating inflammatory cell chemotaxis. While the effects observed in this study were relatively minor, we were able to detect some significant differences in macrophage homing across transwell inserts after only serum pretreatment. By placing scaffolds directly in transwells after protein adsorption, we were able to negate the chemotactic

effects of normal serum [96]. Therefore, these differences, predominantly observed in the -NH_2 modification group, may presumably occur through release of soluble chemotactic protein components or results from sensation of proteins reversibly exchanging with surrounding aqueous media [41].

Having established to an extent that protein interactions can mediate inflammatory cell chemotaxis, and given the vast array of data (reviewed in Chapter 1) regarding inflammatory cell behavior after adherence to biomaterial surface, we next examined the effects of these responses on subsequent inflammatory cell recruitment. A recent series of studies have shown significantly altered cytokine secretion profiles of macrophage adhered to different functionalized surfaces [81-83]. This resulted in variable production of chemokines associated with inflammatory cell recruitment. Given this information, we were able to quantify theses alterations by showing macrophage migration could be differentially stimulated by preconditioned media from macrophage seeded scaffolds. Emerging as a recurrent theme in these in vitro studies, the -NH_2 functionality along with unmodified PLGA surfaces, after macrophage adherence exhibited significantly more chemotactic potential than modification with -OH or -COOH. Interestingly, in vivo studies have detected inflammatory cell accumulation on -OH and -COOH modified surfaces after implantation. Though only limited groups have investigated -NH_2 functionality in comparison with other functionalities, studies are numerous and consistent in their findings regarding fewer macrophages/inflammatory cells on -COOH modified surfaces [59, 97], in agreement with these in vitro findings. Our results show that this may indeed be due a decreased production of inflammatory chemokines by biomaterial adherent cells. In fact, neutralization of implicated inflammatory chemokines from this preconditioned media differentially downregulated the chemotactic potential. This was especially evident in the control and -NH_2 groups which had more chemotactic potential. In fact, antibody neutralization was differentially effective at limiting chemotaxis in these groups, with MCP-1 neutralization being more effective in the control group and TNF-α having more

effectiveness in the -NH_2 modified group. This supports differential surface mediated activation of inflammatory cells, which could exert influence on downstream inflammatory and fibrotic responses.

Unfortunately, as previously stated, many in vitro surface functionality findings have shown far less effectiveness in vivo [60, 88]. However, this is likely due to the dynamic parts of the in vivo response, which cannot be simulated adequately in vitro. One such prominent player is the mast cell, for which very few in vitro biomaterial-mediated interactions have been investigated. To further elucidate the potential performance of these surface modified scaffolds in vivo, a co-culture system consisting of mast cell and macrophages to precondition media was developed and examined for macrophage chemotactic potential. Somewhat to our anticipation, the addition of the mast cell component muddled chemotactic analysis, with only -COOH significantly reducing chemotaxis, a finding with some in vivo support. However, the less significant interactions may be due to cross-interactions between the two cell types as many mast cell products have actions predominantly on macrophages. Unfortunately, our analysis did not cover cell behavior post seeding with regards to mast cell activation and macrophage behavior. We expect that the cytokine profiles of these conditioned media would be substantially more complex than macrophage preconditioned media alone.

Neutralization was overall ineffective with only MCP-1 significantly reducing chemotaxis to control scaffolds, interestingly in agreement with that observed in the previous macrophage alone preconditioned study. MCP-1 neutralization and deficiency have been investigated with regard to the inflammatory response in wound repair [65], for which findings indicated that MCP-1 is not critical for macrophage influx during inflammation, but rather activates effector functions. Effects such as these may explain why neutralization in the more complex culture system was less effective. Given evidence that surface functionality appears to successful modulate inflammatory responses in vitro, we next set out to examine these responses in the in vivo system.

2.4 Interface Interactions with Surface Modified Scaffolds at 2 Weeks Implantation

2.4.1 Purpose

Many previous studies have analyzed the effect of surface functionality in vivo using biomaterial films and biomaterial microparticles [59, 60, 98]. In addition, many of these studies have focused on acute tissue responses over the context of the first couple weeks after implantation [59, 60]. The purpose of this study was to analyze the similarity between the host responses to biomaterial scaffolds and to correlate any potential observed alterations in the inflammatory response with those responses observed in vitro. Specifically, this study is interested in analyzing potential alterations in the accumulation of inflammatory cells at the interface between the scaffold and the native tissue, and how this translates into alterations in the fibrotic response downstream.

2.4.2 Materials and Methods

2.4.2.1 Animal Implantation Model

Scaffolds were implanted in the subcutaneous cavity of Balb/C mice as established in early studies [40]. For implantation, mice were anesthetized with isofluorane and the incision site marked and sterilized with 70% ethanol. A vertical incision was made down the midline of the back. Scaffolds were implanted subcutaneous and tucked away from incision. At the end of the experiments, animals were sacrificed by CO_2 inhalation and implants and surrounding tissue were recovered and embedded in OCT and sectioned for histological and immunohistochemical analyses.

2.4.2.2 Inflammatory Responses to Surface Functionalized Scaffolds

To determine the extent of inflammatory responses to scaffold implants, slides were stained with Hematoxylin and Eosin Y (H&E stain, Sigma, St. Louis, MO) according to the manufacturer's instruction. The participation of inflammatory cells in the host reaction was assessed by examining expression of CD11b at the interface between the scaffold and healthy tissue [99]. Primary antibodies were labeled with either FITC or Texas Red conjugated

secondary antibodies based on primary antibody isotype (Pro Sci, Poway, CA). The measurements of tissue thickness and cell densities at the material:tissue interface were then performed in Image J [100].

2.4.3 Results

2.4.3.1 Histology of the Scaffold Interfaces

H&E staining revealed infiltration of cells at the interface between the scaffolds and the native tissue (Figure 2.8). Despite surface modifications, the scaffolds elicited a similar degree of cell infiltration as no significant differences could be observed between the cell density at the interface and the thickness of the infiltrated cell layer.

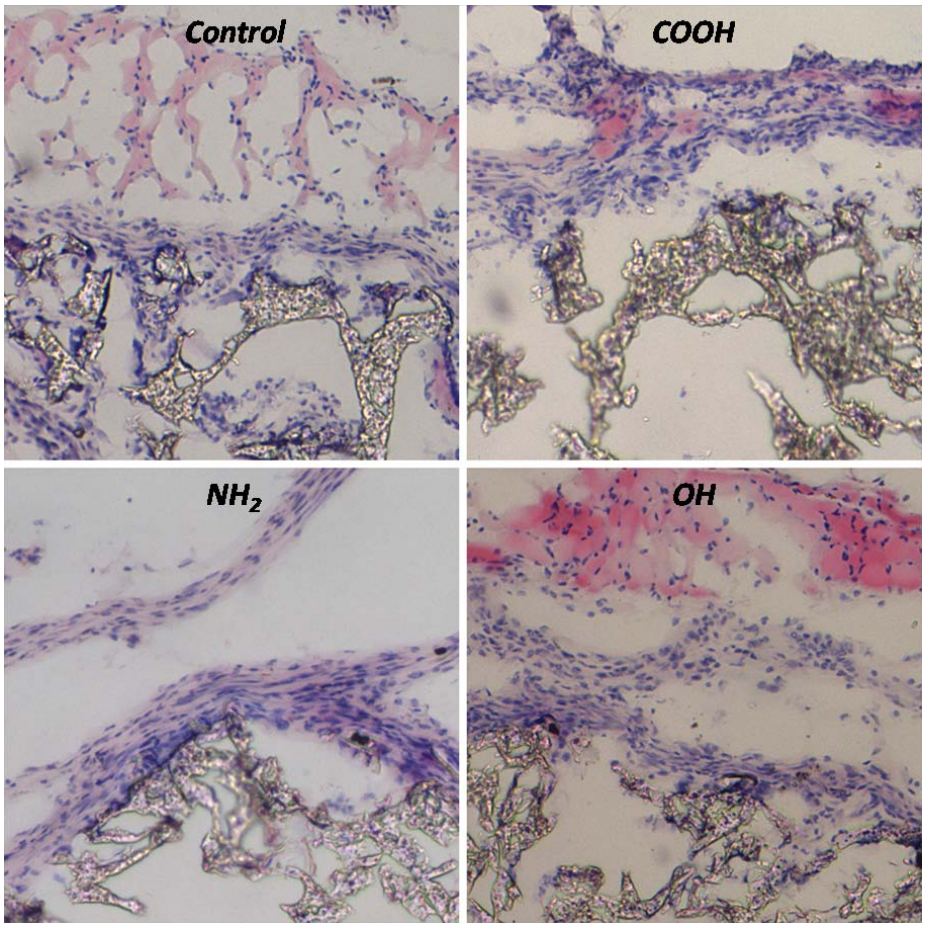

Figure 2.8 H&E staining of the skin side interface tissue between the scaffold implant and the native healthy tissue. Images are labeled by surface modification group.

2.4.3.2 Inflammatory Cell Composition of the Scaffold Interface

Despite the similarity of the interfaces seen in H&E staining of the scaffolds, several previous investigations have shown that the composition of the inflammatory cells is altered by surface modification. To verify these responses in surface modified scaffolds, sections were analyzed for the presence of $CD11b^+$ inflammatory cells. As expected, the presence of $CD11b^+$ cells is readily observed for all scaffold treatments (Figure 2.9). However, the degree of responses does not appear to be similar between modification groups. Control unmodified scaffolds have a prominent layer of CD11b cells throughout the interface observed in the H&E stains. The distribution of CD11b cells in the -COOH modification groups appears lower than that of control, with fewer cells observed in the implant interface. The distribution of cells in –NH and –OH modification groups appears more similar to that of controls, with CD11b cells distributed throughout the interface though apparently at a slightly lower density than that of controls. To quantify these responses, the percentage of $CD11b^+$ cells was plotted over the total number of observed cells at the interface using 4 -diamino-2-phenylindole dihydrochrolide (DAPI) (Invitrogen; Carlsbad, CA) staining. Consistent with the observed immunofluorescence staining, the percentage of CD11b cells is significantly different among groups. Specifically, the percentage of inflammatory cells in the –COOH and –OH groups is significantly lower than those observed in –NH2 and unmodified scaffold groups ($P < 0.05$, ANOVA with Dunnet test).

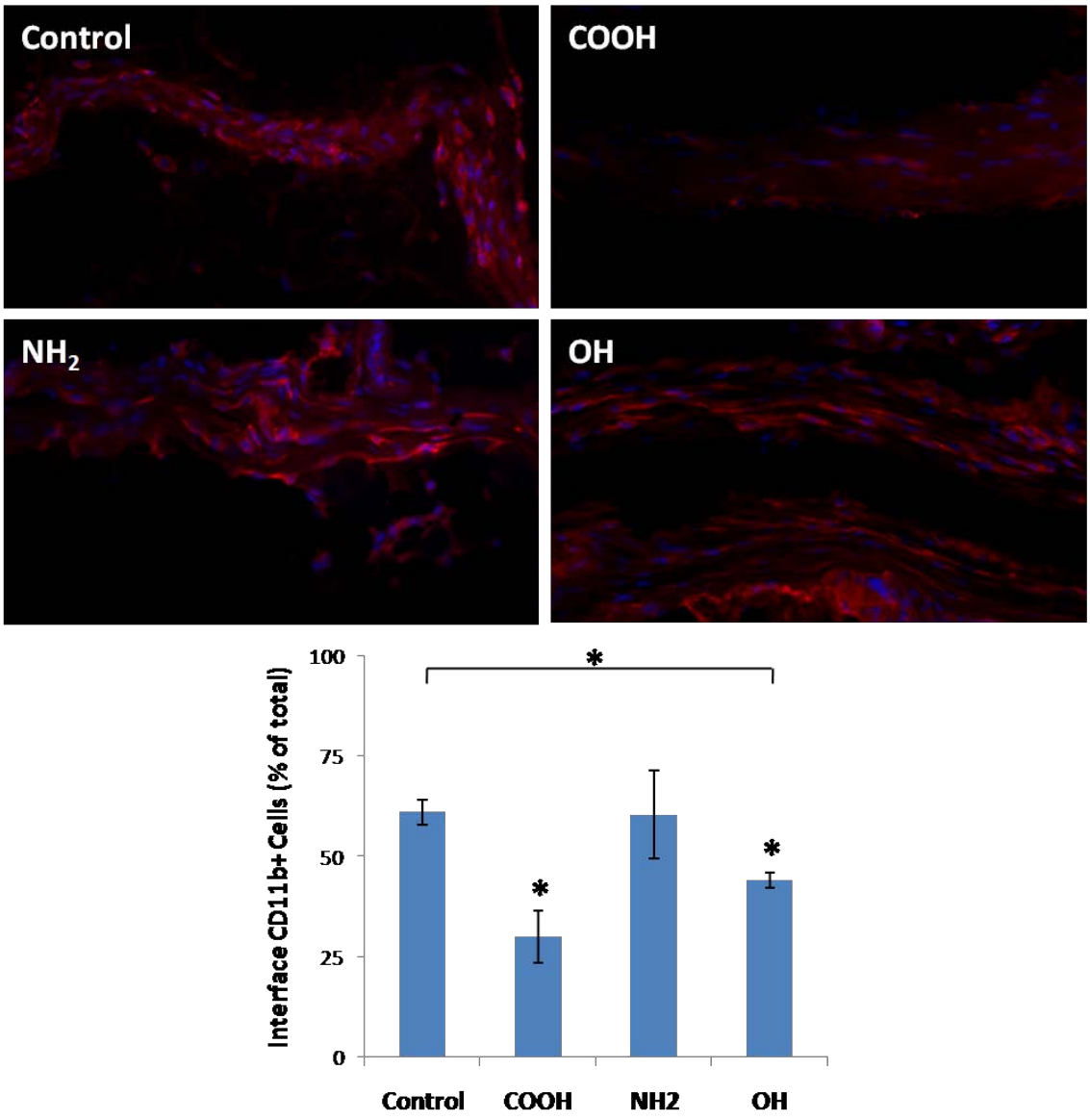

Figure 2.9 CD11b inflammatory cell responses in the interface tissue between the scaffold implants and the native healthy tissue. Images are labeled by scaffold treatment group. Graph displays the percentage of inflammatory cells per total cells at the implant interface and reveals significant differences between groups, with –COOH and –OH modification groups having significantly fewer inflammatory cells at the interfaces (* represents significant from control group $P < 0.05$.)

2.4.4 Discussion

Several in vitro studies have shown that surface modification of biomaterial wettability and charge can affect protein adsorption, and thus inflammatory cell adherence [101, 102] and

subsequent interactions [46], with hydrophobic surfaces (PLGA) favoring macrophage adherence over hydrophilic surfaces (-COOH, -NH_2, -OH). Though many in vivo studies support alterations in inflammatory cell responses to model biomaterial surfaces [98, 103, 104], there are few investigations regarding surface modification of TE scaffolds [14]. In fact, some in vivo studies have shown that alterations in cytokine response between different polymer and surface chemistry groups are negligible [103-105], despite differences in number of recruited inflammatory cells. In vitro, we found that scaffold surface modification altered the responses of macrophages, especially regarding the chemotactic potential of cytokine products after adherence to the scaffold. Preconditioned media from these studies showed significant differences regarding their ability to recruit macrophages through chemotaxis, which is most likely linked to production of inflammatory cytokines by the adherent macrophages. This is presumably influenced by their interaction with control or modified biomaterial surfaces as is supported by previous studies which analyzed inflammatory proteins produced after macrophage adherence to surfaces with different chemical properties [81, 83]. As Study 2.3 and other studies suggest [46], the adherence of macrophages to a surface of a certain wettability does not directly correlate to protein synthesis by these adherent cells. Therefore, though the in vitro system can give indications of potential cell interactions in vivo, the observed in vivo responses may be quite different given the effects of macrophage soluble products on other aspects of the inflammatory response.

In examining the in vivo responses, we find the appearance of the interface between the biomaterial and the native tissue to be similar based on H&E staining at 2 weeks. However, closer inspection of the phenotype of recruited cells reveals that indeed the composition of inflammatory cells is quite different between treatment groups, suggesting that surface functionality does alter the cascade of inflammatory cell responses in vivo. Interestingly, the observed CD11b responses for the surface modified PLGA scaffolds closely approximate that of a previous investigation of surface modified microparticles implanted in the subcutaneous

compartment evaluated at the 2 week time point [59, 60]. Specifically, we find the density of $CD11b^+$ inflammatory cells to decrease in the following manner (control > NH_2 > OH > COOH). We have observed this phenomenon of altered CD11b+ cell percentages [59, 60], though a group using cage implants with different biomaterials showed no significance changes in cell percentages despite significantly different biomaterial properties [103]. This divergence may be due to material properties and the quantity of and accessibility of the functional groups.

Many previous studies have shown that hydrophobic surfaces in vivo elicit significant adsorption of serum proteins [104, 106], resulting in higher degrees of inflammatory cell infiltration [97], supporting the interactions observed in this study. The -NH_2 modified surface, having hydrophilic functionality and positive charge, has been shown to enhance protein adsorption and denaturation despite altered wettability and charge compared to untreated control [63, 107]. Denatured serum protein, specifically fibrinogen, has previously been linked with enhancing the infiltration of inflammatory cells to implantation site [63], as observed in this study. The –OH surface, having hydrophilic and anionic properties, have been shown in vivo to lead to coagulation, resulting in fibrin formation and platelet aggregation, thus facilitating complement activation and inflammatory cell chemotaxis [62, 94]. Interestingly, in studies which compared –OH verses –COOH functionality, a consistent trend of reduction in complement activation and subsequent inflammatory cell chemotaxis has been observed [95], in support of the further reduction in inflammatory cell density observed in this study. This may predominate due to repulsion or conformational changes in adsorbed protein from the negatively charged –COOH surface [98, 108]. Our next focus was to determine whether these alterations led to downstream influence over fibrotic responses to the scaffolds.

2.5 Host Response to Scaffold Implants at 6 Weeks

2.5.1 Purpose

Results have thus far shown that surface functionality affects macrophage behavior following adhesion to the scaffold in vitro, possibly altering cellular responses including

chemokine production in vivo. Differences observed in macrophage derived products which generated subsequent macrophage chemotaxis in vitro were similar to trends in infiltration of $CD11b^+$ cells to the implantation site of the scaffold in vivo after 2 weeks implantation. Since the $CD11b^+$ inflammatory cell responses are significantly different between scaffold modification conditions at week 2, this may lead to alterations in the downstream fibrotic responses with increasing implant duration.

Hypothesized models of biomaterial mediated fibrotic responses suggest that interactions between macrophages and fibroblasts in the granulation tissue surrounding implants fuel the development of the collagenous matrix [109, 110]. This matrix, comprised of disorganized bands of collagen, surrounds the implant, effectively walling the implant from the native tissue [111]. Our hypothesis is that the altered $CD11b^+$ cell responses at 2 weeks are a measure of the macrophage:fibroblast interactions that subsequently alter the development of fibrotic tissue around the scaffolds. Secondary to this hypothesis, alterations in fibrotic encapsulation may affect the infiltration of cells into the scaffold and mineralization within the scaffold. To further analyze these responses, surface modified scaffolds were implanted for 6 weeks.

2.5.2 Materials and Methods

2.5.2.1 Animal Implantation Model

Surface modified scaffolds from the previous studies were implanted using identical protocols in Balb/c mice and explanted after 6 weeks implantation.

2.5.2.2 Masson Trichrome Staining to Visualize Collagen Deposition

Collagen deposited around and inside surface modified scaffolds was visualized and quantified using Masson Trichrome staining (Sigma Aldrich, St. Louis, MO) and Image J. The thickness of the collagen layer around the implants was quantified by measuring collagen deposition from the scaffold through the interface to the native healthy tissue for each sample group (n=4). The densities of cells inside the scaffolds were quantified based on the number of

hematoxylin staining cells per scaffold cross-sectional area. Collagen deposition within the implants was quantified by measuring the area of blue collagen staining within the scaffold cross-section compared to the total area of collagen and scaffold cross-sectional area.

2.5.3 Results

2.5.3.1 Collagen Deposition in Surface Modified Scaffolds at Week 2

Prior to examining fibrotic responses at 6 weeks, week 2 implants were stained with Masson Trichrome to examine interface collagen deposition and matrix deposition inside the scaffold cross-section. For all scaffold treatment groups, minimal cell infiltration was observed beyond the extreme edge sections. As a result of poor cell infiltration, and thus lack of mineralization, at 2 weeks, cross-sections of this time point had severe loss of the interior of the scaffold in the section. Left in the cross-sections was only the thin layer of cell infiltrate from the skin side and muscle side of the subcutaneous implant, and the surrounding tissue. However, this did allow visualization of the initial stages of the fibrotic response at the interface. Masson Trichrome staining of the scaffold interfaces (Figure 2.10, reference H&E stains in Figure 2.8), showed only minor differences in the degree of collagen deposition with exception to control scaffolds, which had an histology consistent with granulation tissue of the late inflammatory phase. Control scaffolds therefore had an inconsistent distribution of collagen in the interface tissue compared with other groups and a slightly larger interface thickness. Otherwise, the appearance and thickness of the collagen stain in the interface was not drastically different between groups.

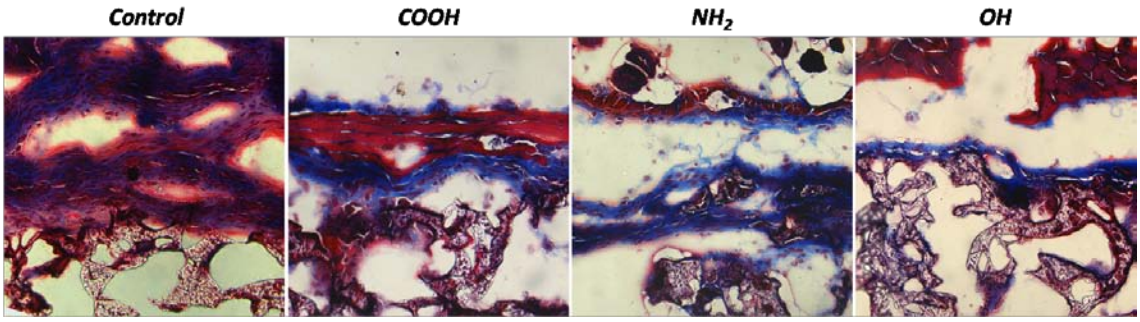

Figure 2.10 Collagen deposition at the interface of surface modified scaffolds after 2 weeks. Scaffold cross-sections were stained with Masson Trichrome to visual collagen. Surace modification groups label each image in the upper-left corner.

2.5.3.2 Collagen Deposition in Surface Modified Scaffolds at Week 6

The downstream fibrotic response was assessed at week 6. Similar to week 2 results, the thickness of the collagen interface does not appear to be drastically differ among treatment groups. However, in contrast to the appearance of the collagenous matrix at week 2, there are noticeable differences in the histology of the interface based on the surface modification group (Figure 2.11). First the organization of cells at the interface is not standard among functional groups. Both control and –COOH modified interfaces have a regular, somewhat uniform distribution of cells throughout the interface. In contrast to this trend, the $–NH_2$ interfaces have a lower cell frequency with a more prominent collagen stain, observed by the more prominent Methylene Blue uptake. Of interest, these areas of enhanced blue staining also form a continuous sheet, running the length of the interface. The –OH modified group has a higher density of cells inside the interface, though with a collagen staining similar to the control and –COOH groups, without the prominent Methylene Blue staining bands seen in the $–NH_2$ group. Quantification of the average thickness of the collagen layer at the interface, measuring from scaffold surface to native healthy tissue reveals only minor differences, with exception to –OF treatment.

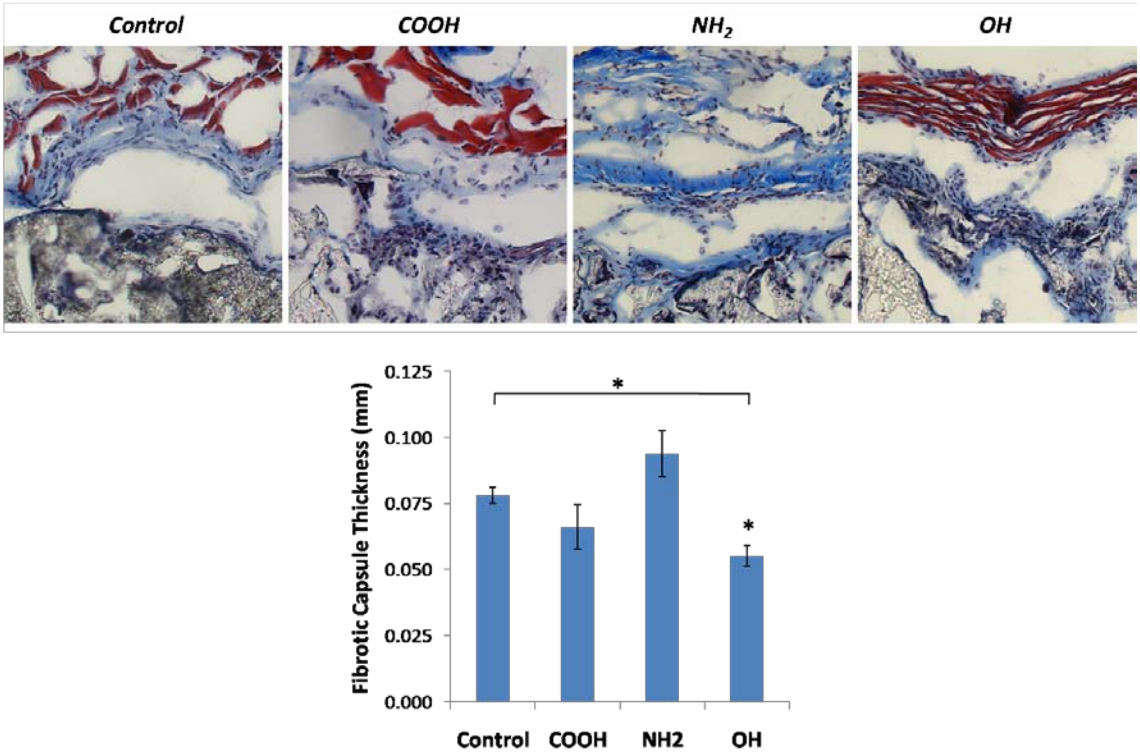

Figure 2.11 Collagen deposition 6 weeks after implantation. The degree of intensity of collagen staining at the interface appears different based on surface modification condition. Modification groups are labeled on the upper-left hand corner of each image taken at 20X magnification. The thickness of the collagenous interface was measure using Image J (n=4) and plotted. (ANOVA significant at $P<0.05$, (*) represents significant from control group $P<0.05$ by Dunnett comparison)

2.5.3.3 Cell Infiltration and Matrix Deposition at Week 6

Though our focus was to investigate the link between surface functionality and fibrotic outcomes, the intra-scaffold histology seen in Masson Trichrome staining revealed some interesting interactions with possible implications in the field of TE. Examination of the intra-scaffold regions of the tissue section revealed some interesting differences between modification groups, specifically related to the density of cells inside the scaffold and the degree of collagen deposition within the scaffold (Figure 2.12). Gross examination of the interior regions of the 5 x 5 x 5 mm cube scaffolds showed major differences the presence of cells and collagenous matrix. Control unmodified scaffolds had very little cell infiltration into the scaffold

interior, measuring about 1800 cells/mm^2. However, surface modification with $–NH_2$, -OH, or –COOH groups increased cell infiltration densities to greater than 3X the density of control scaffolds. Despite the similar intra-scaffold cell densities of the surface modified groups, the amount of collagen mineralization differed among modification groups, though all were significantly higher than unmodified scaffolds. Scaffolds surface modified with –COOH groups had the highest percentage of collagens staining, with about 75% of the scaffold:matrix area staining positive for collagen. Though $–NH_2$ modified scaffolds had the most prominent collagen staining at the interface, scaffold infiltration was still elevated with respect to control and accompanied by 60% collagen area percentages inside the scaffold. Hydroxyl modified scaffolds, which had a high density of cells at the interface observed in the gross histological examination, had a intra-scaffold density similar to $–NH_2$ modified scaffolds, and of modification groups had the lowest percentage of collagen inside the cross-section (50%).

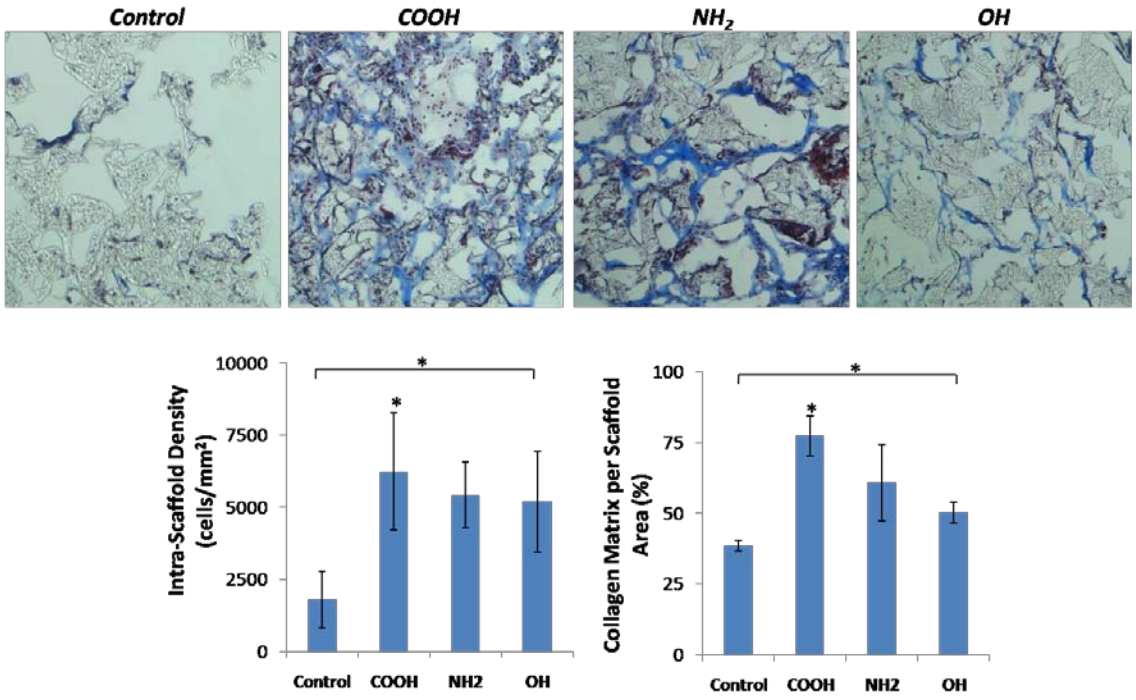

Figure 2.12 Collagen deposition inside the scaffold. Cell density was quantified via Hemotoxylin stained nuclei counts per scaffold cross-sectionl area and plotted. To quantify collagen deposition, the area of collagen per total scaffold and matrix area was quantified using Image J. (* with brackets represents significant ANOVA at P<0.05, (*) above groups represents significant from control group by Dunnett test, P<0.05.)

2.5.4 Discussion

As suggested in literature, most biomaterials adsorb proteins in vivo, which trigger activation of the foreign body response [14, 24, 60, 63]. This results in inflammatory cell infiltration to the implantation site, the formation of granulation tissue consisting of inflammatory cells and fibroblasts around the implant, followed by deposition of collagen around the implant. In this study, we investigated the effects of surface functionality in possibly altering this fibrotic process for a given biomaterial (PLGA porous scaffolds). Based on Masson Trichrome staining to detect collagen, we find that changing surface functionality leads to minor differences in collagen deposition at the biomaterial:tissue interface, similar to previous reports using a surface modified microparticle system in the same tissue compartment and time point [60, 63]. At 2 weeks after implantation, surface modification appeared to hasten the transition between

granulation tissue formation and fibrosis, initiating an interface which stained positive for collagen and had a thinner scaffold to healthy tissue measurement. In comparison, unmodified scaffolds had a disorganized development of collagen in the interface with a thicker interface. Though hydrophilicity has been linked to reduction in biomaterial-mediated fibrosis [14, 112], the speed of its development in the context of the biomaterial response has not been well addressed. However there are some known factors which may influence collagen maturation in the biomaterial mediated responses, specifically cell-mediated collagen breakdown, cytokine influences on collagen secretion and degradation, and vascularity of the region [15, 113]. As our in vitro studies have shown a chemokine influence, and preliminary in vivo protein content results suggest altered protein expression, these two factors may contribute to the altered state of collagen deposition at week 2. In addition, at week 2 we do not observe any alterations in vessel formation either intra-scaffold or in the interface region. Therefore, changes in vascularity may not be the primary contributor to these observations.

Given altered inflammatory cell responses at week 2 potential altered macrophage activation based on altered cytokine profiles, we expected a more measurable downstream influence on the fibrotic response. In addition, in vitro studies have also shown that in addition surface functionality influence on macrophages, surface functionality can also affect fibroblast responses related to collagen production [114]. In fact, many studies have shown surface functionality influences inflammatory responses with little effect on downstream fibrotic responses [59, 63, 98, 115]. As expected, surface functionality did lead to altered fibrotic responses at the interface. However, more predominant were the effects on intra-scaffold interactions, where surface modification increased the infiltration and collagen deposition inside the scaffold.

Several in vitro [116-118] and in vivo investigations [59, 60] have linked improved cell infiltration with hydrophilicity, supporting our finding that surface modification greatly increased the degree of cell infiltration into the scaffold at 6 weeks. However, the differences in collagen

deposition within the scaffold were not expected and may be related to the depth of functionalization. Due to limited investigations involving equivalent scaffold materials with different surface chemistries [14], previous observations of this phenomenon are extremely limited. However, some hypothesis to justify this response can be developed. Surface chemistry is known to effect protein adsorption; however, the depth functional monomer deposition was not quantitatively determined in these studies. However, qualitative assessment of functionality revealed some differences in the modification depth, of which -NH_2 modified scaffolds appeared to have uniform cross-sectional modification and -OH modified scaffolds having a surface corona modification as viewed from the cross-section. Modification throughout the scaffold in the -NH_2 modified scaffolds may have allowed for altered protein interactions throughout the porous structure, thereby effecting cellular responses related to collagen deposition. A study investigating polymer:fibrinogen blends showed that cell-mediated collagen production was greatly influenced by the fibrinogen content [119]. Fibrinogen is known to strongly interact and dentaure on -NH_2 surfaces, which may facilitate increased cell infiltration. Since –NH_2 modification had the highest power and functionalization depth, the increase in cell infiltration and collagen production may be linked to these processes. However, -COOH modification increased cell infiltration and intrascaffold collagen production, despite having different fibrinogen interactions. These findings seem to hint at a more complex interaction, for which in vivo literature is limited, and thus may necessitate additional studies understand these interactions.

Though surface modification literature on in vivo cell infiltration in porous scaffolds is limited, we and others have observed that cell infiltration in PLGA salt-leached scaffolds is minimal after 2 weeks implantation [44, 120, 121]. Despite surface modification, we find a similar result in this study 2 weeks after subcutaneous implantation. Previous studies have shown that by week 6, cells may begin to infiltrate the porous structure [120, 122]. We also find some degree of cell infiltration in unmodified PGLA scaffolds, though infiltration is greatly

enhanced with scaffold modification. In addition, we also observe a more prominent collagen deposition within surface modified scaffolds.

Our previous studies have linked fibrotic interactions with -OH and -NH_2, though these investigations were focused on capsular formation around the biomaterial. Therefore, the increased intra-scaffold collagen deposition observed in the -COOH functionalized scaffolds is somewhat surprising. Qualitatively, we were unable to visualize deep intra-scaffold functionalization with vinyl acetic acid monomer which was used to generate the -COOH functionality. Though –COOH modification seems to beneficially influence cell behaviors in vitro, literature supporting these influences in vivo is somewhat limited. Therefore, it is difficult to discern whether hydrophilic surface functionality, or cellular interactions with protein adsorbed to these different functionalities may be responsible for altered intra-scaffold responses.

2.6 Conclusions

In order to improve fibrotic responses, enhancing the porosity of the implant was thought to be a viable approach to reducing collagen buildup and contraction around the implants. In fact, many results subsequently supported this hypothesis. As discussed previously, surface functionality was shown to exert influence over inflammatory cell responses, and to some degree, fibrotic responses to non-porous biomaterials. Therefore, we sought to analyze whether the combination of biomaterial porosity and surface functionality could further improve fibrotic reactions. However, in terms of fibrotic reactions at the implant interface, these effects appeared minimal. In the following study, we therefore considered another approach to improving inflammatory and fibrotic reactions to TE scaffolds.

CHAPTER 3

THE INFLUENCE OF SDF-1α RELEASE ON INFLAMMATORY AND FIBROTIC RESPONSES TO PLGA SCAFFOLDS

3.1 Introduction

As previously discussed, despite considerable advancements in biomaterial synthesis and modification techniques, most TE scaffolds, both acellular and seeded, elicit fibrotic reactions resulting in encapsulation of the implant. Such fibrotic reactions often hinder the vascularization of scaffold implants which leads to a bare necrotic core in cell seeded constructs as shown in many recent publications [1, 29]. It is generally believed that controlled wound healing and angiogenesis are critical to the short-term survival/behavior and long-term functionality/integration of seeded cells [24]. For cells to survive in vivo, it has been estimated that cells must reside within 200μm of a capillary bed [22]. Indeed, many studies have shown that cells seeded below the scaffold exterior surface do not survive and require some degree of prevascularization in vitro to survive in vivo [23]. In a recent investigation, MSC seeded by various methods onto scaffolds implanted subcutaneously showed the majority of cells (~75% depending on seeding method) die within 2 weeks [21]. To improve cell survival and functionality, better approaches to reduce fibrotic tissue formation associated with biomaterial implants is urgently required.

To minimize fibrotic reactions to implants, the majority of the past and current research focuses on reducing cell:material interactions. However, the major drawback of this approach is that scaffold implants induce very little short term cell infiltration, resulting in cell buildup at the tissue:material interface, inducing a significant fibrotic response effectively walling off the biomaterial implant. Thus the ability to control the extent and duration of inflammatory response has emerged as a critical design parameter which may ultimately dictate the success of TE designs in vivo [25]. However, traditional anti-inflammatory treatments, such as the use of

Dex (Dexamethasone), may impair wound healing and tissue regeneration [123]. There is still a need for the development of novel treatment to reduce fibrotic reactions while to promote tissue regeneration and angiogenesis.

Due to their unique pluripotency and regenerative properties, stem cells have been intensively studied as powerful therapeutic tools for a variety of diseases and conditions. Recently, groups have focused on the beneficial effects of stem cell participation in inflammation, with mounting evidence supporting improved wound healing outcomes possibly through physical and paracrine influences [124]. Following induced injury, local delivery of stem cells has been shown to reduce inflammation, angiogenesis, and to improve function outcomes in many different models [125, 126]. However most of these models employ transplanted exogenous stem cells. These approaches are complicated by many limitations due to cell sources, expense to achieve sufficient cells for a dose response, xenogenic components necessary to expand the cells, control over the functionality and behavior of these cells, and potential host vs. graft responses. In addition, transplanted cultured and differentiated stem cells may not respond to the physiological microenvironmental stimuli like circulating stem cells [17]. Since stem cells are recruited to the injury sites to participate in wound healing and tissue regeneration, it is our belief that the complications associated with biomaterial scaffold implantation may be reduced or even eliminated if autologous stem cells are purposefully recruited to the tissue scaffold and implantation sites.

Recently, studies have uncovered that the implantation of foreign bodies, including biomaterials, may prompt the recruitment and local engraftment of autologous stem cells [109, 127, 128]. The recruitment of autologous stem cells may be substantially enhanced with localized release of stem cell chemokines. We are specifically interested in stromal derived factor-1 alpha (SDF-1α), since many prior publications have shown that SDF-1α is critical to hematopoietic stem cell (HSC), and possibly MSC migration, and can be used to target stem cells to a desired site within the body [129]. Coincidentally, SDF-1α is also involved in the

recruitment of inflammatory cells and other types of stem cells including tissue committed stem cells [130]. Based on these observations, we hypothesized that localized release of SDF-1α may facilitate the recruitment of autologous stem cells to TE scaffolds and subsequently enhance tissue regeneration.

To test the hypothesis, degradable scaffolds capable of locally releasing SDF-1α via physical adsorption (short term release) or osmotic pumps (long term release), were produced and then implanted in the subcutaneous space of mice. Our objectives were to (1) monitor the effects of SDF-1α on stem cell recruitment, (2) quantify the effects of increased host stem cell responses on the inflammatory response, and (3) examine long term effects on fibrotic and angiogenic processes on SDF-1α supplemented implants.

3.2 Methodology

Chemokine delivery can result in a multi-faceted outcome, upon which outcomes could be based on many known and unknown variables and interactions. Therefore, prior to experimentation, it is critically important to understand the known functions of the cytokine to be delivered, as well as many of the potential components for which interactions may occur in an manner for which interaction was not anticipated or interaction for which previous data is limiting. In this case, we are interested in testing the ability of SDF-1α to recruit MSC to the site of scaffold implantation in vivo, for which controversial data exists. However, SDF-1α has well established and understood interactions as a chemotaxin via its receptor CXCR4, which will be elaborated on in the subsequent section. However, expression of CXCR4 is abundant among the cells of the inflammatory and fibrotic responses. Therefore, throughout this chapter, hypothesized mechanism diagrams will be continually developed to attempt to quantify both hypothesized and potential unanticipated interactions of the chemokine during the context of the inflammatory and fibrotic responses.

3.3 SDF-1α Background

3.3.1 Structure, Properties, and Physiological Function during Homeostasis

SDF-1α (CXCL12) was first characterized for its growth stimulating properties to B cells. Subsequently, SDF-1α was identified as a chemoattractive cytokine with structural properties similar to large family of low molecular weight cytokines with chemotactic properties. It binds specifically only to the receptor CXCR4 [131], which is expressed on a number of different cell types including MSC [132]. In addition to its involvement in several differentiation pathways of differentiation and proliferation, SDF-1α is constitutively expressed in both lymphoid and non-lymphoid systems, unlike inflammatory chemokines in inflamed tissue [131]. This signaling axis has been found to be critical in hematopoiesis, including B cell development and HSC colonization of bone marrow [133]. In fact, antagonizing CXCR4 increases mobilization of HSC to the peripheral blood, suggesting a role for CXCL12 in retaining HSC [134, 135]. In fact, studies have shown that stromal cell production of SDF-1α along with HSC expression of CXCR4 is indeed critical to maintaining HSC in their niches. Based on this observation, it was additionally shown that SDF-1α supplementation can HSC mobilization to the peripheral blood [136].

3.3.2 Influence on Stem Cell Mobilization

Despite its physiological bone marrow retention function, SDF-1α has shown chemotactic potential for recruiting bone marrow derived cells to the periphery [137]. Recent studies have shown additional involvement in stem cell recruitment and retention, especially with proangiogenic HSC trapping and retention in the peripheral tissue [137]. This presumably occurs via VEGF upregulation, which increases SDF-1α expression in the peripheral tissue, where it is normally quiescent. In addition to HSC migration, several groups have shown that SDF-1α is able to induce MSC chemotaxis in vitro [138, 139], migrating at an optimal concentration of around 100ng/ml. In addition, in vivo studies have shown SDF-1α induced

chemotaxis of labeled MSC to the site of injury and engraftment into the damaged tissue [140, 141]. Some recent studies suggest that retention signal receptors expressed by stem cells such as cKit receptor, fibronectin and VCAM-1 may actually facilitate their residence at the injury site [137]. Surprisingly however, there still remains some controversy as to whether MSC can be recruited and maintained in the peripheral tissue via SDF-1α [142].

3.3.3 Influence on Inflammatory and Fibrotic Responses

Recent studies have demonstrated that the SDF-1α-CXCR4 axis is one of the principal regulators of stress-induced stem cell responses [143]. Studies have linked SDF-1α to the recruitment of EPC to the site of injury to control wound healing responses [144]. Previous studies with SDF-1α have noted synergistic relationships between SDF-1α and other cytokines [131]. Interestingly, part of this synergy appears in relationship between SDF-1α mechanisms of stem cell chemotaxis, and reliance upon VEGF, prominently expressed during states of inflammation [137]. In support of this, it has been recently shown that in the absence of injury, the addition of exogenous SDF-1α does not stimulate stem cell migration [145]. However, supplementation of SDF-1α was shown to enhance the formation of granulation tissue [146].

Due to the many recent studies showing anti-inflammatory effects and improved wound healing outcomes of MSC possibly related to cell:cell and paracrine interactions, we hypothesized that controlling the homing response of MSC could be used as a therapeutic agent to improve fibrotic outcomes related to biomaterial-mediated responses. MSC have been shown to home to injured tissues in vivo [140, 147], and there is evidence to support that SDF-1α may be critically involved in this process [129].

3.3.4 Hypothesized Interaction in the Context of Biomaterial Mediated Responses

Based upon this information, we have developed a hypothesis of interaction wherein SDF-1α locally release from tissue engineering scaffold may be able to facilitate improve host-derived MSC homing and retention. In addition to recruitment of proangiogenic HSC, we hypothesized that these interactions may facilitate influence over the foreign body response,

improving host-scaffold integration and limiting foreign body responses to the implanted scaffolds. As previously outlined, in the context of biomaterial-mediated foreign body responses, many inflammatory cells are recruited to the implantation site, subsequently functioning to decontaminate the area, phagocytise any foreign material, and set up granulation tissue to facilitate separation of the foreign body from the local tissue. The enhanced stem cell influence may be able to avert these responses by jumpstarting the wound healing process over the fibrotic process. Based on this hypothesis (Figure 3.1), we proceeded with an in vitro investigation of whether recruited MSC could be engrafted onto tissue engineering scaffolds.

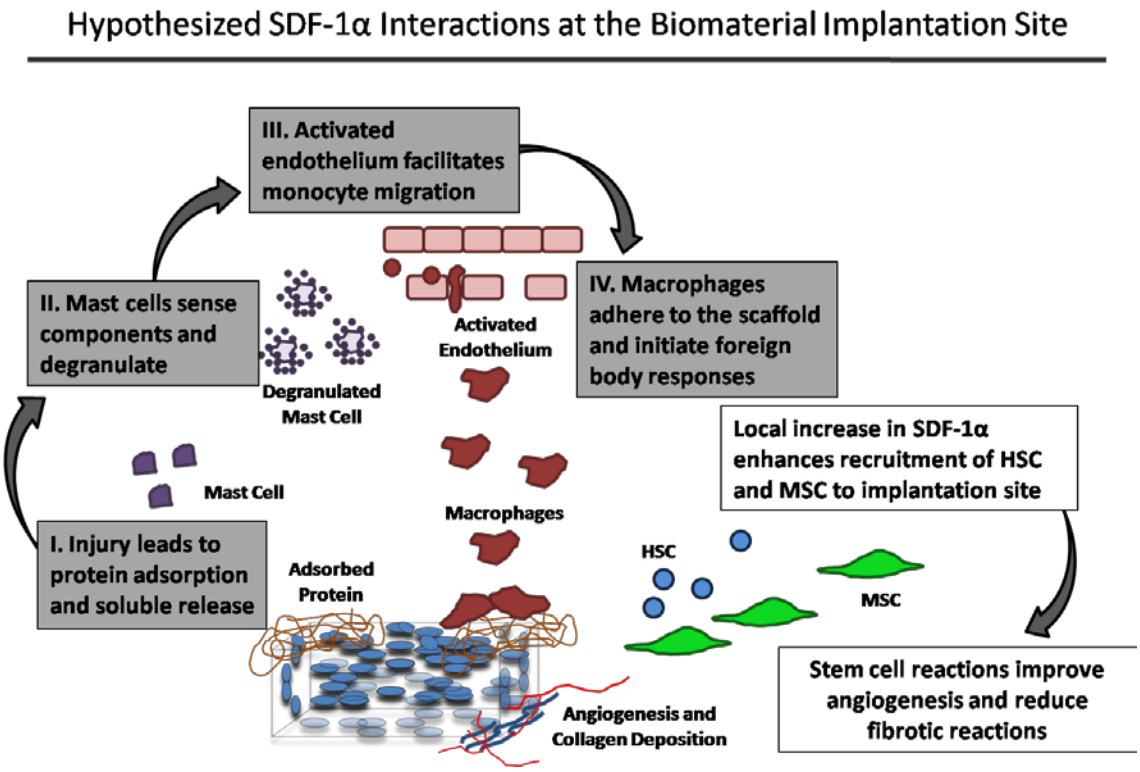

Figure 3.1 Hypothesized interactions of SDF-1α in biomaterial-mediated foreign body responses.

3.4 In Vitro Evaluation of SDF-1α Releasing PLGA Scaffold System to Induce MSC Chemotaxis and Engraftment

3.4.1 Purpose

Many previous studies have established that MSC contain the capacity to migrate along SDF-1α gradients. In addition, some in vivo studies have also implicated SDF-1α as being critical to MSC chemotaxis to sites of injury. Therefore, we believe that modulating SDF-1α at the site of scaffold implantation may increase the local recruitment of MSC which may alter inflammatory and fibrotic outcomes. However, we are interested in further augmenting this process to potentially address TE parameters, by having the MSC not only participate in the wound healing response, but also potentially engraft into the scaffold and differentiate into cells to regenerate damaged ECM. To investigate this possibility, we have designed in vitro experiments to verify whether migrating MSC will engraft into an SDF-1α source, in this case a porous PLGA scaffold adsorbed with SDF-1α placed in the lower chamber of Boyden chambers.

3.4.2 Materials and Methods

PLGA scaffolds used in this study were fabricated using protocols described in Chapter 2. To examine the site directed homing capability of the scaffold:SDF-1α system, a homing and engraftment transwell model was developed. Briefly, scaffolds were injected with 50 ul (approximate to the scaffold retention volume) of SDF-1α (Prospec-Tany TechnoGene, Rehovot, Israel) at 1 μg/mL or PBS (as control). Our preliminary studies have found that such methods provided the release of SDF-1α for approximately 5 days [80]. Scaffolds were then cut to fit beside transwell inserts (3 x 3 x 1 mm) in the lower chamber of 8μm pore membranes of 24-well plates (Corning Costar, Corning, NY). Primary murine bone marrow derived MSC were obtained as previously described [148, 149]. Briefly, the femur and tibia bone marrow of 6-8wk old Balb/c was flushed with DMEM containing 20% FBS and plated into 75cm^2 tissue culture flasks. Non-adherent cells were removed from the culture at day 3, with fresh media supplied at 50% with the remaining 50% conditioned media from which non-adherent cells were removed.

Media was continually renewed every 3 days with subculture upon confluence up to the fourth passage. At fourth passage, MSC were verified for phenotype by positive stain for SSEA-4 and negative expression of CD45 (Santa Cruz Biotech, Santa Cruz, CA). Prior to scaffold placement, bone marrow derived MSC were labeled with the cell tracer dye CDFA-SE (Invitrogen) and seeded onto transwell inserts. The MSC expansion media was removed and replaced with fresh media in the upper and lower chambers. SDF-1α was allowed to release from the scaffolds into the lower chamber, and the percentage of transmigrated MSC from top chamber to bottom chamber was quantified. Briefly membranes were scraped on the upper side to remove adherent cells, detached from insert, and H&E stained to visualize and quantify cell migration to the lower side of the membrane. To verify cell engraftment, scaffolds were removed from the bottom wells, fixed in cold methanol, and visualized via CFDA-SE staining as previously described [31].

3.4.3 Results

3.4.3.1 Mesenchymal Stem Cell Morphology and Expression

Bone marrow MSC were acquired and expanded in culture to fourth passage. The morphology of the cells was consistent with literature, with MSC adhering to tissue culture plastic and growing in colonies after subculture (Figure 3.2). MSC had a fibroblast-like morphology and routinely stained positive for CD90 and CD73 (Figure 3.2) and CD44 and CD105 (Figure 3.2), reaching a purity of approximately 95% at the time of experimentation. For transwell engraftment experiments, a model engraftment system was designed. MSC were allowed to migrate across transwell insert to the bottom surface of the membrane (Figure 3.2). The engraftment of CFDA-SE labeled cells was then monitored on the surface of the PLGA scaffold by observing tracer fluorescence.

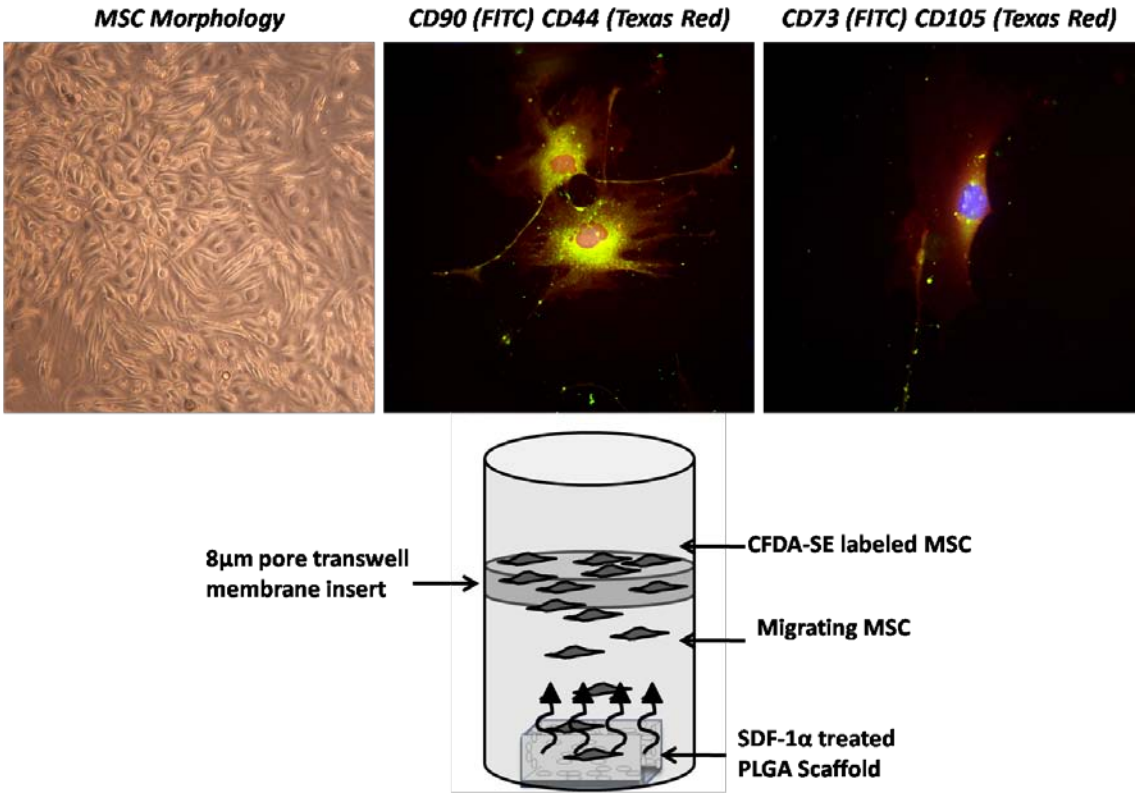

Figure 3.2 In vitro model of bone marrow-derived MSC chemotaxis and engraftment. MSC were purified from the bone marrow and imaged under phase contrast to observe a spindle shaped morphology. MSC expression was verified in vitro by examining of expression of MSC markers CD90 and CD44 and CD73 and CD105. Schematic model of in vitro chemotaxis and engraftment through utilization of a modified Boyden chamber assay.

3.4.3.2 SDF-1α Mediated Effects on MSC Chemotaxis and Engraftment

Using the transwell engraftment system, we monitored the effects of SDF-1α on inducing MSC migration. Placement of SDF-α treated scaffolds in the lower chamber led to MSC chemotaxis to the other side of the membranes (Figure 3.3). In addition, after 48hrs MSC labeled with CFDA-SE tracer dye were found engrafted onto the surface of the PLGA scaffolds treated with SDF-1α placed in the lower chamber (Figure 3.3). In quantifying chemotactic responses, we found a significant increase in the percentage of cells which crossed the transwell membrane in SDF-1α treated scaffolds compared with untreated scaffolds and media control. Refreshing media in the lower chamber at 24hr and 12hr intervals for 48hrs increased

the percentage of migrating MSC dependent upon how often the SDF-1α gradient was refreshed (Figure 3.3).

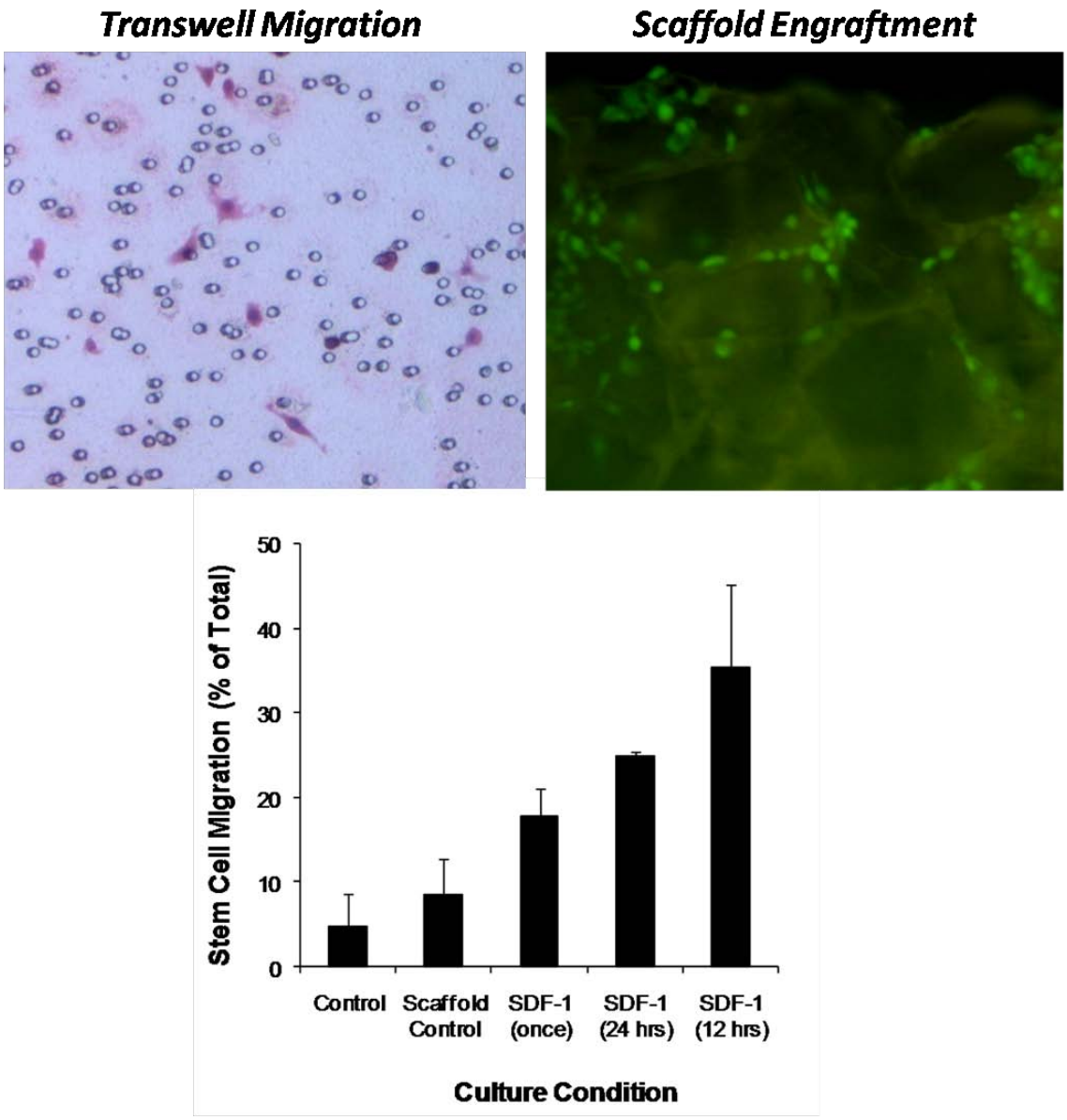

Figure 3.3 MSC homing and engraftment to SDF-1α and SDF-1α modified scaffolds in vitro. (A) After exposure to SDF-1α, MSC exhibited migration to the lower surface of the transwell inserts as verified by H&E staining. After extended culture periods, MSC migration and attachment could be observed on the PLGA scaffolds through staining of viable cells with CFDA-SE (B). Quantification of SDF-1α mediated migration was observed and quantified based on total migrated cells per cell input (C).

3.4.4 Discussion

As expected, SDF-1α was able to induce MSC chemotaxis in vitro, as shown in many previous investigations [138, 139], migrating at an optimal concentration of around 100ng/ml. Scaffolds in this study were filled with 100µl of SDF-1α (1µg/ml) and placed into the lower chamber. This configuration would have put the concentration of SDF-1α near this optimal value. Transwells which were not disturbed for quantification began to show CFDA-SE positive stained cells after 24hrs. These cells attached to the surface of the PLGA scaffold and assumed a fibroblast-like adherent morphology on the scaffold. Though this model provides a unique approach to this concept, prior studies have shown that SDF-1α induced chemotaxis of labeled MSC to the site of injury and engraftment into the damaged tissue [140, 141]. This supports our in vitro finding, which shows that MSC where able to transverse the polycarbonate membrane and engraft to the SDF-1α source scaffold. We next set out to determine whether this process could be replicated in vivo.

3.5 Influence of Short Term Scaffold Treatment with SDF-1α on MSC Responses In Vivo

3.5.1 Purpose

Having established that SDF-1α-mediated MSC recruitment also demonstrates potential for MSC engraftment into the scaffold, we next sought to examine whether scaffold treatment with SDF-1α could improve the mobilization and engraftment of MSC at the scaffold implantation site. We first examined whether, following scaffold implantation, culture-expanded MSC supplemented into the peritoneal space could migrate and preferentially engraft to SDF-1α treated scaffolds. We next examined whether SDF-1α treated scaffolds could improve MSC responses over the course of the inflammatory response up to 2 weeks. Additionally, the infiltration of HSC to the implantation site was also monitored.

3.5.2 Materials and Methods

3.5.2.1 Animal Implantation Model

Scaffolds were implanted in the subcutaneous cavity of Balb/C mice as established in early studies [40]. Scaffolds were implanted as described in the previous chapter with exception to implant treatment group configurations in each treatment animal. Control PLGA scaffolds were implanted to one side of the incision and tucked subcutaneous away from the incision. For short term study, the scaffolds were injected with 50 µL (approximate to the scaffold retention volume) of SDF-1α at 1 µg/mL or PBS (as control). Implants were recovered and processed as outline in the previous chapter.

3.5.2.2 Assessment of Supplemented MSC Migration to SDF-1α Treated Scaffolds

The engraftment of MSC from the blood was quantified using an in vivo model of stem cell mobilization. Briefly, Balb/c mice were implanted with either control or SDF-1α supplemented scaffolds using procedures described previously. To minimize interference from the incision site and maximize the distance between scaffold treatment groups, scaffolds were placed vertical along the back of the mice opposite to the incision site on the opposite side of the mouse. The configuration of implants with respect to upper verses lower position on the back was randomized to account for the effects of implant placement. Bone marrow-derived MSC were recovered from Balb/c mice and purified using plastic adhesion and verified for MSC expression as outline for in vitro transwell studies. Cells were loaded with Xsite 761 (Carestream Health, New Haven CT) at a concentration of 2µM for a period of 3hrs. After detaching MSC, uptake was assessed by NIR fluorescence intensity (excitation-761nm emission-789nm) using Kodak FX Pro imaging system (Carestream). After implantation for 2 days, a 100µL PBS solution containing 1 x 10^6 bone marrow-derived MSC was injected into the peritoneal space. The location of MSC cells in relation to implanted scaffolds was monitored and fluorescent intensity measurements taken over the region of interest daily until signal subsided.

3.5.2.3 Assessment of Host-Derived MSC and HSC Localization at the Implantation Site

Stem cell engraftment was monitored in implant cross-sections using immunofluorescence. All antibodies employed in this study were purchased from Santa Cruz Biotech (Santa Cruz, CA) with staining protocols as specified by the manufacturer. Specifically, $SSEA4^{+}/CD45^{-}$ [150] was used to identify MSC. HSC were detected by expression of the HSC markers c-kit, CD34, or Sca-1. Secondary antibody labeling for immunfluorescence was performed as described in the previous chapter. Cell densities and percentages were quantified per total interface DAPI cells as described in the previous chapter. After cell morphology for positive staining cells was established, merged DAPI layers were shielded to increase cell visibility in immunofluorescence images. Measurement of cell density were collected from the average of multiple counts taken from the scaffold interface over the center of the scaffold on the skin side of the biomaterial interface for each sample (n=4). For these calculations, density was measured in a representative area of the capsule extending from biomaterial to native healthy tissue with the area held constant for all treatment group quantifications.

3.5.2.3 Differentiation of Implant Derived Stem Cells

MSC were recovered using a subcutaneous wound chamber system, and cultured as previously described [151]. Briefly, the biomaterial wound chamber system consisted of PLGA conduits fabricated by dip-coating PLGA in 1,4-dioxane (7.5% w/v) onto Teflon rods. Coated rods (1.5cm long, and 3mm inner diameter) were then frozen in liquid nitrogen and solvent extracted by freeze drying. Conduits were sterilized and implanted subcutaneously as described for PLGA films. After 1 week implantation, Balb/c mice were anesthetized and conduits were flushed aseptically with PBS to recover cells inside the conduits. The exudate was centrifuged to obtain cells and recovered cells cultured in DMEM containing 20% FBS. Non-adherent cells were removed after 48hrs and media replaced subsequently every third day. Cells were detached using a cell scraper and replated into new $75cm^2$ flasks weekly for 4 weeks prior to

verification of phenotype by immunofluorescent staining of cells adhered to coverslips. Expression was verified for CD44, CD73, CD90, and CD105 for seeded coverslips.

After verifying expression, cells were prepared for differentiation studies. All basal media consisted of DMEM supplemented with 10% FBS. To induce osteogenic differentiation [152], cells where cultured for 2 weeks in media containing 10^{-8} M Dex, 0.2mM ascorbic acid, and 10mM β-glycerol phosphate (Sigma Aldrich, St. Louis, MO). Osteogenic differentiation was assessed by mineral deposition using Alizarin Red staining (Sigma Aldrich, St. Louis, MO). Adipogenic differentiation [153, 154] was induced by incubation in media consisting of 100nM IGF-1, 1 μM Dex, 0.5mM isobutylmethylxanthine, and 200 μM indomethacin (Sigma Aldrich, St. Louis, MO). Adipogenic differentiation was assessed by Oil Red O (Sigma Aldrich, St. Louis, MO) staining after 2 weeks of culture. Finally, chondrogenic differentiation was induced by centrifuging MSC to a pellet, and culturing the pellet in media consisting of 10nM Dex, 10ng/mL of TGF-β1 and 100ng/mL IGF-1 (Prospec-Tany TechnoGene, Rehovot, Israel) for 2 weeks [155, 156]. After differentiation, cultures were examined for chondrocytes using Alcian Blue (Sigma Aldrich, St. Louis, MO).

3.5.3 Results

3.5.3.1 Differentiation of Host-Derived MSC Recruited to Implantation Sites

To verify the pluripotency of recruited mesenchymal stem cells, a biomaterial wound chamber model was used to recover these cells in vivo. After purifying through culture and verifying that a portion of the cell population had an MSC phenotype, the cells were induced to differentiate into different mesenchymal lineages. Under phase contrast, adherent cells contained a mixture of spindle-shaped cells growing in a non-colonial fashion and a separate smaller population of cells which also maintained a spindle shaped yet proliferated in colonies (Figure 3.4). Cells from this population placed in the appropriate differentiation media, deposited Ca containing minerals which stained positive with Alizarin Red indicating

osteoblasts, formed intracellular oil droplets consistent with adipocytes, and altered to GAG producing chondrocytes which stained positive with Alcian Blue.

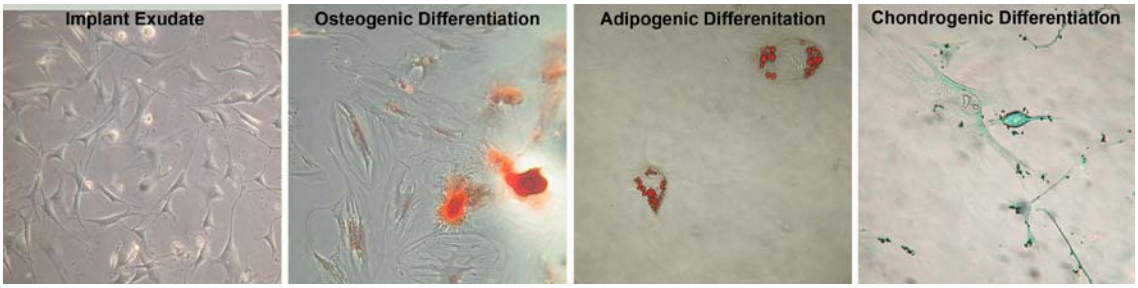

Figure 3.4 Pluripotency of implant recruited MSC following biomaterial implantation. Cells recovered from the biomaterial implant and purified through plastic adherence (far left) contained pluripotent cell populations. These cells could be differentiated in osteoblasts (Alizarin Red – second from the left), adipocytes (Oil Red O – third from the left), and chondrocytes (Alcian Blue – fourth from the left).

3.5.3.2 Homing of Intraperitoneally Injected MSC to SDF-1α Treated Scaffolds

In order to establish whether SDF-1α release was effective at mobilizing MSC from the circulation, an in vivo imaging experiment with NIR labeled MSC was performed. Imaging 24hrs after injection showed faint signal dispersed throughout the peritoneal space with some fluorescent signal near the SDF-1α treated scaffold. No fluorescent signal was observed near control scaffolds at 24hrs. At 48hrs after peritoneal injection (3 days implantation), the faint fluorescent signal in the peritoneal space had subsided while SDF-1α supplemented scaffolds were able to attract and engraft supplemented MSC based on co-localization of NIR fluorescent signal over the region of scaffold implantation (Figure 3.5). In contrast, no fluorescent signal was detected near the untreated PLGA scaffold.

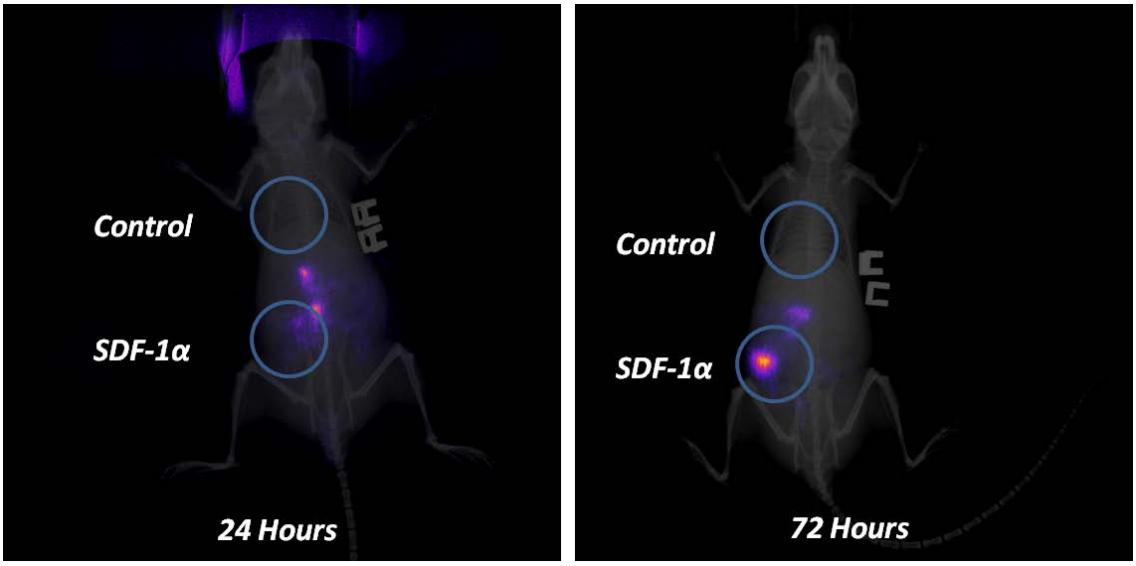

Figure 3.5 Preferential migration of bone marrow derived MSC to SDF-1α treated scaffolds. Control unmodified or SDF-1α soaked scaffolds were implanted into the subcutaneous space for 2 days. Xsite-761 labeled MSC where then injected and found to preferentially localize at the SDF-1α treated scaffold by 24hrs with maximal accumulation at 72hrs as imaged for the NIR probe with Fx Pro.

3.5.3.1 Expression of SDF-1α in Tissue Surrounding Scaffold Implants

To verify bioactive local release of SDF-1α, implant cross-sections were stained using monoclonal antibody to CXCL12 (Figure 3.6). Peroxidase staining shows a more prominent distribution of SDF-1α at the interface surrounding treated implants compared to untreated controls. Interestingly, as opposed to an even distribution of SDF-1α in the interface as expected, SDF-1α appears to be predominantly cell-associated in both control and treated scaffolds. However, the density of these SDF-1α producing cells appears qualitatively to be more prominent in the SDF-1α treated scaffold group.

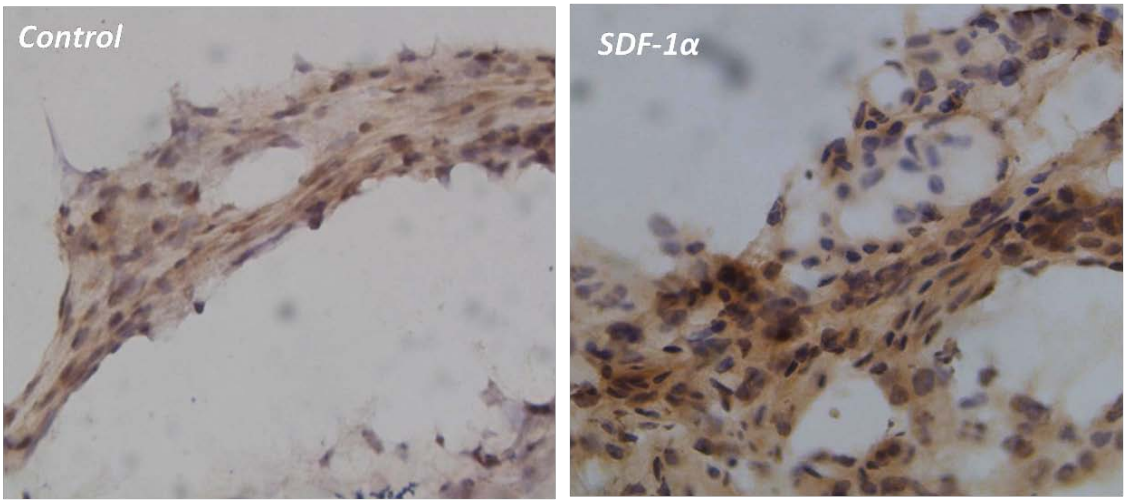

Figure 3.6 SDF-1α (CXCL12) distribution in the matrix surrounding scaffold implants. The distribution of SDF-1α was assessed by peroxidase staining with monocloncal antibody to mouse CXCL12. The distribution of SDF-1α expression appears more predominant in SDF-1α treated scaffolds.

3.5.3.3 SDF-1α Effects on Recruitment of Host Derived MSC to Scaffold Implantation Sites

We next sought to determine whether scaffold treatment with SDF-1α could result in measurable alterations in the stem cell response to subcutaneous implant scaffolds. We find that biomaterial-mediated inflammatory responses stimulate the recruitment of bone marrow derived MSC, staining positive for SSEA-4 (FITC) and negative (Texas Red) in Figure 3.7. After implantation for one week, control scaffolds (Figure 3.7) were found to have attracted substantially less MSC compared with SDF-1α soaked scaffolds (Figure 3.7). Specifically, the density of MSC surrounding SDF-1α soaked scaffolds is about 3 times higher than those associated with control scaffolds at both 3-day and 7-day time points (Figure 3.8). In addition to an increase in interface density, we also find enhanced (2-fold increase) density of MSC within the matrix of SDF-1α soaked scaffold compared with control scaffolds at day 7 (Figure 3.8).

Since SDF-1α treatment improved MSC responses, and given precedent for SDF-1α mediated HSC chemotactic responses, we quantified the time-scale recruitment of c-kit$^+$ HSC to the site of scaffold implantation using fluorescent IHC. Consistent with MSC responses, we observe a progressive increase in c-kit$^+$ cell density over the course of the implantation study

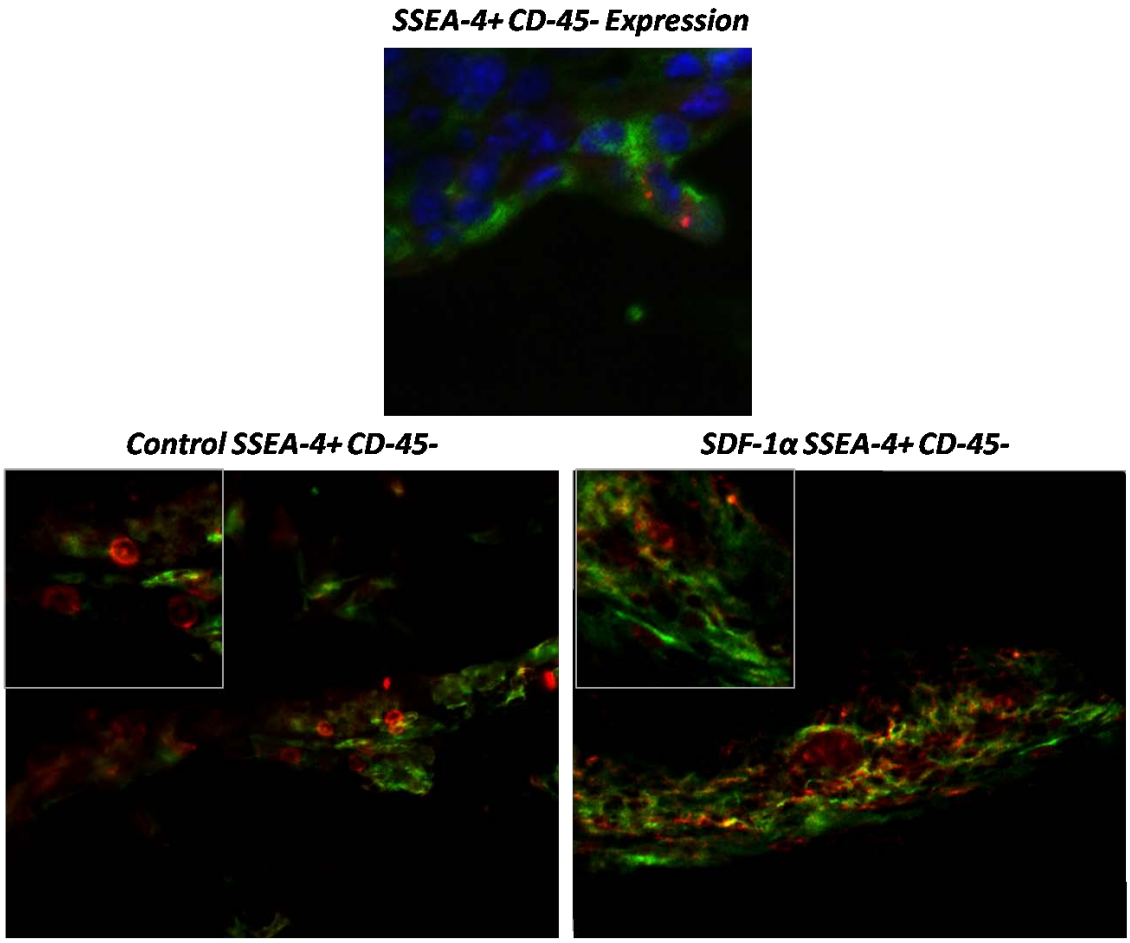

Figure 3.7 Visualization of MSC recruited to the interface of SDF-1α treated and untreated scaffolds. The cell based expression of an SSEA-4^{+} CD45^{-} phenotype was verified by overlapping first with DAPI. Scaffold interfaces of control and SDF-1α treated scaffolds were then examined for the presence of cells having this expression and morphology. (SSEA-4 conjugated to FITC (green) and CD45 conjugated to Texas Red (red).

(Figure 3.9 & 3.9). Quantification of these responses on basis of cell density reveals significant increase at time points of 3 days and 7 days compared to unmodified scaffolds (Figure 3.10). To further investigate this response, we quantified the density of other common markers used to identify HSC, namely CD34 and Sca-1, between SDF-1α treatment and control groups. In accordance with c-kit results, we observe a significant week 1 increase in the density of both CD34 and Sca-1 positive cells with respect to control. Quantification reveals a greater than 2-fold increase consistent with c-kit^{+} cells at the same time point (Figure 3.10).

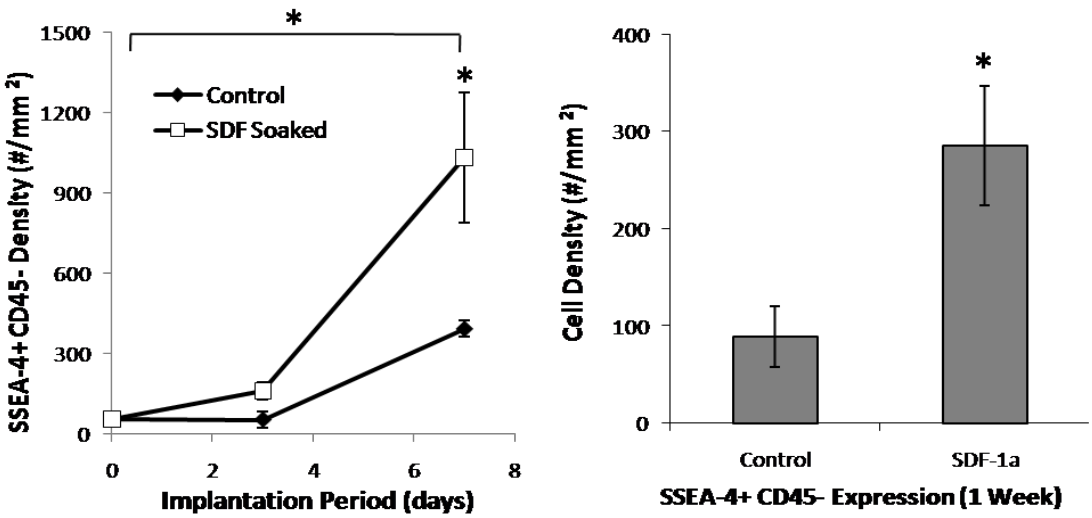

Figure 3.8 Density and kinetics of MSC recruited to the scaffold implantation site. (A) The density of MSC was determined in normal skin tissue, and then quantified at the scaffold interfaces at Day 3 and Day 7 and analyzed for treatment effects (Two-way Repeated Measures ANOVA, bracket and * indicates significant treatment effect $P<0.05$, * above data point represents significance by Bonferroni test $P<0.05$). (B) The MSC intra-scaffold density was also compared after 1 week showing enhanced MSC infiltration (Student t-test, * represents significance at $P<0.05$).

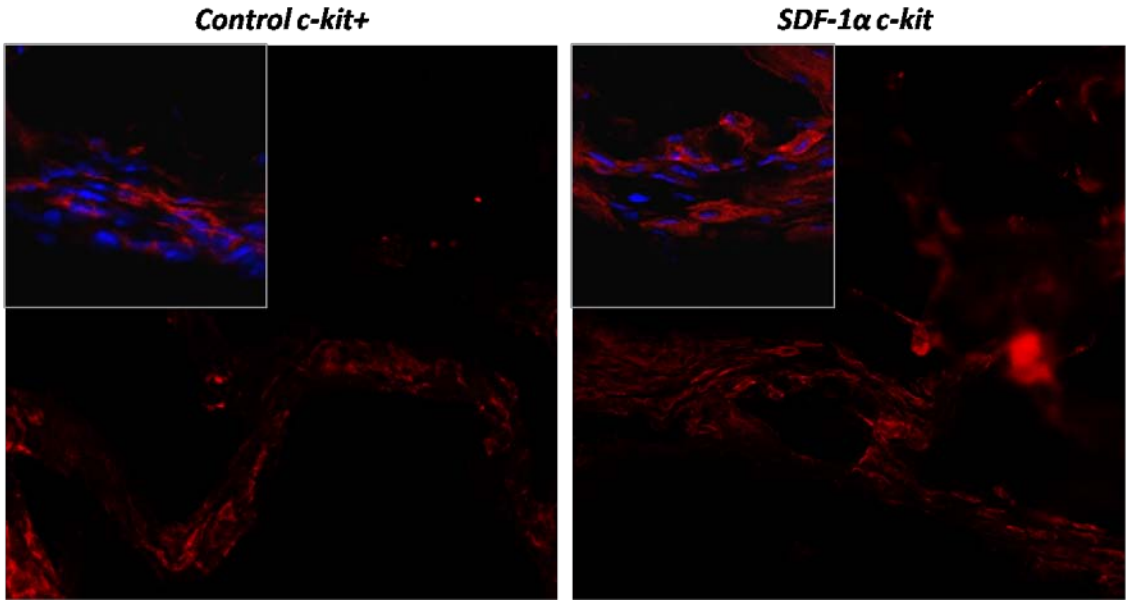

Figure 3.9 HSC recruitment to the biomaterial interface in SDF-1α treated scaffolds. HSC recruitment was visualized through through staining for c-kit. The total cell density was visualized using DAPI staining. Control implants (A) appear to have a lower degree of HSC recruitment after 1 week compared to SDF-1α treated scaffolds (B).

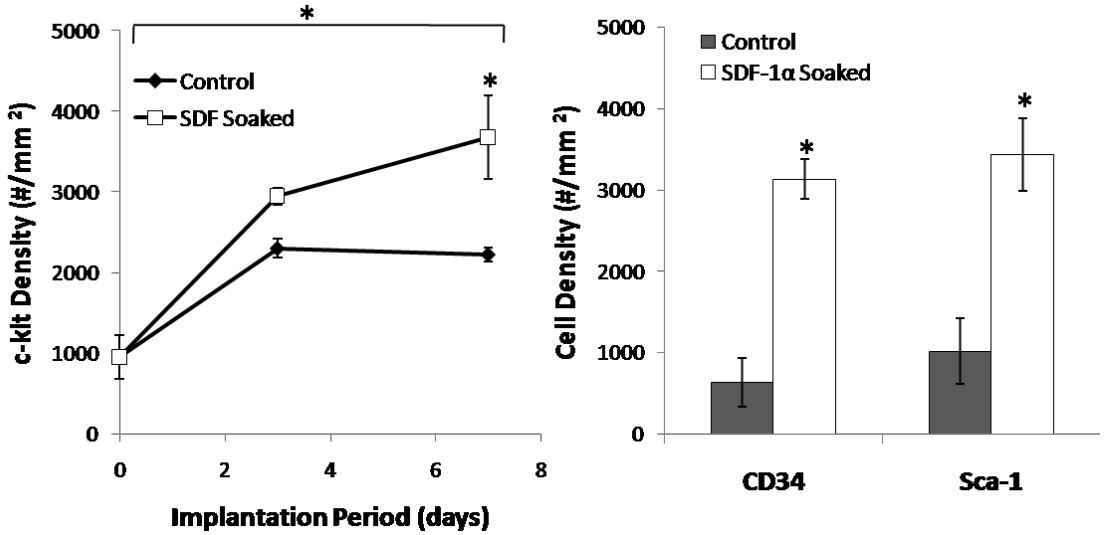

Figure 3.10 Recruitment density of HSC at the scaffold interface. The density of c-kit^{+} cells was quantified in normal control skin and compared between implants at 3 and 7 days, revealing significantly higher c-kit cells in SDF-1α treatment group (Two-way Repeated Measures ANOVA, bracket and * indicates significant treatment effect $P<0.05$, * above data point represents significance by Bonferroni test $P<0.05$). HSC where also assessed with other common markers with similar inter-group significance for CD34 and Sca-1.

3.5.4 Discussion

In this study we investigated whether host derived stem cells could be triggered to home and engraft to scaffold implants through treatment with a stem cell chemokine, SDF-1α. Although SDF-1α has shown stem cell chemotactic properties in vitro [129], it has remained controversial as to whether MSC migration in response to SDF-1α supplementation could be achieved in vivo [142]. To test our hypothesis, two different strategies were employed in PLGA scaffolds with physical adsorption of SDF-1α for short term release. The first was to monitor the migration of murine MSC injected into the peritoneum to an SDF-1α scaffold source. The second was to monitor MSC density at the implantation site over a 1 week course. In support of our assumption, SDF-1α was found to substantially increase the number of MSC (SSEA-4^+/$CD45^-$) at the implantation site of PLGA scaffolds over the course of the inflammatory response. Surprisingly at 2 weeks, beyond short term release by physical adsorption, we find the MSC density in treatment verse control group scaffolds to be roughly equivalent. Interestingly, we also find an increase in SDF-1α producing cells early in the inflammatory response. The additional host cell mediated production of SDF-1α may be magnifying the effects of the initial treatment. Cellular production of SDF-1α during the inflammatory response has been linked to a number of potential cells including epithelial cells, endothelial cells, pericytes, dendritic cells, fibroblasts, and myofibroblasts [144], in addition to stromal progenitor cells [146]. The reduced number of SDF-1α producing cells in the control at Day 3 may indicate the initial sign of an altered response occurring at the implant interface.

In addition to enhanced MSC recruitment, we also observed increased HSC (c-kit^+, $CD34^+$, and Sca-1^+) recruitment to SDF-1α soaked implants. HSC, along with MSC, express the receptor CXCR4 [129, 130] and are held in the bone marrow through CXCL12-CXCR4 interactions [157]. The gradients of exogenous SDF-1α can lead to the stem cell mobilization and homing [157, 158]. Some recent studies suggest that retention signal receptors expressed

by stem cells such as cKit receptor, fibronectin and VCAM-1 may actually facilitate their residence at the injury site [137].

Recently, it was shown that in the absence of injury, the addition of exogenous SDF-1α does not stimulate stem cell migration [145]. In fact, it appears that VEGF and possibly other inflammatory factors may be interrelated to SDF-1α mediated responses and therefore be required to facilitate homing and retention of recruited stem cells in the peripheral tissue [137, 159]. Therefore, the inflammatory stimuli due to scaffold implantation in combination with SDF-1α is likely the factor leading to increases beyond those stem cells normally recruited to participate in healing. To quantify these influences, we first set out to examine how SDF-1α and stem cell responses may be affecting the inflammatory response.

3.6 The Effects of Improved MSC Responses on the Inflammatory Response to PLGA Scaffolds

3.6.1 Purpose

Due to its role as a model FDA approved biomaterial and commonplace in academic studies, the host response to PLGA has been well characterized [44, 121, 160]. Given the increase in MSC and HSC responses and data suggesting their presence can influence inflammatory responses [161-164], we sought to analyze the histology of the implant interface to observe these outcomes. The drastic differences in stem cell responses after 1 week of implantation led us to begin investigating the gross response and specific inflammatory cell response at this time point. Our hypothesis, based on previous reports [12, 161, 162], is that the increase in MSC would have an influence over the composition and density of inflammatory cells at the scaffold interface. In the host inflammatory response to PLGA scaffolds, a significant accumulation of inflammatory cells is to be expected [44, 80, 121], though increased MSC influence prior to and at the 1 week time point may have altered these responses.

3.6.2 Materials and Methods

3.6.2.1 Histological and Immunohistochemical Evaluation of Scaffolds

Implants from the previous study were cryosectioned and analyzed using histology and immunohistochemistry. H&E staining (Sigma Aldrich, St. Louis, MO) was used to identify cell and matrix characteristics of scaffold interface. Toluidine Blue staining was used to visualize mast cells. CD11b (Santa Cruz Biotech, Santa Cruz, CA), neutrophil antibody, and MOMA-2 (AbD Serotec Raleigh, NC) staining was used to identify inflammatory cells (neutrophils, macrophages, and dendritic cells) and macrophages respectively. Collagen I antibody was used to visualize collagen I after visualizing total collagen with Masson Trichrome staining. Thickness of inflammatory cell infiltrate was measure from implant to native healthy tissue on the skin side of the subcutaneous implant. Cell density at the interface was quantified as described in the previous chapter. For mast cell quantification, mast cells were considered degranulated based on the presence of extracellular granules with diminished stain intensity.

3.6.3 Results

3.6.3.1 Effects of SDF-1α-mediated Stem Cells Response on Mast Cell Responses

We next sought to examine whether these interactions had measurable effects on the inflammatory response. Given that our current understanding of the mechanism of foreign body reactions suggests that mast cell activation and its products effect the initial recruitment of inflammatory cells, it is possible that SDF-1α release may also affect mast cell reactions. To test the hypothesis, the densities of mast cells surrounding both scaffold groups were examined. As expected, control scaffolds prompted the recruitment and degranulation of large numbers of mast cells (Figure 3.11 top row), especially over the course of the acute inflammatory response at 3-7 days. In contrast, we found that SDF-1α soaked scaffolds elicited substantially less accumulation of mast cells (mostly non-activated) compared with controls (Figure 3.11 bottom row). Quantification of density in the reaction tissue reveals a 62% and 75% reduction in mast cell density around the treated implants at Day 3 and Day 7 (Figure 3.11, bars

and asterisks Student t-test $P<0.05$ between treatment groups), respectively. By Day 14, we observe a similar number of mast cells in the region surrounding the scaffolds. After 5 weeks, control scaffolds are surrounding by a prominent layer of mast cells comprising a thickened matrix surrounding these scaffolds (Figure 3.12). SDF-1α treated scaffolds have a much thinner interface matrix with fewer mast cells surrounding the implant. Mast cells around control implants still have a degranulated morphology while mast cells in SDF-1α treated scaffolds have normal, unactivated mast cell morphology. In addition, mast cells infiltrated inside control scaffolds also have a degranulated morphology while treatment group has fewer infiltrating mast cells.

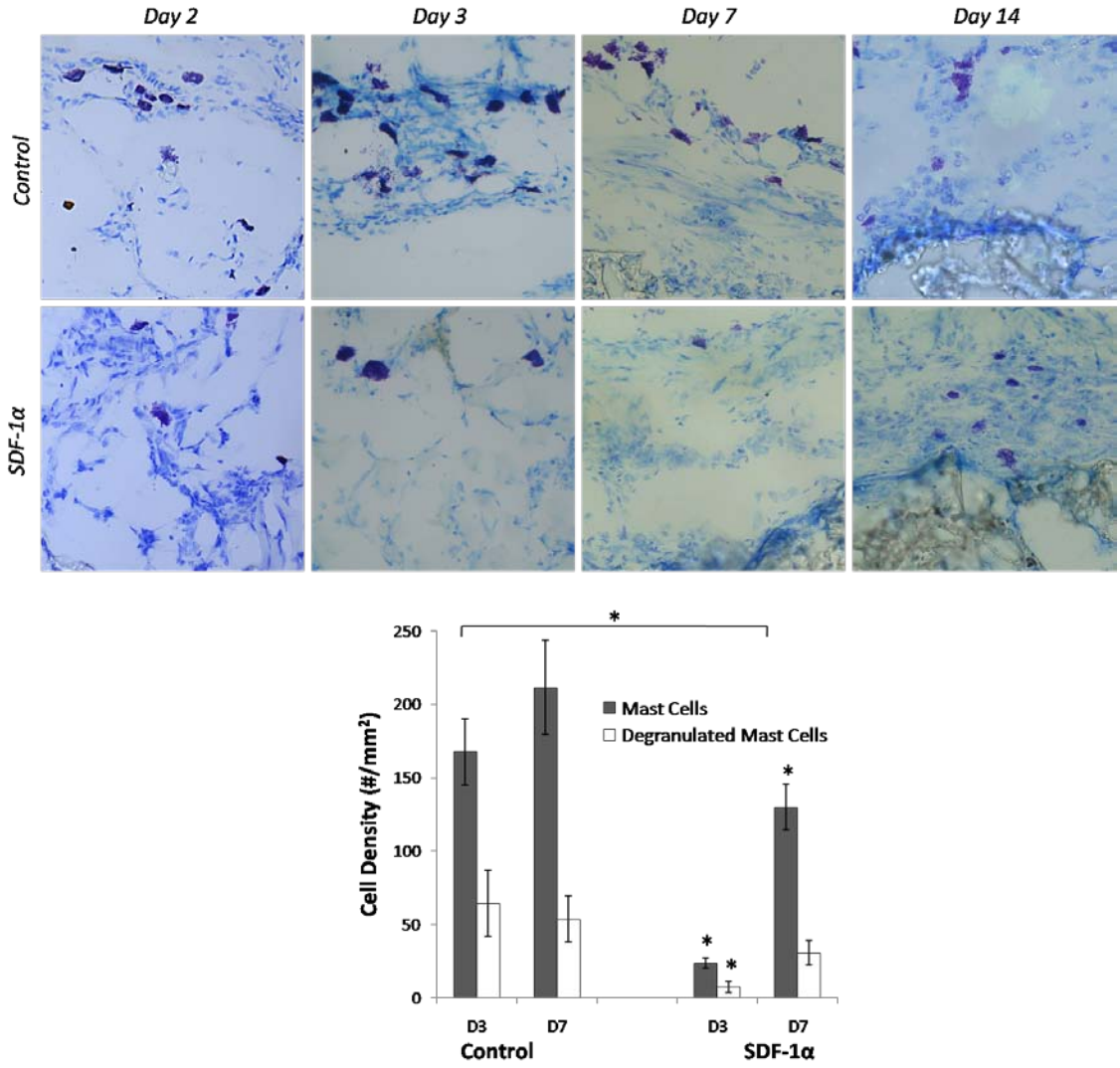

Figure 3.11 Mast cell behavior in the inflammatory response to SDF-1α treated scaffolds. The mast cell response was observed using Toluidine Blue staining. At each time point examined over the course of the first week, fewer total mast cells were observed in SDF-1α treatment groups accompanied by fewer degranulated mast cells. These responses appear to stabilize 14 days after implantation. Quantification total mast cell density and degranulated mast cell density reveals significant differences among treatment group (Two-way Repeated Measures ANOVA, bracket and * indicates significant treatment effect $P<0.05$, * above data point represents significance by Bonferroni test $P<0.05$).

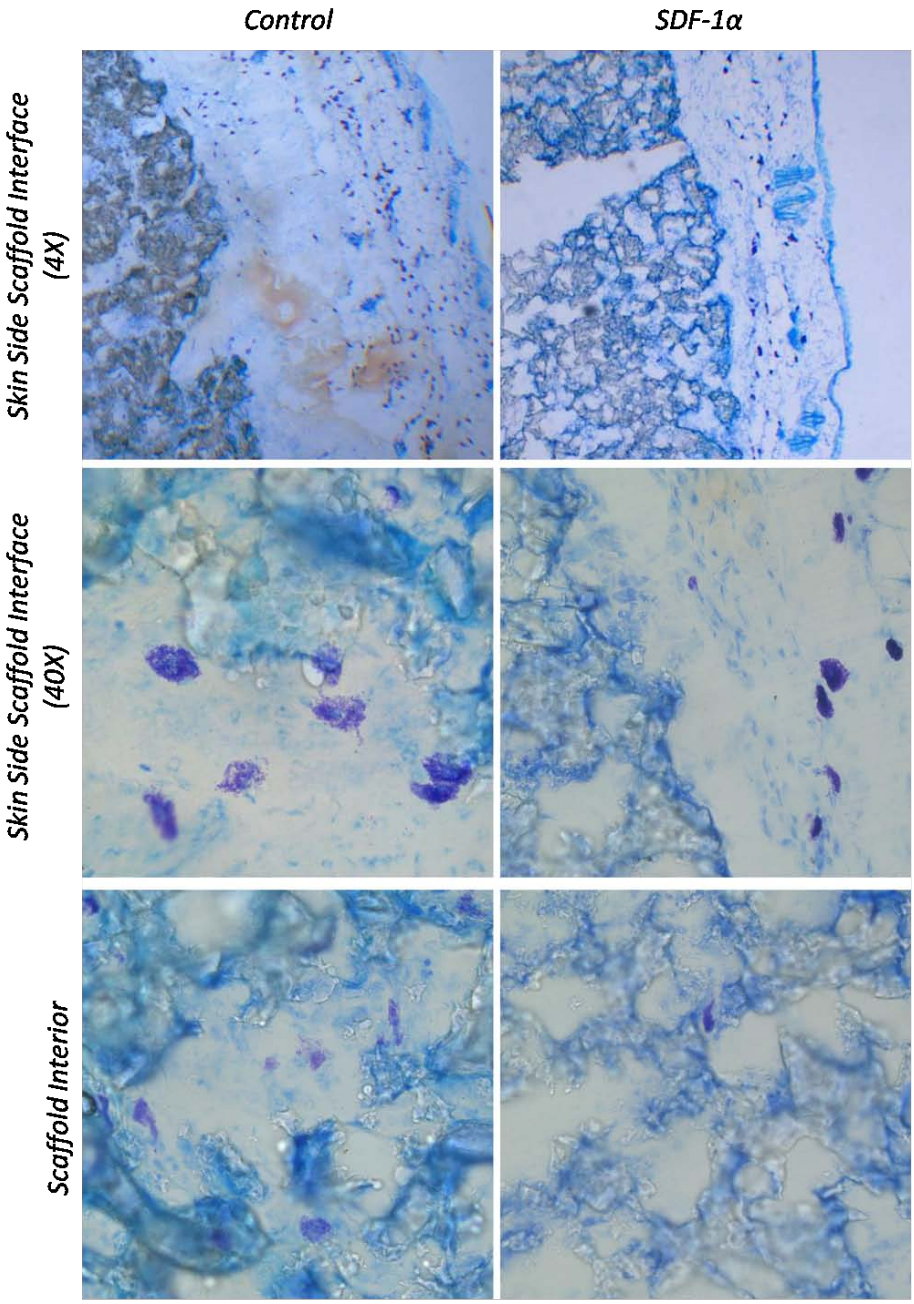

Figure 3.12 SDF-1α alters downstream mast cell responses. The mast cell response was also examined after 5 weeks implantation. Control scaffolds have a prominent thickening of the interface characterized by a prominent layer of mast cells outside the capsular region, in contrast to SDF-1α having a thinner interface a decrease mast cell density. Interfaces of control implants still contain degranulating mast cells while treatment interfaces have stable mast cells at the interface. In addition, degranulated mast cells are observed within the scaffold cross-sections of control scaffolds while intra-scaffold mast cells are less prominent in treatment group.

3.6.3.2 Effects on Macrophage and Neutrophil Responses and Implant Infiltration

Since inflammatory cells are the major component of the fibrotic capsule surrounding biomaterial implants, and their participation may be linked to mast cell activation, we hypothesized that altering the stem cell and mast cell responses may reduce the accumulation of inflammatory cells ($CD11b^+$ cells) at the implant interface. In addition, these interactions may also effect the infiltration of inflammatory cells into the scaffold. As expected, examination of scaffold interiors at Day 3 reveals infiltration of neutrophils and macrophage (Figure 3.13). The extent of these responses is similar between treatment groups. However, at Week 1, these cell responses begin to diverge. Control scaffolds appear infiltrated by predominantly neutrophils while SDF-1α scaffolds are predominantly infiltrated with macrophages (Figure 3.14).

Since intra-scaffold response quantifications may be potentially be affected by section depth differences and local porosity, we next focused on the implant interfaces where a more uniform response could be quantified. Indeed, control implants were found to have a thick, dense band of $CD11b^+$ cells while SDF-1α soaked implants have a substantially reduced density of inflammatory cells (Figure 3.15). By quantifying the cell density, we find that SDF-1α soaked implants elicited little influence on inflammatory cell recruitment at day 3. However, SDF-1α release profoundly reduced inflammatory cell accumulation, 3-fold less than control implants after one week of implantation.

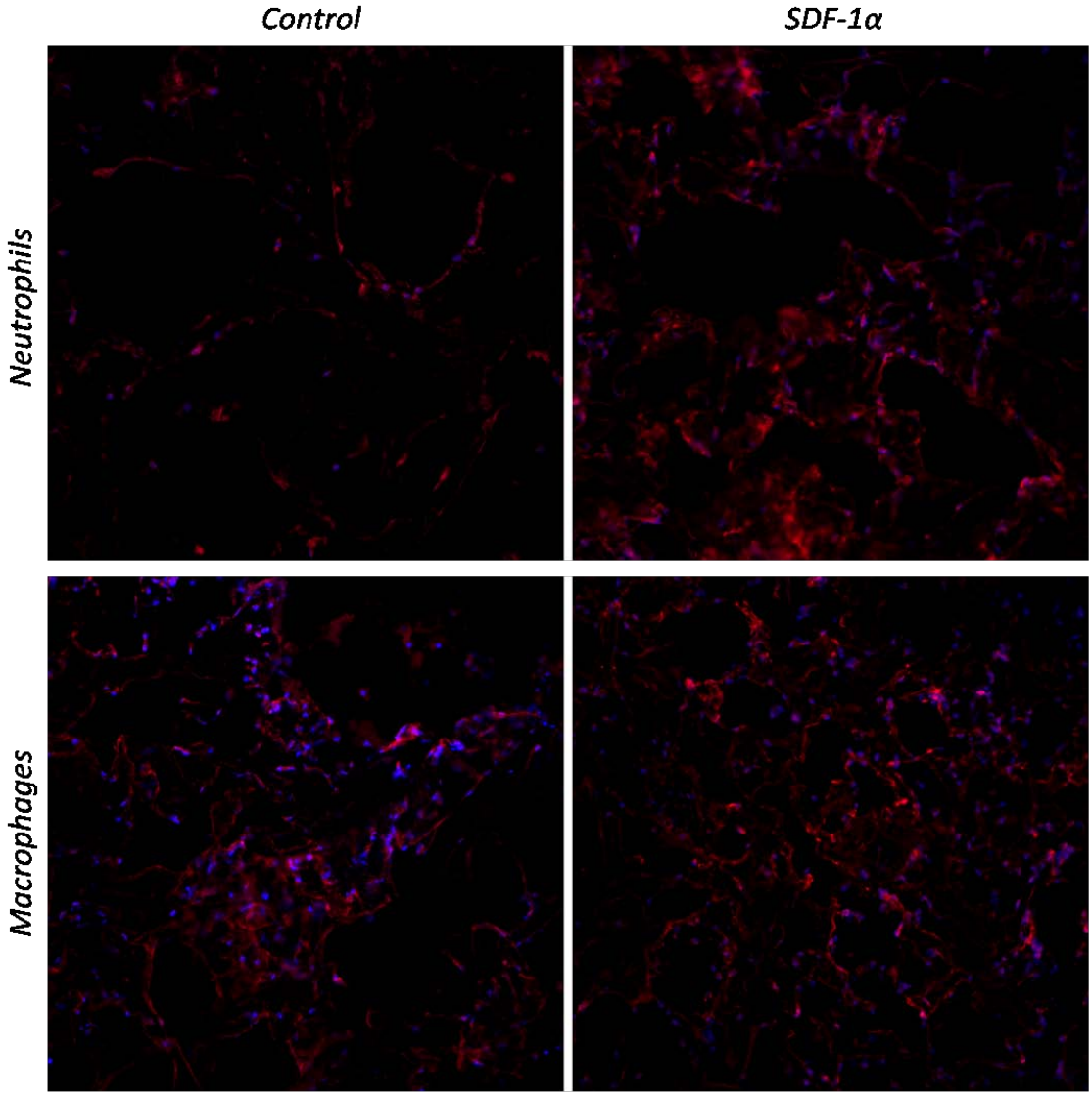

Figure 3.13 Neutrophil and macrophage infiltration 3 days after implantation. Antibodies specific for neutrophils and macrophages were examined using immunofluorescence staining with Texas Red. SDF-1α have a more prominent degree of neutrophil infiltration into the scaffold. However, macrophage infiltration appears similar between treatment groups.

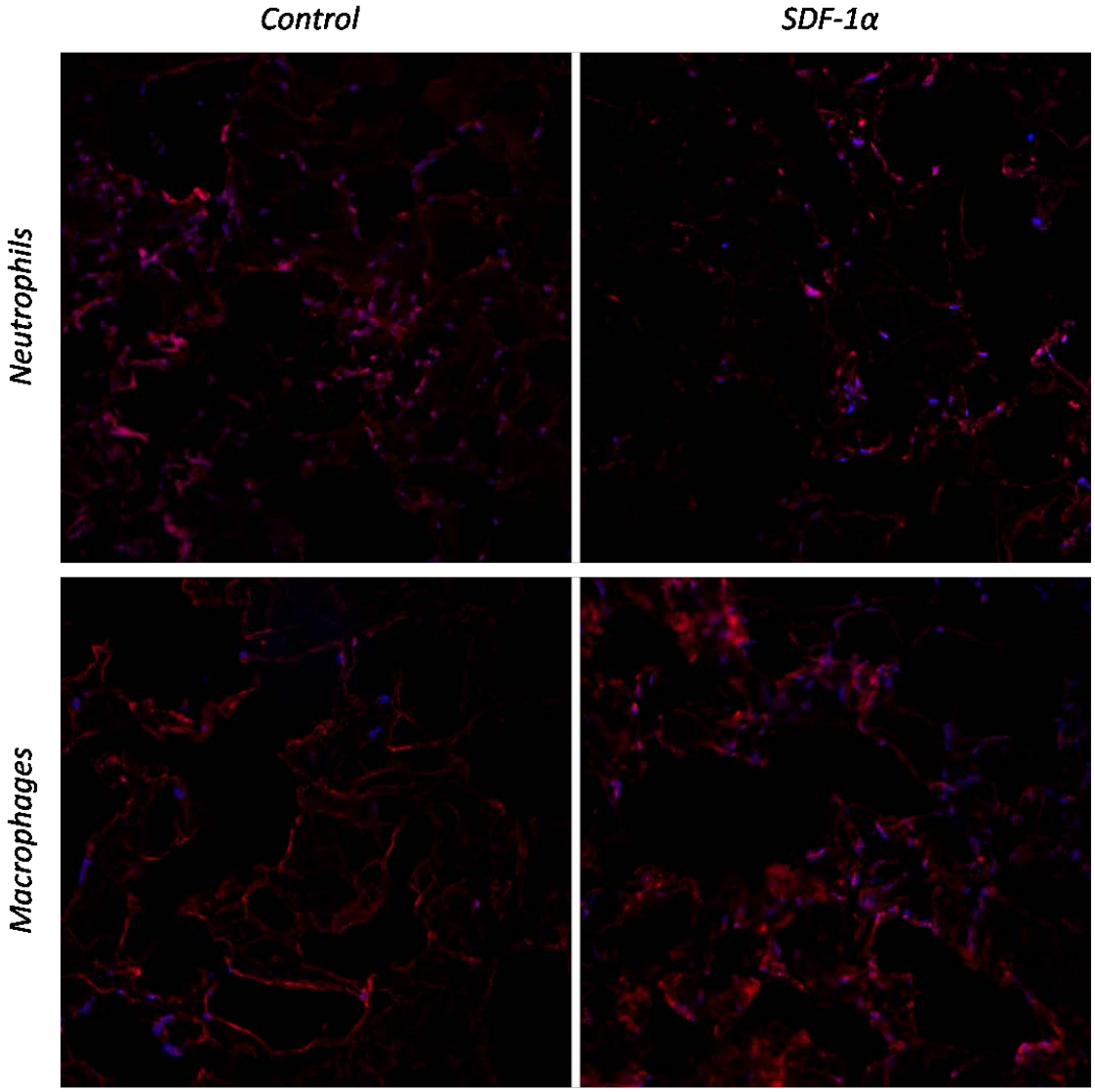

Figure 3.14 Neutrophil and macrophage infiltration 7 days after implantation. One week after implantation, the prominence of neutrophils has greatly increased in control scaffolds, while decreasing in SDF-1α treated scaffolds. Interestingly, the number of macrophages inside control scaffold has also been significantly reduced, while SDF-1α have prominent macrophage infiltration.

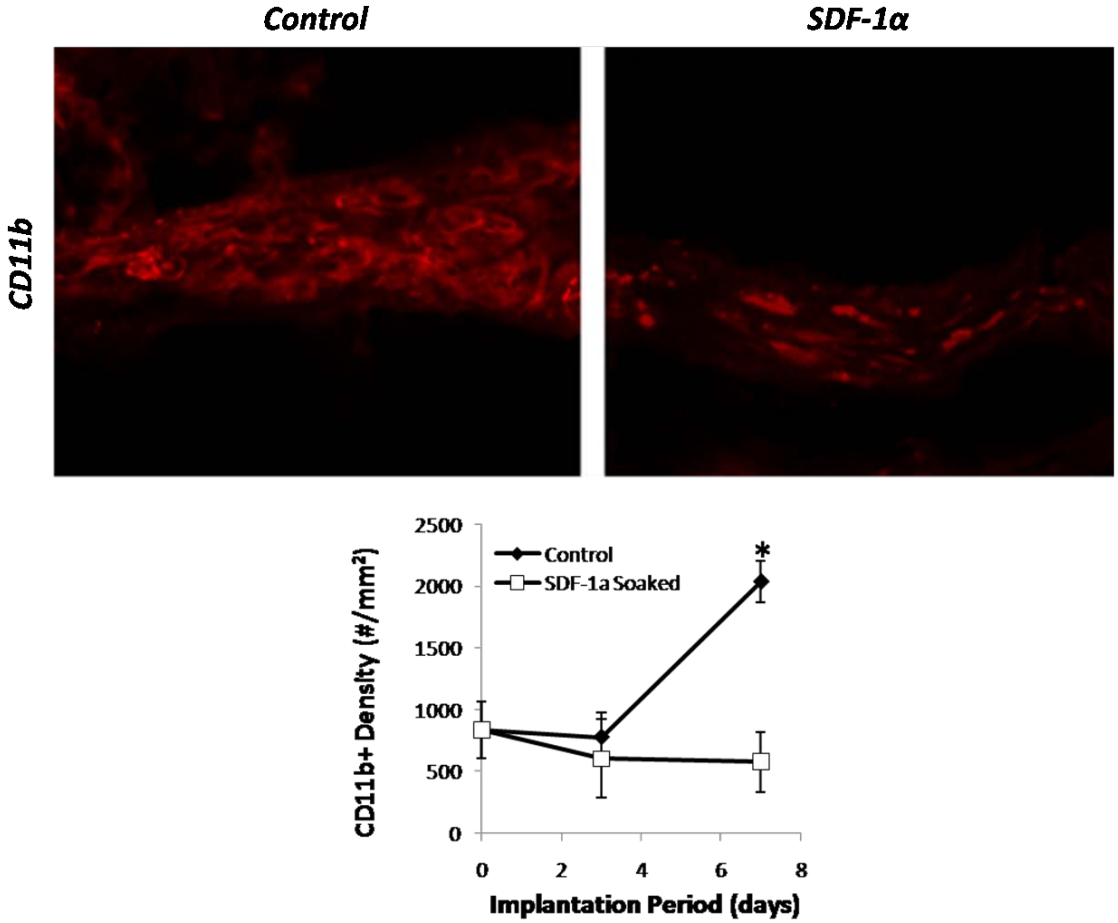

Figure 3.15 Buildup of inflammatory cells at the scaffold interfaces. Inflammatory cells (based on CD11b expression) where characterized at the implant interface and visualized with immunofluorescence conjugating to Texas Red. Visualization reveals a much higher density in control scaffolds. Quantification on the basis of cell density at the interface also reveals a significant differences between treatment groups as the inflammatory response progressed (Two-way Repeated Measures ANOVA, bracket and * indicates significant treatment effect $P<0.05$, * above data point represents significance by Bonferroni test $P<0.05$).

3.6.3.3 Influence of Altered Inflammatory Cell Responses on the Histology and Population of Cell at the Implant Interface

With mast cell responses significantly altered at Day 3, we began our histological assessment at at this point and additional examined histology at Weeks 1, 2, and 5. At Day 3 (Figure 3.16) H&E staining reveals on a modest influence in interface histology. SDF-1α treated scaffolds have a slightly lower cell density at the interface and a slight reduction in the thickness of the inflammatory cell infiltrate between the scaffold and native tissue. In addition, H&E

staining of the control scaffold cross-section shows very little matrix staining inside the scaffold despite detection of neutrophils and macrophages by immunofluorescenece. However, SDF-1α cross-sections have a higher degree of cell infiltration and some matrix deposition already beginning inside the scaffolds. As indicated by the area on the SDF-1α cross-section image, cells can observe penetrating through a surface pore into the interior pororsity of the scaffold establishing a network of cell:cell interactions which allow the cells to distribute throughout the open pore in the cross section.

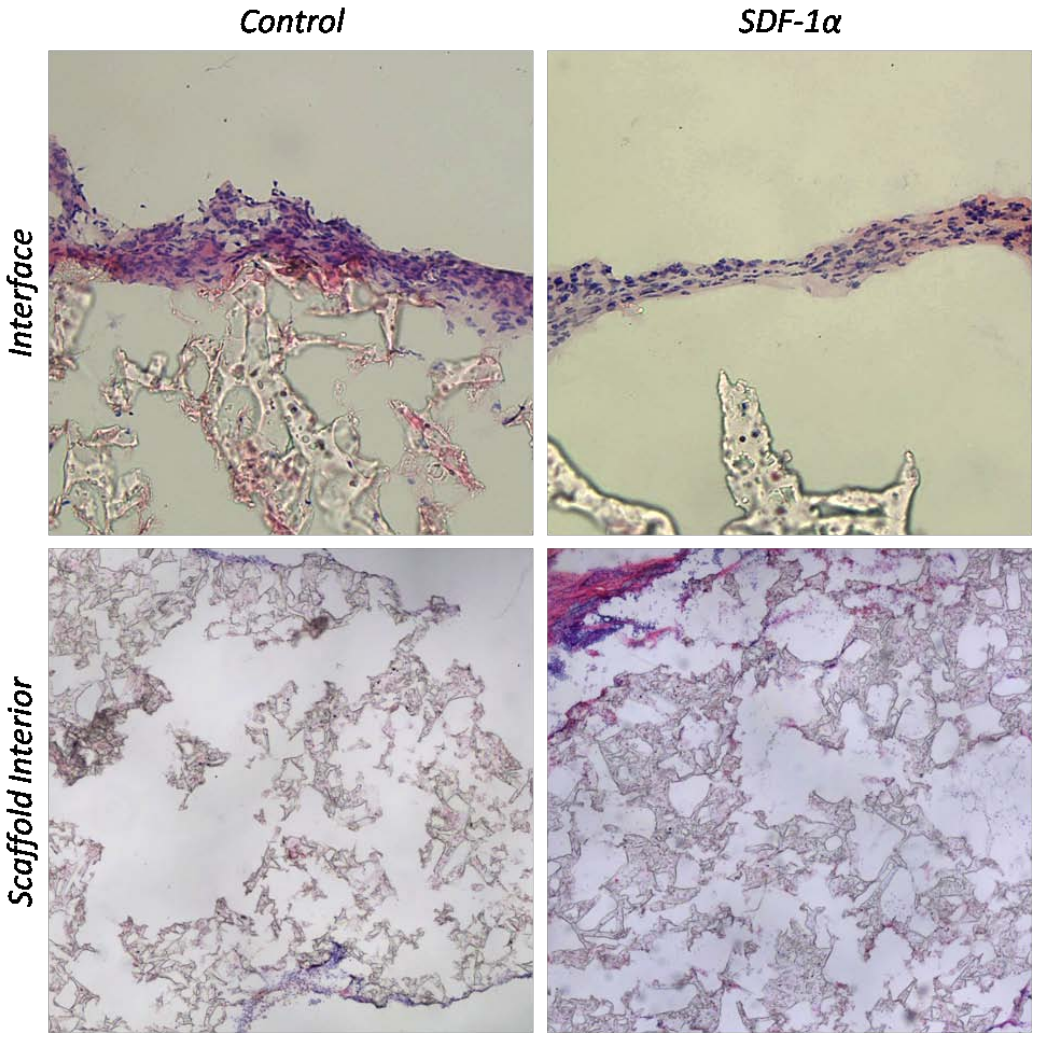

Figure 3.16 Histological characterization of scaffold interface and cross-section after 3 days. H&E staining reveals SDF-1α has a reduced cell accumulation at the interface which is accompanied by increase cell infiltration into the cross-section.

We next examined the histology of the scaffold at Week 1. Since inflammatory cells, especially $CD11b^+$ macrophages, at the interface participate in the formation of granulation tissue and subsequent fibroblast interactions, we hypothesized that the observed differences in $CD11b^+$ inflammatory cells and stem cells may have exerted a more profound influence on interface histology between treatment conditions. First, as anticipated, we found that SDF-1α soaked scaffolds exert substantially less inflammatory cell infiltration and granulation tissue formation than control scaffolds at day 7 (Figure 3.17). Untreated scaffolds have a thick band of infiltrated cells surrounding the scaffolds, accompanied by a more prominent eosin stain indicating a higher degree of matrix production consistent with the initial formation of granulation tissue. Treated implants have a 2 fold reduction in thickness of the inflammatory infiltrate and a ~1 fold decrease in cell density (Figure 3.17) compared to control implants. In addition, the density of cells inside the interface is significantly higher in control scaffolds (Figure 3.17).

Using our calculation of the cell density at the Week 1 time point as well as previous calculations of the stem cell and inflammatory cell densities at the implant, we developed a cell composition histogram. Cells which were not identified through positive expression of stem cell markers and the general inflammatory cell marker CD11b were assumed to be implant associated fibroblasts. Using H&E stained cross-sections, spindle shaped cells in the interface were estimated based on density and closely estimated the unaccounted percentage of cells left over from subtracting stem cell and inflammatory cell densities. Thus this residual density was defined and plotted in the histogram as fibroblasts. In control scaffolds at week 1, the scaffold interface was composed of approximately 75% inflammatory ($CD11b^+$) cells and fibroblasts (residual spindle shaped cells of the interface which do not stain positive for the specified marker set). In contrast, implants treated with SDF-1α prior to implantation leads to a week 1 interface with approximately 75% composition of MSC and HSC.

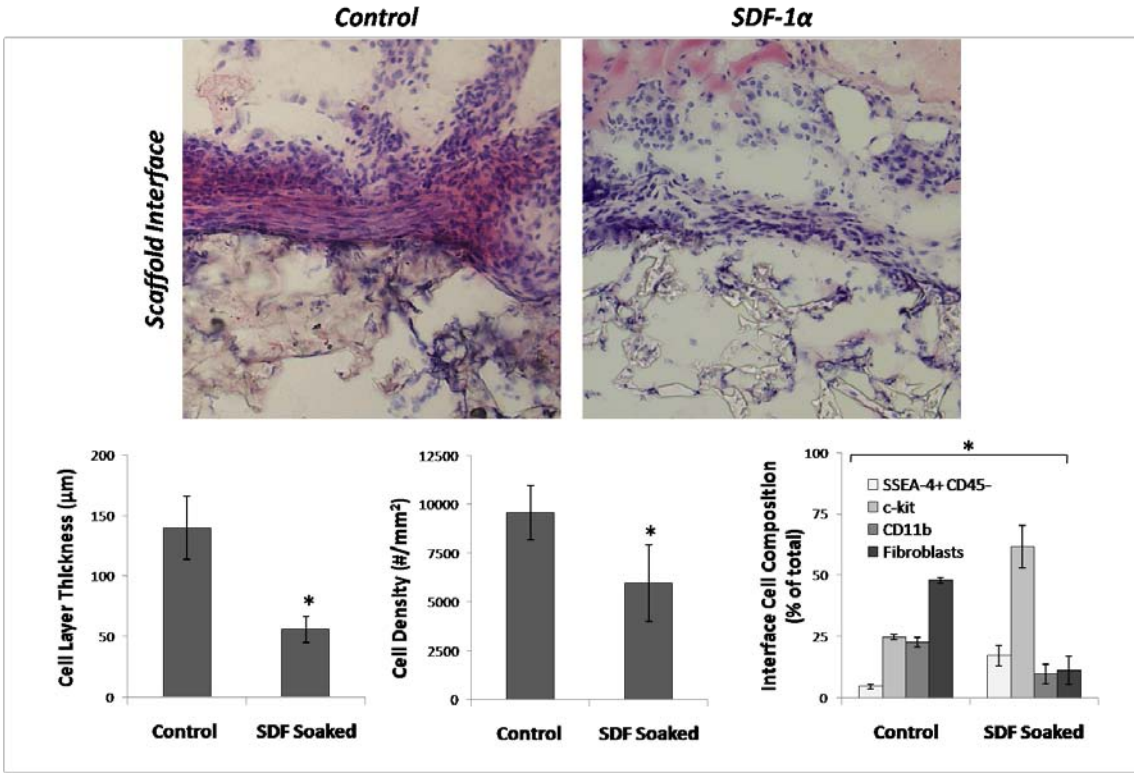

Figure 3.17 Characterization of granulation tissue at the interface of SDF-1α treated scaffolds. H&E staining shows a prominent infiltration of cells around the fibrotic region encompassing the control implant interface. However, SDF-1α treated implants appear to have a reduced infiltrated cell load and less prominent spindle shaped encapsulating layer. Quantification reveals significant decreases in thickness and density parameters (Student t test, * represents significance at $P<0.05$). Using the quantified implant interface density, the populations of examined cell populations was estimated and reveals a significantly different population of stem cells, inflammatory cells, and fibroblast between implant treatment conditions (ANOVA, * represents significance at $P<0.05$).

Next, we examined the cross-sections of 1 Week scaffold implants with regards to cell infiltration and intra-scaffold matrix deposition (Figure 3.18). Control scaffolds have a slight increase in the penetration depth compared with the previous Day 3 time point, advancing approximately 500μm into the scaffold cross-section. However, as observed at Day 3 in treated scaffolds, the addition of SDF-1α to the scaffolds has influenced cell infiltration as cells consistently could be identified at deeper depths within the scaffold, greater than 1mm within the cross-section. In addition, the infiltrated cells had a fibroblast-like morphology observed

from eosin staining cell projections which connected these cells and formed networks covering some of the interior scaffold pores.

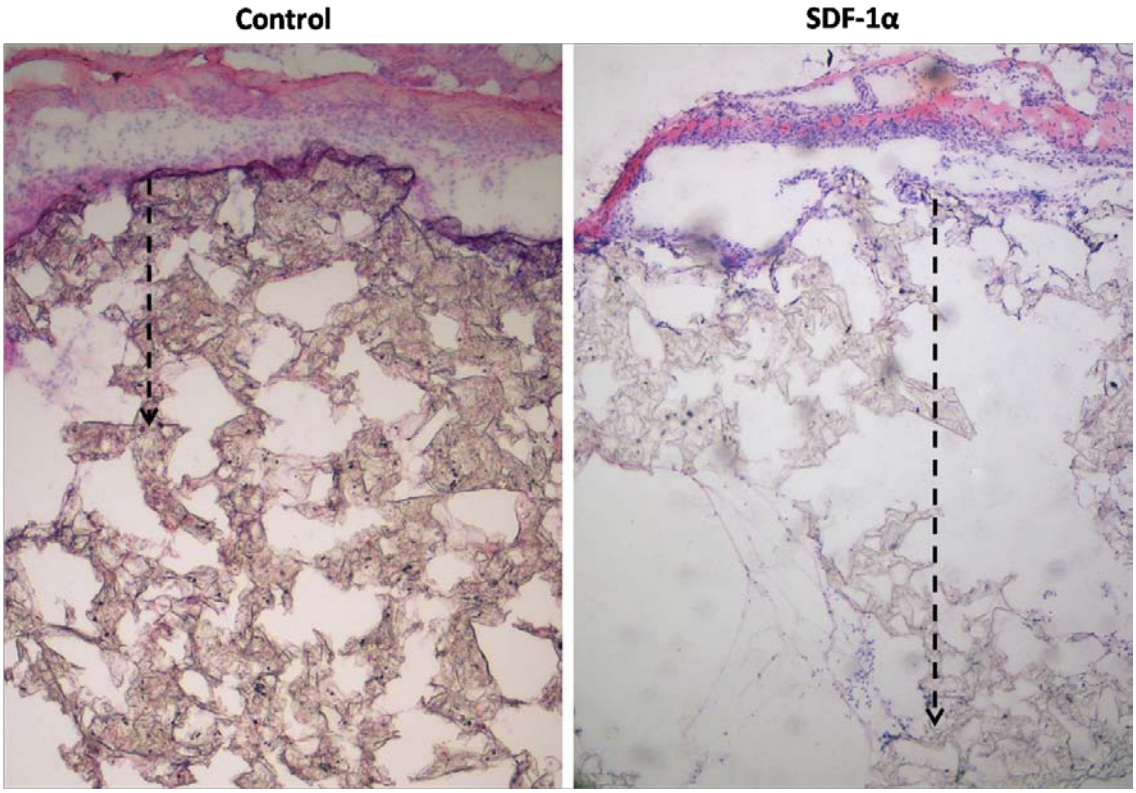

Figure 3.18 Comparison of 1 week cell infiltration among scaffold treatment groups. Scaffold cross-sections were H&E stained than examined for intra-scaffold cell pockets. The penetration of cells in control scaffolds was restricted to the first few pore layers in depth form the skin side of scaffold implant. However, SDF-1α scaffolds had far deeper cell infiltration extending multiple pore layers inside the scaffold matrix.

Though we did not find significant alterations in the MSC response between scaffold treatment conditions beyond the first week of implantation, the growing difference in implant histology led us to consider whether SDF-1α : MSC interactions could continue to influence foreign body response downstream. We began by again assessing the interface between the scaffold and native tissue at Week 2 (Figure 3.19). Interestingly, we see similar trends progressing from the previous week. SDF-1α treated scaffolds have a persistent reduction in the thickness and density of cell surrounding the scaffold implants. Prominent eosin staining in control implants is becoming more organized and reminiscent of the initial stages of fibrosis,

while SDF-1α scaffolds do not stain prominently with eosin at the interface. Surprisingly, we instead find new blood vessels running throughout the skin side of the interface (indicated by arrow) of SDF-1α scaffolds. This led us to consider whether differences in cell infiltration may have been influenced by the differences in vessel formation between treatment groups. To qualitatively assess this, we again looked at the cell infiltration into the scaffold. A series of H&E images were taken of each implant, in order to completely comprise the cross-section, which were then assimilated into a mosaic image of the entire cross-section. Both scaffolds have a corona shape of cell infiltration around the scaffold cross-section. However, the SDF-1α treated scaffolds appear to have a higher degree of intra-scaffold penentration, though cores are still readily observeable in both treatment conditions. Another observation from these histology mosaics, is the severe cross-sectional degradation associated with the untreated scaffolds. This can be observed by the shape of the cross-section (triangular) which has been worn down from the square cross-section of the original implant. Interestingly however, there appears to be less cross-sectional wear on the SDF-1α, again accompanied by a higher degree of cell infiltration.

Given these observations, we considered whether $CD11b^+$ cells (of which a significant portion of cells are likely macrophages) are likely still distinct between treatment conditions given the still prominently dense cell infiltrate and cross-sectional wear differences between treatment conditions. For reference, mast cell images and density graphs from Week 2 are included (Figure 3.20) at which point we observed a return to similar mast cell density and activation state between treatment conditions. As expected, we still find a more prominent layer of CD11b cells in untreated implants compared with SDF-1α. The difference in $CD11b^+$ responses at the interface remains statistically significant between treatment groups at Week 2.

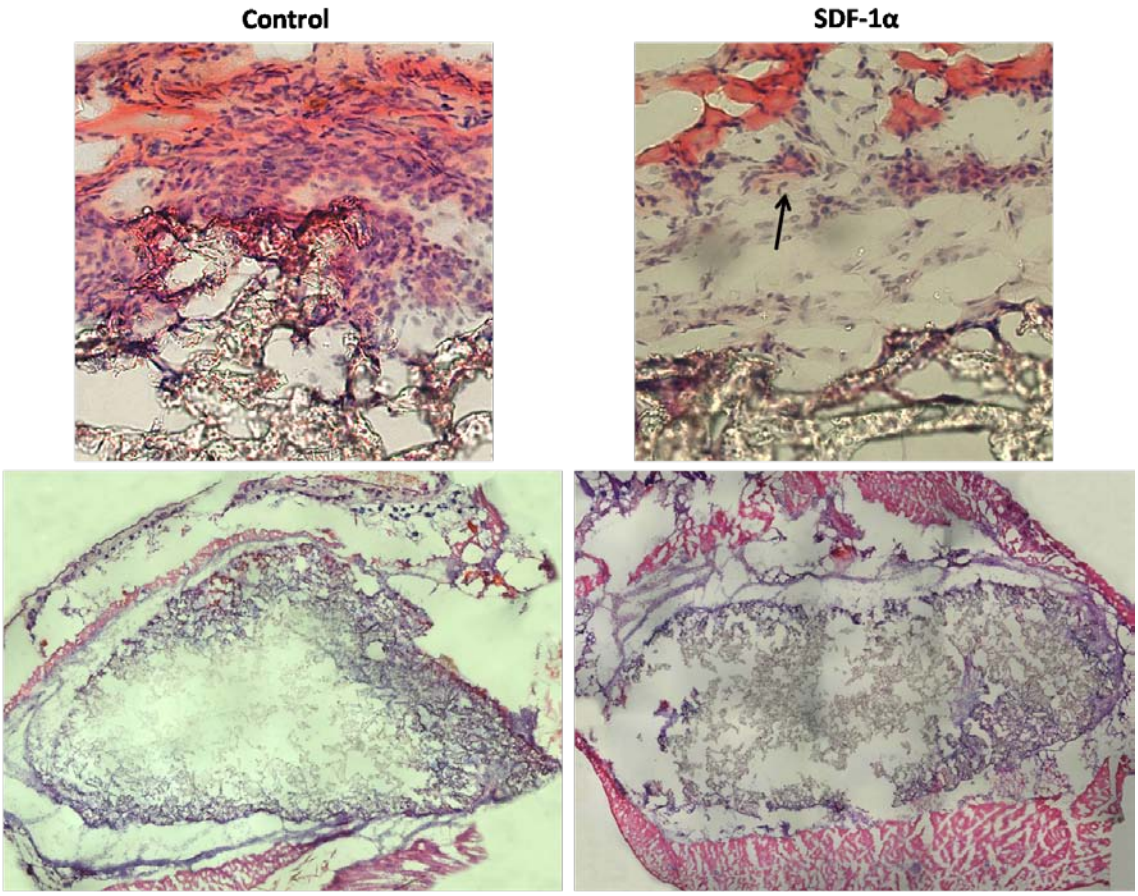

Figure 3.19 Cell behavior at the interface and within the scaffold cross-section 2 weeks after implantation. Multi-cell thick bands of cells tightly packed around the interface of control scaffolds is observed. Cross-sections show a prominent void within the scaffold with cell infiltration corona limited to the exterior edge. In contrast, SDF-1α treated scaffolds have a reduced cell density and less cell packing at the interface. Vessels can also be observed inside the interface between the scaffold and native tissue (arrow). Vertical bands of cell infiltration extend prominently from the muscle interface beyond the center of the scaffold. Though more irregular, cell infiltration can be observed at deeper depths compared to control scaffolds. Overall wear on the rectangular shaped implant cross-sections also appears higher in control scaffolds.

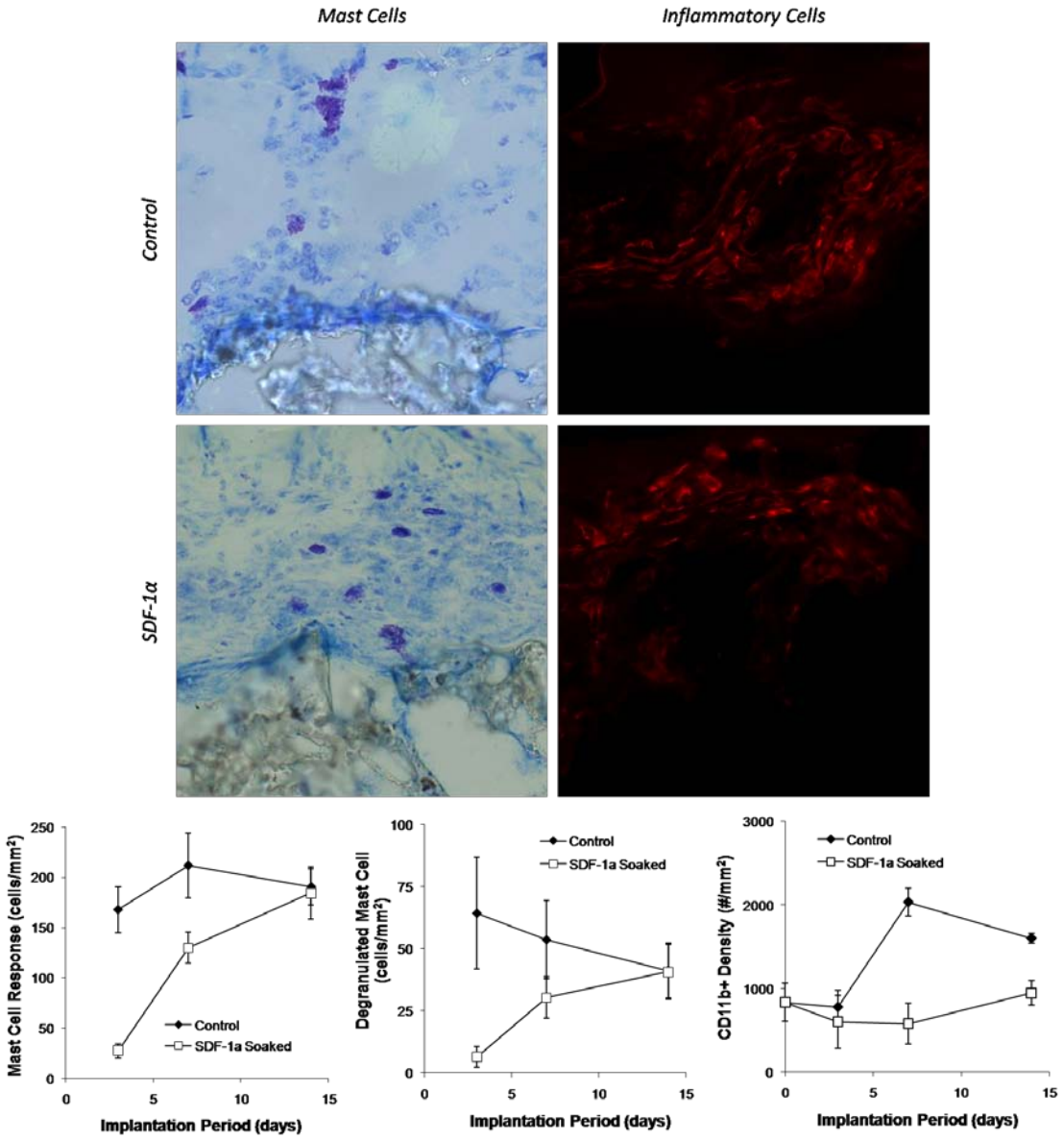

Figure 3.20 Inflammatory cell stabilization in week 2 scaffold interfaces. Mast cell (Toluidine Blue) and inflammatory cell (CD11b) populations were analyzed between scaffold groups. By week 2, less drastic differences in both mast cell and CD11b divergence is evident. These responses were quantified and added to kinetic plots, which indicates this pattern in total mast cells, degranultated mast cells, and $CD11b^{+}$ inflammatory cells.

3.6.3.4 Short-Term Scaffolds Treatment with SDF-1α Affects Long Term Fibrotic Responses

Our primary focus for this study was to correlate whether increasing stem cell responses to scaffold implants could have effects on fibrotic interactions. Given the substantial alterations in inflammatory cell responses, improved cell infiltration, and reduction in cell infiltrate around the implants throughout the inflammatory response, we believed this approach should have been successful at providing some influence over fibrotic reactions downstream. To examine these influences, 5 Week scaffold implants were H&E stained to analyze the cellular composition at the interface and intra-scaffold, Masson Trichrome stained to visualize collagen deposition, and stained with anti-collagen I antibodies to examine cell distribution relative to collagen production (Figure 3.21).

As expected from previous histology trends, the interface between untreated and treated scaffolds is substantially altered at 5 weeks. Control scaffolds are surrounding by a thick encapsulating layer of cells within prominent bands of eosin stain while SDF-1α treated scaffolds have a substantially reduced cell density with a faint eosin stain. Masson Trichrome staining of control interfaces shows deep blue patches and bands of collagen disorganized throughout the interface. In contrast, SDF-1α have fewer deep blue staining areas, instead having well organized, but faintly blue bands of collagen running parallel to the scaffold interface. Collagen I staining of control scaffolds shows prominent staining (FITC immunofluorescence). Finally, H&E images were aligned into a mosaic to display a high resolution view of the scaffold cross-section (Figure 3.22). As expected, control scaffolds are mostly acellular inside the scaffold with high matrix deposition while treated scaffolds have a higher degree of cell infiltration visible through the pore structure accompanied by a lower degree of acellular matrix deposition. However, cell infiltration ceases toward the extreme muscle side of the scaffold.

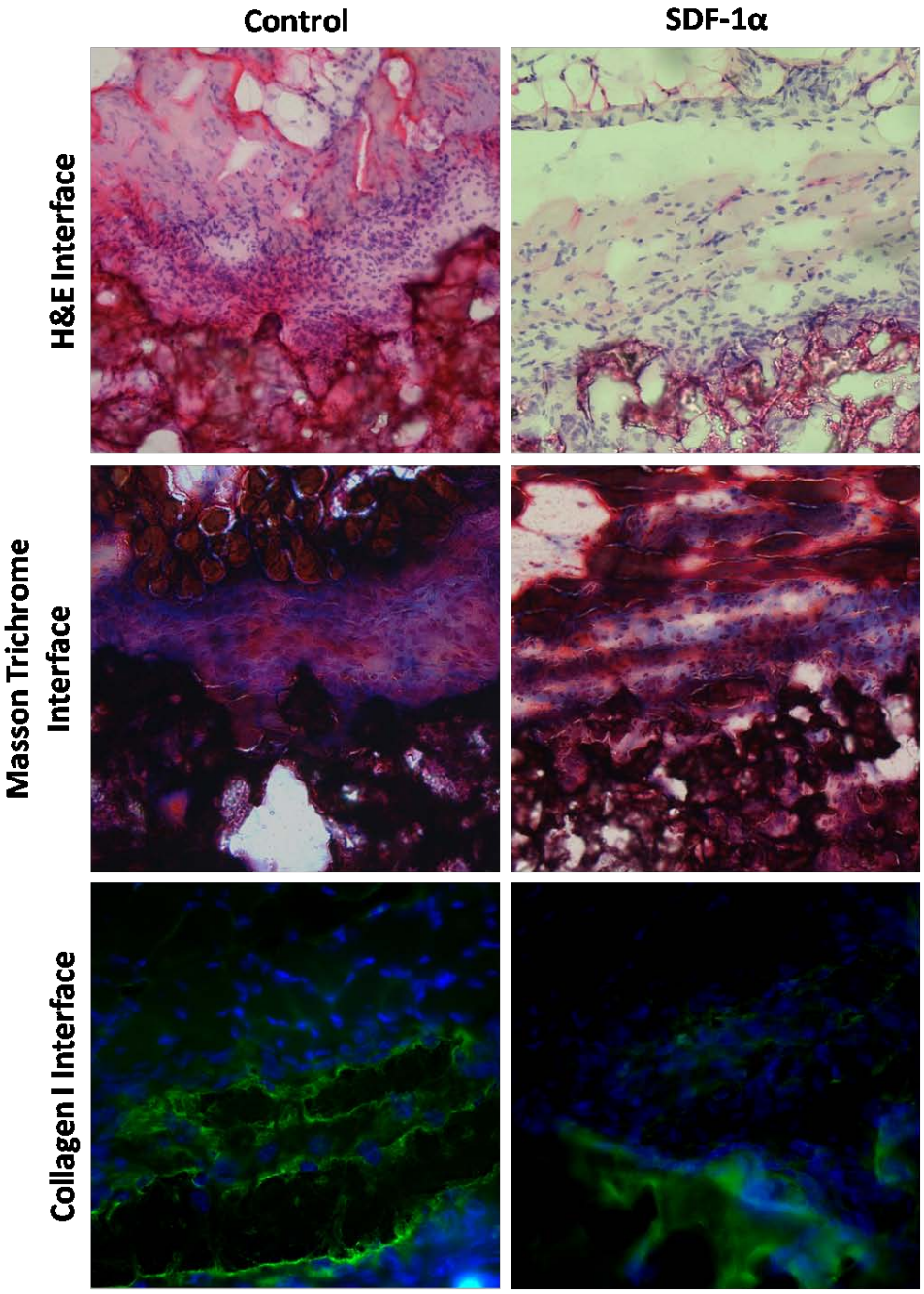

Figure 3.21 SDF-1α treated scaffolds have reduced fibrotic responses at 5 weeks after implantation. Compared to control scaffolds, SDF-1α scaffolds have a reduced cell density at the implant interface and a passive transition from healthy tissue to the scaffold in comparison of H&E stains. Masson Trichrome staining reveals thin organized collagen bands at the scaffold interface of SDF-1α scaffolds compared to the thick disorganized collagenous matrix in control. Finally, staining with Collagen I reveals only minor expression at SDF-1α interface with prominent expression bands are observed in controls.

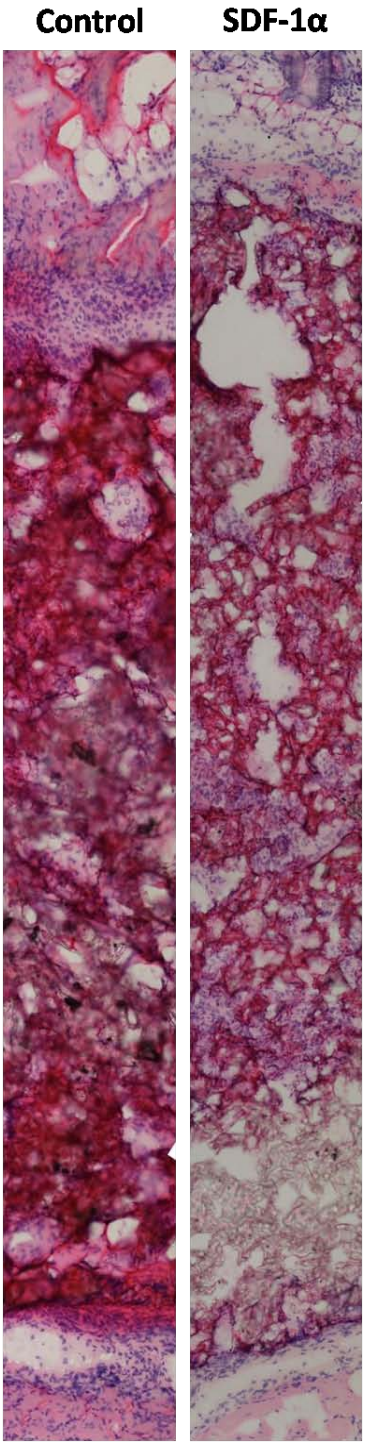

Figure 3.22 Mosaic image of H&E stains in a column through the center of the scaffold. Prominent fibrotic interfaces can be observed in control scaffolds with heavy collagenous matrix deposition. However, in SDF-1α scaffolds, cells infiltrate throughout scaffold pores in a more organized manner with little fibrotic encapsulation observed at either interface.

3.6.4 Discussion

In this implantation study, we examined the influence of SDF-1α and SDF-1α-mediated stem cell responses on the biomaterial-mediated inflammatory response. Recently, it was shown that in the absence of injury, the addition of exogenous SDF-1α does not stimulate stem cell migration [145]. Therefore, the inflammatory stimuli due to scaffold implantation in combination with SDF-1α is likely the factor leading to increases beyond those stem cells normally recruited to participate in healing. Having improved the stem cells response, we analyzed components of the inflammatory response in comparison to their normal biomaterial mediated responses to unmodified PLGA scaffolds.

We began by investigating the mast cell response as their degranulation at the implantation initiates the first wave of inflammatory cell responses [40]. Interestingly, our results show a substantial alteration in both the total mast cell response (3-4X times less prominent in SDF-1α treated scaffolds) as well as the degree of mast cell activation (3-4X fewer activated cells in SDF-1α scaffolds). These alterations remain constant and significant up to 2 weeks after implantation. Previous studies have shown that reducing the products of mast cell activation can lead to a decrease in inflammatory cell responses [39, 40]. Unfortunately, there has been very little work relating MSC and HSC responses to mast cell behavior in vivo. One study however has shown that MSC conditioned media as well as MSC supplementation can accelerate wound healing responses and these responses were linked to an increase in c-kit$^+$ endothelial progenitor cells [165], in agreement with our finding of SDF-1α increasing c-kit cell density. Of interest, this report and other studies also showed that MSC conditioned media contained higher amounts of SDF-1α along with other chemokines and growth factors [146, 165, 166]. However, these studies did not specifically investigate mast cell responses to these treatments. One of the few studies which does showed that administration of MSC did not substantially increase the number of mast cells, though this study was not conducted with mouse MSC and was performed in the brain [167].

There have been published reports on the influence of SDF-1α directly on mast cell behavior [168-170], though SDF-1α-mediated reduction of mast cell reactions appears to be due to interactions for which a detailed mechanism has not yet been developed. Receptor expression studies have shown that mast cell progenitors express CXCR4 [170] and both mature and progenitor mast cells respond to SDF-1α gradients in vitro [171]. This suggests that CXCR4 may be, at least partially, responsible for mast cell chemotaxis to peripheral tissues [172]. However, in this study we find decreased mast cell numbers in the local response around the implant and reduction in activation. In support of this finding, recent evidence has shown that mast cell treatment with SDF-1α in vitro does not stimulate degranulation [173], instead selectively stimulates production of IL-8, a mast cell product responsible for initiating neutrophil chemotaxis to the site of inflammation [174]. This finding led us to subsequently investigate CD11b (expressed by both mature neutrophils and macrophages) as well as specific neutrophil and macrophage responses using markers specific to these cell types.

Shortly after implantation, macrophages can be found infiltrating to the implantation site and within the scaffold pores, as expected. In accordance with study of Lin et al. [168], we find a more prominent neutrophil infiltration inside the SDF-1α scaffolds, though quantification of this density was insignificant at Day 3. Interestingly however, at approximately the same time when MSC infiltration between treatment groups begins to deviate, we find substantial differences in the CD11b cell responses. At 1 week after implantation, the number of neutrophils inside control scaffolds increases while those inside SDF-1α appears to decrease, accompanied by an apparent decrease in macrophages inside control scaffolds. At the SDF-1α implant interface, we were surprised to find a significant decrease in the density of inflammatory ($CD11b^+$) cells in the subcutaneous space around the implant. A previous study investigating MSC supplementation have shown increases in macrophages (which express CD11b) to the wound site after MSC administration [165]. Interestingly however we find that increases in these two cell populations (neutrophils and macrophages) over a week foreign-body mediated

inflammatory response was actually reduced. However several lines of evidence suggest that SDF-1α in coordination with other growth factors may contribute to facilitating macrophage differentiation in a manner which improves wound healing responses by increasing angiogenesis [163, 175]. This possibility was assessed in later studies of this dissertation.

This shift in inflammatory cell responses appears to have consequences on the development of granulation tissue, and is likely related to findings which have shown that SDF-1α may coordinate the transition from inflammation to the initiation of tissue repair [176]. In the context of this first week response, we consistently observe a thicker (3X) and denser (2X) cell response at the interface in control scaffold with a reduced infiltration of fibroblast-like cells into the scaffold (observed as having large cytoplasmic extension by Eosin Y staining). In addition, examination of cell populations shows a significant shift from a predominant inflammatory cell and fibroblast population in control implants to include substantially more stem cells in SDF-1α scaffolds and thus a reduction in fibroblast and inflammatory cell numbers and percentage. It is possible that since foreign body reactions are initiated by implant-associated mast cell recruitment and activation [40], that exogenous SDF-1α may directly or indirectly alter the extent of mast cell responses, leading to a stage whereby stem cells impart influence over the development of the inflammatory response, as shown in previous supplementation studies [165]. Next we analyzed whether these upstream influences could indeed translate to downstream responses including the buildup and development of fibrotic tissue around the scaffold implants.

Despite the limited quantity and delivery period of SDF-1α, the preliminary influence over the inflammatory response and subsequent stem cell responses translate into many downstream alterations in fibrotic responses. Extending outside our intended evaluation period (5 weeks implantation), we find a thinner, less dense cell infiltration around SDF-1α treated scaffolds as well as a profound decrease in eosin banding at the interface around the implant. This was accompanied by the appearance of vessels at the SDF-1α scaffold interface and

higher degrees of cell infiltration. As previously discussed SDF-1α has been linked with improved angiogenic responses [137, 175], in addition to this we hypothesized that, based on the reduced eosin staining bands in the interface tissue, that SDF-1α and the improved MSC response may also be modulating fibrosis. In addition to the histological appearance of the interface, the increase in cell infiltration seems to support this hypothesis. To address this, we observed the responses further downstream after 5 weeks of implantation.

After extended implantation, mast cell staining reveals a drastic difference in the thickening of the tissue around the implantation site and is characterized by an accumulation of mast cells in this region and an ongoing state of mast cell activation in control PLGA scaffolds. Tissue thickening and the mast cell agitation do not appear to the same degree in SDF-1α treated scaffolds. At least one study has linked continued mast cell agitation with chronic inflammation and fibrosis due to stimulation of fibroblast proliferation and collagen synthesis by tryptase, chymase, and histamine in the granular content [177]. In agreement with these findings, we find a higher degree of total collagen around untreated implants combined with a high density of collagen I producing cells inside the fibrous layer surrounding the implants. Type I collagen is prominently produced by fibroblasts and myofibroblasts and, based on its prominence and structure around the implant, signifies fibrotic encapsulation [178]. In addition, fibrosis is of considerable concern in TE as it can limit cell infiltration and reconstitution of the matrix due to permeability and nutrient restrictions [15, 16, 179]. The lower degree of fibrotic encapsulation in SDF-1α afforded a higher degree of cell infiltration in comparison to control scaffolds which have restricted cell infiltration and an acellular matrix appearance inside the scaffold architecture.

Treatment of scaffolds with SDF-1α was highly successful in increasing stem cell participation at the scaffold interface and modulating the inflammatory response thereby reducing fibrotic encapsulation of the scaffold implants. This was accompanied by an increase in cell infiltration beyond that normally observed with PLGA scaffolds [121, 160]. However, this

study investigated the responses due to a relatively short term low dose delivery of SDF-1α. We hypothesized that alternative delivery strategies may improve responses based on a few different observations from this study. First, SDF-1α altered mast cell responses for a period of time consistent with the release duration expected from physical adsorption and soaking of the scaffold. In addition, MSC responses were also increased for duration consistent with this period. This led us to speculate whether controlled delivery may further improve host stem cell responses and modulate inflammation improving wound healing and reducing fibrosis.

Alternatively, our results support that maximal biomaterial induced MSC response occur at approximately 1 week after implantation. In the normal physiological response, SDF-1α levels reach a maximum tissue concentration post injury approximately 4-7 days after injury [180, 181], which hypothetically constitutes a major contributor to subsequent stem cell responses. Given this, we also considered whether delaying SDF-1α release to correspond with the physiological mechanism may scale this response. Based on mast cell responses to SDF-1α treated implants, and given that mast cell influence appears to predominate only during the first few days post implantation, delaying delivery until after mast cell response would also allow us to analyze the influence SDF-1α mediated mast cell responses.

3.7 Influence of SDF-1α Dosing Time and Duration on Biomaterial Mediated Tissue Responses

3.7.1 Purpose

The previous study confirms the utility of SDF-1α as a means to modulate host stem cell responses in the foreign body response to biomaterials. Based on this study, some mechanistic hypothesis governing these responses emerged regarding delivery time post implantation and duration of delivery. In this study, we set out to examine whether SDF-1α supplementation following mast cell responses led to a more prominent host response. In addition, controlled release of SDF-1α at the implantation site over a 2 week period was investigated using slow release mini-osmotic pumps.

3.7.2 Materials and Methods

3.7.2.1 SDF-1α Scaffold Supplementation

To verify whether delayed delivery enhanced SDF-1α-mediated effects, PLGA scaffolds were implanted subcutaneous as previously described and Balb/C- scaffold bearing mice were then returned to housing. Following implantation for 3 days, scaffolds were supplemented with 100μL SDF-1α solution at 100ng/mL (noted in figures and graphs as D3). Animal study procedures were otherwise as previously outlined. After 7 days, scaffolds were removed and analyzed for cellular composition.

3.7.2.2 Controlled Delivery of SDF-1α from PLGA Scaffolds

To achieve long term release, 2 week delivery mini-osmotic pumps (Alzet Model 1002, Alza Corporation, Palo Alsot, CA) delivering SDF-1α at a rate of 0.25ng/hour were connected to the scaffold via a polyvinyl chloride catheter (Alzet, Durect Corporation, Cupertino, CA) were inserted into the center of the scaffold (5 x 5 x 5 mm). Control scaffolds received sterile saline via osmotic pump. Pump-connected scaffolds were then implanted subcutaneous on the back of Balb/C mice with mice receiving only 1 scaffold treatment grouped at n=4 per treatment condition. After 2 weeks implantation, scaffolds were recovered and analyzed.

3.7.2.3 Histological and Immunohistochemical Evaluation of Scaffolds

Recovered implants were embedded and cryosectioned as outline in previous sections. In addition to characterizations outline in previous sections, MSC phenotype [182] was further validated by examining immunofluorescent co-expression of CD90, CD44, CD105, CD73 (Santa Cruz Biotech, Santa Cruz, CA). Vessel formation around and inside the scaffolds was verified using antibodies to laminin and CD31 to identify vessel basal lumina[183] and endothelial cells[163] respectively. Endothelial progenitor cells were identified by co-expression of CD34 and CD133 as previously described [184]. Masson Trichrome staining was used quantify collagen deposition and additionally was used to examine vessel formation by comparing stains with erythrocyte autofluorescence detected on FITC emission channel [185].

3.7.2.4 Inflammatory Protein Array

The profile of inflammatory protein production by implant-associated cells was determined using mouse cytokine antibody array III (Raybiotech, Norcros, GA) compared with control implants (n=3). Briefly, 30 slices of tissue sections from both control and treated groups were incubated with lysis buffer at -80°C 30 minutes followed by 30 minutes at room temperature for 3 cycles to extract proteins produced by cells adjacent to the implants. The protein concentrations in each sample were then determined using bicinchoninic acid (BCA) assay (Thermo Fisher Scientific Pierce Protein Research Products, Rockford, IL) as recommended by the manufacturer. For the antibody array, 50 µg of each protein sample was used in the mouse cytokine antibody array III, following manufacture's instruction. Finally, the slides were subjected to image analysis by Axon GenePix 4000B microarray scanner (Molecular Devices, Sunnyvale, CA) using Cy3 channel. The ratio of relative expression of SDF-1α treated scaffolds was calculated after subtraction of the background intensity and comparison with untreated controls. The fluorescence ratio for each spot was further processed to identify the species of up-regulated and down-regulated cytokines/growth factors.

3.7.3 Results

3.7.3.1 Effects of Delayed SDF-1α Delivery on Stem Cell and Inflammatory Cell Responses

We first quantified the effects of delaying SDF-1α until after peak mast cell degranulation to more closely correspond with peak physiological injury responses. Explant analysis at Day 7 reveals unexpectedly that delayed delivery leads to an intermediate response compared to control and scaffolds treated with SDF-1α prior to implantation (labeled as D0) (Figure 3.23). SDF-1α treatment at Day 0 and Day 3 resulted in a significant increase in MSC engraftment at the scaffold interface compared to no treatment, though differences between SDF-1α treatment intervals were not significant. However, delaying the chemokine until Day 3 resulted in an intermediate $CD11b^+$ inflammatory cell response, significantly less than control yet greater than treatment prior to implantation.

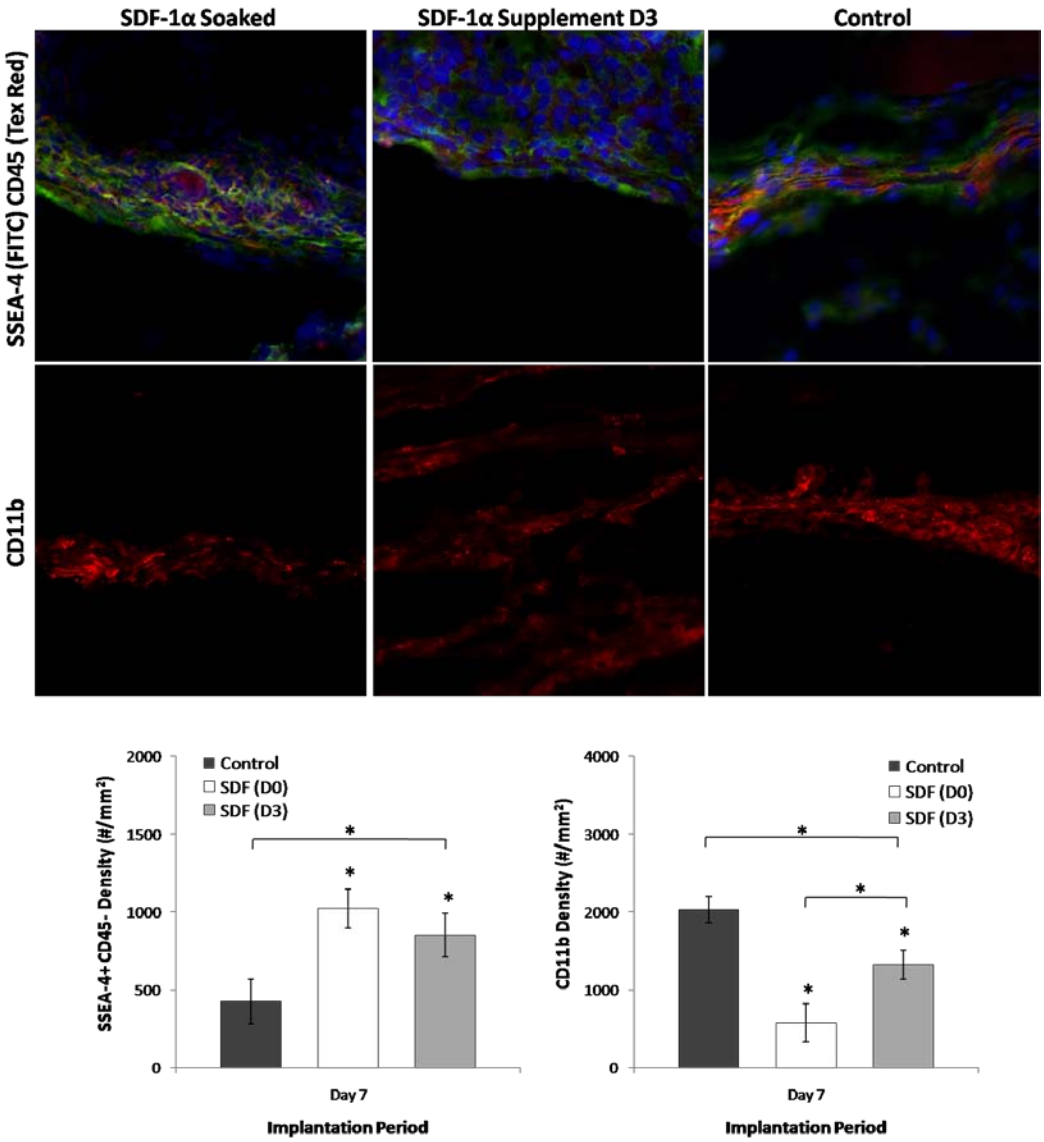

Figure 3.23 Delayed SDF-1α delivery results in intermittent MSC and inflammatory cell responses. Delayed delivery of SDF-1α until day 3 improves SSEA-4^{+} CD45^{-} density compared to no treatment. In addition, CD11b^{+} cell density also appears reduced compared to controls. Quantification reveals that these increases were significant with respect to control (bracket with * represents significant ANOVA at $P<0.05$, Dunnet test for control comparison significance indicated by * above bar plot $P<0.05$), while delaying SDF-1α delivery resulted in similar recruitment compared to soaking before implantation (insignificant Bonferroni intergroup test). However, soaking before implantation resulted in a more dramatic decrease in CD11b cell responses compared to delayed delivery (significant Bonferroni intergroup test indicated by bracket between two data groups with *, $P<0.05$).

3.7.3.2 Controlled Release of SDF-1α from Scaffold Implants

To analyze cellular and tissue response parameters beyond 7 days, scaffolds were implanted with either saline mini-osmotic pumps as control or pumps delivering SDF-1α at 100ng/mL for 2 weeks. As expected, the controlled delivery of SDF-1α was able to increase and extend the engraftment of MSC at the scaffold implantation site (Figure 3.24). Immunofluorescent staining also revealed a significant population of c-kit$^+$ and CD34$^+$ stem cells in the peri-implant region. Since SSEA-4 expression is characteristic of embryonic-like stem cell isolated from the bone marrow [186, 187], we additionally examined markers more consistent with literature on MSC phenotype [182]. The interface of SDF-1α treated scaffold implants also contains significant quantities of cells co-expressing these markers. Quantification of MSC density revealed an increase more dramatic than pretreatment studies, with the density and percentage of MSC in the SDF-1α approximately 3X higher for both parameters (Figure 3.25). Interestingly though, the density and percentage of c-kit$^+$ was not altered between treatment groups at week 2 as observed in week 1 of pretreatment studies.

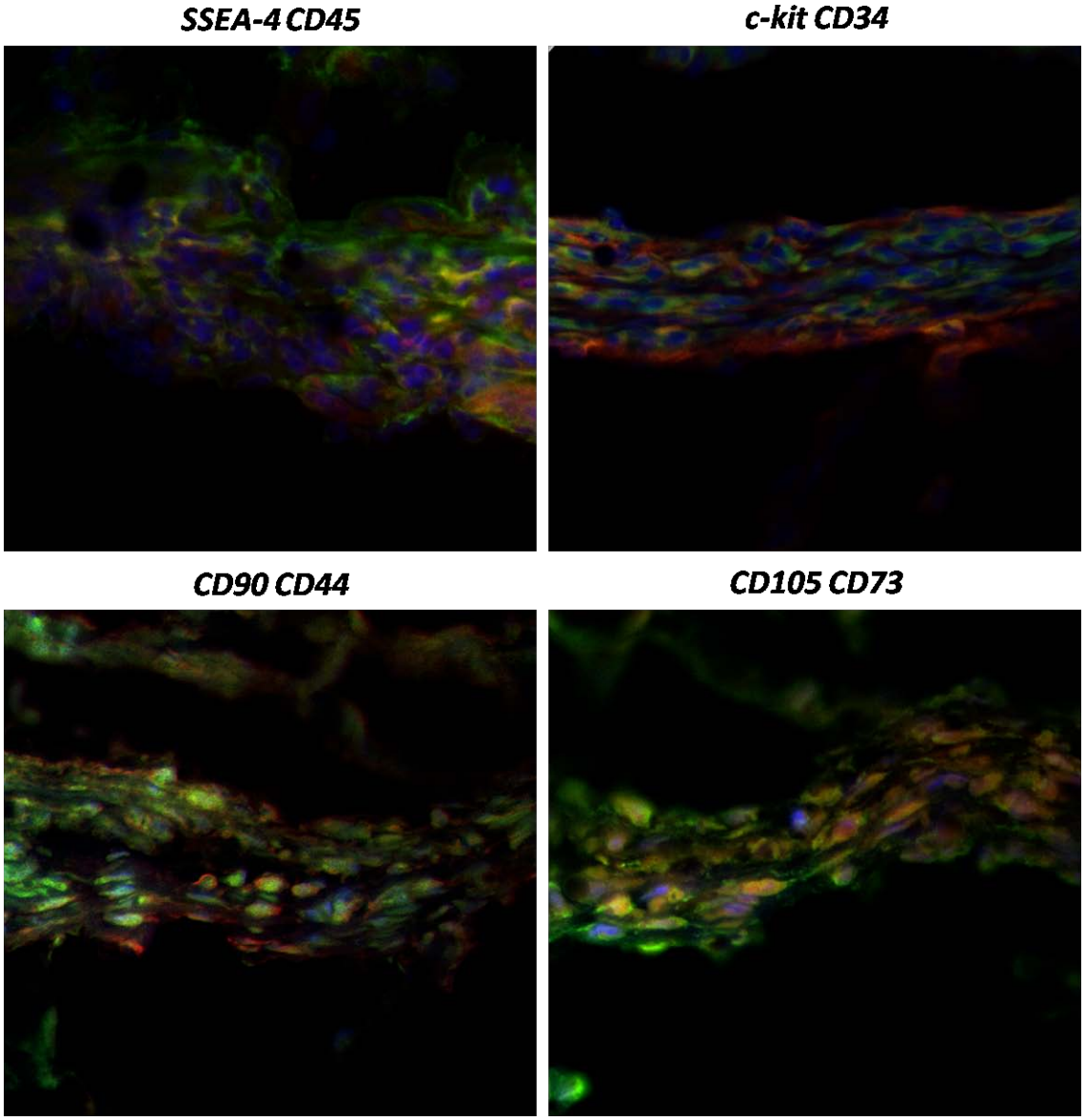

Figure 3.24 Stem cell expression at the interface of SDF-1α pump scaffolds. MSC expression of SSEA-4 (FITC-green) and CD45 (Texas Red – red) showed significant accumulation of MSC at scaffold interfaces. HSC expression of c-kit (FITC-green) and CD34 (Texas Red – red) showed cells expressing both HSC markers independently, as well as some with overlap of both markers. MSC at the scaffold interfaces also overlapped for many other MSC markers including CD90 (FITC – green) with CD44 (Texas Red – red) and CD105 (FITC – green) with CD73 (Texas Red – red).

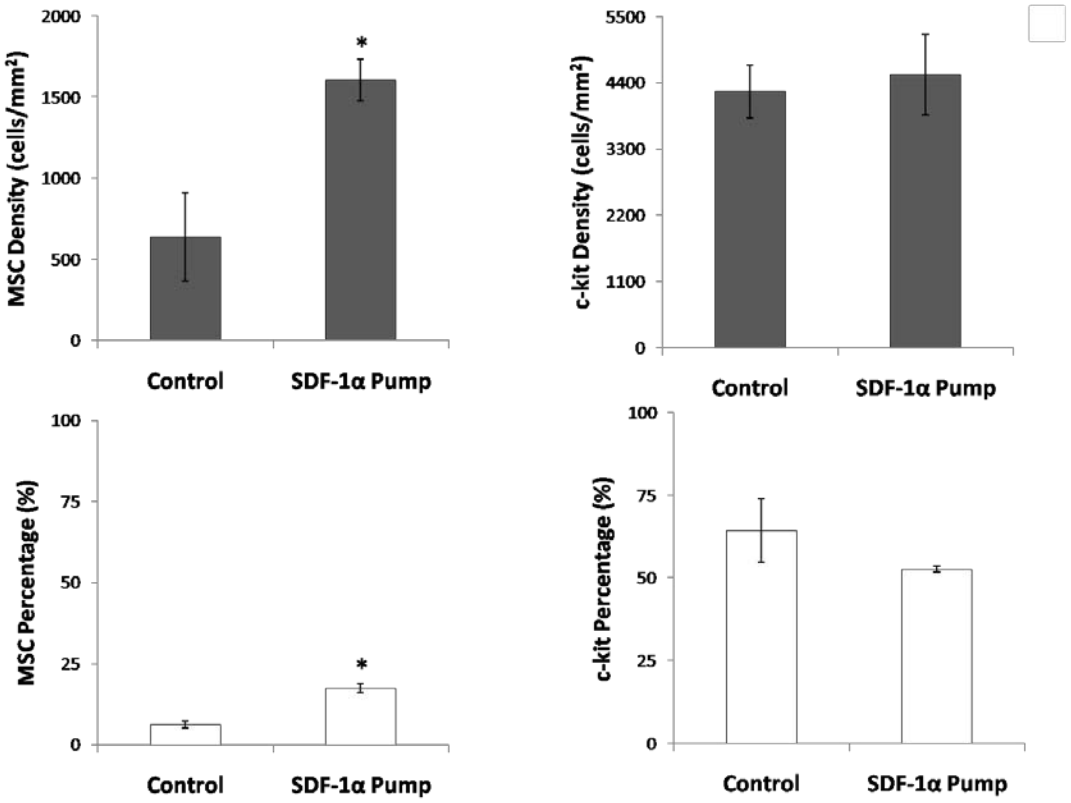

Figure 3.25 Quantified stem cell responses in SDF-1α pump scaffolds. Plotting the density and percentage of MSC reveals significant differences in both parameters after 2 weeks implantation (* indicates significant Student t tests, $P<0.05$). However, there was little quantified variation in c-kit expression between treatment groups.

Similar to pre-implantation soaking, we observe an altered mast cell response around the scaffold implants after 2 weeks. In the absence of SDF-1α, control scaffolds were surrounded by degranulated mast cells. However, the SDF-1α pump implants had a reduced total presence of mast cells and very few degranulated mast cells (Figure 3.26). These differences were quantified as a 59% reduction in mast cell response and a 75% decrease in degranulated mast cells at day 14 with respect to control implants.

Given that current models of biomaterial-mediated inflammatory responses suggest long-term effect of macrophages on foreign body reactions [16, 46, 72, 83], we used antibodies specific to murine macrophages as an additional comparison against the more general $CD11b^+$ marker which may include other cell types such as neutrophils. The density of $CD11b^+$ cells at the implant interfaces is much higher in control scaffold compared to SDF-1α pumps (Figure

3.26), similar to pretreatment studies. As expected, this trend is also apparent with regard to macrophages, as control scaffolds have a higher density of macrophages surrounding implants compared to SDF-1α scaffolds which have a lower density, with distribution restricted to small pockets long the skin side of the scaffold interface.

We next examined the relationship which emerged in soaked studies between MSC responses and $CD11b^+$ inflammatory cell responses. Interestingly, the same stem cell : inflammatory cell trend was present in the pump implants as previously witnessed in pretreatment implants, where MSC density is elevated with reduced inflammatory cell density with respect to control at 2 weeks. In addition, comparison of the inflammatory cell density between control saline and SDF-1α mini-osmotic pumps reveals a significant decrease with respect to untreated control.

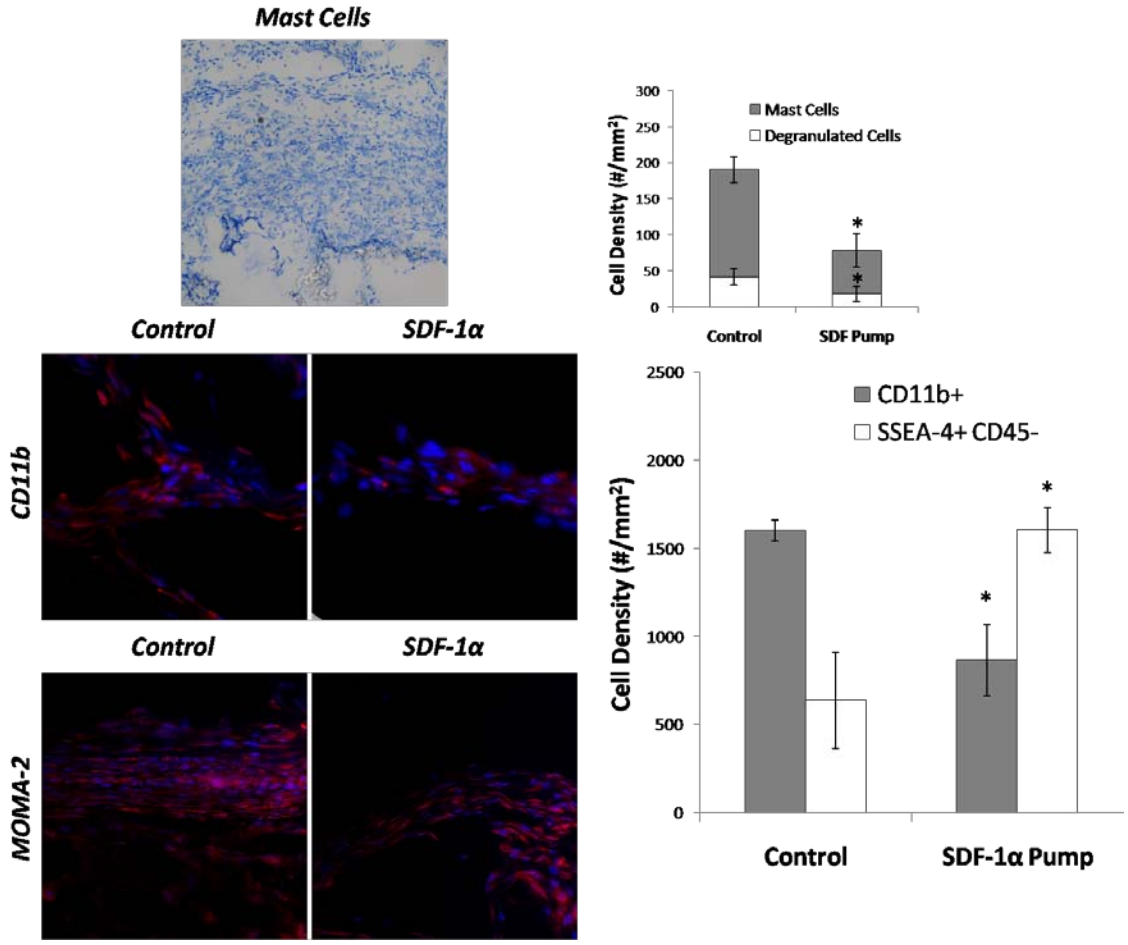

Figure 3.26 Effects of controlled SDF-1α release on inflammatory cell responses. Extended SDF-1α release was able to significantly reduce the density of both total and degranulated mast cells compared to control (* indicates significant Student t test, $P<0.05$). The density of CD11b cells and macrophage (assessed by MOMA-2 expression) were also less prominent in SDF-1α group. Plotting of CD11b and SSEA-4^{+} CD45^{-} cells reveals an inverse trend similar to soaking studies, with significantly altered values (* indicates significant Student t test, $P<0.05$).

Similar to the previous study, we next examined how these altered inflammatory cell response may be affecting the host response at the scaffold interface and interior. Histological analyses show onset of granulation tissue in control implants with a multi-cell thick leukocyte and fibroblast layer forming between the implants and surrounding tissue (Figure 3.27). In contrast, SDF-1α pump implants have reduced cell density and a less organized tissue capsule around the implants. Interestingly, we also found a 35% reduction in capsule thickness (data not shown) and 60% reduction in capsular cell density in SDF-1α pump connected implants. In

conjunction with the absence of this multi-cell thick granulation tissue, SDF-1α pump implants also had many vessels organized throughout the interface between the native tissue and the scaffold. Notably, this vessel formation in the interface at 2 weeks was less evident in control scaffolds.

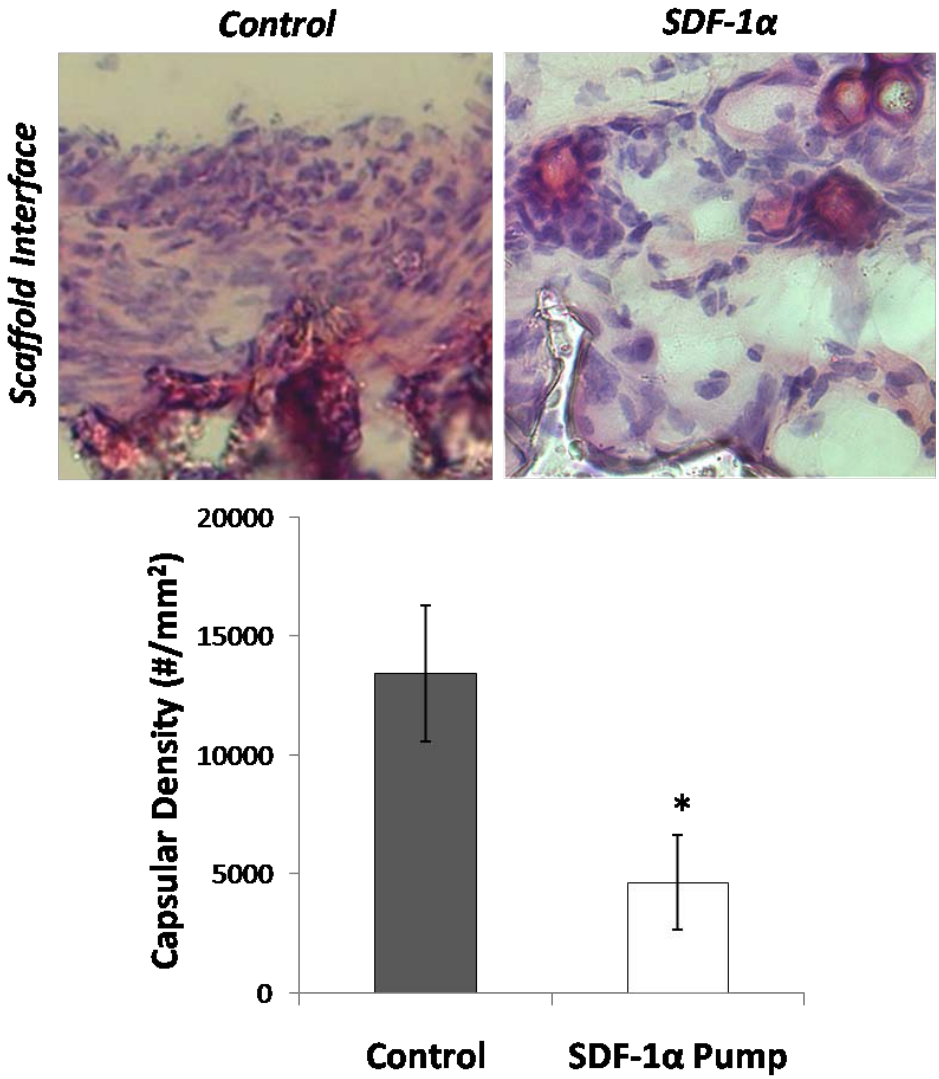

Figure 3.27 Controlled SDF-1α delivery reduces interface density and increases interface vessel formation. Similar to soaking studies, SDF-1α led to a decreased cell density at the interface, with less packed spindle shaped cells stacked above the scaffold interface. In addition, budding vessels could be identified in close proximity to the scaffold interface in SDF-1α scaffolds. Quantification of the cell density at the interface revealed significant differences between treatment groups (* indicates significant Student t test, $P<0.05$).

Having seen decreased inflammatory cell density and increased angiogenesis at the scaffold interface, we expected to find an increase in cellular infiltration into the scaffold. Indeed, we find substantial vertical and horizontal cell infiltration into scaffold resulting in only a small central area of the scaffold acellular at week 2 (Figure 3.28). Closer inspection reveals large bands of cells branching throughout the interconnected porosity of the scaffold. These bands appear to seamlessly transition from the interface of the scaffold through surface porosity, as opposed to the termination of cell infiltration at the fibroblast layer surrounding control scaffolds.

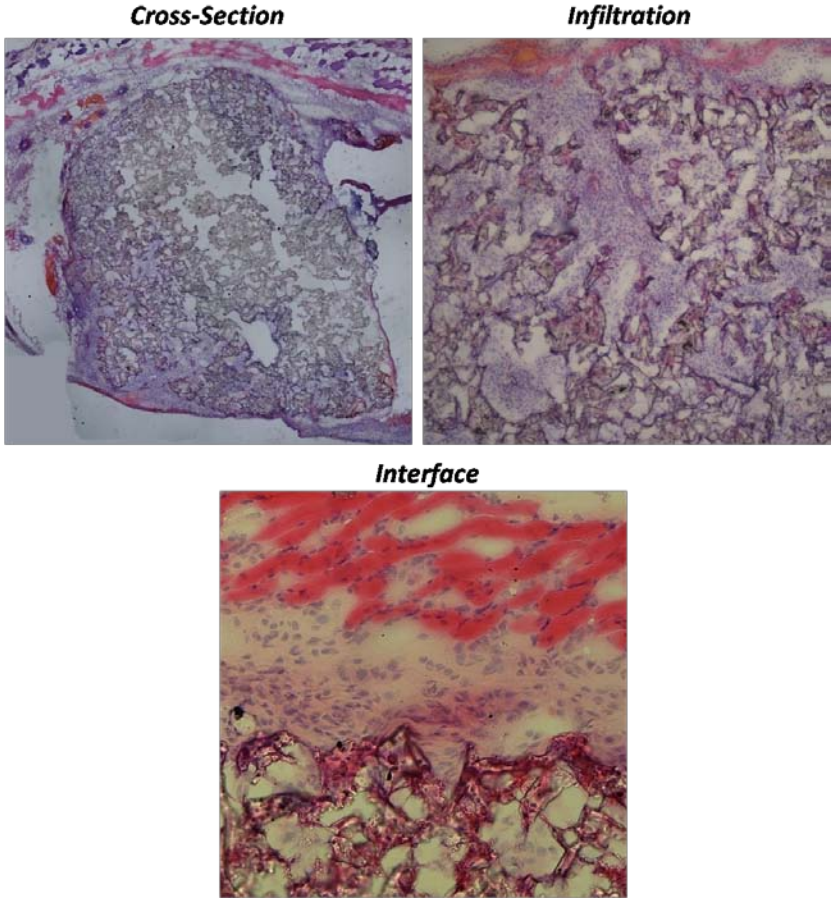

Figure 3.28 Histology of 2 week SDF-1α pump implants. H&E staining of scaffold cross-sections showing significant vessel formation and cell infiltration into the scaffold. Magnified view of the scaffold core shows cells infiltrated throughout the porous structure of the scaffold. Magnified view of scaffold interface depicts a low density interface without hallmark signs of fibrotic encapsulation.

As previously mentioned, 2 week control implants were characterized by a thick encapsulating cell layer as part of the developing fibrotic tissue around the scaffold implants. However, SDF-1α consistently altered these cellular responses. Specifically in all cases SDF-1α administration from onset was accompanied by an increase in MSC at the interface and decrease in $CD11b^+$ cells. These implant interfaces are normally dominated by $CD11b^+$ during the acute and chronic inflammatory responses. These trends led us to consider that the differences in $CD11b^+$ cell responses and macrophage responses may be due to altered activation of the macrophages, leading to macrophage participation in other aspects of wound healing. Though we have previously investigated both $CD11b^+$ cell responses and macrophage responses independently, and qualitatively noticed a smaller than usual percentage of macrophage relative to total $CD11b^+$, we employed co-expression of the two markers to verify this finding (Figure 3.29). Indeed we find that roughly half of the already reduced density of $CD11b^+$ cells co-express the macrophage marker MOMA-2. Recent evidence suggests that bone marrow-derived macrophages participate in angiogenesis and lymphogenesis at the sites of inflammation [50, 188]. We thus investigated the potential role of bone marrow-derived macrophages in scaffold-associated tissue responses based on the co-expression of $CD11b^+$ $VEGFR\text{-}1^+$ (mononuclear myeloid cells with the capacity to induce proangiogenic activities) [50] and $CD11b^+$ $LYVE\text{-}1^+$ (macrophages which participate in lymphangiogenesis in healing tissue) [188]. Interestingly, we observed little participation of these specialized $CD11b^+$ $VEGFR1^+$ macrophages in control implants. However, at sites of vessel formation in SDF-1α treated implants we observe co-staining identifying these cells in the presence of budding vessels. In addition, we see a few $CD11b^+$ $LYVE\text{-}1^+$ cells in control scaffolds, with these cells expressed at specific locations throughout the interface in SDF-1α treated implants.

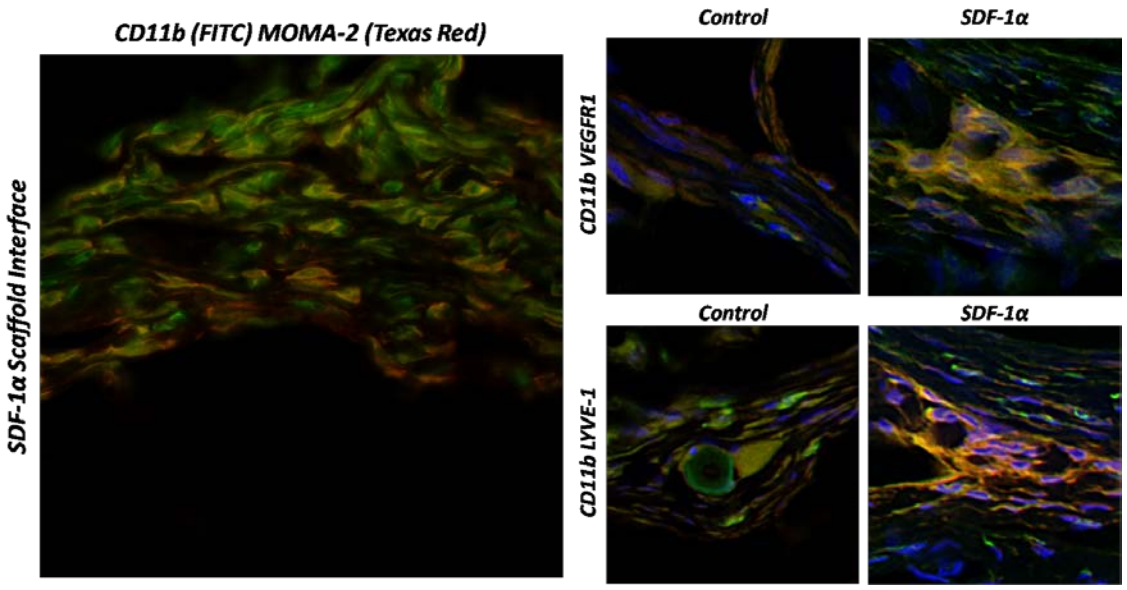

Figure 3.29 Analysis of macrophage and macrophage phenotypes at the tissue interface. The percentage of macrophages at the implant interface was visualized by double staining for CD11b and MOMA-2, representing dually expressed markers for macrophages. These cells represent a slight majority of $CD11b^{+}$ cells at the implant interface. Further analysis of macrophage phenotype which participate in wound healing processes reveals prominent expression of CD11b (FITC – green) VEGFR1 (Texas Red – red) and CD11b (FITC – green) LYVE-1 (Texas Red – red) positive macrophages in SDF-1α treatment group.

Since the interfaces of SDF-1α treated scaffolds showed increased vessel formation at the interface along with the presence of macrophage phenotypes linked with angiogenesis and, given previous literature studies which have suggested angiogenic properties of SDF-1α, we further investigated the presence of endothelial precursor cells. These studies have shown that SDF-1α levels in peripheral tissue serve as a trap for angiogenic stem cells recruited to the circulation from the bone marrow [137, 164, 189]. Therefore, using 2 week SDF-1α pump implants from which we observe improved angiogenesis in histological analysis, we additionally analyzed interfaces for endothelial progenitor cell (EPC) engraftment (Figure 3.30). First, interfacial vessels identified in H&E stains were tested for expression of laminin, a component of basal lamina. As expected, vessel-like formations at the scaffold interface expressed laminin prominently within spherical rings of DAPI positive cells forming the vessel. To verify that these cell formations were endothelial cells, CD31 expression was verified. Additionally, CD31

expression was double stained against CD133, a marker expressed by endothelial progenitor cells which is lost after terminal differentiation [190]. CD31 positive endothelial cell formations contain cells co-expressing CD31 and CD133 consistent with EPC expression. However these cells are not restricted to the interface. Within the scaffold interior, vessel formation could be identified expressing even more plastic markers of EPC, specifically CD34 and CD133.

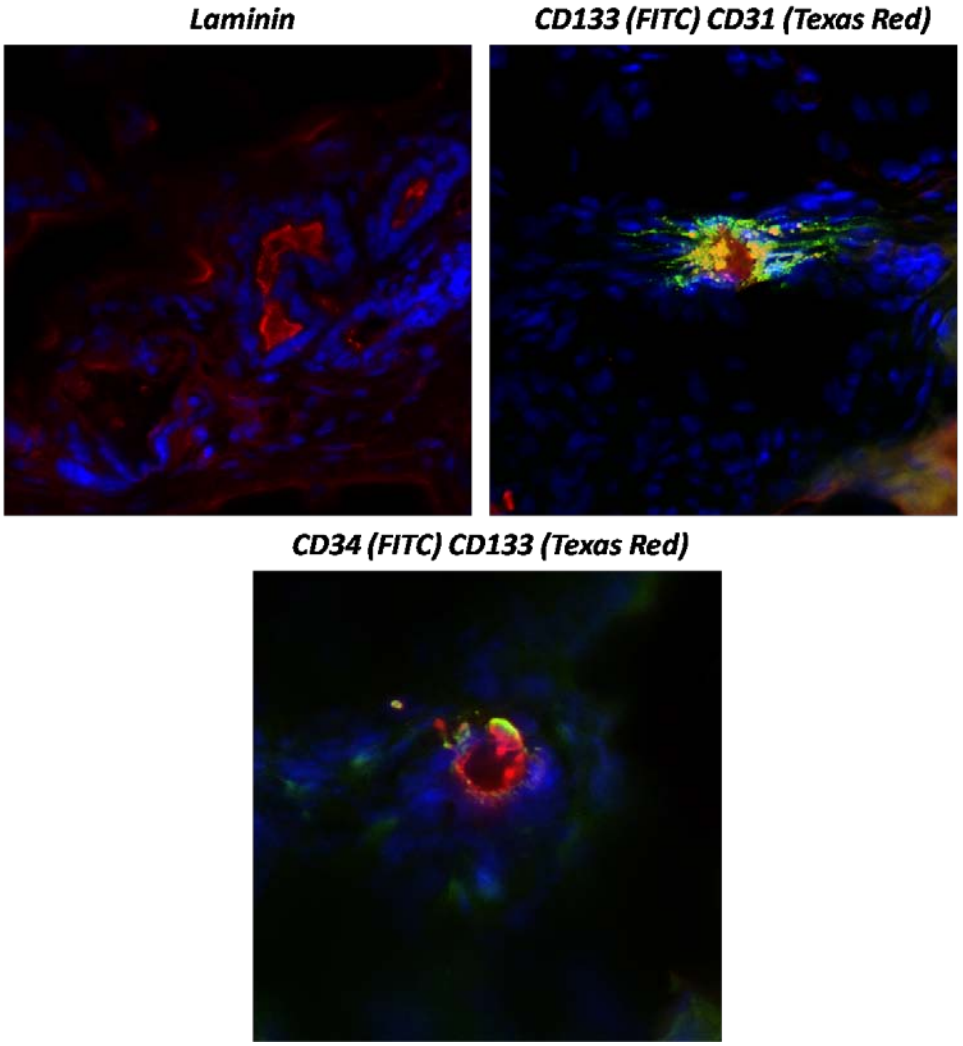

Figure 3.30 Endothelial progenitor cell participation in interface vessel formation due to SDF-1α delivery. The presence of properly structured vessels at the SDF-1α interface was verified by examining expression of laminin. Endothelial cells in vessels was verified by CD31 staining (Texas Red – red). The possible participation of EPC in vessel formation was examine using CD133 (FITC – green) overlapped with CD31 (Texas Red – red). To further characterize EPC, CD34 (FITC – green) and CD133 (Texas Red – red) was examined. In all cases targets could be identified consistently at the interface of SDF-1α treated scaffolds.

The balance between constructive remodeling and fibrosis was additionally assessed through quantification of collagen deposition around the exterior of the biomaterial. Given that SDF-1α decreased inflammatory cell responses while still increasing MSC and EPC response, we hypothesized that these interactions may have affected this balance, away from fibrotic reactions. We therefore examine the deposition of collagen around scaffold implant using Masson Trichrome staining. Notably, through this stain, we were able to more clearly identify both the exterior and interior presence and structure of vessel formation in SDF-1α scaffolds (Figure 3.31). In addition, control scaffolds show a characteristic 2 week fibrotic response with a thick layer of collagen deposition surround the scaffold implants (Figure 3.32). In contrast, SDF-1α treated scaffolds had a very thin layer of collagen formation compared with controls.

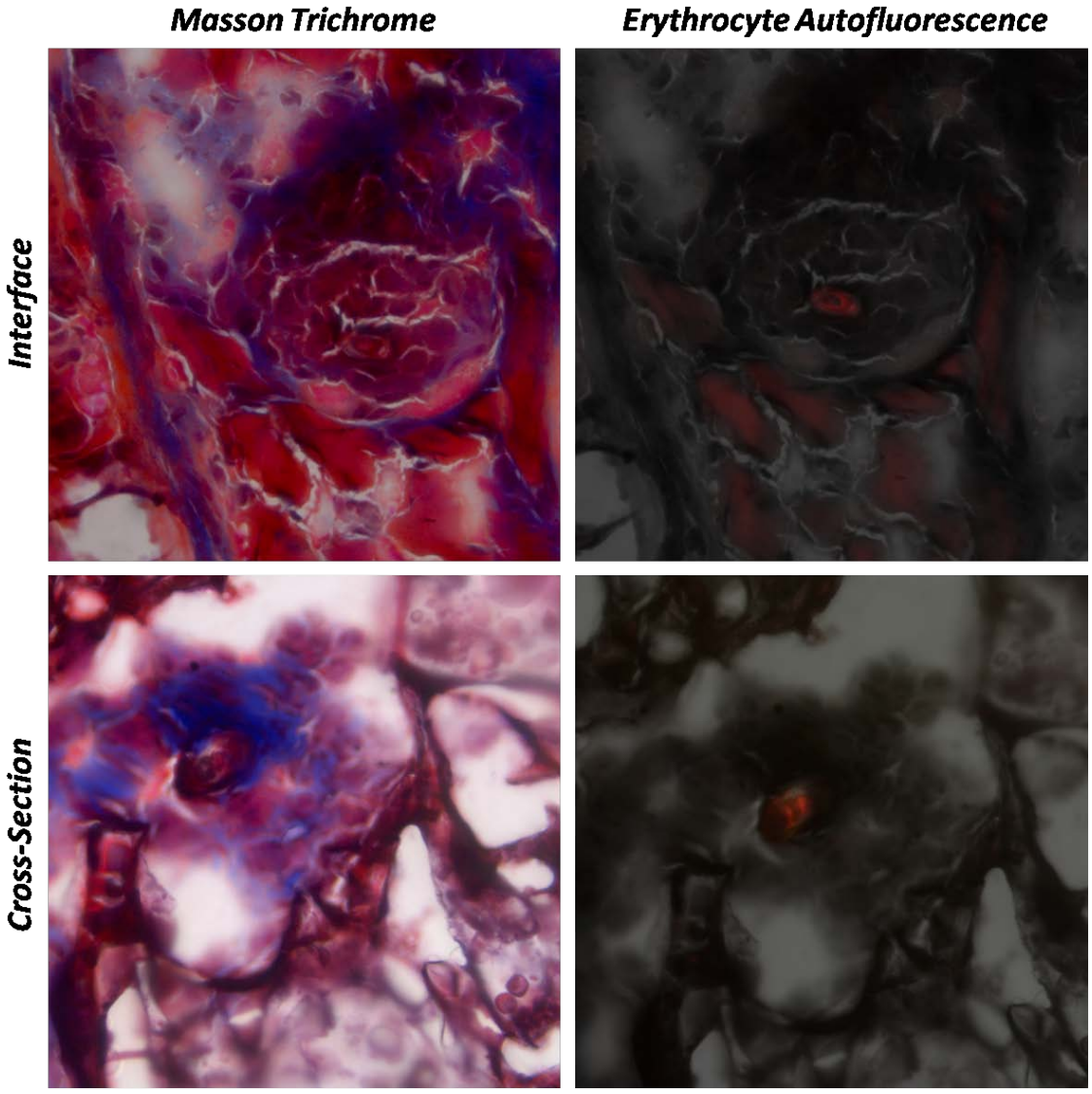

Figure 3.31 Blood vessel formation at SDF-1α scaffold interfaces and intra-scaffold. Masson Trichrome staining was able to clearly distinguish the structure of newly formed vessels by comparing stains with autofluorescent emission from erythrocytes within the vessels.

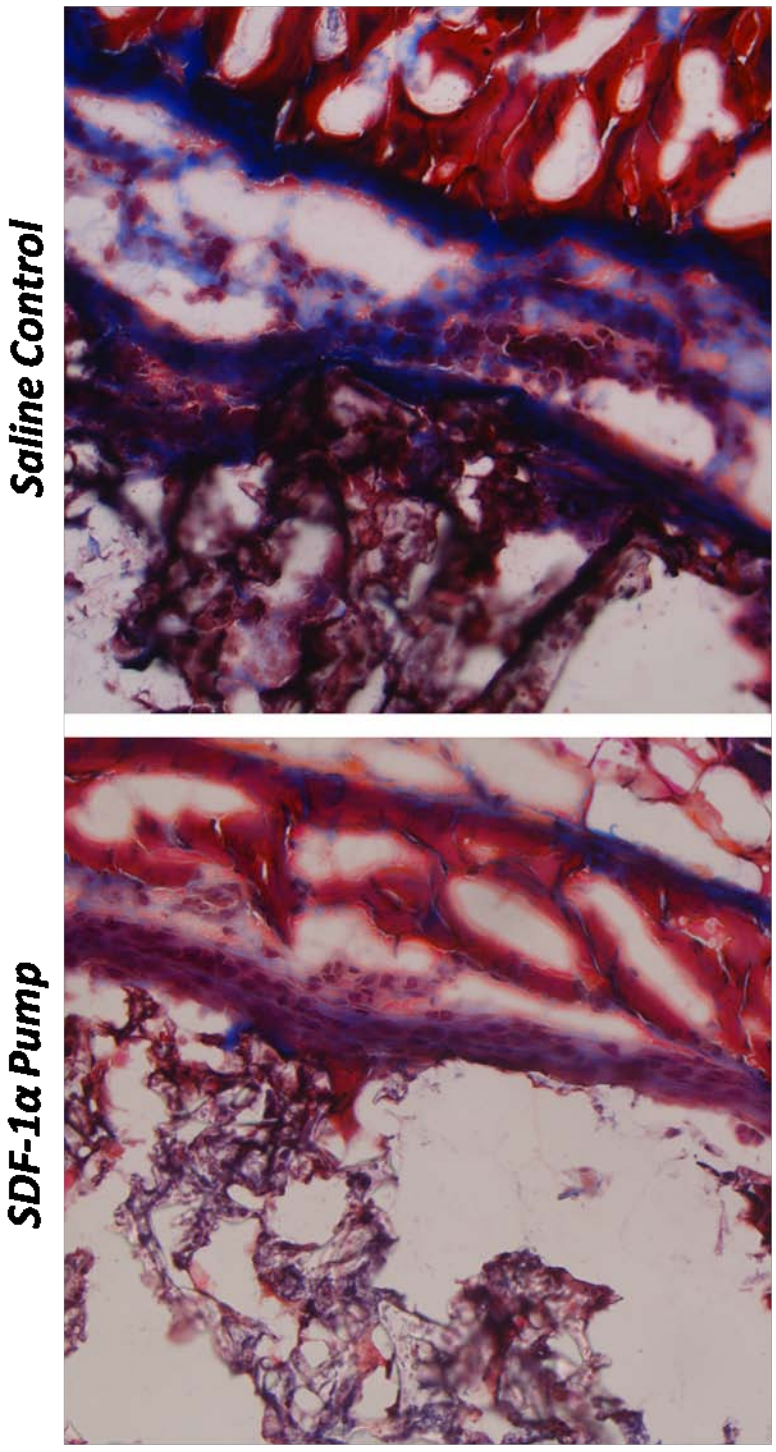

Figure 3.32 Collagen deposition at the interface of treated and untreated scaffolds. Masson trichrome staining showed significant collagen deposition at the interface of control implants. However, collagen staining of SDF-1α pump scaffolds showed a substantially decreased presence of collagen at the interface, indicated by the lack of methylene blue staining.

Given that studies suggested a complex relationship between inflammatory cells, fibroblasts, and granulation tissue as well as subsequent fibrotic responses, and since SDF-1α release appears to alter these processes, we determined the characteristics of the local cytokine/chemokine environment using protein micro-arrays. In agreement with histological evaluation, we have found that the presence of SDF-1α reduced the production of a variety of inflammatory cytokines and chemokines produced by a variety of cells during inflammation, including IL-13, IL-3Rβ, IL-4, IL-5, IL-9, Leptin R, L-selectin, Lymphotactin, MIP-3α/β, TCA3/CCL1, and TNF-α (Figure 3.33). Specifically, in support of altered mast cell responses we find the mast cell growth factors IL-3, IL-4, and IL-9 are substantially downregulated. It should also be noted that the treatment with SDF-1α profoundly increased the release of several inflammatory cytokines produced during inflammation, including GCSF, GM-CSF, IL-6, KC/CXCL1, MIP-1α/CCL3, MIP-2/CXCL2, PF-4/CXCL4, sTNF RII/CD120b, TARC/CCL17, and TIMP-1.

Interestingly, the treatment of SDF-1α was found to reduce the production of several pro-fibrotic cytokines, including IL-13, PF-4/CXCL4, and TIMP-1. In addition, in support of SDF-mediated angiogenic responses, we observe high upregulation of many cytokines related to angiogenic processes, including IGFBP-3, VEGF, and GM-CSF. Finally, treatment with SDF-1α appears to have significant influence on many other factors, including G-CSF, VEGF, and CXCL16, related to stem cell mobilization and homing. Surprisingly, the levels of tissue expression for SDF-1α are only slightly higher (< 2X increase) in the tissue and scaffold infiltrating cells of SDF-1α treated implants.

Most convincing of these cytokine comparisons is the uniform decrease in cytokines associated with macrophage activation in SDF-1α scaffolds. Cytokines involved in macrophage activation including CD40 (>2X), TNF-α (>2), IFN-γ (>1.5), IL-4 (>2), IL-10 (>2), IL-13 (>5), IL-1β (>1.2), and Lymphotactin (>3) are decrease in SDF-1α scaffolds with respect to control.

Protein	Expression		Protein	Expression	
	Increase	Decrease		Increase	Decrease
Axl	1.20		IL-9		5.21
BLC/CXCL13	1.55		KC/CXCL1	8.56	
CD30 L		2.62	Leptin		1.80
CD30 T		1.57	Leptin R/CD295		4.26
CD40		2.15	LIX/CXCL5		1.07
CRG-2/CXCL10		2.70	L-Selectin/CD62L		2.08
CTACK/CCL27		2.25	Lymphotactin/XCL1		3.26
CXCL16	2.80		MCP1 /CCL2	1.80	
Eotaxin/CCL11	2.01		MCP-5/CCL12		1.45
Eotaxin-2/CCL24		2.03	M-CSF		1.41
Fas Ligand/CD95L		3.98	MIG/CXCL9	1.32	
Fractalkine		1.49	MIP-1α /CCL3	24.39	
GCSF	81.90		MIP-1γ /CCL9	1.29	
GM-CSF	49.57		MIP-2/CXCL2	120.63	
IFN γ		1.70	MIP-3 β /CCL20		2.14
IGFBP-3	6.01		MIP-3α /CCL19		2.67
IGFBP-5		1.22	PF-4/CXCL4	7.06	
IGFBP-6		1.99	P-Selectin/CD62P		1.12
IL-1 β		1.20	RANTES/CCL5	1.76	
IL-10		2.12	SCF/CD117		1.74
IL-12 p40/p70	3.33		SDF-1α /CXCL12		1.39
IL-12 p70		1.74	sTNF RI/CD120a		1.14
IL-13		5.02	sTNF RII/CD120b	2.91	
IL-17	1.47		TARC/CCL17	3.41	
IL-1α		1.18	TCA-3/CCL1		4.27
IL-2		1.71	TECK/CCL25		1.07
IL-3		1.91	TIMP-1	2.05	
IL-3 Rβ		2.74	TNFα		2.57
IL-4		2.14	TPO		1.24
IL-5		3.46	VCAM-1/CD106	1.13	
IL-6	13.54		VEGF	2.93	

Figure 3.33 Inflammatory cytokine expression in the scaffold and adjacent tissue. Cytokine expression was quantified and compared to control scaffolds. Values tabulated are multiplications increased or decreased for each cytokine examine.

3.7.4 Discussion

Though SDF-1α may not contribute to the degree of inflammatory cell infiltration as shown in some blockage studies [189], it may contribute to activation of macrophages along a particular phenotype as supported by our macrophage phenotypic analysis.

The release of SDF-1α was also found to reduce many potent pro-inflammatory cytokines, including TNFα, IL-1β, MIP3α/β, lymphotactin/CXCL1, L-selectin, leptin receptor, IL-9, IL-5, IL-10, Eotaxin-2, CTACK/CCL27, CRG-2/CXCL10, CD30L. Reduction in these

cytokines may be responsible for the less destructive inflammatory reactions to scaffold implants [16, 191, 192]. Though interestingly, many proinflammatory cytokines which have been linked with stem cell responses and angiogenesis were highly upregulated in SDF-1α treated implants, specifically MIP-2 (120.6X), G-CSF (81.9X), GM-CSF (49.6X), KC (8.6X), MIP-1α (24.4X) and IL-6 (13.5X). In addition, decreases in inflammatory cell engraftment, downregulation in cytokines related to macrophage activation, and the presence of macrophage subsets related to angiogenesis and lymphangiogenesis suggests that stem cell interactions and the presence of SDF-1α is likely improving tissue responses to the biomaterial, thereby preferentially increasing tissue compatibility. These results suggest a potentially complex interaction between SDF-1α, inflammatory responses and stem cell responses.

Since biomaterial-mediated inflammatory responses are often followed by fibrotic tissue reactions [193], it is not surprising to find that SDF-1α treatment reduces not only inflammatory responses but also capsule formation surrounding scaffold implants. It is also possible that SDF-1α treatment may have a more direct influence on the extent of collagen production. Indeed, our protein array results have shown that IL-13, a cytokine implicated in fibroblast proliferation and collagen production [194], is substantially reduced in tissue exposed to SDF-1α. In addition, our results have shown that SDF-1α treatment reduce Fas Ligand production (3.94x). It should be noted that Fas Ligand appears to be involved in biomaterial-mediated fibrosis [195], and reduced Fas Ligand has been shown to attenuate fibrotic tissue reactions [196, 197]. However, the molecular mechanisms governing SDF-1α-mediated reduction in fibrotic reactions to scaffold implants have yet to be determined.

It is well established that inflammatory products play an essential role in promoting tissue regeneration and angiogenesis [198, 199]. Thus, wound healing responses were impaired when treated with anti-inflammatory agents, such as Dex [200]. However, our results show that SDF-1α can not only reduce inflammatory responses, but also promote tissue regeneration/angiogenesis. Many recent results may shed some light on this interesting

phenomenon. First, it was shown that SDF-1α is involved in the recruitment of $CXCR4^+$ $VEGFR1^+$ hematopoietic progenitors (hemangiocytes) which accelerate revascularization [201]. Second, SDF-1α regulates adhesion of stem cells in vitro and in vivo and promotes differentiation of $CD34^+$ cells to endothelial progenitor cells [202]. Finally, a recent study has shown MSC secrete SDF-1α in culture and that MSC conditioned media concentrated and delivered to a wound site resulted in accelerated wound healing [165].

As previously mentioned, though long-term cytokine delivery is commonly included in TE designs, little consideration is generally given to the mechanisms governing their observed responses in lieu of long term histological responses. Although various cytokines (including VEGF, PDGF, and FGF) have been incorporated into scaffolds to enhance angiogenesis [22, 203, 204], these investigations have not explicitly focused on how factors such as these may affect the cascade of the inflammatory and wound healing responses. Here we show that delivery of SDF-1α not only enhanced MSC and HSC migration, but also EPC ($CD34^+$ $CD133^+$) engraftment near the scaffold. In addition, many budding vessel formations identified in H&E stains can be identified through subsequent tissue sections and routinely labeled for CD31, α-SMA, and Laminin, in support of evidence which suggests EPC differentiation in angiogenesis to $CD31^+$ and $\alpha\text{-SMA}^+$ cells [205]. The ability of SDF-1α to generate a pro-angiogenic environment is well supported by the results of a protein assay performed on the scaffolds and surrounding tissue after two weeks of implantation. Though the participation of recruited cells in angiogenesis was not determined, our findings here may provide a novel strategy to improve host responses to biomaterials though recruiting autologous stem cells for tissue regeneration, while providing a suitable environment for transplanted cell-containing scaffold with a reduced fibrotic capsule and improved angiogenic environment.

CHAPTER 4

THE INFLUENCE OF MAST CELL RESPONSES ON THE RECRUITMENT OF FIBROCYTES AND FACTORS DICTATING THEIR SUBSEQUENT PARTICIPATION IN BIOMATERIAL-MEDIATED FIBROTIC RESPONSES

4.1 Introduction

Despite substantial improvements in biomaterial design, almost all biomaterial implants initiate inflammatory and fibrotic responses [179]. These responses are characterized by inflammatory cell adherence to the biomaterial over the first week, subsequently leading to fibroblast proliferation and encapsulation of the implant followed by development of a collagenous matrix [206]. This matrix separates the biomaterial from the native tissue and ultimately contributes to failure of the biomaterial to more naturally integrate with native tissue and regenerate tissue matrix, as shown in previous chapters.

These responses are initiated almost immediately after implantation, when mast cells infiltrate and degranulate near the biomaterial implant (biomaterial-mediated foreign body response summarized Figure 4.1), presumably mediated by the soluble complement components C3a and C5a [41]. Histamine released from degranulated mast cells has previously been linked with subsequent inflammatory cell diapedisis and adherence to biomaterial implants [40]. As time progresses, the mast cell response diminishes around the implant, in conjunction with the progression of macrophage and fibroblast responses, which over time develops into the fibrotic capsule [207]. Additional evidence suggests that the degree of fibrotic reactions may be linked to mast cell production of IL-4 [208], IL-13 [206], FGF-2, TGF-β, and TNF-α [209] as well. However, mast cell release of other chemokines/cytokines in granular contents or by other secretions in relationship to biomaterial mediated responses is not well understood [210, 211].

Though data on mast cell responses governing biomaterial mediated responses is limited [40, 212], there is evidence to show that mast cell activation may be dependent upon biomaterial physical or chemical properties, specifically related to the manner in which opsonizing proteins (complement and fibrinogen) interact with the implant [212]. In fact, the long term presence of mast cells at the implantation site may be related to the degree of fibrotic encapsulation [209].

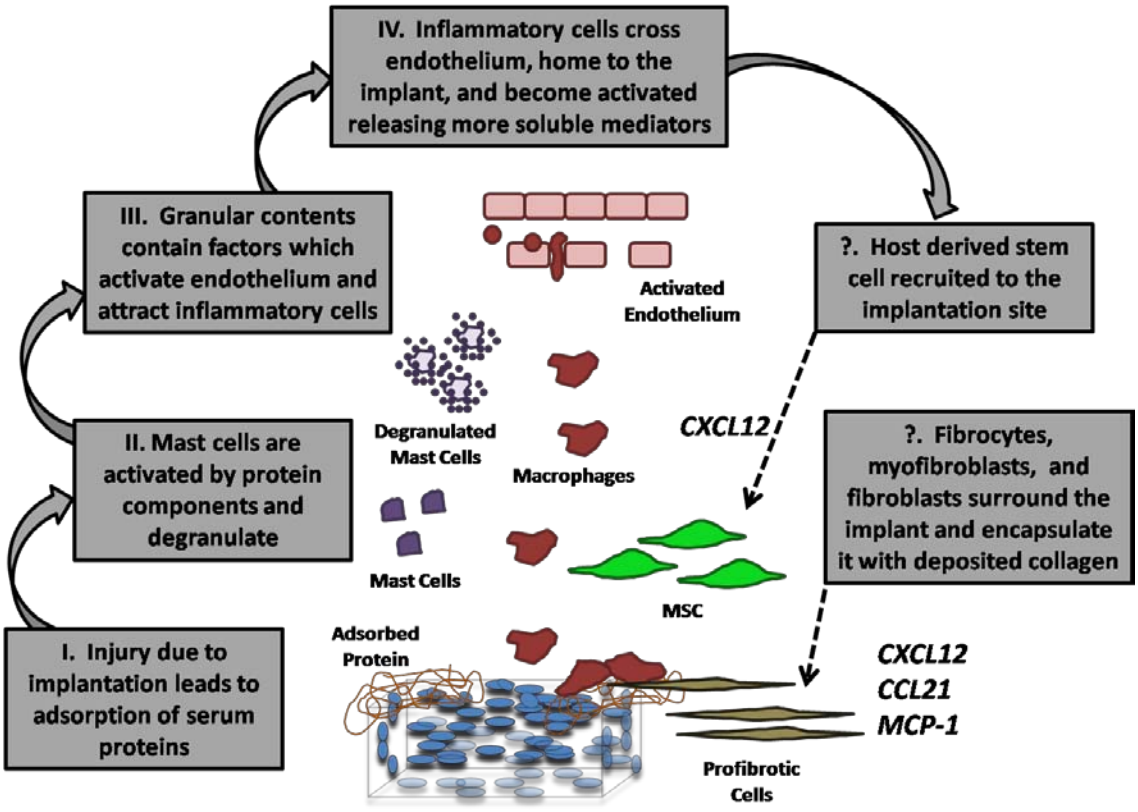

Figure 4.1 Biomaterial-mediated fibrotic responses. Protein interactions with the biomaterial lead to mast cell activation, resulting in the recruitment of leukocytes, fibrocytes, and host derived stem cells. Cytokines release from degranulated mast cells and activated macrophages presumablely represent the source of the chemokines which recruit fibrocytes and host derived stem cells.

We hypothesized that mast cell responses are directly associated with the fibrotic pathogenesis of biomaterial implants. Specifically, we hypothesized that in addition to mast cell influence on downstream inflammatory cell chemotaxis, they may also dictate fibrocyte

recruitment, differentiation, and host derived stem cell recruitment to the implantation site. Our group has recently found that biomaterials appear to initiate a predictable host derived SSEA-4^{+} CD45^{-} mesenchymal stem cell response peaking at 1 week after implantation of the biomaterial in the subcutaneous cavity [44]. This response can be manipulated through incorporation of stem cell chemokines (in our case, SDF-1α) with the scaffold, resulting in increased MSC engraftment and improved inflammatory and fibrotic outcomes [44]. Many groups have reported on the effects of MSC on inflammatory responses, suggesting a beneficial cell:cell and/or paracrine influence [124]. However, recent work on the mechanisms of fibrosis has led to the discovery of the fibrocyte, a CD34^{+} CD45^{+} blood leukocyte which arrives at injury sites within the first week after injury [151, 213-215], which may use the same SDF-1α/CXCR4 axis [216]. However, some conflicting observation on the primary chemotactic regulator of fibrocyte responses exists [217, 218]. Regardless of their homing axis, after arrival fibrocytes (CD45^{+} collagenI^{+}) participate in fibrotic reactions through differentiation to myofibroblasts (α-SMA^{+}) and secretion of collagen I, vimentin, and other proteins which influence the developing fibrotic matrix [214, 216, 217, 219].

Unfortunately, very little is understood regarding the participation of host derived stem cells and fibrocytes in biomaterial mediated host responses. However, our hypothesis is that there may be a relationship between fibrocyte and stem cell responses. Given the response to a particular biomaterial, the relationship between these cells may provide clues as to the downstream fibrotic potential of a biomaterial mediated response as well as therapeutic targets to modify these responses. In addition to previously mentioned fibrocyte responses in fibrosis, recent evidence suggests that modulation of Thy-1 (CD90) expression [220], present on both MSC and fibroblasts, particularly decreased expression, may signal a progression toward fibrosis. Thy-1- fibroblasts have been shown to have increased myofibroblast differentiation potential, a greater proliferative and fibrotic response to inflammatory cytokines (TNF-α and TGF-β), increased collagen deposition, and resistance to apoptosis in a contracting collagen

matrix [221]. Interestingly, Thy-1 knockout mice appear to generate a greater fibrotic response when challenged despite similar inflammatory cell responses [222]. In our previous study of host-derived MSC recruitment to biomaterial implants [223], MSC recruited to the implantation site through incorporation of a MSC chemokine increased MSC recruitment and decreased fibrosis. Thy-1 expression has been well characterized for MSC and is commonly used in conjunction with other markers to identify MSC in vivo [182]. However, the link between Thy-1 expression and myofibroblast differentiation has yet to be determined. We believe these findings support possible interactions between fibrocytes and MSC in the pathogenesis of biomaterial-mediated fibrotic reactions.

Fibrocytes in wounded skin models traffic into wound sites expressing CD34 and CD45 in combination with markers of mesenchymal cells, including Collagen I (prolyl hydroxylase) and vimentin [151, 224]. As their progression shifts toward myofibroblast differentiation, expression of CD34 and CD45 is diminished with increasing expression of α-SMA [216, 225, 226]. We hypothesize that interactions between upstream inflammatory cells, recruited host-derived MSC, and fibrocytes may be linked with the degree of myofibroblast differentiation and density at the implantation site and the loss of Thy-1 expression in fibroblasts near the implantation site.

Therefore, this study was designed to investigate the potential influence of mast cells on host-derived stem cell and fibrocyte responses. In order to analyze these responses, PLGA (a commonly employed, FDA approved biomaterial) films were incorporated with mast cell destabilizing or stabilizing chemicals in addition to unmodified films. Films were incorporated with either Compound 48/80 or Cromolyn, both having well documented mast cell interactions, to generate variable biomaterial-independent mast cell responses. Downstream host interactions to the films were then monitored with regards to inflammatory and fibrotic outcomes.

4.2 Characterization of the Cell Populations which Constitute the Granulation and Fibrotic Tissue in Biomaterial Implants

4.2.1 Introduction

Fibrocytes have been shown to mediate many pathological fibrotic conditions [226]. However, their potential involvement in biomaterial-mediated responses has not been well established. However, we hypothesized that they are the likely source of α-SMA producing cells, which tend to gather near the biomaterial interface shortly (about 1 week) after implantation. Interestingly, this arrival period coincides with the arrival of macrophages to the implantation site, bringing into question (a) the possibility of similar cascades leading to macrophage and α-SMA expressing cell recruitment, and (b) the question of whether fibrocytes, the progenitor cell which differentiates to α-SMA producing cells, may arrive in the context of macrophage recruitment or prior to macrophage recruitment. Our hope in proposing these experimental questions is to identify potential targets to modulate their recruitment and activation to improve biomaterial mediated fibrotic responses. Additionally, we are interested in reporting the possibility of coordination or correlation between fibrocyte recruitment and host stem cell recruitment, as shifts in the balance of these two cells may dictate downstream wound healing verses fibrosis.

4.2.2 Materials and Methods

4.2.2.1 Biomaterial film fabrication and implantation

PLGA films were fabricated using the solvent casting technique. Briefly, PLGA (75:25, 113kDa, Medisorb Inc., Birmingham, AL) was dissolved at 10% w/v in dichloromethane (Sigma Aldrich, St Louis, MO). Films were then cast into Teflon molds with the solvent allowed to evaporate overnight in a chemical fume hood. For all film conditions, the resulting film had a thickness of ~ 1mm. Films were cut into 5mm disks and stored at -20°C until implantation. C57 mice (Jackson Labs) were selected for equal age and sex prior to housing by implantation condition. Biomaterial implantations were performed as previously described. Briefly, each mouse (n=3 for all studies) was implanted with two films of equal treatment condition, with films

placed laterally on either side of the dorsal incision tucked into the subcutaneous space approximately 15mm away from the midline incision. The incision was closed with surgical clips and the mice returned to housing. The mice were monitored daily for irritation around the implantation for 1 week until explantation.

4.2.2.2 Histological evaluation of the inflammatory and fibrotic cells at the biomaterial interface.

Implant recovery, cryosectioning, and histological and immunohistochemical analyses were performed as described in previous chapters. The recruitment of specific cell populations was monitored through immunofluorescence staining of interface cells. Specifically, the presence of macrophages was monitored using MOMA-2 antibody (Serotec, Oxford, UK). Myofibroblasts were estimated via detection of α-SMA (Santa Cruz Biotech, Santa Cruz, CA) expressing cells inside the interface. MSC were monitored by positive expression for SSEA-4 and CD90 (Santa Cruz Biotech, Santa Cruz, CA).

4.2.2.3 Recovery, characterization, and culture of tissue fibrocytes

Fibrocytes were recovered using a subcutaneous wound chamber system, and cultured as previously described [151]. Modifications to this system were employed as previously described in Chapter 3. Conduits were sterilized and implanted subcutaneously as described for PLGA films. After 1 week implantation, C57 mice were anesthetized and conduits were flushed aseptically with PBS to recover cells inside the conduits. The exudate was centrifuged to obtain cells and the remaining supernatant was stored at -20°C. Cells were also obtained by cardiac puncture as previously described [151]. The heparinized blood collected or implant exudates were centrifuged and recovered cells cultured in DMEM containing 20% FBS. Non-adherent cells were removed after 48hrs and media replaced subsequently every third day. Cells were detached using a cell scraper and replated into new 75cm^2 flasks weekly for 4 weeks prior to verification of phenotype by FACS array and immunofluorescent staining of cells adhered to coverslips. Fibrocytes were verified via expression of a hematologic marker CD45

with connective tissue matrix synthesis markers collagen I and vimentin on cell seeded coverslips (Santa Cruz Biotech, Santa Cruz, CA).

4.2.3 Results

First, we characterize the tissue response to PLGA implants in C57 mice (Figure 4.2). H&E staining of the biomaterial interface after 1 week implantation reveals an accumulation of cells at the interface between the material and native skin tissue. In addition, Masson Trichrome staining for collagen indicates prominent staining of the interface. As expected, this layer is well infiltrated with cells staining positive for MOMA-2 indicating a macrophage phenotype consistent with presence of leukocyte morphology cells in H&E stains. Since developing fibrotic tissue contains contractile α-SMA^{+} cells, the collagen staining region at the interface was investigated for expression. These fibroblast-like cells are also present, in random distributions, throughout the interface. Also present in this interface are cells with a fibroblast morphology expressing CD45 and CI consistent with a fibrocyte phenotype. Since fibrocytes could be identified at the biomaterial interface, we analyzed expression of CD45 and α-SMA consistent with expression of fibrocyte-derived myofibroblasts. These cells could also be prominently visualized at the biomaterial interface. Finally, using DAPI to assess the total cells at the interface, the percentage of each of these cell populations was quantified at the interface. Quantification revealed that roughly 54% of the cells at the interface where macrophages and approximately 29% expressed α-SMA. In addition, about 12% of the cells showed fibrocyte expression while 16% had markers consistent with fibrocyte-derived myofibroblasts.

Finally, we examined CD90 expression in both MSC and α-SMA expressing cell populations (Figure 4.3), as a progressive loss of CD90 expression in the granulation tissue has been linked with the generation of fibroblasts with a high fibrotic potential. We find expression that roughly 22% of the cells at the interface express SSEA-4 alone while 35% of cells express

CD90 alone. Interestingly, we find also found that only roughly 32% of SSEA-4^{+} cells also express CD90. In addition, only 28% of α-SMA^{+} cells still show expression of CD90.

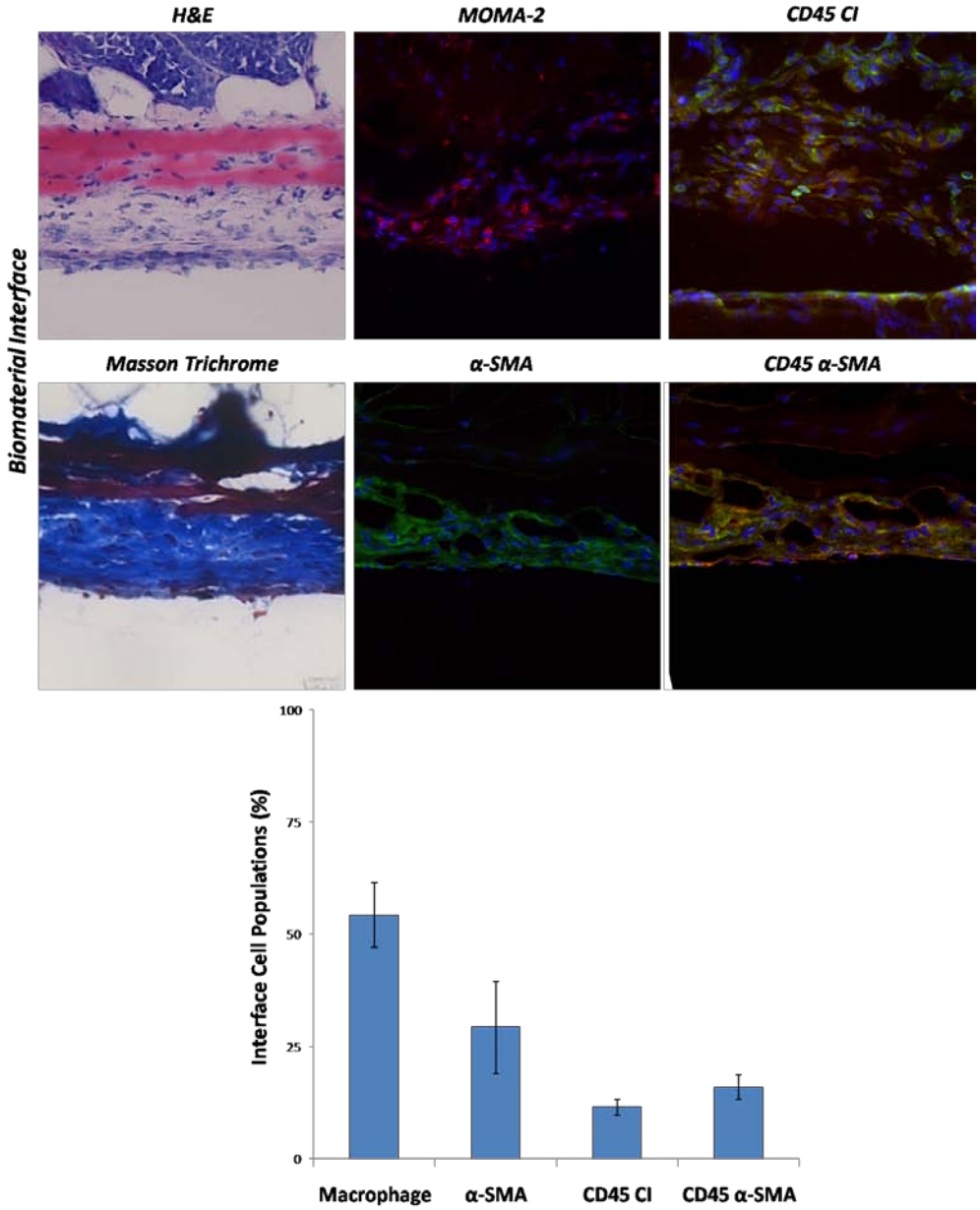

Figure 4.2 Characterization of cells in the fibrotic tissue surrounding biomaterial implants. PLGA scaffolds were implanted for 1 week and stained using H&E and Masson Trichrome (inset) to examine the infiltrated cell layer and quantify collagen deposition. Immunofluorescence showed cells in the interface expressing markers characteristic of macrophages, myofibroblasts, and MSC.

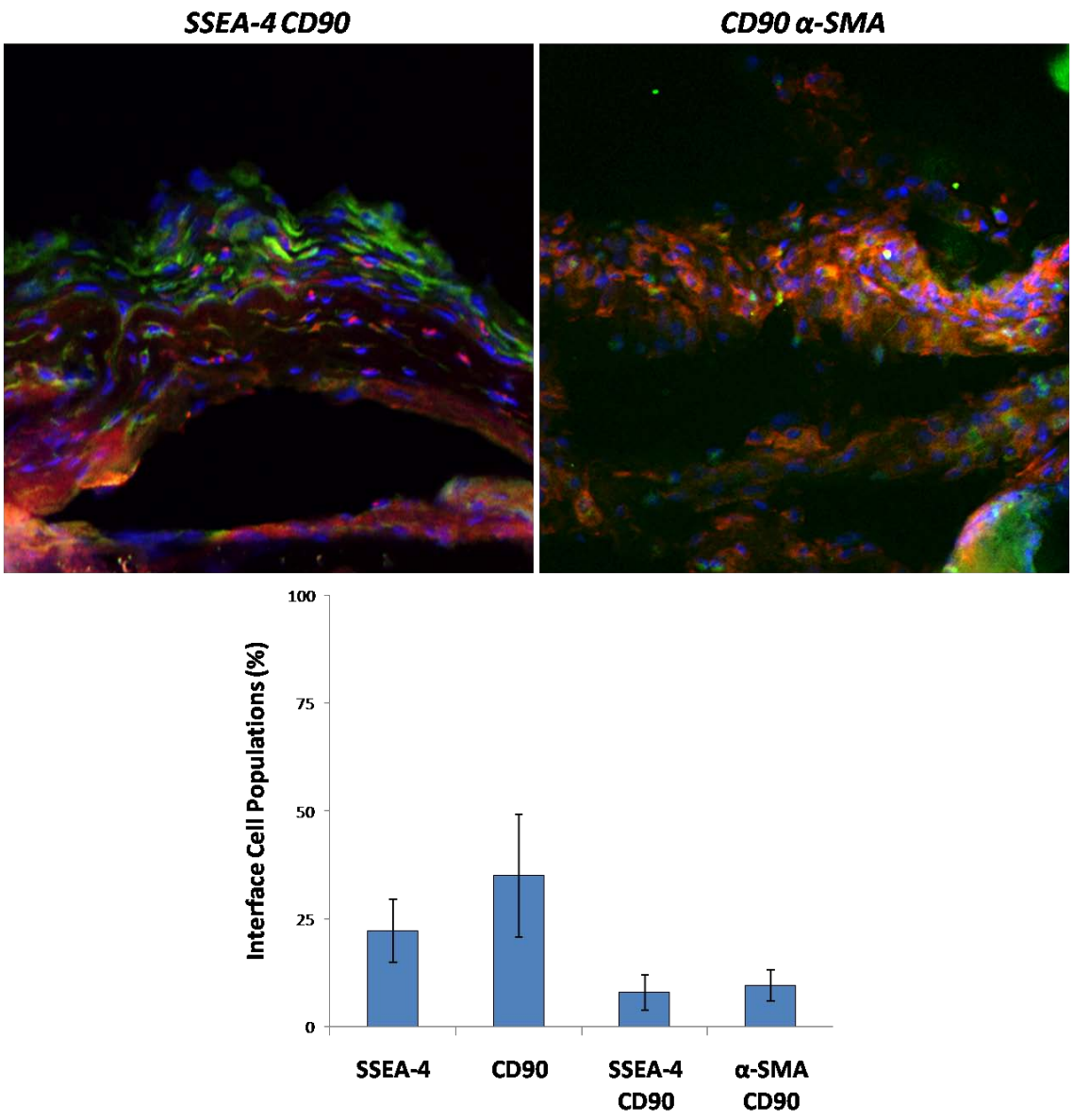

Figure 4.3 Characterization of stem cell and myofibroblast CD90 expression at the biomaterial interface. We used SSEA-4 CD90 and CD90 α-SMA expression to analyze the potential contribution of myofibroblasts and stem cells as the predominant cells with expression of CD90 at the biomaterial interface.

4.2.4 Discussion

Though we are developing a more complete understanding of biomaterial mediated host responses [206, 227, 228], strategies to control inflammatory and fibrotic responses while maximizing integration and regeneration are limited due to complex interactions between both processes [229, 230]. Our previous work has established the importance of mast cell

responses in controlling phagocyte chemotaxis to the site of biomaterial implantation [39, 40]. Downstream from this event, others have shown that the nature of the macrophage response can influence the balance between regenerative and fibrotic responses to biomaterial implants [52, 64, 206]. Controlling this balance may ultimately determine the success of both biomaterial and TE strategies [227]. Though many have investigated strategies to control biomaterial-mediated fibrotic responses (reviewed in [47]), thus far these strategies have been extremely limited in their effectiveness. Modifying cellular responses by altering implant surface chemistry have shown limited downstream effects [60, 193]. Anti-inflammatory treatments, while successful at reducing inflammation (reviewed in [47]), stall wound healing responses, delaying regeneration of the damaged tissue [123]. These examples point to the fact that our understanding of the biomaterial-mediated fibrotic mechanisms and thus strategic targets may not be sufficient.

Our recent study using the chemokine SDF-1α to improve host derived stem cell participation in wound healing was conducted under the hypothesis that MSC could improve fibrotic responses by improving regenerative responses and stimulating biomaterial integration. Though our results were promising, SDF-1α appeared to exert influence on the development of a full-scale inflammatory response, specifically through stabilizing mast cell responses shortly after implantation [223]. Additionally, literature supports the potential role of the SDF-1α/CXCR4 axis in fibrocyte recruitment to injury sites, and the subsequent role of the fibrocyte in facilitating fibrotic responses [226]. However, potentially due to SDF-1α-mediated mast cell effects or MSC influence, PLGA scaffolds treated with SDF-1α showed significant reduction in fibrotic responses [223]. Current literature characterization of MSC and fibrocytes shows that MSC prominently express Thy-1 [182, 231] while fibrocytes do not [232, 233]. However, wound sites have been characterized as being constituted by both Thy-1^{+} and Thy-1- fibroblasts [234], though the factors regulating their differentiation in vivo are not completely delineated. However, in vitro shedding of Thy-1 may be related to fibroblast exposure to IL-1β and TNF-α

exposure [234]. In fact, the ability to fully differentiate into a myofibroblast may be related to Thy-1 expression [235]. It is possible that these different fibroblasts phenotypes arise from differential inflammatory stimuli in vivo, and possibly different progenitor sources. This led us to consider the role of the mast cell in facilitating biomaterial-mediated fibrotic responses through fibrocyte interactions. However, literature regarding biomaterial-mediated fibrocyte responses is extremely limited. And though PVA sponges have been used to induce fibrocyte infiltration in wound chamber studies, no further characterizations of this response were investigated [214].

We first characterized the interface of PLGA films to establish a baseline for fibrotic responses to the biomaterial. As many groups have shown, macrophages prominently characterize implant interface within 1 week of implantation [16, 44, 46, 57, 199]. During this period, the initial deposition of collagen occurs at implant interface, based on our previous murine biomaterial implantation studies in the subcutaneous space [44]. In addition, our recent studies have also identified that stem cell are recruited to participate in these interactions, though their participation seems to be ineffective with regards to fibrosis, as most biomaterial implants generate a collagenous capsule which surrounds the implant [44]. Possibly the influence of collagen producing cells, present at only slightly higher concentrations in the interface may be swaying influence toward fibrosis. Though previous studies in different pathological conditions suggest this process may be influence by fibrocytes [151, 213, 218, 219, 225, 226], their participation has yet to be verified in biomaterial-mediated responses.

To investigate these responses, we first verified participation of fibrocytes in biomaterial mediated responses. Indeed, we observe the recruitment of fibrocytes, peaking at 1 week after implantation as shown in previous induced injury studies [151, 217]. These cells could be identified through expression of leukocyte markers such as CD34, CD45, and CD11b (for which data was not presented here but expression was verified by FACS array) along with co-expression of collagen I and vimentin [214, 216, 217, 225, 232]. Additionally, culture of these

implant recruited cells maintained expression of these markers after detachment and media changing cycles to remove contaminating cells.

Interestingly, we find that SSEA-4, a marker we have employed to identify cells with mutlipotent characteristics recruited to the biomaterial interface, shows relatively low levels of CD90 expression. Expression of CD90, and therefore the potential to lose expression, is much more characteristic of α-SMA positive cells in the developing fibrotic tissue [234, 235]. Given their prominence with respect to the MSC expressing cells (roughly 3-4X more cells), this suggests they are the likely target of cells which may alter CD90 expression in vivo. It appears that upon reaching the implantation site MSC, which do not express CD34 and CD45, may lose CD90 expression. However SSEA-4 expression remains as a marker of MSC lineage. A small percentage of cells remain which express both markers. Fibrocytes, which express CD34 and CD45 prominently [225, 232], do not express CD90, therefore it is difficult to ascertain whether shedding of CD90 by fibroblast like cells is directly related to fibrocytes . The contribution of recruited MSC to the injury site which then subsequently lose CD90 expression may be a more prominent possibility.

4.3 Influence of Inflammatory Cytokines on Fibrocyte Recruitment In Vitro and In Vivo

4.3.1 Introduction

Despite their characterization in many pathological conditions, there is still some debate regarding the chemokine responsible for fibrocyte chemotaxis [217, 218, 226]. However, a very limited pool of chemokines are thought to be potential primary contributors to fibrocyte chemotaxis. These chemokines are SDF-1α [226, 236-239], CCL21 [238, 240, 241], and MCP-1 [241-243]. Previous studies have shown that fibrocytes express the receptors necessary to respond to these chemokines, CXCR4 [215, 226, 244], CCR7 [218, 226, 240], and CCR2 [218, 225] respectively. Unfortunately, many of these studies have focused on fibrocyte chemotaxis to the lungs and liver and involve processes involves with many diverse clinical manifestations [215, 218, 225, 226, 232, 237, 239, 244]. The purpose of this study was to investigate

biomaterial-derived fibrocyte chemotaxis in vitro using a panel of implicated cytokines and their respective neutralizing antibodies. Following identification of the most potent chemokines, in vivo neutralization studies were undertaken to examine whether blocking the receptor in vitro, following by injection into implant bearing mice blocked fibrocyte homing to the implantation site.

4.3.2 Materials and methods

4.3.2.1 Fibrocyte Recovery and Chemotaxis

Fibrocytes were recovered using a biomaterial wound chamber system and culture in DMEM with 20% FBS as described for the previous experiment. Non-adherent cells were removed after 48hrs and media replaced subsequently every third day. Cells were detached using a cell scraper and replated into new 75cm^2 flasks weekly for 4 weeks prior to verification of phenotype by expression of CD45 coexpressed with collagen I and vimentin on seeded coverslips.

Fibrocyte chemotaxis was examined using wound chamber exudates in transwell plates (8μm pore, Corning Costar, Corning, NY). Fibrocytes were starved overnight in serum free DMEM, then detached using cold 0.05% EDTA and seeded onto transwell inserts at 5 x 10^4 cells per insert and allowed 6hrs to attach. Exudate from wound chamber studies was heated to 37°C and divided into four groups: untreated exudates (positive control), SDF-1α neutralized exudates, CCL21 neutralized exudate, MCP-1 neutralized exudates, and PBS alone (negative control). All neutralizing antibodies were purchased from R&D Systems (Minneapolis, MN). Neutralizing antibodies were added to 600μL of exudate at x μg/ml (SDF-1α), x μg/ml (CCL21), and x μg/ml (MCP-1). All transwell treatments were incubated for 30min prior to addition to the lower chamber. After addition, plates were incubated for 4hrs, after which cells on the upper surface were removed with a cotton swab, membranes were fixed in cold methanol, H&E stained, and quantified as cells per 40X view field on the lower surface of the membranes.

4.3.3 Results

4.3.3.1 Chemokines governing biomaterial mediated fibrocyte recruitment in vitro

To analyze what chemokines may be responsible for fibrocyte recruitment to the biomaterial interfaces, exudates from wound chamber studies were treated with different neutralizing antibodies. Neutralized exudates were compared against untreated exudate as positive control and PBS as negative control (Figure 4.4). Interestingly, SDF-1α neutralization resulted in a significant, approximately 50% reduction in fibrocyte chemotaxis. Neutralization of MCP-1 and CCL21 separately was able to slightly reduce chemotaxis, though values were insignificant from unneutralized exudate.

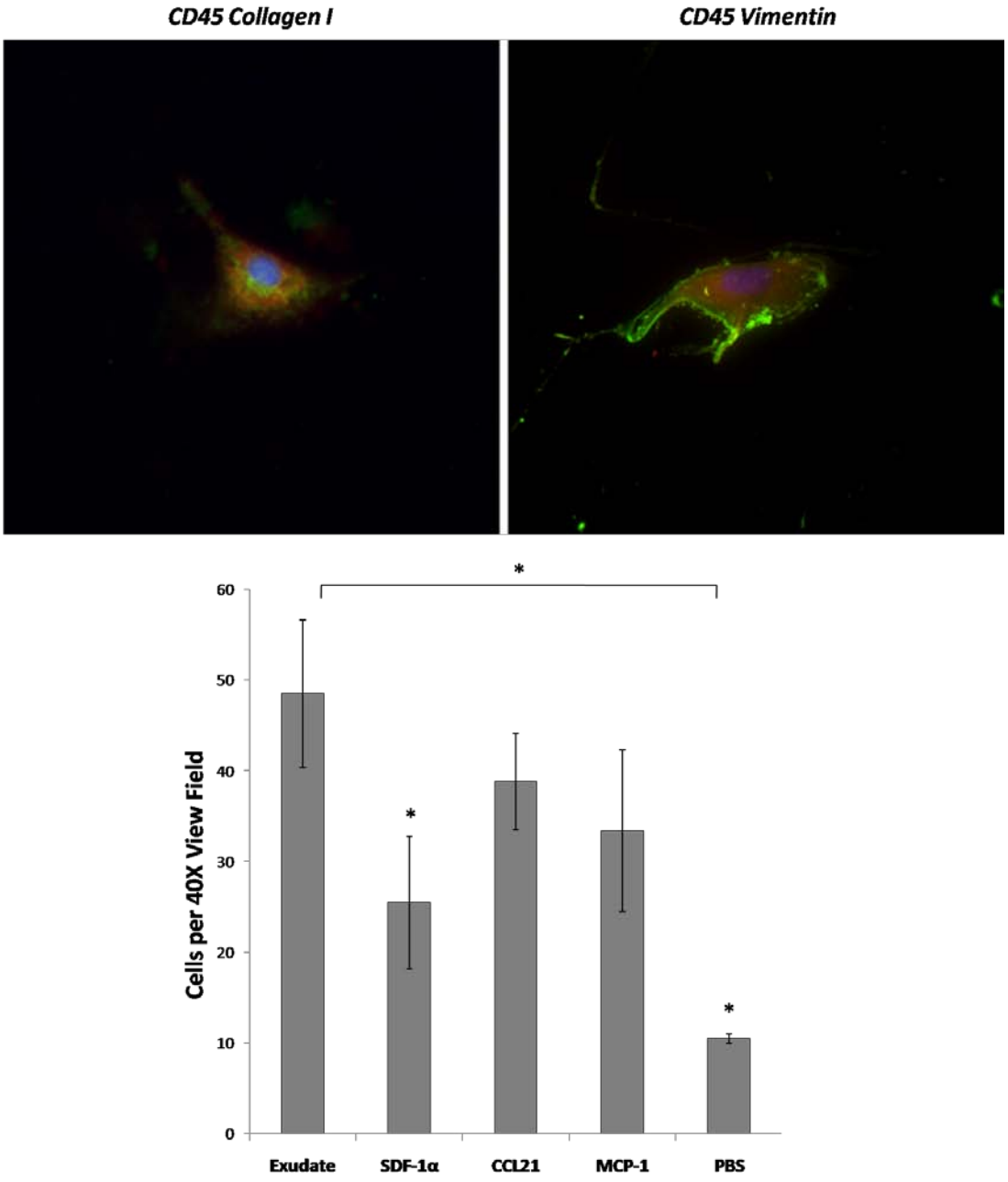

Figure 4.4 Fibrocyte expression and chemotaxis. After identification at the interface, PLGA conduits implanted for 1 week were flushed and purified for adherent cells from the exudates. These cells also expressed CD45 CI and CD45 vimentin after purification in culture. In Vitro fibrocyte chemotaxis to biomaterial implant exudate and chemokine neutralized exudates was then quantified. Fibrocytes exhibited significant migration toward control biomaterial exudate. However, neutralization of chemokines decreased fibrocyte migration. Anti-CXCL12 significantly reduced fibrocyte chemotaxis, while anti-CCL21 and anti-MCP-1 had moderate effects on fibrocyte chemotaxis (bracket and * represent significant ANOVA at $P<0.05$, * above groups represents significant Dunnett test comparing all groups to control exudates at $P<0.05$).

4.3.4 Discussion

Though several axes have been implicated in fibrocyte chemotaxis [213, 217, 218], data is limited regarding their homing in foreign body responses. Therefore, using exudate from biomaterial implants, we investigated neutralizing different chemokines to identify which of a limited group of implicated chemokines may be facilitating fibrocyte chemotaxis to biomaterial implantation sites. In agreement with some of these reports [215, 226], we find neutralization of SDF-1α was able to substantially inhibit recruitment of fibrocytes to biomaterial wound chamber exudates. Several previous investigations have established fibrocyte expression of CXCR4 and shown their propensity to use the SDF-1α/CXCR4 axis in chemotaxis and have verified expression and utility of the axis in vivo [215, 226]. However, some studies have also identified fibrocytes which do not express CXCR4, yet express CD45 and CI [226]. This may explain why SDF-1α did not completely abolish migration, in addition to CCL21 and MCP-1 having some effectiveness in reducing migration. Recently, studies of induced lung fibrosis have brought about additional chemokines which may influence fibrocyte recruitment, including MIP-1 (CCL3) and MCP-5 (CCL12) in mice [217, 218].

Given that SDF-1α appears to be a prominent target in the biomaterial-mediated response, we proceeded with in vivo studies designed to limit inflammatory responses to assess the effects on fibrocyte-mediated responses.

4.4 Effects of Dexamethasone Treatment on Fibrocyte Responses

4.4.1 Introduction

Recently tissue engineering approaches have seen an increase in design methodologies which attempt to induce repair in vivo by influencing inflammatory and stem cell populations to influence the balance between regeneration and fibrosis [245, 246]. In these preliminary investigations, we and others have identified the potential for links between inflammation and stem cell responses in a potentially similar relationship to inflammatory cell responses and fibrotic stimuli [44, 247, 248]. However, our investigations of SDF-1α roles in

MSC and fibrocyte chemotaxis bring up some potential points of conflict. SDF-1α production after injury has been linked to platelets, endothelial cells and fibroblasts [144, 146]. This potentially suggests that both the injury stimulus (platelets and endothelial cells) and biomaterial:blood interactions as well as the inflammatory response (endothelial cells and fibroblasts) may play a role. However, fibrotic stimuli have been causatively linked with many activated macrophage responses [72, 110, 217]. In addition, inflammatory growth factors such as TNF-α may render these cells more responsive to chemokines [138].

Dex has previously been shown to inhibit leuokocyte infiltration to inflammation sites [123, 230]. In addition, local release of Dex has been shown to be effective in mediating this effect in biomaterial-mediated inflammatory responses [230]. Interestingly though, some data suggests that Dex actually upregulates CXCR4 expression [249]. However, information is not readily available regarding the consequences of this treatment on MSC and fibrocyte responses. In order to establish a link between leukocyte responses due to biomaterial-mediated responses, we released Dex locally from PLGA films in the subcutaneous space in order to evaluate two responses specifically. The first was to evaluate whether Dex-mediated reduction of infiltrating $CD45^+$ leukocytes to the biomaterial interface may directly or indirectly affect the behavior of fibrotic cells. Since Dex may not affect fibrocyte chemotaxis, we instead analyzed the interface composition of α-SMA cells as a measure of myofibroblasts, whose differentiation and functionality are more directly linked with leukocyte responses. Our second aim was to analyze whether Dex effected the composition of MSC and Thy-1 (CD90) cells at the implant interface.

4.4.2 Materials and methods

4.4.2.1 PLGA film fabrication, Dexamethasone loading, and implantation

PLGA films were incorporated with Dex (Sigma Aldrich, St Louis, MO) at 1mg/kg body wt/day to decrease leukocyte responses to biomaterial implants and examined against no treatment unmodified PLGA films. The elution of dexamethasone from PLGA films was

approximated based on previous release studies using PLGA fabricated by similar methods [250, 251] and used to set loading values established for anti-inflammatory treatments based on previous murine studies [230, 252]. Control PLGA films were fabricated as desecribed in previous studies. For Dex embedded films, Dex was mixed with the polymer solution, cast into molds, and evaporated as per control films. C57 mice (Jackson Labs) were selected for equal age and sex prior to housing by implantation condition. For implantation, mice were anesthetized and a dorsal midline incision created as previously described [223]. Briefly, each mouse (n=3 for all studies) was implanted with two films of equal treatment condition as described in previous studies. Mice were monitored daily for irritation around the implantation for 1 week until explantation.

4.4.2.2. Immunohistochemical analysis of interface cell populations

After 1 week implantation, biomaterials were recovered and processed as outlined in previous chapters. Cross sections of the tissue and film were cut at 7μm. Leukocytes were detected using CD45 antibodies (Santa Cruz Biotech, Santa Cruz, CA). Macrophages were detected using MOMA-2 antibody (Serotec, Oxford, UK). Myofibroblasts were detected via expression of α-SMA (Santa Cruz Biotech, Santa Cruz, CA). MSC were detected via co-expression of SSEA-4 with CD90 (Santa Cruz Biotech, Santa Cruz, CA). Cell percentages for each marker were assessed at the interface per total DAPI staining nuclei.

4.4.3. Results

4.4.3.1 Effects of dexamethasone on leukocyte and myofibroblast responses

As expected, implant incorporation with Dex appeared to reduce the amount of infiltrated macrophages at the interface of the PLGA films (Figure 4.5). In addition the percentage of $CD45^+$ leukocytes was also substantially reduced. However, there was no significant change in the percentage of $\alpha\text{-SMA}^+$ cells. In accordance with this finding, the percentage of fibrocyte-derived myofibroblasts was also unaltered between treatment groups

after assessing $CD45^+$ α-SMA^+ cells. Fibrocyte infiltration ($CD45^+$ CI^+) was also unaltered due to Dex treatment.

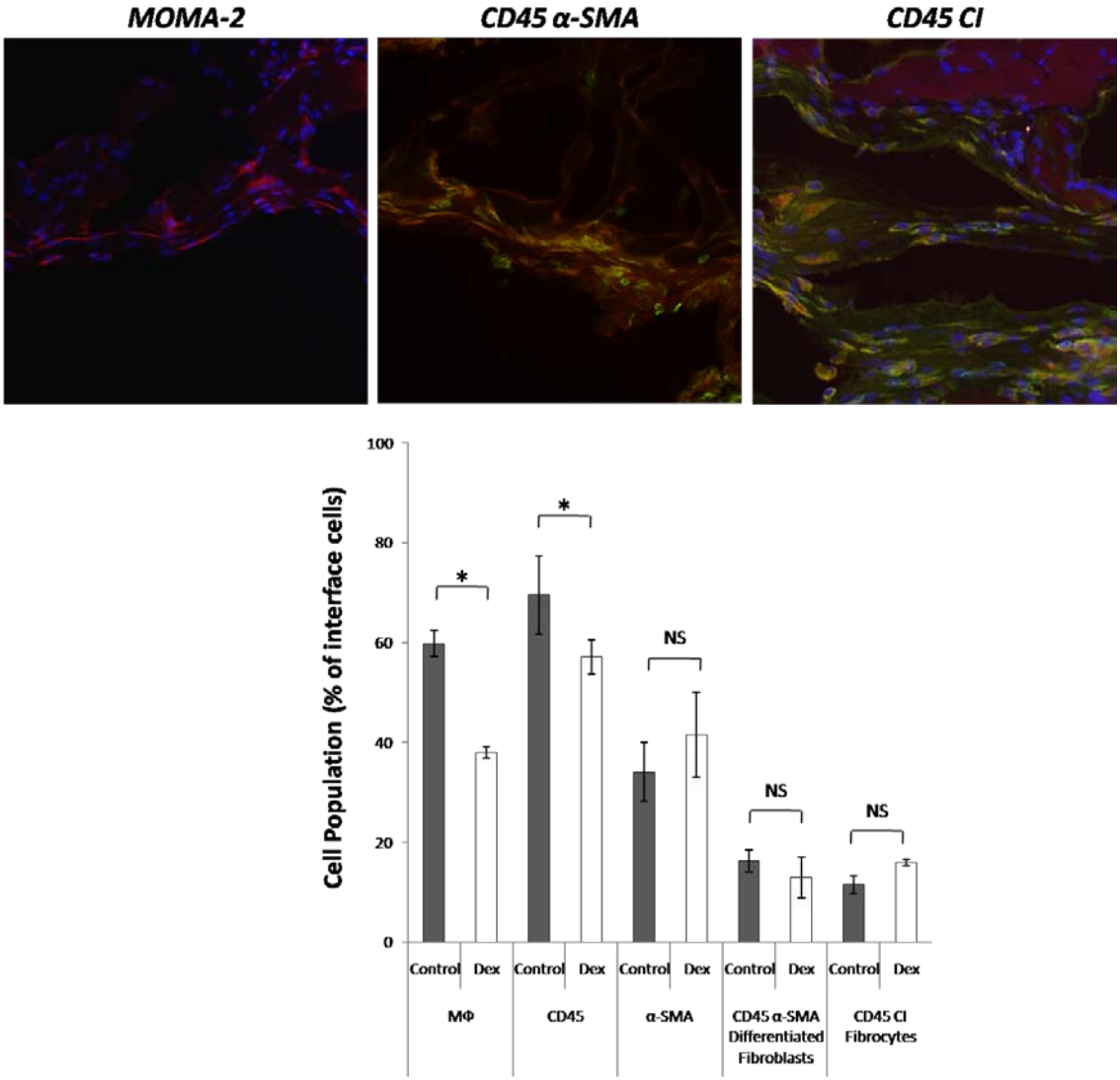

Figure 4.5 Characterization of inflammatory and fibrotic cells in response to Dex. Dex was able to effectively limit macrophage infiltration (MOMA-2 – top left) as well as leukocytes (CD45 labeled with FITC – green, top-middle). However, the number of fibrocytes (CD45 labeled with FITC and CI labeled with Texas Red – red, top-right) per total cells was apparently unaltered. Comparison of each cell grouping to controls revealed significant reductions in only macrophages and leukocytes (One-tailed Student t test, brackets and * represent significance at $P<0.05$).

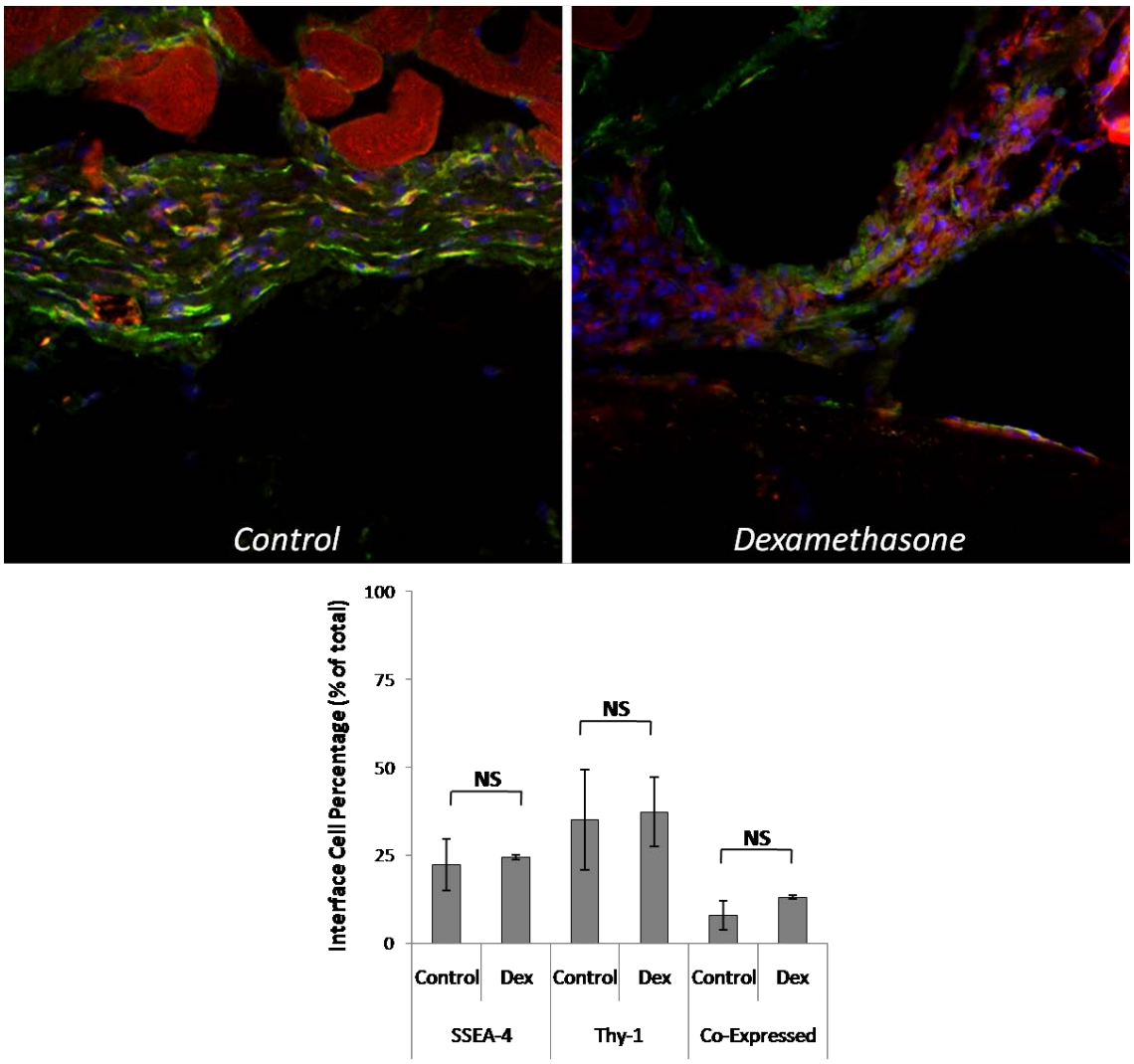

Figure 4.6 Effects of dex on interface cell MSC marker expression. The expression of MSC markers was unaltered between dex treatment groups.

In the second series of assessments, we analyzed whether Dex downregulation of macrophage responses at the biomaterial interface may have an effect on host derived MSC. As per our previous studies, we find a small percentage of SSEA-4 Thy-1 double positive MSC at the implantation site of both control and Dex treated implants (Figure 4.6). In dex treated implants, we see no significant differences between these cell populations between treatment conditions.

4.4.4 Discussion

Given in vitro chemotaxis results, we speculated as to whether reducing inflammation through biomaterial treatment with Dex may have any effects on fibrocyte responses. We hypothesized limited influence since although Dex may limit leukocyte infiltration [123, 230, 249], processes resulting from tissue damage and subsequent biomaterial mediated protein interactions may play an equally important role in fibrotic cell recruitment. Though we find reduced cell infiltrate, and more specifically reduced macrophage and leukocyte infiltration, the number of α-SMA cells was nearly unaltered. Though Dex appears to be effective in treating pulmonary fibrosis [253], the short-term success appears related to anti-inflammatory effects. Unfortunately, these effects are relatively ineffective at reducing fibrosis due to the persistence of myofibroblasts [254]. In agreement with this finding, we find that Dex is ineffective at reducing myofibroblast populations in developing fibrotic tissue surrounding biomaterial implants. However, there are some studies in pulmonary fibrotic models which do show slight reductions in the number of myofibroblasts [255]. As such, the effectiveness of Dex treatment to reduce myofibroblast accumulation in these models is still controversial based on the model employed and experimental techniques. This is supported by the fact that Dex only partially inhibits leukocyte recruitment chemokine pathways [256]. However, it is well understood that Dex can reduce levels of TGF-β1 which is necessary for initiation of the profibrotic functions of myofibroblasts [255]. As such, Dex likely alters the activation of myofibroblasts pending its continuous bioavailability to prevent the activation cascade from resuming.

Since our previous results support SDF-1α-mediated effects on stem cell recruitment to sites of peripheral tissue injury [44], we hypothesized that Dex treated may have some effect on host derived stem cell recruitment. However, we find no significant differences in stem cell recruitment. Dex functions by inhibiting many cytokines related to inflammatory cell chemotaxis and diapedesis, including RANTES [257, 258], IL-6 [259, 260], TNF-α [261, 262], and GM-CSF [263, 264]. Though MSC have shown limited chemotactic responses to many inflammatory

chemokines including MCP-1, MIP-1, and RANTES, responsiveness to these chemokines may be enhanced by TNF-α [138]. TNF-α is believed to be one of the factors prominently effected by Dex treatment, though results are controversial [265]. Our group has previously observed a decrease in the recruitment of host-derived MSC to the subcutaneous space bearing microparticle implants combined with Dex treatment (unpublished observations). However, experimental deviations and the possible over-estimation of MSC using SSEA-4 alone may have contributed to these differences. SDF-1α and other chemokines have been shown to increase the recruitment of tissue committed stem cells to participate in wound healing [266]. It may be possible that SSEA-4^+ $CD90^-$ stem cell populations may represent tissue committed or differentiated stem cells. Regardless of this hypothesis, recent papers have shown that SSEA-4^+ Oct-4^+ stem cells are recruited to sites of tissue injury [187]. Unfortunately, a change in expression and, more generally, the fate of stem cells recruited to the biomaterial implantation site is not well defined.

The ineffectiveness of Dex at inhibiting myofibroblast and stem cell percentages led us to speculate whether neutralization of SDF-1α in vivo may lead to a more prominent decrease in fibrocyte recruitment in biomaterial mediated responses. Therefore, we took a more direct approach based on our in vitro investigations of fibrocyte chemotaxis, specifically by incorporating Chalcone-4 to neutralize CXCL12 in vivo.

4.5 Effects of SDF-1α Neutralization on Fibrocyte Recruitment and Collagen Deposition

4.5.1 Introduction

While Dex was effective at limiting leukocyte infiltration and macrophage percentages at the implantation site, it was ultimately ineffective at limiting fibrocyte responses and myofibroblast responses. Given our in vitro findings, we next were interested in examining whether neutralization of SDF-1α in vivo could limit fibrocyte infiltration and collagen deposition in the biomaterial-mediated foreign body response. Previous investigations in lung fibrosis models has shown potential of CXCL12 neutralization [215, 267], however this has not been

established in model of foreign body responses. These models could possibly differ in effectiveness, given that populations of fibrocytes have been identified in fibrotic lung models which do not express CXCR4, and thus their migration was minimally effected by CXCR4 neutralization [268], though this represented a small percentage of total fibrocytes. We have also established the importance of SDF-1α in biomaterial-mediated wound healing responses through increased recruitment and retention of MSC and other multipotent cells at the implantation site to participate in these interactions [44]. It is unclear what effect CXCL12 neutralization will have on these responses.

To neutralize SDF-1α in vivo, we have developed PLGA films which can release Chalcone-4. Chalcone-4 binds to a portion of CXCL12 effectively inhibiting its biological functions in interacting with its receptor CXCR4 [269]. We then investigated the effectiveness of this inhibitor in reducing fibrocyte recruitment and collagen deposition, as well as potential side-effects related to SSEA-4$^+$ and SSEA-4$^+$ CD90$^+$ cell populations to the implant interface.

4.5.2 Materials and Methods

4.5.2.1 PLGA films fabrication and drug loading

PLGA films were fabricated as described in previous experiments. Films were incorporated with SDF-1α (CXCL12) inhibitor Chalcone 4 (Sigma Aldrich, St Louis, MO) at 350μmol/kg body wt/day as per previous studies [269] or no treatment unmodified PLGA films. Compound release from PLGA was estimated as decribed for Dex studies. PLGA films were fabricated using the solvent casting technique. Briefly, PLGA (75:25, 113kDa, Medisorb Inc., Birmingham, AL) was dissolved at 10% w/v in dichloromethane (Sigma Aldrich, St Louis, MO). Films were cast as described in previous sections. For Chalcone-4 embedded films, Chalcone-4 was dissolved in dimethylsulfoxide (Sigma Aldrich, St Louis, MO) and the solution mixed with the polymer solution prior to casting. For all film conditions, the resulting film had a thickness of ~ 1mm. Films were cut into 5mm disks and stored at -20°C until implantation.

4.5.2.2 Implantation studies

C57 mice (Jackson Labs) were selected for equal age and sex prior to housing by implantation condition. Implantation procedures were identical to those of the previous section of this chapter.

4.5.2.3 Evaluation of drug loaded films

Implant recovery and analysis were identical to the previous section with exception to the following. Fibrosis was assessed using both Masson Trichrome (Sigma Aldrich, St Louis, MO) and Picosirius Red (Sigma Aldrich, St Louis, MO) staining. Picosirius Red staining was visualized using polarized light microscopy. The degree of collagen I in the fibrotic layer was quantified using Image J to measure the percentage of red/yellow birefringence per total interface area (between the implant and hypodermis).

4.5.3 Results

4.5.3.1 Effect of Chalcone-4 on development of fibrotic tissue and fibrocyte recruitment

We first examined the histology of the implant interface using H&E staining (Figure 4.7). Treatment with Chalcone-4 resulted in a reduction in the infiltration of inflammatory cells after one week implantation. However, we were interested in whether Chalcone-4 could limit the deposition of collagen at the implant interface. We assessed this parameter using Masson Trichrome staining. The amount of collagen in the interface was investigated further using Picosirius Red to compare and quantify the area percentage of collagen I fibers. In agreement with Masson Trichrome staining, the deposition of collagen I fibers is drastically different between treatment groups. Finally, we stained the sections to examine co-expression of CD45 and vimentin consistent with a fibrocyte phenotype. As expected, there are also substantial differences between these cells at the interfaces between treatment groups. As a result, the thickness of the granulation was significantly different between treatment groups. As expected, we find a substantial reduction in the amount of collagen deposited around the biomaterial films.

Finally, we quantified the percentage of collagen I coverage between treatment groups and also quantified a significant difference due to treatment group.

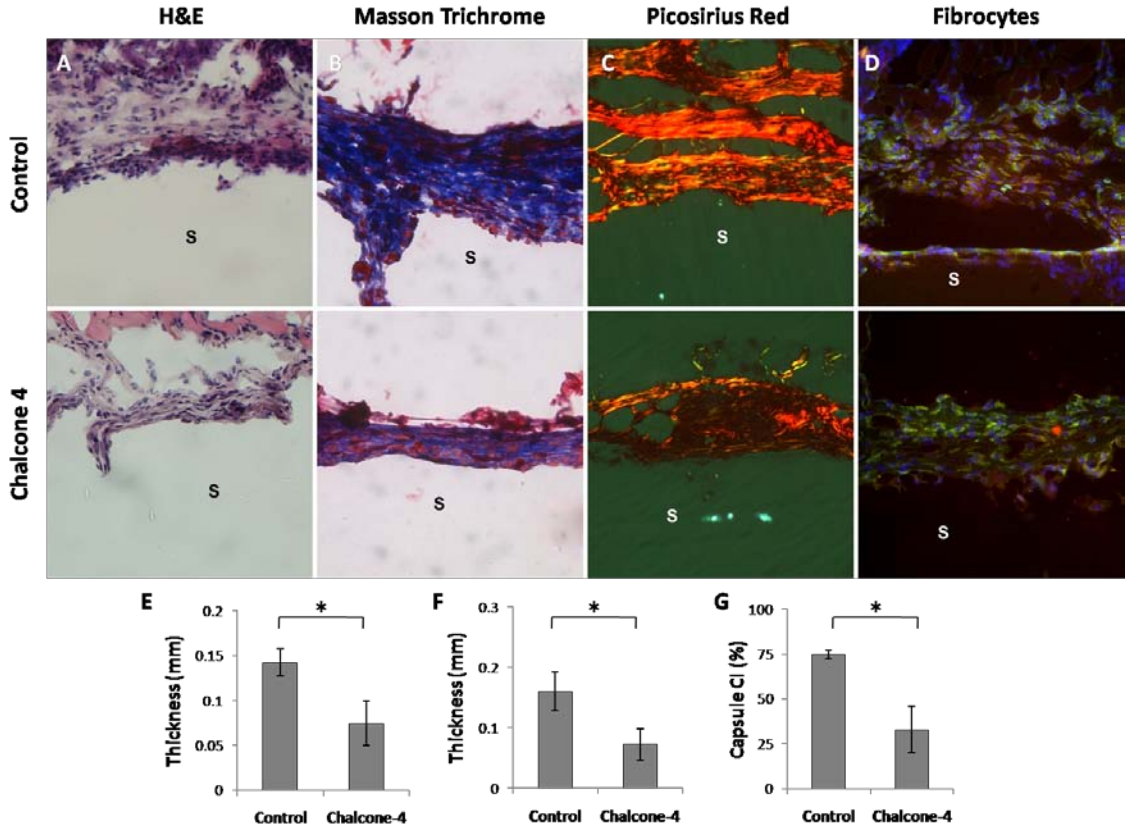

Figure 4.7 Characterization of the fibrotic response to Chalcone-4 loaded PLGA films. H&E staining comparing the buildup of inflammatory cells at the material interface. Masson Trichrome staining to identify the deposition of total collagen around the implant. Picosirius red staining of collagen I fibers inside the fibrotic capsule. CD45 (FITC – green) Vimentin (Texas Red – red) immunofluorescent staining of fibrocytes inside the collagenous interface. Histological parameters of interface thickness, collagen layer thickness, and percent coverage of interface by collagen I all reveal significant decreases in the Chalcone-4 treatment group (Student t test, bracket and * represent significance at $P<0.05$).

4.5.3.2 Influence of Chalcone-4 on inflammatory and fibrotic cell composition of the interface

We next sought to link cell responses in the interface to the observed changes in collagen deposition. We quantified the percentages leukocytes (CD45), myofibroblasts (α-SMA), and fibrocytes (CD45 CI and CD45 vimentin) in the interface tissue. Interestingly, the percentage of CD45 positive cells was significantly reduced after Chalcone-4 treatment (Figure

4.8). However, the percentage of α-SMA positive cells was unaffected by CXCL12 inhibition. The percentage of CD45 CI positive fibrocytes was also significantly decreased and the percentage of CD45 vimentin positive fibrocytes also decreased but not to a significant degree.

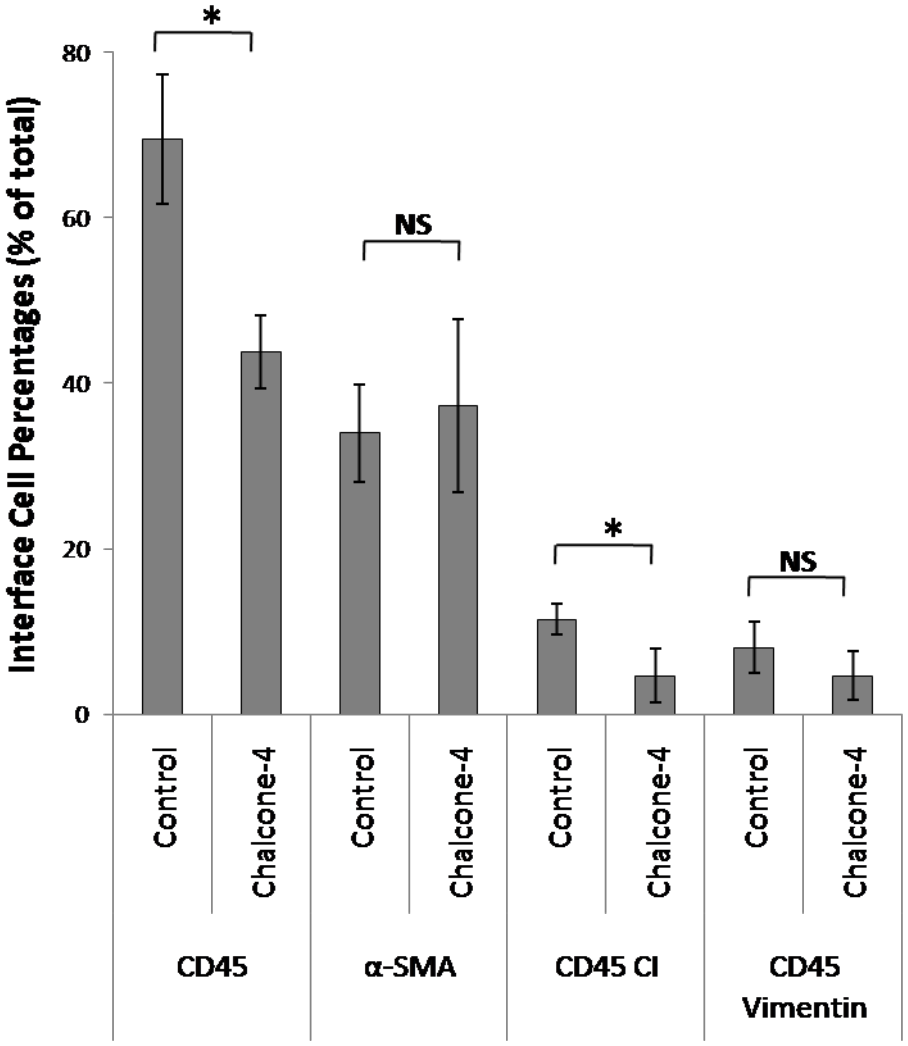

Figure 4.8 Compositional changes in fibrocyte density at the interface of Chalcone-4 implants. The percentage of interface cells expressing CD45 (leukocytes), α-SMA (myofibroblasts) and co-expressing CD45 CI and CD45 vimentin (fibrocytes) were quantified per total DAPI cells.

We next analyzed co-expression of CD45 and α-SMA as a measure of fibrocyte differentiation. We find cells in the biomaterial interface decreasing in a trend from control > Dex > Chalcone-4 though the differences between steps are insignificant (Figure 4.9).

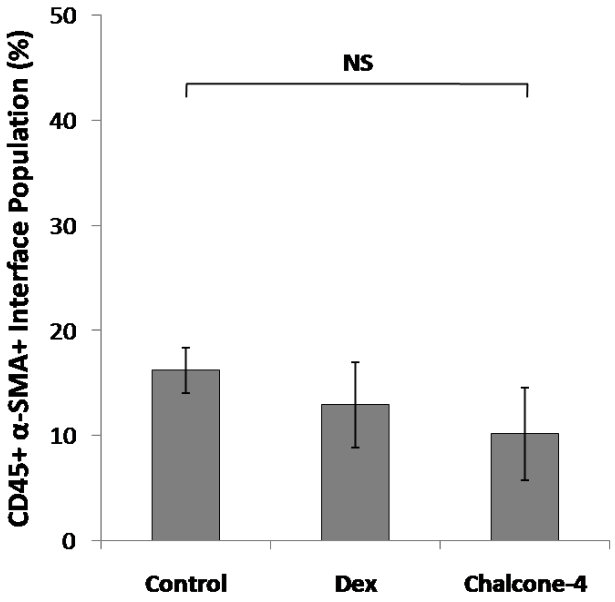

Figure 4.9 Effects of fibrocyte intervention on differentiation of fibrocytes to myofibroblasts. ANOVA testing reveals no significant differences between treatment groups, though Dex and Chalcone-4 did reduced the percentage of fibrocyte-derived myofibroblasts and substantially reduce the number of total cells at the interface.

4.5.4 Discussion

Having established that fibrocytes were recruited to biomaterial implantation site and migrated predominantly via SDF-1α in vitro, we hypothesized that limiting inflammatory cell interactions via Dex would limit fibrocyte recruitment and α-SMA positive cell responses. However, we found that limiting inflammatory cell influx had little effect on fibrocyte percentages or myofibroblast-like cells at the interface. In addition, our previous studies have shown that SDF-1α is not significantly altered between low inflammatory and high inflammatory biomaterial reactions (unpublished observations). Therefore, we considered the possibility that biomaterial-mediated inflammatory cytokine responses may not be the predominant mechanism leading to fibrocyte infiltration, but rather may affect their activation status and differentiation after arrival.

Therefore, to attempt to limit fibrocyte infiltration, we investigated the effect of combining a CXCL12 inhibitor with the PLGA film. The inhibitor was able to substantially

decrease inflammatory cell infiltration as observed in H&E stained cross-sections. SDF-1α has been implicated with HSC migration to peripheral tissue [44, 130, 137, 164, 201] as well as many inflammatory cells [176], both of which prominently express CD45. SDF-1α has been shown to have many anti-apoptotic effects on HSC and other myeloid cells [135], and thus neutralization of the chemokine in the local peripheral tissue may affect the behavior of these cells as evident in the reduced percentage of $CD45^+$ cells. As witnessed in the Dex study, we would expect that in addition to potential effects on fibrocyte chemotaxis, the decrease in inflammatory stimuli produced by these cells may contribute to altered TGF-β1 levels and thus effect collagen deposition.

Several studies in lung fibrotic models have shown that neutralization of CXCL12 and blocking CXCR4 can reduce, but not completely eliminate, fibrosis [176, 226, 239, 244]. Therefore, in lungs, several redundant pathways likely exist [218, 225, 238, 240, 243, 267]. In biomaterial-mediated fibrosis, the understanding of factors governing these responses is much less prevalent. Though tissue injury and the inflammatory response, which lead to both the accumulation of cells and production of many target chemokines, proceed by similar mechanisms, differences in the activation of these cells may alter recruitment redundancies to increase or decrease complexity [81, 103, 161]. For instance, in our recent study of methods to improve MSC chemotaxis, increasing stem cell responses via SDF-1α actually reduced fibrosis, potentially by increasing mesenchymal stem cell responses and overriding fibrocyte mediated interactions [44]. Here, by neutralizing CXCL12, we were able to reduce fibrotic responses by pushing the axis in the opposite direction.

Interestingly, though fibrotic collagen deposition appeared significantly altered, the percentage of fibrocytes in the local tissue was only slightly decreased using one marker convention (CD45 vimentin) and significantly reduced using another (CD collagen I). However, similar to Dex treatment, no difference in α-SMA positive cells was observed. Fibrocytes begin to express α-SMA in the peripheral tissue under the influence of TGF-β1 while also reducing

their expression of CD34 and CD45 [219]. TGF-β1 was not directly assessed in these investigations, but a more detailed cytokine evaluation in vivo may be necessary to quantify why Dex and Chalcone-4 were ineffective at reducing α-SMA positive cells at the implant interface.

To provide some insight into this issue, we examined co-expression of CD45 and α-SMA as a measure of fibrocyte differentiation through staining fibrocyte-derived α-SMA as previously described [151]. Previous results show that approximately 40% of cells in full thickness wounded tissue after 7 days express CD45 and α-SMA, which represent myofibroblasts which have differentiated from fibrocytes [151]. Using this as a benchmark for comparison, we find approximately half this percentage of cells in the biomaterial interface in a trend decreasing from control > Dex > Chalcone-4 though the differences between steps are insignificant. Though the treatments were ineffective at limiting myofibroblast infiltration, it appears that they were able to affect fibrocyte infiltration and differentiation with increasing effectiveness up to CXCL12 neutralization.

Since treatment with Dex did not appear to influence fibrocyte infiltration or α-SMA reactivity and Chalcone-4 had some influence on these parameters, we decided to move further upstream to assess what influences may dictate these parameters. Specifically we were interested in analyzing a cellular response which could correlate with cytokine release or cascades leading to inflammatory cytokine release which could possibly substantially influence fibrocyte responses. Our previous work and that of a few other groups have highlighted the importance of mast cells in initiating and influencing the biomaterial-mediated foreign body responses [15, 16, 39, 40, 212]. More importantly, some other groups have presented work which appears to show a link between mast cell responses and the degree of fibrotic encapsulation [44, 177, 208, 270, 271]. However, studies of fibrotic potential using liver and lung disease models in mast cell deficient animals did not verify this link [272, 273], though these models may significantly differ from biomaterial-mediated foreign body responses. Therefore, we set out to analyze a condition where biomaterial properties were held constant,

while a variable mast cell response was generated in order to analyze downstream effects on fibrocytes and fibrotic outcomes.

4.6 Influence of Different States of Mast Cell Activation on Fibrocyte Responses and Collagen Deposition

4.6.1 Introduction

Prior to investigating mast cell influence, we have examined whether Dex treatment to reduce inflammatory cell responses and local distraction of the SDF-1α axis with SDF-1 inhibitor Chalcone-4 in vivo obstructed fibrocyte responses. We found that Dex reduced infiltrating CD45 positive cells, but had little influence on the presence of α-SMA positive cells or fibrocytes. In addition, Dex did not appear to influence fibrocyte differentiation to α-SMA positive cells based on CD45 α-SMA expression. Chalcone-4 embedded into PLGA films was able to substantially reduce collagen deposition at the biomaterial interface, possibly through limiting fibrocyte infiltration into the developing granulation tissue.

If fibrocyte responses were unaffected by leukocyte infiltration, yet local inhibition of SDF-1α was effective, we hypothesized that stabilizing or destabilizing mast cell responses may potentially be more effective. Mast cell responses are critical in initiating leukocyte infiltration in biomaterial-mediated inflammatory responses. In addition, kinetic analysis of fibrocyte infiltration seems to support that leukocyte and fibrocytes arrive at a similar time point (4 days), suggesting a common mechanism may be leading to their infiltration, even if the implicated chemokines differ [151]. Therefore, we hypothesized that in comparison to the normal biomaterial-mediated response, creating variable levels of mast cell influence to the same biomaterial implant may vary the infiltration of fibrocytes and the degree of fibrosis at the biomaterial interface.

We approached this design by incorporating mast cell stabilizing (Cromolyn) and destabilizing (Compound 48/80) agents into the polymer. This allows us to validate the normal response, in addition to a response with substantially reduced mast cell influence and also with exaggerated mast cell influence.

4.6.2 Materials and Methods

4.6.2.1 PLGA film fabrication and drug loading

PLGA films were fabricated to incorporate drugs and chemicals for three separate treatment groups to study variable mast cell responses. Films were incorporated with the mast cell stabilizing agent cromolyn (Sigma Aldrich, St Louis, MO) supplemented at 640 µg/kg body wt/day, mast cell destabilizing agent compound 48/80 (Sigma Aldrich, St Louis, MO) at 1 mg/kg body wt/day, or no treatment unmodified PLGA films. PLGA films were fabricated using the solvent casting technique. Briefly, PLGA (75:25, 113kDa, Medisorb Inc., Birmingham, AL) was dissolved at 10% w/v in dichloromethane (Sigma Aldrich, St Louis, MO). Films were then cast into Teflon molds with the solvent allowed to evaporate overnight in a chemical fume hood. For cromolyn embedded films, cromolyn salt was mixed with the polymer solution and cast into molds and evaporated as per control films. For compound 48/80 embedded films, 10mg of compound 48/80 was dissolved in dimethylsulfoxide (Sigma Aldrich, St Louis, MO). The solution was then blended with the polymer solution and cast into molds. For all film conditions, the resulting film had a thickness of ~ 1mm. Dosing values were set based on previous studies [274, 275] and delivery parameters estimated as previously described. Films were cut into 5mm disks and stored at -20°C until implantation.

4.6.2.2 Film implantation

C57 mice (Jackson Labs) were selected for equal age and sex prior to housing by implantation condition. For implantation, mice were anesthetized and a dorsal midline incision created as previously described [223]. Briefly, each mouse (n=3 for all studies) was implanted with two films of equal treatment condition, with films placed laterally on either side of the dorsal incision tucked into the subcutaneous space approximately 15mm away from the midline incision. The incision was closed with surgical clips and the mice returned to housing. The mice were monitored daily for irritation around the implantation for 1 week or 2 weeks until explantation.

4.6.2.3 Histological evaluation of drug loaded films

Biomaterials were recovered and process for histological and immunohistochemical staining as described in previous section. Primary antibodies were used to detect inflammatory and fibrotic cells as described in the previous sections. Finally, quantification of histological parameters related to interfacial responses, total collagen deposition, and collagen percentages were described in previous sections.

4.6.3 Results

4.6.3.1 Correlation between mast cell responses, implant histology, and collagen deposition

H&E staining of the implants reveals some significant differences related to both the organization and thickness of the infiltrated cell layer at the interface (Figure 4.10). Unmodified PLGA films have a dense layer of spindle-shaped cells next to the implant ~5 cells thick with a less dense area of cells above the fibroblast layer. Films embedded with Compound 48/80 have a uniformly dense, thick cell layer with a mix of cells of rounded and spindle-shaped morphology throughout. Cromolyn embedded films have an interface cell mixture similar to that of Compound 48/80 implants, but of lower density and thickness. The thickness of the infiltrated cell layer was measured from implant surface dorsal to the hypodermal layer of non-inflammatory cell infiltrated tissue. Compound 48/80 treatment to induce mast cell degranulation results in a significant 2X thickening of the infiltrated cell layer in comparison to other treatments. However, there were only minor differences in the total cell density.

We next examined whether the degree of mast cell response correlated with downstream fibrotic reactions at 2 weeks (Figure 4.10). Masson Trichrome staining was used to stain collagen at the interface. As expected, the interface of PLGA films stains lightly, but uniformly for collagen from the implant dorsal to the hypodermis. Compound 48/80 treatment results in a more prominent collagen staining, with more developed collagen formation observed as thick bands of collagen staining darker shade of blue. Collagen deposition in Cromolyn treated implant more closely resembles unmodified films with a uniform, light staining for total

collagen from implant to hypodermis. The thickness of the collagen staining layer was measured and resembles the trend for total cell infiltrate thickness, with Compound 48/80 initiating a thicker collagen layer surrounding the implants.

The layering of collagen I in fibrotic tissue provides a measure of the degree of fibrosis. In order to compare fibrotic degree among implants, Picosirius red staining was used under polarized light microscopy to view collagen I fibers (Figure 4.10). Unmodified films had discontinuous collagen I deposition, pronounced near the implant interface becoming segmented away from the implant with a mix of collagen III. Compound 48/80 embedded implants had a continuous, well formed layer of collagen I extending from the implant surface throughout the interface tissue with no evident collagen III. Cromolyn embedded implants had a thin collagen I layer which was segmented similar to PLGA unmodified films with a mix of collagen III throughout the interface. Interfaces of each treatment condition were characterized for the percentage of collagen I area per interface area. Compound 48/80 embedded implants had a significantly higher percentage of collagen I deposition (95%), significantly higher than both PLGA unmodified (80%) and Cromolyn embedded films (55%). In addition, Cromolyn embedded implants had significantly reduced collagen I deposition compared to PLGA unmodified films.

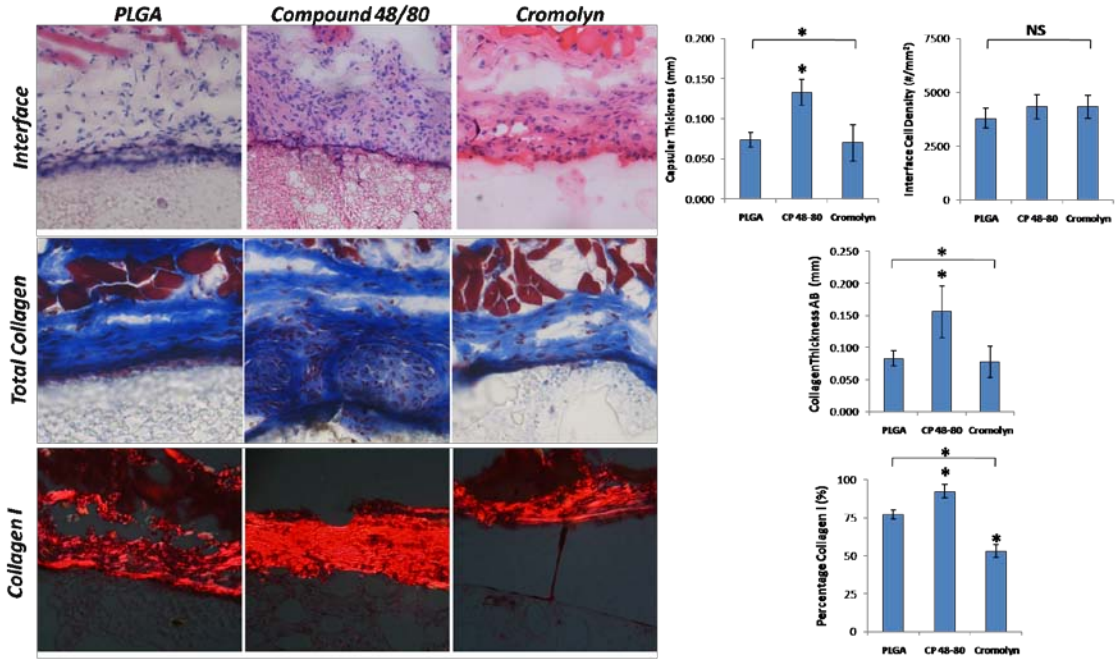

Figure 4.10 Interfacial responses and collagen deposition in the context of variable mast cell responses. H&E stains show differential cellular composition at the interface, further evident in quantification of the thickness of cells at the interface though the density is similar. Masson Trichrome staining for total collagen reveals differences in the nature of the fibrotic response, for which quantification of the thickness of the collagen layer reveals significant differences between treatment groups. Examination of collagen I content with Picosirius Red shows nearly 100% coverage in the Compound 48/80 group decreasing through control to Cromolyn treatment (All statistics are ANOVA with Dunnett intergroup comparison to control values, bracket with * and * above groups represent significant tests at $P<0.05$).

4.6.3.2 Mast cell responses affect fibrocyte and macrophage responses while also influencing Thy-1 and MSC responses

As mentioned previously, our studies have linked the degree of phagocyte responses to the degree of mast cell degranulation. Therefore, we would expect that a variable mast cell response would correlate directly with a variable macrophage response given this link. As expected, we see a high density of macrophages at the interface of Compound 48/80 embedded films compared to other treatment groups (Figure 4.11). Quantification reveals that the density of macrophage is significantly higher in Compound 48/80 treated films, while the percentage of macrophages per total cells is significantly reduced in cromolyn treated films.

Thus far, we have observed that mast cell response appears to correlate with the fibrotic outcome. Since fibrocytes participate in fibrotic reaction, we would expect to find differences in their responses to a biomaterial with variable mast cell effector tendencies. We therefore assessed the fibrocyte response by examining the density of $CD45^{+}CI^{+}$ fibrocytes at the biomaterial:tissue interface. Indeed we observe that the dispersion of these cells at the biomaterial interface is inconsistent between treatment groups, with the mast cell stabilizer cromolyn appearing to have reduced the recruitment of fibrocytes to the biomaterial implantation site (Figure 4.11). To quantify these responses, we examine both the density and percentage of fibrocytes at the biomaterial interface. Indeed we find that implant combination with the mast cell stabilizer cromolyn was able to significantly reduce the recruitment density and percentage of fibrocytes to the PLGA films.

We next examined Thy-1 expression, as loss of Thy-1 expression has been linked with a terminal differentiation state of fibroblasts and participation in fibrosis. In agreement with fibrotic histology assessments, we see more prominent expression of Thy-1 in less fibrotic condition and decreased Thy-1 expression in more fibrotic conditions, specifically higher expression in PLGA and lower expression in Compound 48-80 (Figure 4.11). In addition, Cromolyn treated implants also had higher Thy-1 expression. The percentage of $Thy\text{-}1^{+}$ cells at the interface was higher in PLGA and Cromolyn groups compared with Compound 48-80.

Though there is no established mechanism for biomaterial-mediated recruitment of host derived stem cells, based on our previous observations we hypothesized that mast cell behavior may contribute to the degree of MSC recruitment. In addition, a reduction in the number of $Thy\text{-}1^{+}$ cells may represent conditions in which a reduced number of MSC (which express Thy-1) would have been recruited from host stores. Consistent with our previous observations, we observe a small percentage of cells at the biomaterial interface expressing markers of multipotent MSC (Figure 4.11). Though we qualitatively observe a higher number of cells at the interface of Compound 48/80 embedded implants, the number of host derived MSC is lower

than that of untreated controls. In contrast, Cromolyn embedded implants appear similar to unmodified PLGA implants, with a considerable percentage of MSC present at the biomaterial interface. The percentage of MSC for each treatment condition was compared and reveals that the percentage of MSC was significantly lower than unmodified and Cromolyn embedded implant groups.

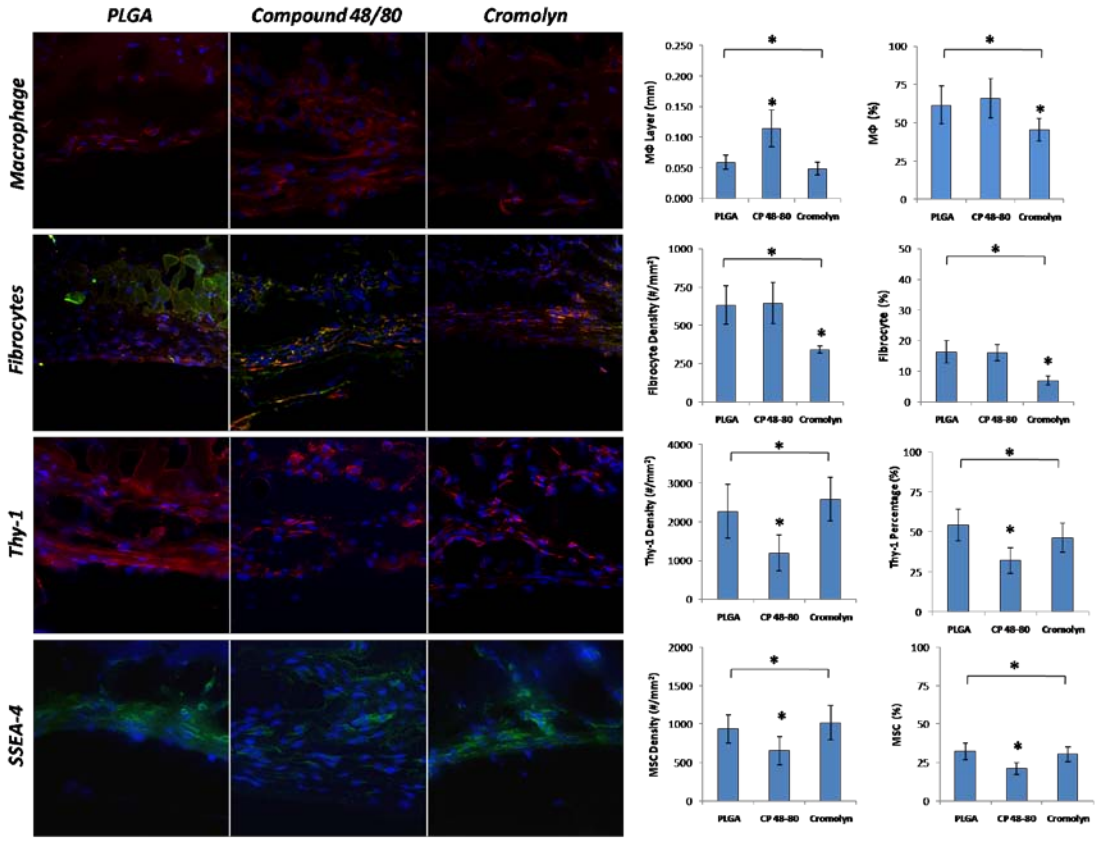

Figure 4.11 Fibrocyte, macrophage, CD90, and stem cell responses due to variable mast cell responses. Cromolyn treatment appeared to reduce the infiltration of fibrocytes into the interfacial tissue, which could be verified by examining both the density and percentage of fibrocytes. In addition, the macrophage response was also altered, with macrophage buildup highest in Compound 48/80 treatment groups and lower number by percentage in Cromolyn treatment group. In addition, the expression of Thy-1 was altered between treatment groups with percentage lowest due to Compound 48/80 treatment. Finally, the MSC response assessed by SSEA-4 expression was also reduced due to Compound 48/80 treatment. All statistics were ANOVA with Dunnett intergroup comparison to control, with brackets and * and * above treatment group representing significant tests at $P<0.05$.

Finally, we examined the cell populations at the interface in a similar format to previous sections. Interestingly, as seen in our previous studies, treatment for variable mast cell responses significantly altered the macrophage response, however at the 2 week time point imparted little influence over CD45 cells at the interface (Figure 4.12). In addition, we find a slight decrease in the number of total α-SMA positive cells at the interface. In conjunction with this, we observe significant decreases in the percentage of fibrocyte-derived myofibroblasts as

well as fibrocyte. Cromolyn significantly reduced fibrocyte-derived myofibroblasts with respect to control while also decreasing fibrocyte percentages with respect to compound 48/80 treatment.

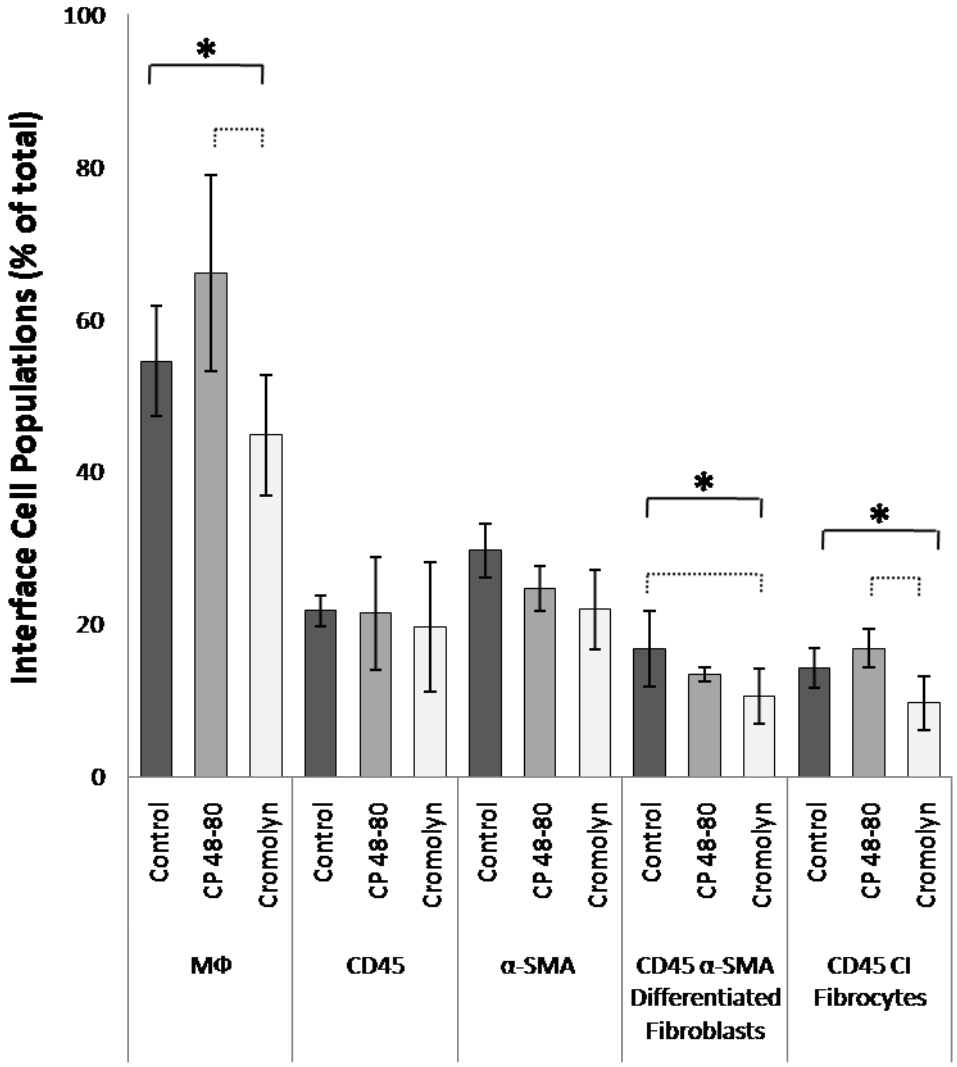

Figure 4.12 Effect of mast cell response on cell populations at the biomaterial interface. Cromolyn treatment effectively reduced inflammatory cells and fibrotic cells at the biomaterial interface in comparison to other treatment groups (ANOVA bracket and * P<0.05, Bonferroni or Dunnett intergroup tests, dashed brackets P<0.05).

4.6.4 Discussion

Based on the fact that both leukocyte responses were minimally involved in fibrocyte responses and CXCL12 neutralization was only slightly effective, this led us to consider the role of the mast cell in facilitating biomaterial-mediated fibrotic responses through fibrocyte interactions. However, literature regarding biomaterial-mediated fibrocyte responses are extremely limited [214].

We based this hypothesis on the assumption that though Dex may limit leukocyte infiltration [123, 230], processes resulting from peripheral tissue damage and subsequent biomaterial mediated protein interactions may play a more prominent role [35, 37, 72, 82]. Though we find reduced cell infiltrate, and more specifically reduced macrophage and leukocyte infiltration, the number of fibrocytes was nearly unaltered. This supported our assumption that mast cells may play a more decisive role in dictating fibrocyte recruitment, and subsequently implant-mediated fibrosis. Prior to investigating mast cell influence, we examined whether local distraction of the SDF-1α axis with SDF-1 inhibitor Chalcone-4 in vivo would obstruct fibrocyte responses. As expected, we found that Chalcone-4 embedded into PLGA films was able to substantially reduce collagen deposition at the biomaterial interface, likely through limiting fibrocyte chemotaxis and activation in the developing granulation tissue through SDF-1α-dependent interactions.

If fibrocyte responses were unaffected by leukocyte infiltration, yet local inhibition of SDF-1α was effective, we hypothesized that stabilizing or destabilizing mast cell responses in comparison to the normal biomaterial-mediated response, creating variable levels of mast cell influence to the same biomaterial implant, should vary the infiltration of fibrocytes and the degree of fibrosis at the biomaterial interface. In line with our hypothesis, stabilizing the mast cell response was able to reduce macrophage infiltration, reduce fibrocyte infiltration, and significantly decrease the thickness of the collagen encapsulating layer while limiting the deposition of collagen I fibers at the interface.

Previous results have suggested that mast cells may be critical determinants of the fibrotic potential of a given biomaterial, especially, given their critical role in inflammatory cell recruitment to the sites of biomaterial implantation [24, 40, 208, 212]. It is plausible that mast cell release of histamine and tryptase as well as cytokines such as TNF-α, GM-CSF, IL-4, IL-6, IL-10, IL-13, IL-16 and chemokines MIP-1α, MCP-1 may result in the proper signals to initiate significant fibrocyte infiltration around 4 days after implantation based on tissue injury and fibrotic model studies [40, 276]. In fact, a recent study suggests that mast cell tryptase may be linked to autocrine TGF-β1 signaling which initiates α-SMA expression [277].

TGF-β1 has been linked to fibrocyte differentiation to myofibroblasts, detected by expression of α-SMA in conjunction with a decrease in CD45 and CD34 expression. The influence of mast cells on this response appears to result in both insuffiecient stimuli for normal fibrocyte infiltration and significant reductions in the presence of α-SMA^{+} myofibroblasts. These alterations were linked to decreases in cell infiltration at the implant interface, decreased total collagen at the interface, and a significant disruption in collagen I synthesis and organization at the implant interface. Though SDF-1α production has not been directly linked with mast cells, several mast cell dependent processes, including fibroblast activation and cytokine production as well as endothelial cell activation, has been linked and these cells have been implicated in SDF-1α production. As we have previously shown, downstream modulation of SDF-1α by inactivating through local release of Chalcone-4 was also able to significantly alter collagen deposition at the interface.

In summary, this aim has established that fibrocytes and fibrocyte-derived myofibroblasts are responsible for collagen deposition at the implant interface. Mast cell activation as a result of biomaterial-mediated protein interactions initiates an influx of inflammatory cells and fibrotic progenitors. The degree of fibrocyte and inflammatory cell influx could be varied by altering the degree of mast cell activation, which additionally altered the deposition of collagen at the implantation site. The recruitment of fibrocytes to the implantation

site is co-dependent upon both inflammatory chemokines as well as SDF-1α, which was able to reduce fibrocyte chemotaxis in vitro as well as reduce collagen deposition in vivo. However, treatment with Dex to reduce inflammatory responses did not significantly alter the recruitment of fibrocytes, however, likely influenced the activation of fibrocytes based on TGF-β1 dependent processes through reduction of macrophage and leukocyte responses. Therefore, the mast cell response appears to be a primary target for reducing biomaterial-mediated foreign body responses.

CHAPTER 5

SUMMARY AND CONCLUSION

5.1 Summary

In this dissertation, two promising strategies to reduce biomaterial-mediated foreign body responses were investigated. The first of these strategies, modification of the biomaterial surface to increase wetability, was able to moderately influence inflammatory cell interactions with the scaffolds. Exposure of macrophages to surface modified scaffolds in vitro altered cytokine secretion as analyzed through macrophage chemotaxis to preconditioned media. In addition, in vivo scaffold modification was able to slightly alter inflammatory cell influx to the biomaterial interface dependent upon surface functional group. Surface modification to increase hydrophilicity also influenced the penetration of cells into the scaffold with time as well as infiltration density and matrix production. However surface modification exerted only minor influence over the thickness of the fibrotic capsule surrounding the biomaterial implants.

The second approach was primarily focused on increasing the participation of host-derived stem cells using stem cell chemokines to reduce biomaterial-mediated fibrotic responses. The increase in host-derived stem cells was able to significantly alter the deposition of collagen at the biomaterial interface. In addition, SDF-1α dependent recruitment of angiogenic progenitors was also increased, resulting in better vasculogenesis accompanied by improved cell infiltration into the scaffolds. In addition, inflammatory cytokine analysis revealed drastic changes in the implant cytokine environment. These changes were accompanied by shifts in macrophage phenotype, revealing the participation of macrophage shown to selectively participate in wound healing responses. In searching for a primary influence of SDF-1α on these responses, the mast cell emerged as a critical parameter which was influenced almost immediately after implantation. Based on the delivery duration of the chemokine, these

responses appear to be continually modulated over the course of biomaterial-mediated host reaction.

Interestingly, when delivery of SDF-1α was delayed until after primary biomaterial-induced mast cell degranulation, the effect of SDF-1α supplementation was less substantial. This led us to consider whether the mast cell responses were primarily regulating the biomaterial-mediated fibrotic response. To test this hypothesis, we first identified what cells at the biomaterial interface where primarly contributing to the deposition of collagen, from which the fibrotic progenitor cells (fibrocytes) and the downstream fibrotcyte-derived myofibroblast were primarily implicated. Based on their implication in several disease conditions as primary contributors to fibrosis, we proceeded in indentifying their arrival at the implantation site and chemokines which may be governing their arrival. Interestingly, we found that fibrocytes recovered from the biomaterial implantation site appeared to predominantely migrate in response to SDF-1α, prominently produced in the weeks following tissue injury. Using this target, we investigated downregulation of the inflammatory response using the drug Dex. Though this greatly affected inflammatory cell influx, the percentage of recruited fibrocytes and the generation of myofibroblasts was not significantly influenced. We therefore, directly targeted SDF-1α in vivo to reduce fibrocyte infiltration.

In agreement with in vitro chemotaxis studies, SDF-1α neutralization was able to significantly reduce the influx of fibrocytes as well as the generation of fibrocyte-derived myofibroblasts in addition to reducing inflammatory cell influx. This condition led to a significant reduction in fibrotic responses at the conclusion of the first week of implantation. Since mast cells influence the acute inflammatory response to biomaterial implants, we hypothesized that creating different degrees of mast cell responses to the same implant would result in differentiatal stimulation of cells responsible for producing SDF-1α in addition to reducing inflammatory stimuli. We further suspected this would influence not only inflammatory cell

recruitment and fibrocyte recruitment, but substantially alter the generation of fibrocyte-derived myofibroblasts and the degree of fibrotic responses.

Analysis of biomaterial implants two weeks after implantation showed that reducing the mast cell response with Cromolyn was able to significantly reduce macrophage influx in addition to fibrocyte and fibrocyte-derived myofibroblast influx to the biomaterial interface. As expected, Cromolyn treatment was therefore able to significant reduce fibrotic encapsulation and collagen I structure around the biomaterial, implicating mast cells as the initiator of the fibrotic response to biomaterial implants.

Based on these results, we propose the following hypothetical sequence of events leading to the formation of fibrotic tissue around biomaterial implants. Shortly following implantation, direct protein interactions and protein interactions leading to release of soluble mediators lead to mast cell activation. This results in the degranulation of mast cells, leading to activation of endothelial cells and recruitment of inflammatory cells and fibrotic progenitors. Through local influence of implant activated macrophage nd mast cells, fibrocytes differentiate into myofibroblasts which align at the biomaterial interface and begin to produce collagen. This collagen production results in fibrotic encapsulation of the implant.

5.2 Conclusion

Mast cells, which have been less significantly investigated in biomaterial-mediated responses, appear to control many aspects of downstream host responses. Their behavior can be linked to both inflammatory and fibrotic progenitor responses, through which modulation of the mast cell response appears to significantly influence both of these parameters. Despite links between SDF-1α mediated recruitment of fibrocytes in this process, SDF-1α supplementation was able to significantly improve the host-derived stem cell response, and thereby improve the integration of the scaffold by reducing fibrotic encapsultation. However, this process appeared be to be linked with selective modulation of mast cell responses, resulting in a decrease in mast cell activation. Therefore, here were able to identify both the

critical involvement of the mast cell response in biomaterial-mediated fibrosis, as well as identify a strategy to reduce mast cell activation while improving host-derived stem cell responses to improve the response to biomaterial scaffolds in the subcutaneous space.

5.3 Future Prospectives

Controlling the host response to biomaterial implants is of great interest to both biomaterial scientists and tissue engineers moving forward. Pending the arrival of a broader selection of clinically applicable biomaterials, methods to alter the host response to available biomaterials is critically important. Here we have begun to investigate the influence of improving host-derived stem cell response to improve these parameters. Though successful, the pleitrophic effects of chemokines especially with regard to inflammatory and fibrotic response must be fully appreciated. We must continue to seek a balance between modulation of the factors which control unregulated fibrotic response and those which enhance tissue integration. Identification of these factors will open up possibilities to altering cell responses potentially through protein and surface interactions, which may reduce the need for recombinant cytokine therapy, increasing the translatability of biomaterial designs.

The following questions remained to be addressed regarding the biomaterial-mediated fibrotic responses. There is still some debate as to source of fibrotic progenitor cells, specifically regarding their phenotype prior to and after signaling to home to the implant interface. Though SDF-1α appears to be primarily involved based on our results, several other chemokines have been implicated in other models, which may implicate a redundant, more complicated pathway of chemotaxis. In addition, fibrocytes which do not express CXCR-4 have been identified which highlights our incomplete understanding of fibrotic progenitors. While the influence of inflammatory cells on fibrocytes has been thoroughly investigated, the influence of host-derived stem cells, with regards to both their potential involvement as source of fibrosis and potential paracrine influence over fibrocyte differentiation has not been well investigated. In addition, the potential interactions of novel biomaterials designed to reduce mast cell responses

has not been well developed and represents an interesting new track for biomaterial development to reduced fibrotic host responses to polymeric scaffolds implants.

REFERENCES

1. Muschler GF, Nakamoto C, Griffith LG. Engineering principles of clinical cell-based tissue engineering. J Bone Joint Surg Am 2004;86-A(7):1541-1558.
2. Ikada Y. Challenges in tissue engineering. J R Soc Interface 2006;3(10):589-601.
3. Centeno CJ, Busse D, Kisiday J, Keohan C, Freeman M, Karli D. Regeneration of meniscus cartilage in a knee treated with percutaneously implanted autologous mesenchymal stem cells. Med Hypotheses 2008;71(6):900-908.
4. Payne N, Siatskas C, Bernard CC. The promise of stem cell and regenerative therapies for multiple sclerosis. J Autoimmun 2008;31(3):288-294.
5. Park HC, Shim YS, Ha Y, Yoon SH, Park SR, Choi BH, et al. Treatment of complete spinal cord injury patients by autologous bone marrow cell transplantation and administration of granulocyte-macrophage colony stimulating factor. Tissue Eng 2005;11(5-6):913-922.
6. Janssens S, Dubois C, Bogaert J, Theunissen K, Deroose C, Desmet W, et al. Autologous bone marrow-derived stem-cell transfer in patients with ST-segment elevation myocardial infarction: double-blind, randomised controlled trial. Lancet 2006;367(9505):113-121.
7. Enzmann V, Yolcu E, Kaplan HJ, Ildstad ST. Stem cells as tools in regenerative therapy for retinal degeneration. Arch Ophthalmol 2009;127(4):563-571.
8. Jawad H, Lyon AR, Harding SE, Ali NN, Boccaccini AR. Myocardial tissue engineering. Br Med Bull 2008;87:31-47.
9. Ugurlucan M, Yerebakan C, Furlani D, Ma N, Steinhoff G. Cell sources for cardiovascular tissue regeneration and engineering. Thorac Cardiovasc Surg 2009;57(2):63-73.
10. Roth CC, Kropp BP. Recent advances in urologic tissue engineering. Curr Urol Rep 2009;10(2):119-125.
11. Ekdahl M, Wang JH, Ronga M, Fu FH. Graft healing in anterior cruciate ligament reconstruction. Knee Surg Sports Traumatol Arthrosc 2008;16(10):935-947.
12. Arthur A, Zannettino A, Gronthos S. The therapeutic applications of multipotential mesenchymal/stromal stem cells in skeletal tissue repair. J Cell Physiol 2009;218(2):237-245.
13. Aframian DJ, Cukierman E, Nikolovski J, Mooney DJ, Yamada KM, Baum BJ. The growth and morphological behavior of salivary epithelial cells on matrix protein-coated biodegradable substrata. Tissue Engineering 2000;6(3):209-216.
14. Thevenot P, Hu W, Tang L. Surface chemistry influences implant biocompatibility. Current Topics In Medicinal Chemistry 2008;8(4):270-280.
15. Luttikhuizen DIT, Harmsen MC, Luyn MJAV. Cellular and molecular dynamics in the foreign body reaction. Tissue Engineering 2006;12(7):1955-1970.
16. Anderson JM, Rodriguez A, Chang DT. Foreign body reaction to biomaterials. Semin Immunol 2008;20(2):86-100.
17. Mikos AG, Herring SW, Ochareon P, Elisseeff J, Lu HH, Kandel R, et al. Engineering complex tissues. Tissue Eng 2006;12(12):3307-3339.
18. Rouwkema J, Westerweel PE, de Boer J, Verhaar MC, van Blitterswijk CA. The use of endothelial progenitor cells for prevascularized bone tissue engineering. Tissue Engineering Part A 2009;15(8):2015-2027.
19. Lysaght MJ, Hazlehurst AL. Tissue engineering: The end of the beginning. Tissue Engineering 2004;10(1-2):309-320.
20. Hunziker E, Spector M, Libera J, Gertzman A, Woo SL, Ratcliffe A, et al. Translation from research to applications. Tissue Eng 2006;12(12):3341-3364.

21. Seitz S, Ern K, Lamper G, Docheva D, Drosse I, Milz S, et al. Influence of in vitro cultivation on the integration of cell-matrix constructs after subcutaneous implantation. Tissue Eng 2007;13(5):1059-1067.
22. Laschke MW, Harder Y, Amon M, Martin I, Farhadi J, Ring A, et al. Angiogenesis in tissue engineering: breathing life into constructed tissue substitutes. Tissue Eng 2006;12(8):2093-2104.
23. Smith MK, Peters MC, Richardson TP, Garbern JC, Mooney DJ. Locally enhanced angiogenesis promotes transplanted cell survival. Tissue Eng 2004;10(1-2):63-71.
24. Jones KS. Effects of biomaterial-induced inflammation on fibrosis and rejection. Semin Immunol 2008;20(2):130-136.
25. Mountziaris PM, Mikos AG. Modulation of the inflammatory response for enhanced bone tissue regeneration. Tissue Eng Part B Rev 2008;14(2):179-186.
26. Jones KS. Assays on the influence of biomaterials on allogeneic rejection in tissue engineering. Tissue Eng Part B Rev 2008;14(4):407-417.
27. Kaully T, Kaufman-Francis K, Lesman A, Levenberg S. Vascularization-the conduit to viable engineered tissues. Tissue Eng Part B Rev 2009;15(2):159-169.
28. Yang J, Yamato M, Kohno C, Nishimoto A, Sekine H, Fukai F, et al. Cell sheet engineering: recreating tissues without biodegradable scaffolds. Biomaterials 2005;26(33):6415-6422.
29. Silva MM, Cyster LA, Barry JJ, Yang XB, Oreffo RO, Grant DM, et al. The effect of anisotropic architecture on cell and tissue infiltration into tissue engineering scaffolds. Biomaterials 2006;27(35):5909-5917.
30. Scheufler O, Schaefer DJ, Jaquiery C, Braccini A, Wendt DJ, Gasser JA, et al. Spatial and temporal patterns of bone formation in ectopically pre-fabricated, autologous cell-based engineered bone flaps in rabbits. J Cell Mol Med 2008;12(4):1238-1249.
31. Thevenot P, Nair A, Dey J, Yang J, Tang L. Method to analyze three-dimensional cell distribution and infiltration in degradable scaffolds. Tissue Eng Part C Methods 2008;14(4):319-331.
32. Wu X, Rabkin-Aikawa E, Guleserian KJ, Perry TE, Masuda Y, Sutherland FWH, et al. Tissue-engineered microvessels on three-dimensional biodegradable scaffolds using human endothelial progenitor cells. Am J Physiol Heart Circ Physiol 2004;287(2):H480-487.
33. Ko HC, Milthorpe BK, McFarland CD. Engineering thick tissues--the vascularisation problem. Eur Cell Mater 2007;14:1-18; discussion 18-19.
34. Griffith LG, Naughton G. Tissue engineering--current challenges and expanding opportunities. Science 2002;295(5557):1009-1014.
35. Kao WJ. Evaluation of protein-modulated macrophage behavior on biomaterials: designing biomimetic materials for cellular engineering. Biomaterials 1999;20(23-24):2213-2221.
36. Anderson JM. Inflammatory Response to Implants. ASAIO Journal 1988;34(2):101-107.
37. Hu W-J, Eaton JW, Ugarova TP, Tang L. Molecular basis of biomaterial-mediated foreign body reactions. Blood 2001;98(4):1231-1238.
38. Tang L. Mechanisms of fibrinogen domains : biomaterial interactions. Journal of Biomaterials Science, Polymer Edition 1998;9:1257-1266.
39. Zdolsek J, Eaton JW, Tang L. Histamine release and fibrinogen adsorption mediate acute inflammatory responses to biomaterial implants in humans. J Transl Med 2007;5:31.
40. Tang L, Jennings TA, Eaton JW. Mast cells mediate acute inflammatory responses to implanted biomaterials. Proc Natl Acad Sci U S A 1998;95(15):8841-8846.
41. Nilsson B, Ekdahl KN, Mollnes TE, Lambris JD. The role of complement in biomaterial-induced inflammation. Molecular Immunology 2007;44(1-3):82-94.
42. Schmid-Schonbein GW. Analysis of Inflammation. Annual Review of Biomedical Engineering 2006;8(1):93-151.

43. Oki T, Kitaura J, Eto K, Lu Y, Maeda-Yamamoto M, Inagaki N, et al. Integrin {alpha}IIb{beta}3 induces the adhesion and activation of mast cells through interaction with fibrinogen. J Immunol 2006;176(1):52-60.
44. Thevenot PT, Nair AM, Shen J, Lotfi P, Ko CY, Tang L. The effect of incorporation of SDF-1alpha into PLGA scaffolds on stem cell recruitment and the inflammatory response. Biomaterials;31(14):3997-4008.
45. Kyriakides TR, Foster MJ, Keeney GE, Tsai A, Giachelli CM, Clark-Lewis I, et al. The cc chemokine ligand, CCL2/MCP1, participates in macrophage fusion and foreign body giant cell formation. Am J Pathol 2004;165(6):2157-2166.
46. Anderson JM, Jones JA. Phenotypic dichotomies in the foreign body reaction. Biomaterials 2007;28(34):5114-5120.
47. Novak MT, Bryers JD, Reichert WM. Biomimetic strategies based on viruses and bacteria for the development of immune evasive biomaterials. Biomaterials 2009;30(11):1989-2005.
48. Bridges AW, Garcia AJ. Anti-inflammatory polymeric coatings for implantable biomaterials and devices. J Diabetes Sci Technol 2008;2(6):984-994.
49. Viola A, Luster AD. Chemokines and their receptors: Drug targets in immunity and inflammation. Annual Review of Pharmacology and Toxicology 2008;48(1):171-197.
50. Grunewald M, Avraham I, Dor Y, Bachar-Lustig E, Itin A, Jung S, et al. VEGF-induced adult neovascularization: recruitment, retention, and role of accessory cells. Cell 2006;124(1):175-189.
51. Schledzewski K, Falkowski M, Moldenhauer G, Metharom P, Kzhyshkowska J, Ganss R, et al. Lymphatic endothelium-specific hyaluronan receptor LYVE-1 is expressed by stabilin-1+, F4/80+, CD11b+ macrophages in malignant tumours and wound healing tissue in vivo and in bone marrow cultures in vitro: implications for the assessment of lymphangiogenesis. The Journal of Pathology 2006;209(1):67-77.
52. Badylak SF, Valentin JE, Ravindra AK, McCabe GP, Stewart-Akers AM. Macrophage Phenotype as a Determinant of Biologic Scaffold Remodeling. Tissue Engineering Part A 2008;14(11):1835-1842.
53. Halaby IA, Lyden SP, Davies MG, Roztocil E, Salamone LJ, Brooks AI, et al. Glucocorticoid-regulated VEGF expression in ischemic skeletal muscle. Mol Ther 2002;5(3):300-306.
54. Ma Z, Mao Z, Gao C. Surface modification and property analysis of biomedical polymers used for tissue engineering. Colloids and Surfaces B: Biointerfaces 2007;60(2):137-157.
55. Jiao YP, Cui FZ. Surface modification of polyester biomaterials for tissue engineering. Biomed Mater 2007;2(4):R24-37.
56. Williams DF. On the mechanisms of biocompatibility. Biomaterials 2008;29(20):2941-2953.
57. Chen S, Jones JA, Xu Y, Low H-Y, Anderson JM, Leong KW. Characterization of topographical effects on macrophage behavior in a foreign body response model. Biomaterials;31(13):3479-3491.
58. Roach P, Eglin D, Rohde K, Perry C. Modern biomaterials: a review—bulk properties and implications of surface modifications. Journal of Materials Science: Materials in Medicine 2007;18(7):1263-1277.
59. Kamath S, Bhattacharyya D, Padukudru C, Timmons RB, Tang L. Surface chemistry influences implant-mediated host tissue responses. Journal of Biomedical Materials Research Part A 2008;86A(3):617-626.
60. Nair A, Zou L, Bhattacharyya D, Timmons RB, Tang L. Species and density of implant surface chemistry affect the extent of foreign body reactions. Langmuir 2008;24(5):2015-2024.
61. Chen C, Raghunath M. Focus on collagen: in vitro systems to study fibrogenesis and antifibrosis - state of the art. Fibrogenesis & Tissue Repair 2009;2(1):7.

62. Tang L, Liu L, Elwing HB. Complement activation and inflammation triggered by model biomaterial surfaces. J Biomed Mater Res 1998;41(2):333-340.
63. Tang L, Wu Y, Timmons RB. Fibrinogen adsorption and host tissue responses to plasma functionalized surfaces. J Biomed Mater Res 1998;42(1):156-163.
64. Badylak SF, Gilbert TW. Immune response to biologic scaffold materials. Seminars in Immunology 2008;20(2):109-116.
65. Low QEH, Drugea IA, Duffner LA, Quinn DG, Cook DN, Rollins BJ, et al. Wound healing in MIP-1{alpha}-/- and MCP-1-/- mice. Am J Pathol 2001;159(2):457-463.
66. Jones JA, McNally AK, Chang DT, Qin LA, Meyerson H, Colton E, et al. Matrix metalloproteinases and their inhibitors in the foreign body reaction on biomaterials. Journal of Biomedical Materials Research Part A 2008;84A(1):158-166.
67. Moss AJ, Sharma S, Brindle NPJ. Rational design and protein engineering of growth factors for regenerative medicine and tissue engineering. Biochemical Society Transactions 2009;037(4):717-721.
68. Tayalia P, Mooney DJ. Controlled growth factor delivery for tissue engineering. Advanced Materials 2009;21(32-33):3269-3285.
69. Babensee JE, McIntire LV, Mikos AG. Growth factor delivery for tissue engineering. Pharm Res 2000;17(5):497-504.
70. Onuki Y, Bhardwaj U, Papadimitrakopoulos F, Burgess DJ. A review of the biocompatibility of implantable devices: current challenges to overcome foreign body response. J Diabetes Sci Technol 2008;2(6):1003-1015.
71. Yoon SJ, Kim SH, Ha HJ, Ko YK, So JW, Kim MS, et al. Reduction of inflammatory reaction of poly(D,L-lactic-co-glycolic acid) using demineralized bone particles. Tissue Engineering Part A 2008;14(4):539-547.
72. Kenneth Ward W. A review of the foreign-body response to subcutaneously-implanted devices: the role of macrophages and cytokines in biofouling and fibrosis. J Diabetes Sci Technol 2008;2(5):768-777.
73. Morais J, Papadimitrakopoulos F, Burgess D. Biomaterials/Tissue interactions: Possible solutions to overcome foreign body response. The AAPS Journal 2010.
74. Chan G, Mooney DJ. New materials for tissue engineering: towards greater control over the biological response. Trends in Biotechnology 2008;26(7):382-392.
75. Chu PK, Chen JY, Wang LP, Huang N. Plasma-surface modification of biomaterials. Materials Science and Engineering: R: Reports 2002;36(5-6):143-206.
76. Wu YJ, Timmons RB, Jen JS, Molock FE. Non-fouling surfaces produced by gas phase pulsed plasma polymerization of an ultra low molecular weight ethylene oxide containing monomer. Colloids and Surfaces B: Biointerfaces 2000;18(3-4):235-248.
77. Thevenot P, Cho J, Wavhal D, Timmons RB, Tang L. Surface chemistry influences cancer killing effect of TiO2 nanoparticles. Nanomedicine 2008;4(3):226-236.
78. Cho J, Denes FS, Timmons RB. Plasma processing approach to molecular surface tailoring of nanoparticles: Improved photocatalytic activity of TiO2. Chemistry of Materials 2006;18(13):2989-2996.
79. Yang J, Shi G, Bei J, Wang S, Cao Y, Shang Q, et al. Fabrication and surface modification of macroporous poly(L-lactic acid) and poly(L-lactic-co-glycolic acid) (70/30) cell scaffolds for human skin fibroblast cell culture. J Biomed Mater Res 2002;62(3):438-446.
80. Nair A, Thevenot PT, Dey J, Shen J, Sun MW, Yang J, et al. Novel polymeric scaffolds using protein microbubbles as porogen and growth factor carriers. Tissue Eng Part C Methods 2009.
81. Brodbeck WG, Nakayama Y, Matsuda T, Colton E, Ziats NP, Anderson JM. Biomaterial surface chemistry dictates adherent monocyte/macrophage cytokine expression in vitro. Cytokine 2002;18(6):311-319.
82. Chang DT, Jones JA, Meyerson H, Colton E, Kwon IK, Matsuda T, et al. Lymphocyte/macrophage interactions: Biomaterial surface-dependent cytokine, chemokine, and

matrix protein production. Journal of Biomedical Materials Research Part A 2008;87A(3):676-687.
83. Jones JA, Chang DT, Meyerson H, Colton E, Kwon IK, Matsuda T, et al. Proteomic analysis and quantification of cytokines and chemokines from biomaterial surface-adherent macrophages and foreign body giant cells. Journal of Biomedical Materials Research Part A 2007;83A(3):585-596.
84. Nishida K, Hasegawa A, Nakae S, Oboki K, Saito H, Yamasaki S, et al. Zinc transporter Znt5/Slc30a5 is required for the mast cell-mediated delayed-type allergic reaction but not the immediate-type reaction. J Exp Med 2009;206(6):1351-1364.
85. Ali K, Camps M, Pearce WP, Ji H, Ruckle T, Kuehn N, et al. Isoform-Specific functions of phosphoinositide 3-kinases: p110{delta} but not p110{gamma} promotes optimal allergic responses in vivo. J Immunol 2008;180(4):2538-2544.
86. Szuster-Ciesielska A, Plewka K, Daniluk J, Kandefer-Szerszen M. Zinc supplementation attenuates ethanol- and acetaldehyde-induced liver stellate cell activation by inhibiting reactive oxygen species (ROS) production and by influencing intracellular signaling. Biochemical Pharmacology 2009;78(3):301-314.
87. Zhuang S, Yan Y, Daubert RA, Schnellmann RG. Epiregulin promotes proliferation and migration of renal proximal tubular cells. Am J Physiol Renal Physiol 2007;293(1):F219-226.
88. Ratner BD, Bryant SJ. Biomaterials: where we have been and where we are going. Annu Rev Biomed Eng 2004;6:41-75.
89. Wan Y, Tu C, Yang J, Bei J, Wang S. Influences of ammonia plasma treatment on modifying depth and degradation of poly(l-lactide) scaffolds. Biomaterials 2006;27(13):2699-2704.
90. Rodrigues SN, Gonçalves IC, Martins MCL, Barbosa MA, Ratner BD. Fibrinogen adsorption, platelet adhesion and activation on mixed hydroxyl-/methyl-terminated self-assembled monolayers. Biomaterials 2006;27(31):5357-5367.
91. Sivaraman B, Latour RA. The relationship between platelet adhesion on surfaces and the structure versus the amount of adsorbed fibrinogen. Biomaterials;31(5):832-839.
92. Agashe M, Raut V, Stuart SJ, Latour RA. Molecular simulation to characterize the adsorption behavior of a fibrinogen Î³-chain fragment. Langmuir 2004;21(3):1103-1117.
93. Lan MA, Gersbach CA, Michael KE, Keselowsky BG, García AJ. Myoblast proliferation and differentiation on fibronectin-coated self assembled monolayers presenting different surface chemistries. Biomaterials 2005;26(22):4523-4531.
94. Hirata I, Hioki Y, Toda M, Kitazawa T, Murakami Y, Kitano E, et al. Deposition of complement protein C3b on mixed self-assembled monolayers carrying surface hydroxyl and methyl groups studied by surface plasmon resonance. J Biomed Mater Res A 2003;66(3):669-676.
95. Liu L, Elwing H. Complement activation on thiol-modified gold surfaces. J Biomed Mater Res 1996;30(4):535-541.
96. Shan D, Chen L, Njardarson JT, Gaul C, Ma X, Danishefsky SJ, et al. Synthetic analogues of migrastatin that inhibit mammary tumor metastasis in mice. Proceedings of the National Academy of Sciences of the United States of America 2005;102(10):3772-3776.
97. Barbosa JN, Barbosa MA, Águas AP. Inflammatory responses and cell adhesion to self-assembled monolayers of alkanethiolates on gold. Biomaterials 2004;25(13):2557-2563.
98. Barbosa JN, Madureira P, Barbosa MA, Águas AP. The attraction of Mac-1+ phagocytes during acute inflammation by methyl-coated self-assembled monolayers. Biomaterials 2005;26(16):3021-3027.
99. Solovjov DA, Pluskota E, Plow EF. Distinct roles for the alpha and beta subunits in the functions of integrin alphaMbeta2. J Biol Chem 2005;280(2):1336-1345.
100. Abramoff, Magelhaes, Ram. Image processing with ImageJ. Biophotonics Int 2004;11(7):36-42.

101. Shen M, Horbett TA. The effects of surface chemistry and adsorbed proteins on monocyte/macrophage adhesion to chemically modified polystyrene surfaces. Journal of Biomedical Materials Research 2001;57(3):336-345.
102. Shen M, Pan YV, Wagner MS, Hauch KD, Castner DG, Ratner BD, et al. Inhibition of monocyte adhesion and fibrinogen adsorption on glow discharge plasma deposited tetraethylene glycol dimethyl ether. Journal of Biomaterials Science, Polymer Edition 2001;12:961-978.
103. Schutte RJ, Xie L, Klitzman B, Reichert WM. In vivo cytokine-associated responses to biomaterials. Biomaterials 2009;30(2):160-168.
104. Källtorp M, Oblogina S, Jacobsson S, Karlsson A, Tengvall P, Thomsen P. In vivo cell recruitment, cytokine release and chemiluminescence response at gold, and thiol functionalized surfaces. Biomaterials 1999;20(22):2123-2137.
105. Hunt JA, Flanagan BF, McLaughlin PJ, Strickland I, Williams DF. Effect of biomaterial surface charge on the inflammatory reponse: Evaluation of cellular infiltration and TNF-alpha production. Journal of Biomedical Materials Research 1996;31(1):139-144.
106. Lindblad M, Lestelius M, Johansson A, Tengvall P, Thomsen P. Cell and soft tissue interactions with methyl- and hydroxyl-terminated alkane thiols on gold surfaces. Biomaterials 1997;18(15):1059-1068.
107. Evans-Nguyen KM, Tolles LR, Gorkun OV, Lord ST, Schoenfisch MH. Interactions of thrombin with fibrinogen adsorbed on methyl-, hydroxyl-, amine-, and carboxyl-terminated self-assembled monolayers. Biochemistry 2005;44(47):15561-15568.
108. Mirenghi L, Ramires PA, Pentassuglia RE, Rotolo P, Romito A. Growth of human endothelial cells on plasma-treated polyethyleneterephthalate surfaces. J Mater Sci Mater Med 2000;11(5):327-331.
109. Vranken I, De Visscher G, Lebacq A, Verbeken E, Flameng W. The recruitment of primitive Lin(-) Sca-1(+), CD34(+), c-kit(+) and CD271(+) cells during the early intraperitoneal foreign body reaction. Biomaterials 2008;29(7):797-808.
110. Jabs A, Moncada GA, Nichols CE, Waller EK, Wilcox JN. Peripheral blood mononuclear cells acquire myofibroblast characteristics in granulation tissue. J Vasc Res 2005;42(2):174-180.
111. Gurtner GC, Werner S, Barrandon Y, Longaker MT. Wound repair and regeneration. Nature 2008;453(7193):314-321.
112. Shu XZ, Liu Y, Luo Y, Roberts MC, Prestwich GD. Disulfide Cross-Linked Hyaluronan Hydrogels. Biomacromolecules 2002;3(6):1304-1311.
113. Kojima K, Okamoto Y, Miyatake K, Yukisato K, Minami S. Collagen typing of granulation tissue induced by chitin and chitosan. Carbohydrate Polymers 1998;37(2):109-113.
114. Marinucci L, Lilli C, Guerra M, Belcastro S, Becchetti E, Stabellini G, et al. Biocompatibility of collagen membranes crosslinked with glutaraldehyde or diphenylphosphoryl azide: an in vitro study. J Biomed Mater Res A 2003;67(2):504-509.
115. Koschwanez HE, Yap FY, Klitzman B, Reichert WM. In vitro and in vivo characterization of porous poly-L-lactic acid coatings for subcutaneously implanted glucose sensors. J Biomed Mater Res A 2008;87(3):792-807.
116. Dar A, Shachar M, Leor J, Cohen S. Cardiac tissue engineering Optimization of cardiac cell seeding and distribution in 3D porous alginate scaffolds. Biotechnology and Bioengineering 2002;80(3):305-312.
117. Park H, Radisic M, Lim J, Chang B, Vunjak-Novakovic G. A novel composite scaffold for cardiac tissue engineering. In Vitro Cellular & Developmental Biology - Animal 2005;41(7):188-196.
118. Lee SJ, Lim GJ, Lee J-W, Atala A, Yoo JJ. In vitro evaluation of a poly(lactide-co-glycolide)-collagen composite scaffold for bone regeneration. Biomaterials 2006;27(18):3466-3472.

119. Sell SA, Francis MP, Garg K, McClure MJ, Simpson DG, Bowlin GL. Cross-linking methods of electrospun fibrinogen scaffolds for tissue engineering applications. Biomed Mater 2008;3(4):45001.
120. Cao Y, Mitchell G, Messina A, Price L, Thompson E, Penington A, et al. The influence of architecture on degradation and tissue ingrowth into three-dimensional poly(lactic-co-glycolic acid) scaffolds in vitro and in vivo. Biomaterials 2006;27(14):2854-2864.
121. Kim MS, Ahn HH, Shin YN, Cho MH, Khang G, Lee HB. An in vivo study of the host tissue response to subcutaneous implantation of PLGA- and/or porcine small intestinal submucosa-based scaffolds. Biomaterials 2007;28(34):5137-5143.
122. Silva MMCG, Cyster LA, Barry JJA, Yang XB, Oreffo ROC, Grant DM, et al. The effect of anisotropic architecture on cell and tissue infiltration into tissue engineering scaffolds. Biomaterials 2006;27(35):5909-5917.
123. Greco KV, Lara PF, Oliveira-Filho RM, Greco RV, Sudo-Hayashi LS. Lymphatic regeneration across an incisional wound: Inhibition by dexamethasone and aspirin, and acceleration by a micronized purified flavonoid fraction. European Journal of Pharmacology 2006;551(1-3):131-142.
124. Copland IB, Lord-Dufour S, Cuerquis J, Coutu D, Annabi B, Wang E, et al. Improved autograft survival of mesenchymal stromal cells by plasminogen activator inhibitor 1 inhibition. Stem Cells 2009;27(2):467-477.
125. Pacini S, Spinabella S, Trombi L, Fazzi R, Galimberti S, Dini F, et al. Suspension of bone marrow-derived undifferentiated mesenchymal stromal cells for repair of superficial digital flexor tendon in race horses. Tissue Eng 2007;13(12):2949-2955.
126. Caplan AI. Review: mesenchymal stem cells: cell-based reconstructive therapy in orthopedics. Tissue Eng 2005;11(7-8):1198-1211.
127. Kollet O, Shivtiel S, Chen YQ, Suriawinata J, Thung SN, Dabeva MD, et al. HGF, SDF-1, and MMP-9 are involved in stress-induced human CD34+ stem cell recruitment to the liver. J Clin Invest 2003;112(2):160-169.
128. Lapidot T, Dar A, Kollet O. How do stem cells find their way home? Blood 2005;106(6):1901-1910.
129. Sordi V, Malosio ML, Marchesi F, Mercalli A, Melzi R, Giordano T, et al. Bone marrow mesenchymal stem cells express a restricted set of functionally active chemokine receptors capable of promoting migration to pancreatic islets. Blood 2005;106(2):419-427.
130. Zhang G, Nakamura Y, Wang X, Hu Q, Suggs LJ, Zhang J. Controlled release of stromal cell-derived factor-1 alpha in situ increases c-kit+ cell homing to the infarcted heart. Tissue Eng 2007;13(8):2063-2071.
131. Lee Y, Gotoh A, Kwon H-J, You M, Kohli L, Mantel C, et al. Enhancement of intracellular signaling associated with hematopoietic progenitor cell survival in response to SDF-1/CXCL12 in synergy with other cytokines. Blood 2002;99(12):4307-4317.
132. Honczarenko M, Le Y, Swierkowski M, Ghiran I, Glodek AM, Silberstein LE. Human bone marrow stromal cells express a distinct set of biologically functional chemokine receptors. Stem Cells 2006;24(4):1030-1041.
133. Nagasawa T, Kikutani H, Kishimoto T. Molecular cloning and structure of a pre-B-cell growth-stimulating factor. Proc Natl Acad Sci U S A 1994;91(6):2305-2309.
134. Sugiyama T, Kohara H, Noda M, Nagasawa T. Maintenance of the hematopoietic stem cell pool by CXCL12-CXCR4 chemokine signaling in bone marrow stromal cell niches. 2006;25(6):977-988.
135. Broxmeyer HE, Kohli L, Kim CH, Lee Y, Mantel C, Cooper S, et al. Stromal cell-derived factor-1/CXCL12 directly enhances survival/antiapoptosis of myeloid progenitor cells through CXCR4 and G(alpha)i proteins and enhances engraftment of competitive, repopulating stem cells. J Leukoc Biol 2003;73(5):630-638.
136. Kopp H-G, Avecilla ST, Hooper AT, Rafii S. The bone marrow vascular niche: Home of HSC differentiation and mobilization. Physiology 2005;20(5):349-356.

137. Ruiz de Almodovar C, Luttun A, Carmeliet P. An SDF-1 trap for myeloid cells stimulates angiogenesis. Cell 2006;124(1):18-21.
138. Ponte AL, Marais E, Gallay N, Langonné A, Delorme B, Hérault O, et al. The in vitro migration capacity of human bone marrow mesenchymal stem cells: Comparison of chemokine and growth factor chemotactic activities. Stem Cells 2007;25(7):1737-1745.
139. Wynn RF, Hart CA, Corradi-Perini C, O'Neill L, Evans CA, Wraith JE, et al. A small proportion of mesenchymal stem cells strongly expresses functionally active CXCR4 receptor capable of promoting migration to bone marrow. Blood 2004;104(9):2643-2645.
140. Ji JF, He BP, Dheen ST, Tay SSW. Interactions of chemokines and chemokine receptors mediate the migration of mesenchymal stem cells to the impaired site in the brain after hypoglossal nerve injury. Stem Cells 2004;22(3):415-427.
141. Ma J, Ge J, Zhang S, Sun A, Shen J, Chen L, et al. Time course of myocardial stromal cell–derived factor 1 expression and beneficial effects of intravenously administered bone marrow stem cells in rats with experimental myocardial infarction. Basic Research in Cardiology 2005;100(3):217-223.
142. Zhang D, Fan GC, Zhou X, Zhao T, Pasha Z, Xu M, et al. Over-expression of CXCR4 on mesenchymal stem cells augments myoangiogenesis in the infarcted myocardium. J Mol Cell Cardiol 2008;44(2):281-292.
143. Ayelet D, Orit K, Tsvee L. Mutual, reciprocal SDF-1/CXCR4 interactions between hematopoietic and bone marrow stromal cells regulate human stem cell migration and development in NOD/SCID chimeric mice. Experimental hematology 2006;34(8):967-975.
144. Gallagher KA, Liu ZJ, Xiao M, Chen H, Goldstein LJ, Buerk DG, et al. Diabetic impairments in NO-mediated endothelial progenitor cell mobilization and homing are reversed by hyperoxia and SDF-1 alpha. J Clin Invest 2007;117(5):1249-1259.
145. Abbott JD, Huang Y, Liu D, Hickey R, Krause DS, Giordano FJ. Stromal cell-derived factor-1alpha plays a critical role in stem cell recruitment to the heart after myocardial infarction but is not sufficient to induce homing in the absence of injury. Circulation 2004;110(21):3300-3305.
146. Badillo AT, Chung S, Zhang L, Zoltick P, Liechty KW. Lentiviral gene transfer of SDF-1alpha to wounds improves diabetic wound healing. J Surg Res 2007;143(1):35-42.
147. Barbash IM, Chouraqui P, Baron J, Feinberg MS, Etzion S, Tessone A, et al. Systemic delivery of bone marrow-derived mesenchymal stem cells to the infarcted myocardium: Feasibility, cell migration, and body distribution. Circulation 2003;108(7):863-868.
148. Sudres M, Norol F, Trenado A, Gregoire S, Charlotte F, Levacher B, et al. Bone Marrow Mesenchymal Stem Cells Suppress Lymphocyte Proliferation In Vitro but Fail to Prevent Graft-versus-Host Disease in Mice. J Immunol 2006;176(12):7761-7767.
149. Fiorina P, Jurewicz M, Augello A, Vergani A, Dada S, La Rosa S, et al. Immunomodulatory Function of Bone Marrow-Derived Mesenchymal Stem Cells in Experimental Autoimmune Type 1 Diabetes. J Immunol 2009;183(2):993-1004.
150. Gang EJ, Bosnakovski D, Figueiredo CA, Visser JW, Perlingeiro RC. SSEA-4 identifies mesenchymal stem cells from bone marrow. Blood 2007;109(4):1743-1751.
151. Mori L, Bellini A, Stacey MA, Schmidt M, Mattoli S. Fibrocytes contribute to the myofibroblast population in wounded skin and originate from the bone marrow. Experimental Cell Research 2005;304(1):81-90.
152. Colter DC, Sekiya I, Prockop DJ. Identification of a subpopulation of rapidly self-renewing and multipotential adult stem cells in colonies of human marrow stromal cells. Proceedings of the National Academy of Sciences of the United States of America 2001;98(14):7841-7845.
153. Fritton JC, Kawashima Y, Mejia W, Courtland H-W, Elis S, Sun H, et al. The insulin-like growth factor-1 binding protein acid-labile subunit alters mesenchymal stromal cell fate. Journal of Biological Chemistry;285(7):4709-4714.
154. Schutze N, Noth U, Schneidereit J, Hendrich C, Jakob F. Differential expression of CCN-family members in primary human bone marrow-derived mesenchymal stem cells during

osteogenic, chondrogenic and adipogenic differentiation. Cell Communication and Signaling 2005;3(1):5.
155. Kawamura K, Chu CR, Sobajima S, Robbins PD, Fu FH, Izzo NJ, et al. Adenoviral-mediated transfer of TGF-beta1 but not IGF-1 induces chondrogenic differentiation of human mesenchymal stem cells in pellet cultures. Exp Hematol 2005;33(8):865-872.
156. Longobardi L, O'Rear L, Aakula S, Johnstone B, Shimer K, Chytil A, et al. Effect of IGF-I in the chondrogenesis of bone marrow mesenchymal stem cells in the presence or absence of TGF-beta signaling. J Bone Miner Res 2006;21(4):626-636.
157. Hattori K, Heissig B, Tashiro K, Honjo T, Tateno M, Shieh JH, et al. Plasma elevation of stromal cell-derived factor-1 induces mobilization of mature and immature hematopoietic progenitor and stem cells. Blood 2001;97(11):3354-3360.
158. Elmadbouh I, Haider H, Jiang S, Idris NM, Lu G, Ashraf M. Ex vivo delivered stromal cell-derived factor-1alpha promotes stem cell homing and induces angiomyogenesis in the infarcted myocardium. J Mol Cell Cardiol 2007;42(4):792-803.
159. Menon LG, Picinich S, Koneru R, Gao H, Lin SY, Koneru M, et al. Differential gene expression associated with migration of mesenchymal stem cells to conditioned medium from tumor cells or bone marrow cells. Stem Cells 2007;25(2):520-528.
160. Sung HJ, Meredith C, Johnson C, Galis ZS. The effect of scaffold degradation rate on three-dimensional cell growth and angiogenesis. Biomaterials 2004;25(26):5735-5742.
161. Rojas M, Xu J, Woods CR, Mora AL, Spears W, Roman J, et al. Bone marrow-derived mesenchymal stem cells in repair of the injured lung. Am J Respir Cell Mol Biol 2005;33(2):145-152.
162. Gerdoni E, Gallo B, Casazza S, Musio S, Bonanni I, Pedemonte E, et al. Mesenchymal stem cells effectively modulate pathogenic immune response in experimental autoimmune encephalomyelitis. Ann Neurol 2007;61(3):219-227.
163. Morimoto H, Takahashi M, Shiba Y, Izawa A, Ise H, Hongo M, et al. Bone marrow-derived CXCR4+ cells mobilized by macrophage colony-stimulating factor participate in the reduction of infarct area and improvement of cardiac remodeling after myocardial infarction in mice. Am J Pathol 2007;171(3):755-766.
164. Pietramaggiori G, Fiorina P, Scherer S, Mathews J, Jurewicz M, Zwerves H-G, et al. Mobilization of autologous hematopoietic stem cells by targeting the CXCR4-SDF-1a axis to modulate diabetic wound healing. Journal of the American College of Surgeons 2007;205(3, Supplement 1):S66-S66.
165. Chen L, Tredget EE, Wu PY, Wu Y. Paracrine factors of mesenchymal stem cells recruit macrophages and endothelial lineage cells and enhance wound healing. PLoS ONE 2008;3(4):e1886.
166. Kortesidis A, Zannettino A, Isenmann S, Shi S, Lapidot T, Gronthos S. Stromal-derived factor-1 promotes the growth, survival, and development of human bone marrow stromal stem cells. Blood 2005;105(10):3793-3801.
167. Rossignol J, Boyer C, Thinard R, Remy S, Dugast A-S, Dubayle D, et al. Mesenchymal stem cells induce a weak immune response in the rat striatum after allo or xenotransplantation. Journal of Cellular and Molecular Medicine 2009;13(8b):2547-2558.
168. Lin T-J, Issekutz TB, Marshall JS. Human mast cells transmigrate through human umbilical vein endothelial monolayers and selectively produce IL-8 in response to stromal cell-derived factor-1{alpha}. J Immunol 2000;165(1):211-220.
169. Juremalm M, Hjertson M, Olsson N, Harvima I, Nilsson K, Nilsson G. The chemokine receptor CXCR4 is expressed within the mast cell lineage and its ligand stromal cell-derived factor-1alpha acts as a mast cell chemotaxin. European Journal of Immunology 2000;30(12):3614-3622.
170. Juremalm M, Nilsson G. Chemokine receptor expression by mast cells. Chem Immunol Allergy 2005;87:130-144.

171. Godot V, Arock M, Garcia G, Capel F, Flys C, Dy M, et al. H4 histamine receptor mediates optimal migration of mast cell precursors to CXCL12. J Allergy Clin Immunol 2007;120(4):827-834.
172. Belot MP, Abdennebi-Najar L, Gaudin F, Lieberherr M, Godot V, Taieb J, et al. Progesterone reduces the migration of mast cells toward the chemokine stromal cell-derived factor-1/CXCL12 with an accompanying decrease in CXCR4 receptors. Am J Physiol Endocrinol Metab 2007;292(5):E1410-1417.
173. Juremalm M, Hjertson M, Olsson N, Harvima I, Nilsson K, Nilsson G. The chemokine receptor CXCR4 is expressed within the mast cell lineage and its ligand stromal cell-derived factor-1 alpha acts as a mast cell chemotaxin. Eur J Immunol 2000;30(12):3614-3622.
174. Lin TJ, Issekutz TB, Marshall JS. Human mast cells transmigrate through human umbilical vein endothelial monolayers and selectively produce IL-8 in response to stromal cell-derived factor-1 alpha. J Immunol 2000;165(1):211-220.
175. Cho C-H, Jun Koh Y, Han J, Sung H-K, Jong Lee H, Morisada T, et al. Angiogenic role of LYVE-1-positive macrophages in adipose tissue. Circ Res 2007;100(4):e47-57.
176. Petty JM, Sueblinvong V, Lenox CC, Jones CC, Cosgrove GP, Cool CD, et al. Pulmonary stromal-derived factor-1 expression and effect on neutrophil recruitment during acute lung injury. J Immunol 2007;178(12):8148-8157.
177. Fairweather D, Frisancho-Kiss S, Yusung SA, Barrett MA, Davis SE, Gatewood SJL, et al. Interferon-{gamma} protects against chronic viral myocarditis by reducing mast cell degranulation, fibrosis, and the profibrotic cytokines transforming frowth vactor-{beta}1, interleukin-1{beta}, and interleukin-4 in the heart. Am J Pathol 2004;165(6):1883-1894.
178. Tiede S, Ernst N, Bayat A, Paus R, Tronnier V, Zechel C. Basic fibroblast growth factor: A potential new therapeutic tool for the treatment of hypertrophic and keloid scars. Annals of Anatomy - Anatomischer Anzeiger 2009;191(1):33-44.
179. Higgins DM, Basaraba RJ, Hohnbaum AC, Lee EJ, Grainger DW, Gonzalez-Juarrero M. Localized Immunosuppressive Environment in the Foreign Body Response to Implanted Biomaterials. Am J Pathol 2009;175(1):161-170.
180. Toksoy A, Müller V, Gillitzer R, Goebeler M. Biphasic expression of stromal cell-derived factor-1 during human wound healing. British Journal of Dermatology 2007;157(6):1148-1154.
181. Xing D, Marti G, Liu L, Zhang X, Reinblatt M, Semenza GL, et al. Hypoxia colocalizes with increased levels of HIF-1 alpha and its angiogenic transcription products SDF-1 and VEGF in the burn wound. Journal of the American College of Surgeons 2009;209(3, Supplement 1):S74-S74.
182. Oswald J, Boxberger S, Jørgensen B, Feldmann S, Ehninger G, Bornhäuser M, et al. Mesenchymal stem cells can be differentiated into endothelial cells in vitro. Stem Cells 2004;22(3):377-384.
183. Crosby JR, Kaminski WE, Schatteman G, Martin PJ, Raines EW, Seifert RA, et al. Endothelial cells of hematopoietic origin make a significant contribution to adult blood vessel formation. Circ Res 2000;87(9):728-730.
184. Friedrich EB, Walenta K, Scharlau J, Nickenig G, Werner N. CD34-/CD133+/VEGFR-2+ endothelial progenitor cell subpopulation with potent vasoregenerative capacities. Circ Res 2006;98(3):e20-25.
185. Bot I, de Jager SCA, Bot M, van Heiningen SH, de Groot P, Veldhuizen RW, et al. Short communication: The neuropeptide substance P mediates adventitial mast cell activation and induces intraplaque hemorrhage in advanced atherosclerosis. Circ Res;106(1):89-92.
186. Ratajczak MZ, Kucia M, Halasa M, Wysoczynski M, Machalinski B. 24: Morphological and molecular characterization of novel population of CXCR4+ SSEA-4+ Oct-4+ very small embryonic-like (VSEL) cells purfied from human cord blood. Biology of Blood and Marrow Transplantation 2007;13(11):1401-1401.
187. Wojakowski W, Tendera M, Kucia M, Zuba-Surma E, Paczkowska E, Ciosek J, et al. Mobilization of bone marrow-derived Oct-4+ SSEA-4+ very small embryonic-like stem cells in

patients with acute myocardial infarction. Journal of the American College of Cardiology 2009;53(1):1-9.
188. Schledzewski K, Falkowski M, Moldenhauer G, Metharom P, Kzhyshkowska J, Ganss R, et al. Lymphatic endothelium-specific hyaluronan receptor LYVE-1 is expressed by stabilin-1+, F4/80+, CD11b+ macrophages in malignant tumours and wound healing tissue in vivo and in bone marrow cultures in vitro: implications for the assessment of lymphangiogenesis. J Pathol 2006;209(1):67-77.
189. Schober A, Karshovska E, Zernecke A, Weber C. SDF-1[alpha]-mediated tissue repair by stem cells: A promising tool in cardiovascular medicine? Trends in Cardiovascular Medicine 2006;16(4):103-108.
190. Szmitko PE, Fedak PWM, Weisel RD, Stewart DJ, Kutryk MJB, Verma S. Endothelial Progenitor Cells: New Hope for a Broken Heart. Circulation 2003;107(24):3093-3100.
191. Reimold AM. New indications for treatment of chronic inflammation by TNF-alpha blockade. The American Journal of the Medical Sciences 2003;325(2):75-92.
192. Dinarello CA. Proinflammatory Cytokines. Chest 2000;118(2):503-508.
193. Thevenot P, Hu W, Tang L. Surface chemistry influences implant biocompatibility. Curr Top Med Chem 2008;8(4):270-280.
194. TA Wynn. Cellular and molecular mechanisms of fibrosis. The Journal of Pathology 2008;214(2):199-210.
195. Landgraeber S, von Knoch M, Löer F, Wegner A, Tsokos M, Hußmann B, et al. Extrinsic and intrinsic pathways of apoptosis in aseptic loosening after total hip replacement. Biomaterials;29(24-25):3444-3450.
196. Borges VM, Falcao H, Leite-Junior JH, Alvim L, Teixeira GP, Russo M, et al. Fas Ligand Triggers Pulmonary Silicosis. J Exp Med 2001;194(2):155-164.
197. Hohlbaum AM, Saff RR, Marshak-Rothstein A. Fas-Ligand--Iron Fist or Achilles' Heel? Clinical Immunology 2002;103(1):1-6.
198. Okazaki T, Ebihara S, Takahashi H, Asada M, Kanda A, Sasaki H. Macrophage Colony-Stimulating Factor Induces Vascular Endothelial Growth Factor Production in Skeletal Muscle and Promotes Tumor Angiogenesis. J Immunol 2005;174(12):7531-7538.
199. Xia Z, Triffitt JT. A review on macrophage responses to biomaterials. Biomed Mater 2006;1(1):R1-9.
200. Yanshuang Xie, Kai Gao, Lari Häkkinen, Hannu S. Larjava. Mice lacking β6 integrin in skin show accelerated wound repair in dexamethasone impaired wound healing model. Wound Repair and Regeneration 2009;17(3):326-339.
201. Jin DK, Shido K, Kopp HG, Petit I, Shmelkov SV, Young LM, et al. Cytokine-mediated deployment of SDF-1 induces revascularization through recruitment of CXCR4+ hemangiocytes. Nat Med 2006;12(5):557-567.
202. Stellos K, Langer H, Daub K, Schoenberger T, Gauss A, Geisler T, et al. Platelet-derived stromal cell-derived factor-1 regulates adhesion and promotes differentiation of human CD34+ cells to endothelial progenitor cells. Circulation 2008;117(2):206-215.
203. Hosseinkhani H, Hosseinkhani M, Khademhosseini A, Kobayashi H, Tabata Y. Enhanced angiogenesis through controlled release of basic fibroblast growth factor from peptide amphiphile for tissue regeneration. Biomaterials 2006;27(34):5836-5844.
204. Hao X, Silva EA, Mansson-Broberg A, Grinnemo K-H, Siddiqui AJ, Dellgren G, et al. Angiogenic effects of sequential release of VEGF-A165 and PDGF-BB with alginate hydrogels after myocardial infarction. Cardiovasc Res 2007;75(1):178-185.
205. Sales VL, Engelmayr GC, Jr., Mettler BA, Johnson JA, Jr., Sacks MS, Mayer JE, Jr. Transforming growth factor-beta1 modulates extracellular matrix production, proliferation, and apoptosis of endothelial progenitor cells in tissue-engineering scaffolds. Circulation 2006;114(1 Suppl):I193-199.
206. Anderson JM, Rodriguez A, Chang DT. Foreign body reaction to biomaterials. Seminars in Immunology 2008;20(2):86-100.

207. van Wachem PB, Brouwer LA, van Luyn MJA. Absence of muscle regeneration after implantation of a collagen matrix seeded with myoblasts. Biomaterials 1999;20(5):419-426.
208. Al-Saffar N, Iwaki H, Revell PA. Direct activation of mast cells by prosthetic biomaterial particles. Journal of Materials Science: Materials in Medicine 1998;9(12):849-853.
209. Tcacencu I, Wendel M. Collagen-hydroxyapatite composite enhances regeneration of calvaria bone defects in young rats but postpones the regeneration of calvaria bone in aged rats. Journal of Materials Science: Materials in Medicine 2008;19(5):2015-2021.
210. Savarino L, Baldini N, Greco M, Capitani O, Pinna S, Valentini S, et al. The performance of poly-[epsilon]-caprolactone scaffolds in a rabbit femur model with and without autologous stromal cells and BMP4. Biomaterials 2007;28(20):3101-3109.
211. Artuc M, Hermes B, Stckelings UM, Grützkau A, Henz BM. Mast cells and their mediators in cutaneous wound healing – active participants or innocent bystanders? Experimental Dermatology 1999;8(1):1-16.
212. Rezzani R, Rodella L, Tartaglia GM, Paganelli C, Sapelli P, Bianchi R. Mast cells and the inflammatory response to different implanted biomaterials. Archives of Histology and Cytology 2004;67(3):211-217.
213. Bellini A, Mattoli S. The role of the fibrocyte, a bone marrow-derived mesenchymal progenitor, in reactive and reparative fibroses. Lab Invest 2007;87(9):858-870.
214. Bucala R, Spiegel LA, Chesney J, Hogan M, Cerami A. Circulating fibrocytes define a new leukocyte subpopulation that mediates tissue repair. Mol Med 1994;1(1):71-81.
215. Mehrad B, Burdick MD, Strieter RM. Fibrocyte CXCR4 regulation as a therapeutic target in pulmonary fibrosis. The International Journal of Biochemistry & Cell Biology;41(8-9):1708-1718.
216. Quan TE, Cowper S, Wu S-P, Bockenstedt LK, Bucala R. Circulating fibrocytes: collagen-secreting cells of the peripheral blood. The International Journal of Biochemistry & Cell Biology 2004;36(4):598-606.
217. Ishida Y, Kimura A, Kondo T, Hayashi T, Ueno M, Takakura N, et al. Essential roles of the CC chemokine ligand 3-CC chemokine receptor 5 axis in bleomycin-induced pulmonary fibrosis through regulation of macrophage and fibrocyte infiltration. Am J Pathol 2007;170(3):843-854.
218. Moore BB, Murray L, Das A, Wilke CA, Herrygers AB, Toews GB. The role of CCL12 in the recruitment of fibrocytes and lung fibrosis. Am J Respir Cell Mol Biol 2006;35(2):175-181.
219. Quan TE, Cowper SE, Bucala R. The role of circulating fibrocytes in fibrosis. Curr Rheumatol Rep 2006;8(2):145-150.
220. Rege TA, Hagood JS. Thy-1 as a regulator of cell-cell and cell-matrix interactions in axon regeneration, apoptosis, adhesion, migration, cancer, and fibrosis. FASEB J 2006;20(8):1045-1054.
221. Bradley JE, Ramirez G, Hagood JS. Roles and regulation of Thy-1, a context-dependent modulator of cell phenotype. Biofactors 2009;35(3):258-265.
222. Rege TA, Hagood JS. Thy-1, a versatile modulator of signaling affecting cellular adhesion, proliferation, survival, and cytokine/growth factor responses. Biochim Biophys Acta 2006;1763(10):991-999.
223. Thevenot PT, Nair AM, Shen J, Lotfi P, Ko C-Y, Tang L. The effect of incorporation of SDF-1[alpha] into PLGA scaffolds on stem cell recruitment and the inflammatory response. Biomaterials;In Press, Corrected Proof.
224. Schmidt M, Sun G, Stacey MA, Mori L, Mattoli S. Identification of circulating fibrocytes as precursors of bronchial myofibroblasts in asthma. J Immunol 2003;171(1):380-389.
225. Moore BB, Kolodsick JE, Thannickal VJ, Cooke K, Moore TA, Hogaboam C, et al. CCR2-mediated recruitment of fibrocytes to the alveolar space after fibrotic injury. Am J Pathol 2005;166(3):675-684.
226. Phillips RJ, Burdick MD, Hong K, Lutz MA, Murray LA, Xue YY, et al. Circulating fibrocytes traffic to the lungs in response to CXCL12 and mediate fibrosis. The Journal of Clinical Investigation 2004;114(3):438-446.

227. Jones KS. Effects of biomaterial-induced inflammation on fibrosis and rejection. Seminars in Immunology 2008;20(2):130-136.
228. Tang L, Eaton JW. Natural responses to unnatural materials: A molecular mechanism for foreign body reactions. Mol Med 1999;5(6):351-358.
229. Carmi Y, Voronov E, Dotan S, Lahat N, Rahat MA, Fogel M, et al. The role of macrophage-derived IL-1 in induction and maintenance of angiogenesis. J Immunol 2009;183(7):4705-4714.
230. Patil SD, Papadmitrakopoulos F, Burgess DJ. Concurrent delivery of dexamethasone and VEGF for localized inflammation control and angiogenesis. J Control Release 2007;117(1):68-79.
231. Sasaki M, Abe R, Fujita Y, Ando S, Inokuma D, Shimizu H. Mesenchymal stem cells are recruited into wounded skin and contribute to wound repair by transdifferentiation into multiple skin cell type. J Immunol 2008;180(4):2581-2587.
232. Chesney J, Metz C, Stavitsky AB, Bacher M, Bucala R. Regulated production of type I collagen and inflammatory cytokines by peripheral blood fibrocytes. J Immunol 1998;160(1):419-425.
233. Pilling D, Buckley CD, Salmon M, Gomer RH. Inhibition of fibrocyte differentiation by serum amyloid P. J Immunol 2003;171(10):5537-5546.
234. Hagood JS, Prabhakaran P, Kumbla P, Salazar L, MacEwen MW, Barker TH, et al. Loss of fibroblast Thy-1 expression correlates with lung fibrogenesis. Am J Pathol 2005;167(2):365-379.
235. Sanders YY, Pardo A, Selman M, Nuovo GJ, Tollefsbol TO, Siegal GP, et al. Thy-1 promoter hypermethylation: a novel epigenetic pathogenic mechanism in pulmonary fibrosis. Am J Respir Cell Mol Biol 2008;39(5):610-618.
236. Chu P-Y, Mariani J, Finch S, McMullen JR, Sadoshima J, Marshall T, et al. Bone marrow-derived cells contribute to fibrosis in the chronically failing heart. Am J Pathol:ajpath.2010.090574.
237. Chu P-Y, Mariani J, Finch S, McMullen JR, Sadoshima J, Marshall T, et al. Fibrocyte recruitment to the failing heart: Role of stromal derived factor-1 in cardiac fibrosis. Heart, Lung and Circulation 2009;18(Supplement 3):S176-S176.
238. El-Asrar AMA, Struyf S, Van Damme J, Geboes K. Circulating fibrocytes contribute to the myofibroblast population in proliferative vitreoretinopathy epiretinal membranes. British Journal of Ophthalmology 2008;92(5):699-704.
239. Andersson-Sjöland A, de Alba CG, Nihlberg K, Becerril C, Ramírez R, Pardo A, et al. Fibrocytes are a potential source of lung fibroblasts in idiopathic pulmonary fibrosis. The International Journal of Biochemistry & Cell Biology 2008;40(10):2129-2140.
240. Sakai N, Wada T, Yokoyama H, Lipp M, Ueha S, Matsushima K, et al. Secondary lymphoid tissue chemokine (SLC/CCL21)/CCR7 signaling regulates fibrocytes in renal fibrosis. Proceedings of the National Academy of Sciences 2006;103(38):14098-14103.
241. Wada T, Sakai N, Matsushima K, Kaneko S. Fibrocytes: A new insight into kidney fibrosis. Kidney Int 2007;72(3):269-273.
242. Bellini A, Mattoli S. The role of the fibrocyte, a bone marrow-derived mesenchymal progenitor, in reactive and reparative fibroses. Lab Invest 2007;87(9):858-870.
243. Hennrick KT, Keeton AG, Nanua S, Kijek TG, Goldsmith AM, Sajjan US, et al. Lung cells from neonates show a mesenchymal stem cell phenotype. Am J Respir Crit Care Med 2007;175(11):1158-1164.
244. Strieter RM, Keeley EC, Hughes MA, Burdick MD, Mehrad B. The role of circulating mesenchymal progenitor cells (fibrocytes) in the pathogenesis of pulmonary fibrosis. J Leukoc Biol 2009;86(5):1111-1118.
245. Ringe J, Strassburg S, Neumann K, Endres M, Notter M, Burmester GR, et al. Towards in situ tissue repair: human mesenchymal stem cells express chemokine receptors CXCR1, CXCR2 and CCR2, and migrate upon stimulation with CXCL8 but not CCL2. J Cell Biochem 2007;101(1):135-146.

246. Erggelet C, Neumann K, Endres M, Haberstroh K, Sittinger M, Kaps C. Regeneration of ovine articular cartilage defects by cell-free polymer-based implants. Biomaterials 2007;28(36):5570-5580.
247. Zhang F, Tsai S, Kato K, Yamanouchi D, Wang C, Rafii S, et al. Transforming growth factor-beta promotes recruitment of bone marrow cells and bone marrow-derived mesenchymal stem cells through stimulation of MCP-1 production in vascular smooth muscle cells. Journal of Biological Chemistry 2009;284(26):17564-17574.
248. Mourkioti F, Rosenthal N. IGF-1, inflammation and stem cells: interactions during muscle regeneration. Trends in Immunology 2005;26(10):535-542.
249. Felszeghy K, Banisadr G, Rostene W, Nyakas C, Haour F. Dexamethasone downregulates chemokine receptor CXCR4 and exerts neuroprotection against hypoxia/ischemia-induced brain injury in neonatal rats. Neuroimmunomodulation 2004;11(6):404-413.
250. Zilberman M. Dexamethasone loaded bioresorbable films used in medical support devices: Structure, degradation, crystallinity and drug release. Acta Biomaterialia 2005;1(6):615-624.
251. Jee J-P, Choung H-K, Kim C-K, Hwang J-M. Polytetrafluoroethylene/Polylactide-co-Glycolide Laminate Containing Dexamethasone Allows Delayed Adjustable Strabismus Surgery in a Rabbit Model. Invest Ophthalmol Vis Sci 2006;47(6):2485-2490.
252. Klemm P, Harris HJ, Perretti M. Effect of rolipram in a murine model of acute inflammation: comparison with the corticoid dexamethasone. European Journal of Pharmacology 1995;281(1):69-74.
253. Blyth DI, Wharton TF, Pedrick MS, Savage TJ, Sanjar S. Airway subepithelial fibrosis in a murine model of atopic asthma: suppression by dexamethasone or anti-interleukin-5 antibody. Am J Respir Cell Mol Biol 2000;23(2):241-246.
254. Gu L, Zhu YJ, Guo ZJ, Xu XX, Xu WB. Effect of IFN-gamma and dexamethasone on TGF-beta1-induced human fetal lung fibroblast-myofibroblast differentiation. Acta Pharmacol Sin 2004;25(11):1479-1488.
255. Miller M, Cho JY, McElwain K, McElwain S, Shim JY, Manni M, et al. Corticosteroids prevent myofibroblast accumulation and airway remodeling in mice. Am J Physiol Lung Cell Mol Physiol 2006;290(1):L162-169.
256. Tliba O, Amrani Y, Panettieri RA. Is airway smooth muscle the missing link modulating airway inflammation in asthma?*. Chest 2008;133(1):236-242.
257. Kwon OJ, Jose PJ, Robbins RA, Schall TJ, Williams TJ, Barnes PJ. Glucocorticoid inhibition of RANTES expression in human lung epithelial cells. Am J Respir Cell Mol Biol 1995;12(5):488-496.
258. Berkman N, Robichaud A, Krishnan VL, Roesems G, Robbins R, Jose PJ, et al. Expression of RANTES in human airway epithelial cells: effect of corticosteroids and interleukin-4, -10 and -13. Immunology 1996;87(4):599-603.
259. Waage A, Slupphaug G, Shalaby R. Glucocorticoids inhibit the production of IL 6 from monocytes, endothelial cells and fibroblasts. European Journal of Immunology 1990;20(11):2439-2443.
260. Quante T, Ng YC, Ramsay EE, Henness S, Allen JC, Parmentier J, et al. Corticosteroids reduce IL-6 in ASM cells via up-regulation of MKP-1. Am J Respir Cell Mol Biol 2008;39(2):208-217.
261. Tirumurugaan KG, Kang BN, Panettieri RA, Foster DN, Walseth TF, Kannan MS. Regulation of the cd38 promoter in human airway smooth muscle cells by TNF-alpha and dexamethasone. Respir Res 2008;9:26.
262. Kim SH, Kim DH, Lavender P, Seo JH, Kim YS, Park JS, et al. Repression of TNF-alpha-induced IL-8 expression by the glucocorticoid receptor-beta involves inhibition of histone H4 acetylation. Exp Mol Med 2009;41(5):297-306.

263. Mullou J, Xaubet A, Gaya A, Roca-Ferrer J, Lopez E, Fernandez JC, et al. Cytokine gene expression and release from epithelial cells. A comparison study between healthy nasal mucosa and nasal polyps. Clinical & Experimental Allergy 1995;25(7):607-615.
264. Chen G, Grotendorst G, Eichholtz T, Khalil N. GM-CSF increases airway smooth muscle cell connective tissue expression by inducing TGF-beta receptors. Am J Physiol Lung Cell Mol Physiol 2003;284(3):L548-556.
265. Matsuda A, Orihara K, Fukuda S, Fujinaga H, Matsumoto K, Saito H. Corticosteroid enhances TNF-alpha-mediated leukocyte adhesion to pulmonary microvascular endothelial cells. Allergy 2008;63(12):1610-1616.
266. Kucia M, Ratajczak J, Reca R, Janowska-Wieczorek A, Ratajczak MZ. Tissue-specific muscle, neural and liver stem/progenitor cells reside in the bone marrow, respond to an SDF-1 gradient and are mobilized into peripheral blood during stress and tissue injury. Blood Cells Mol Dis 2004;32(1):52-57.
267. Lama VN, Phan SH. The extrapulmonary origin of fibroblasts: Stem/progenitor cells and beyond. Proc Am Thorac Soc 2006;3(4):373-376.
268. Mehrad B, Burdick MD, Zisman DA, Keane MP, Belperio JA, Strieter RM. Circulating peripheral blood fibrocytes in human fibrotic interstitial lung disease. Biochemical and Biophysical Research Communications 2007;353(1):104-108.
269. Hachet-Haas M, Balabanian K, Rohmer Fo, Pons Fo, Franchet C, Lecat S, et al. Small neutralizing molecules to inhibit actions of the chemokine CXCL12. Journal of Biological Chemistry 2008;283(34):23189-23199.
270. Roberts ISD, Brenchley PEC. Mast cells: the forgotten cells of renal fibrosis. Journal of Clinical Pathology 2000;53(11):858-862.
271. Sasaki A, Mueller RV, Xi G, Sipe R, Buck D, Hollinger J. Mast cells: An unexpected finding in the modulation of cutaneous wound repair by charged beads. Plastic and Reconstructive Surgery 2003;111(4):1446-1453.
272. Ayako S, Tohru T, Yukihisa F, Yasuo N, Nobuyuki T. Evaluation of role of mast cells in the development of liver fibrosis using mast cell-deficient rats and mice. Journal of hepatology 1999;30(5):859-867.
273. Okazaki T, Hirota S, Xu ZD, Maeyama K, Nakama A, Kawano S, et al. Increase of mast cells in the liver and lung may be associated with but not a cause of fibrosis: demonstration using mast cell-deficient Ws/Ws rats. Lab Invest 1998;78(11):1431-1438.
274. Gaboury J, Johnston B, Niu X, Kubes P. Mechanisms underlying acute mast cell-induced leukocyte rolling and adhesion in vivo. J Immunol 1995;154(2):804-813.
275. Noel AA, Fallek SR, Hobson Ii RW, Durán WN. Inhibition of nitric oxide synthase attenuates primed microvascular permeability in the in vivo microcirculation. Journal of Vascular Surgery 1995;22(6):661-670.
276. Bryers JD. Medical biofilms. Biotechnology and Bioengineering 2008;100(1):1-18.
277. Woodman L, Siddiqui S, Cruse G, Sutcliffe A, Saunders R, Kaur D, et al. Mast cells promote airway smooth muscle cell differentiation via autocrine up-regulation of TGF-{beta}1. J Immunol 2008;181(7):5001-5007.

BIOGRAPHICAL INFORMATION

Paul Thevenot finished his Bachelor's Degree in Biological Engineering at Louisiana State University. He then began work on his Master's Degree in Biomedical Engineering under Dr. Liping Tang. Paul studied the influence of surface functionality of microparticle toxicity of for his Master's Thesis project. After briefly working on the influence of seeding parameters in tissue engineering, he began working with Dr. Tang on the mechanisms which govern biomaterial mediated host stem cell responses. They began a series of projects design to improve host-derived stem cell responses to improve biomaterial-mediated fibrotic responses and improve/coordinate biomaterial integration and stimulate regeneration. Based on the results of this work, Paul finished his dissertation work examining the recruitment and contribution of biomaterial-mediated fibrotic progenitor cells and strategies to control and influence their behavior at the implantation site. Paul has accepted a post-doctoral position at Louisiana State University Health Science Center in New Orleans, LA with Dr. Stephania Cormier in the Department of Pharmacology. There he plans to continue studying methods to improve immunological parameters related to biomaterial-mediated foreign body responses to improve the clinical translation of tissue engineering strategies.